

3
2007



This is to certify that the
dissertation entitled

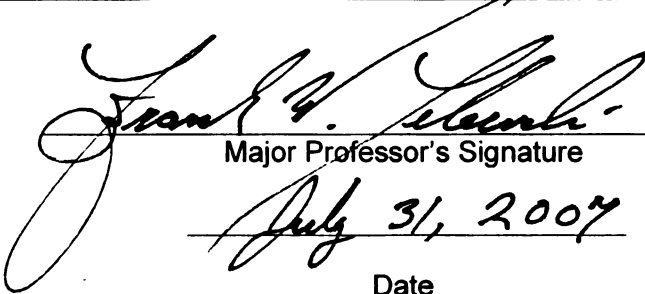
DISTRIBUTION AND ECOPHYSIOLOGY OF THE
PONDEROSAE IN THE SANTA CATALINA MOUNTAINS
OF SOUTHERN ARIZONA

presented by

JASON SCOTT KILGORE

has been accepted towards fulfillment
of the requirements for the

Ph.D. degree in Plant Biology and Ecology,
Evolution, and Behavioral
Biology


Major Professor's Signature
July 31, 2007
Date

PLACE IN RETURN BOX to remove this checkout from your record.
TO AVOID FINES return on or before date due.
MAY BE RECALLED with earlier due date if requested.

DATE DUE	DATE DUE	DATE DUE

**DISTRIBUTION AND ECOPHYSIOLOGY OF THE *PONDEROSAE*
IN THE SANTA CATALINA MOUNTAINS OF SOUTHERN ARIZONA**

By

Jason Scott Kilgore

A DISSERTATION

**Submitted to
Michigan State University
in partial fulfillment of the requirements
for the degree of**

DOCTOR OF PHILOSOPHY

**Department of Plant Biology
Ecology, Evolution, and Behavioral Biology Program**

2007

ABSTRACT

DISTRIBUTION AND ECOPHYSIOLOGY OF THE *PONDEROSAE* IN THE SANTA CATALINA MOUNTAINS OF SOUTHERN ARIZONA

By

Jason Scott Kilgore

I investigated the distribution and ecophysiological factors for establishment and survival for *Ponderosae* in the Santa Catalina Mountains of southern Arizona. The complex topography of this system produces variable microhabitats that obscure a simple elevational pattern of Arizona pine (*Pinus arizonica* Engelman) lower than the Southwestern race of Rocky Mountain ponderosa pine (*P. ponderosa* var. *scopulorum* Engelman). In addition, an intermediate needle morphotype, a putative hybrid between *P. arizonica* and *P. ponderosa* var. *scopulorum*, is recognized from this and other mountain islands in the American Southwest. Following extensive fires, Coronado National Forest identified the need to assess their distributional patterns for reforestation.

Modeling of documented occurrences in relation to climatic variables indicated clear distinction in distribution and ecological niche space between *P. arizonica* and *P. ponderosa* var. *scopulorum*, while the putative hybrid displayed intermediate distribution and occupation of niche space. High intratree variance in needle number and the overlapping distribution and ecological niche space support the hybridization hypothesis.

In controlled tests, germination success and time to initial germination were similar, but *P. arizonica* seeds germinated over a longer period of time. In

the field, neither species germinated in the spring, while, following the monsoon, *P. arizonica* (25%) had lower germination at low and high elevation than did *P. ponderosa* var. *scopulorum* (52%). Controlled whole-plant freezing tests revealed greater cold tolerance in needle, bud, and cambial tissue by *P. ponderosa* var. *scopulorum* seedlings than *P. arizonica* seedlings over periods of simulated fall, winter, and spring. Seedlings of *P. ponderosa* var. *scopulorum* exposed to ambient light and freezing temperatures maintained higher photosynthetic quantum yield than did seedlings of *P. arizonica* and the putative hybrid. In the field, small *P. ponderosa* var. *scopulorum* trees maintained higher net photosynthesis and midday quantum yield than did similarly sized *P. arizonica* trees. When soil water availability was low and incident light levels were high during the winter, small *P. ponderosa* var. *scopulorum* trees maintained higher leaf water status yet similar net photosynthesis than *P. arizonica* trees. During the arid foresummer, diurnal variation in gas exchange was higher in *P. ponderosa* var. *scopulorum* than in *P. arizonica*, suggesting greater stomatal response to water-limiting conditions. However, integrated water-use efficiency and leaf nitrogen content did not differ between species. During severe dehydration, *P. ponderosa* var. *scopulorum* maintained higher photosynthetic quantum yield than did *P. arizonica*. However, xylem conductivity and vulnerability to cavitation did not differ between species. *P. ponderosa* var. *scopulorum* has greater cold tolerance, controls transpirational water loss, and maintains photosynthetic function across the seasons better than *P. arizonica*.

Copyright by
JASON SCOTT KILGORE
2007

ACKNOWLEDGEMENTS

The research described in this dissertation could not have been accomplished without the support of my family and many friends. I especially appreciate the enduring support and love from my wife, Pam, and son, Oliver. My extended family, including Lucy Dueck, Justin Kilgore, Bob and Kathy Reynolds, Kim Reynolds, and Jason Tallant, provided unquestioning support, trust, and curiosity in what I was doing in Arizona or at the lab through the night.

I thank my committee – Drs. Frank Telewski, Peter Murphy, Bryan Epperson, and Brian Maurer – for serving my research interests. Frank was not only my major advisor and mentor but also has become a good friend; I truly appreciate his companionship and contributions to field and labwork. Pete has been my prudent mentor and friend for over a decade. And I eagerly anticipate exploring the genetic complexities of the *Ponderosae* with Bryan in the future.

I have been enormously fortunate to have many people volunteer their time and resources to me through this dissertation research. Friends who trudged the Santa Catalina Mountains with or for me have included Frank Telewski, Kris Kern, Stephanie Blumer, Gretchen Friedlander, Samantha Warwick, Clare and Bob Peterson, Jill Grimes, Tom and Annita Harlan, Holly Bechetti, and Joe and Christina Hoscheidt. Folks from the Coronado National Forest, especially Bill Hart but also Terri Austin, Jennifer Ruyle, and Josh Taiz, have been incredibly supportive and interested in this research; these are the managers of the forest who need this research. Barb Eisele (Trees for Mount

Lemmon) was instrumental in connecting this research with reforestation interests for the Summerhaven community as well as in contributing seedlings to our research program; she was always interested in trading home-cooked meals for research updates. Jim Burns and Steve Leavitt at the Laboratory of Tree-Ring Research provided shipping destinations and nitrogen cylinders, while Carol Mack at Mount Lemmon General Store kindly arranged shipping departures. Bob Peterson and the gang at the Steward Observatory always made sure they had room for us at the top. Loma and Jim Griffith always had a place for us in Tucson and provided transportation, including a 4WD vehicle, whenever needed.

Back in Michigan, I had ample assistance and support from friends. Folks who contributed to lab and greenhouse adventures include Alex Lindsey, Stephanie Blumer, Frank Telewski, Samantha Warwick, Jessica Reif, Tricia Mitchell, Casey Bartrem, Calvin Glaspie, Jameel Al-Haddad, Justin Savu, Pam Kilgore, Crystal Wallace, Will Paddock, Abbie Schrotenboer, Lynn Sage, Todd Robinson, Andrea Corpolongo, Scott Smith, Hope Rankin, Christopher Start, and Andrew Murphy. Anna Jacobsen is a valued friend, colleague, and contributor to this research. Although not serving on my committee, Drs. Lissa Leege, Ken Poff, Bert Cregg, Frank Ewers, Jim Flore, David Rothstein, Carolyn Malmstrom, Merritt Turetsky, Andrew McAdam, and Andy Jarosz provided invaluable advice, equipment, and/or office space. Jeff Wilson, Bob Goodwin, and Nate Siegert assisted me with computer and GIS issues. Lynn Sage, Mark Hammond, and Jim Klug arranged for cold conditions, while Dave Freville's crew ensured warm (greenhouse) conditions. Mike Grillo and Heather Hallen were invaluable friends

and colleagues. No person acts without their departmental staff; I appreciate the support and assistance by Tracey Barner, Kasey Baldwin, Jan McGowan, Jill Richey, and Holly Nieuwma.

Last, I wish to acknowledge those units that have financially contributed to this research. The Department of Plant Biology supported a considerable amount of travel, conference, and non-MSU course-related expenses through the Paul Taylor Fund, as well as supporting me through the experience of teaching assistantships. The College of Natural Science granted me the Dr. Marvin Hensley Endowed Fellowship and the Dissertation Completion Fellowship, while the Ecology, Evolution, and Behavioral Biology (EEBB) program granted me Travel and Summer Fellowships. Campus Planning and Administration has provided logistical support, while Frank has supplemented funding with his research account. I appreciate all that these units have contributed to my research.

TABLE OF CONTENTS

CHAPTER 1	
AN INTRODUCTION TO SOUTHWESTERN PONDEROSA PINE, ARIZONA PINE, AND THEIR ENVIRONMENT	1
CHAPTER 2	
DISTRIBUTION AND ECOLOGICAL NICHE DIFFERENTIATION OF SYMPATRIC <i>PONDEROSAE</i> TAXA IN THE SANTA CATALINA MOUNTAINS OF ARIZONA	23
CHAPTER 3	
INFLUENCE OF SEED GERMINATION ECOLOGY ON THE DISTRIBUTION OF <i>PONDEROSAE</i> IN THE SANTA CATALINA MOUNTAINS OF ARIZONA	82
CHAPTER 4	
DIFFERENTIAL COLD TOLERANCE SEGREGATES DISTRIBUTION OF <i>PONDEROSAE</i> IN THE SANTA CATALINA MOUNTAINS OF ARIZONA	116
CHAPTER 5	
THE ROLE OF DROUGHT TOLERANCE IN STRUCTURING <i>PONDEROSAE</i> DISTRIBUTION IN THE SANTA CATALINA MOUNTAINS OF ARIZONA	160
CHAPTER 6	
GENERAL CONCLUSIONS	220
APPENDIX.....	226
REFERENCES	244

LIST OF TABLES

Table 2-1. Models and environmental variables used in the modeling of species distributions, or suitable habitat (Phillips et al. 2006a), using Maxent (Phillips et al. 2006b).....	43
Table 2-2. Summary statistics for regression of mean number of needles per fascicle per tree by morphotype and combined species against elevation at which the tree was located.....	51
Table 2-3. Comparison of influence of spatial extent by shape of calibration area on model output.....	55
Table 2-4. Performance characteristics and statistics for prediction models generated by Maxent for the rectangular study region.....	58
Table 2-5. Climatically suitable area estimates for the three morphotypes based on cumulative probabilities from the Lit and Lit.Thresh models.....	62
Table 2-6. Thresholds for the three morphotypes based on the Lit.Thresh model.....	64
Table 2-7. Ecological similarity matrix based on the ability of one taxon's model (columns) to predict the documented occurrences of each of the taxa (rows).....	64
Table 3-1. Seeds inventoried from cones collected from the Santa Catalina Mountains in September-October 2005.....	88
Table 3-2. Type II tests of 2-factor ANOVA of percent germination (pergerm), time to first germination (initiate), and time to last realized germination (complete) for PIN_PON seed as a function of site (MTL and PAL), stratification (strat; 0-, 15-, and 30-day), and their interaction.....	99
Table 3-3. Type II tests of 2-factor ANOVA of percent germination (pergerm), time to first germination (initiate), and time to last realized germination (complete) for PIN_ARI seed as a function of site (PAL and RC/LIZ), stratification (strat; 0-, 15-, and 30-day), and their interaction.....	100
Table 3-4. Type II tests of 2-factor ANOVA of percent germination (pergerm), time to first germination (initiate), and time to last realized germination (complete) for the PAL site as a function of morphotype (PIN_PON, Mixed, and PIN_ARI), stratification (strat; 0-, 15-, and 30-day), and their interaction.....	102

Table 3-5. Type II tests of 2-factor ANOVA of natural-log-transformed percent realized germination (pergerm), time to first germination (initiate), and time to last germination (complete) for pooled sites as a function of morphotype (PIN_PON, Mixed, and PIN_ARI), stratification (strat; 0-, 15- and 30-day), and their interaction.....	103
Table 3-6. Pairwise comparisons (Tukey's HSD) of PIN_PON and PIN_ARI seeds for natural-log-transformed percent realized germination (pergerm), time to first germination (initiate), and time to last germination (complete) as a function of stratification treatment for pooled sites.....	103
Table 3-7. ANOVA for germination success of PIN_PON and PIN_ARI seeds at the Mount Lemmon and Willow Canyon sites (adjusted R ² =0.1625).....	104
Table 3-8. Multiple comparisons between site (Mount Lemmon - MTL and Willow Canyon - WC), morphotype, and interactions by Tukey's HSD.....	105
Table 4-1. Seedlings and source trees from the Santa Catalina Mountains used in the controlled whole-seedling experiment.....	125
Table 4-2. Conditions for hardening, acclimating, and deacclimating PIN_PON and PIN_ARI seedlings for the whole-seedling freezing test.....	126
Table 4-3. Temperature profiles for each of the freezing tests outlined in Table 4-2.....	129
Table 4-4. ANOVA results for dark-acclimated chlorophyll fluorescence (DACF), relative conductivity (RC), and cambial (Camb) and bud (Bud) mortality for PIN_PON and PIN_ARI seedlings exposed to freezing treatments (Tx) during the acclimation phase.....	137
Table 4-5. Cold tolerance (LT ₅₀) of PIN_PON and PIN_ARI estimated as a function of needle dark-acclimated chlorophyll fluorescence (ndl - DACF), needle relative conductivity (ndl - RC), and cambium and bud mortality across three stages of cold acclimation: Hardening, Winter, and Deacclimation.....	144
Table 4-6. Type II tests of ANCOVA for PSII quantum yield (LACF) fitted to morphotype and the covariate air temperature (Temp) for 3-year-old potted seedlings with frozen soil water.....	146

Table 4-7. ANCOVA results for predawn dark-acclimated chlorophyll fluorescence (pDA CF), midday light-acclimated chlorophyll fluorescence (mLACF), predawn (ppsi) and midday (mpsi) xylem pressure potential, and midday net photosynthesis (mphoto) for PIN_PON and PIN_ARI trees at three sites (MTL, PAL, and LIZ) in the Santa Catalina Mountains in January 2006.....	148
Table 4-8. Type II ANOVA results for predawn dark-acclimated chlorophyll fluorescence (pDA CF), midday light-acclimated chlorophyll fluorescence (mLACF), predawn (ppsi) and midday (mpsi) xylem pressure potential, and midday net photosynthesis (mphoto) for PIN_PON and PIN_ARI trees at three sites (MTL, PAL, and LIZ) in the Santa Catalina Mountains in January 2006.....	150
Table 4-9. Mean responses by PIN_PON and PIN_ARI trees by site (MTL, PAL, and LIZ) and across sites (Combined) following removal of three outlying data values.....	152
Table 4-10. Cold tolerance (LT_{50}) of combined PIN_PON and PIN_ARI tissues from this study and from Burr et al. (1990) across three stages of cold acclimation: Hardening, Winter, and Deacclimation.....	153
Table 5-1. Characteristics of 'small' trees used for gas exchange and xylem pressure potential measurements in 2005-06 at the Mount Lemmon (MTL), Palisade Rock (PAL), and Lizard Rock (LIZ) sites.....	166
Table 5-2. Comparison of seasonal xylem water potential (Ψ_p) of combined (both), PIN_PON, and PIN_ARI fascicles harvested at predawn, midday, and evening across an elevational gradient.....	190
Table 5-3. Nested ANOVA results xylem pressure potential (Ψ_p) in needles from PIN_PON and PIN_ARI trees across an elevation gradient, 3 seasons ("Arid" is arid foresummer), and 2-3 daytime periods.....	194
Table 5-4. Univariate ANOVA results for carbon isotope ($\delta^{13}C$), nitrogen isotope ($\delta^{15}N$), carbon (%C), nitrogen (%N), and carbon-to-nitrogen (C:N) content in needles for each year from PIN_PON and PIN_ARI trees at PAL.....	195
Table 5-5. Nested ANOVA results for carbon isotope ($\delta^{13}C$), nitrogen isotope ($\delta^{15}N$), carbon (%C), nitrogen (%N), and carbon-to-nitrogen (C:N) content in needles from PIN_PON and PIN_ARI trees at PAL.....	198

Table 5-6. ANCOVA results for fresh mass loss (p _{mass}) and PSII excitation capture efficiency (F_v'/F_m') of dehydrating needles for PIN_PON and PIN_ARI stems from four sites in the Santa Catalina Mountains: MTL, PAL, RCL, and LIZ.....	203
Table 5-7. ANOVA results for xylem pressure potential at 50% loss of hydraulic conductivity (Ψ_{50}) and xylem specific hydraulic conductivity (K_s) for PIN_PON and PIN_ARI stems collected from three sites in the Santa Catalina Mountains: MTL, PAL, and LIZ/RCL.....	207
Table A-1. Geographic coordinates and mean needle number for trees from the distribution study ("SCAT").....	226
Table A-2. Correlation matrix for mean (1971-2000; PRISM 2006) annual and monthly precipitation (Precip, <i>top</i>), minimum temperature (MinTemp, <i>bottom</i>), and maximum temperature (MaxTemp, <i>next page</i>) for the Santa Catalina Mountain study region.....	241

LIST OF FIGURES

Figure 1-1. Vegetation of the Santa Catalina Mountains as drawn by Whittaker and Niering (1965) from 400 vegetation samples in a gradient analysis.....	18
Figure 2-1. General distribution of ponderosa pine (<i>top</i> , <i>Pinus ponderosa</i> , Thompson et al. 1999), and location of study region in the Santa Catalina Mountains in southeastern Arizona (<i>bottom</i> , USGS 2004).....	32
Figure 2-2. Distribution of sampling points collected during the distribution study ("SCAT") and other projects ("Non-SCAT") in the study region of the Santa Catalina Mountains.....	35
Figure 2-3. Frequency of trees (n=671) by mean needle number per fascicle	47
Figure 2-4. Variability in needle number within a tree as a function of its mean needle number.....	48
Figure 2-5. Mean annual needle number (<i>solid</i> , \pm SD) and sample size (<i>hollow</i>) for the PIN_PON (Δ), Mixed (O), and PIN_ARI (\square) morphotypes (Peloquin 1984).....	48
Figure 2-6. Distribution of occurrences for the three morphotypes in the region using the distribution study ("SCAT") data.....	50
Figure 2-7. Mean number of needles per fascicle as a function of elevation for each morphotype.....	51
Figure 2-8. Distribution of the three morphotypes in climatic space with regard to mean monthly minimum and maximum January temperatures.....	52
Figure 2-9. Distribution of the three morphotypes in climatic space with regard to mean monthly maximum June temperature and monthly July precipitation.....	54
Figure 2-10. Distribution of cumulative probability of suitable habitat for PIN_PON relative to maximum June temperature and annual precipitation in two spatial extents ("polygon" and "rectangle") for Maxent model calibration.....	56

Figure 2-11. Distribution of cumulative probability of suitable habitat for the three morphotypes in the region for the Lit model by Maxent.....	61
Figure 2-12. Distribution of cumulative probability of suitable habitat for the three morphotypes in the region for the Lit.Threshold model by Maxent.....	63
Figure 2-13. Distribution of cumulative probability of suitable habitat for the three morphotypes in the region for the NED.Asp model by Maxent.....	70
Figure 3-1. Prepared seedbed within the predator-exclusion cage at the Willow Canyon site.....	94
Figure 3-2. Predator-exclusion cage after placement over sown seeds at the Willow Canyon site (January 2006).....	94
Figure 3-3. Mean seed germination (<i>top</i>), time to first germination (<i>middle</i>), and elapsed time to the last seed germination (<i>bottom</i>) for the full data set.....	97
Figure 3-4. Germination as a function of stratification treatment for seeds from PIN_PON trees at MTL and PAL.....	98
Figure 3-5. Germination as a function of stratification treatment for seeds from PIN_ARI trees at PAL and RC/LIZ.....	100
Figure 3-6. Germination as a function of stratification treatment for combined morphotypes at the PAL site.....	101
Figure 3-7. Germination of PIN_PON and PIN_ARI seeds planted at high (Mount Lemmon) and low (Willow Canyon) elevation.....	104
Figure 3-8. A proposed path of selection for conditional (secondary) dormancy of seeds produced by Arizona and Southwestern ponderosa pine in the mountain islands of the Southwest experiencing bimodal precipitation patterns.....	113
Figure 4-1. Dark-acclimated chlorophyll fluorescence (<i>left</i>) and relative conductivity (<i>right</i>) for PIN_PON and PIN_ARI after different freezing treatments across three stages of cold acclimation: Hardening (<i>top</i>), Acclimation (<i>middle</i>), and Deacclimation (<i>bottom</i>).....	140
Figure 4-2. Cambial and bud mortality for PIN_PON and PIN_ARI after different freezing treatments across three stages of cold acclimation: Hardening (<i>top</i>), Winter (<i>middle</i>), and Deacclimation (<i>bottom</i>).....	141

Figure 4-3. Linear regression of dark-acclimated chlorophyll fluorescence, relative conductivity, and cambial and bud mortality against treatment temperature for PIN_PON (<i>solid line</i>) and PIN_ARI (<i>dashed line</i>) across three stages of cold acclimation: Hardening (<i>thin line</i>), Winter (<i>normal line</i>), and Deacclimation (<i>thick line</i>).....	142
Figure 4-4. Slope (<i>thin line</i>) and intercept (<i>thick line</i>) for regressions of dark-acclimated chlorophyll fluorescence, relative conductivity, and cambial and bud mortality against treatment temperature for PIN_PON (<i>solid line</i>) and PIN_ARI (<i>dashed line</i>) across weeks of cold acclimation.....	144
Figure 4-5. PSII quantum yield (LACF) as a function of air temperature when measured from 3-year-old potted seedlings with frozen soil water: PIN_PON (<i>solid line</i>), Mixed (<i>dotted line</i>), and PIN_ARI (<i>dashed line</i>).....	146
Figure 4-7. Variable chlorophyll fluorescence (F_v/F_m , solid; F_v'/F_m' , empty) as a function of leaf temperature for PIN_PON and PIN_ARI trees combined across sites in January 2006.....	147
Figure 4-8. Xylem pressure potential (Ψ_p) from excised needles of PIN_PON and PIN_ARI trees at three sites (MTL, PAL, and LIZ) in the Santa Catalina Mountains in January 2006.....	151
Figure 4-9. Midday net photosynthesis (A) results for PIN_PON and PIN_ARI trees at three sites (MTL, PAL, and LIZ) in the Santa Catalina Mountains in January 2006.....	151
Figure 5-1. Diurnal variation in net photosynthetic rate (A) and transpiration (Tr) as a function of incident radiation (PAR) and temperature (T_{leaf}) for paired PIN_PON and PIN_ARI trees at PAL during winter (January 2006).....	181
Figure 5-2. Diurnal variation in net photosynthetic rate (A) and transpiration (Tr) as a function of incident radiation (PAR) and temperature (T_{leaf}) for paired PIN_PON and PIN_ARI trees at PAL during the arid foresummer (June 2005).....	183
Figure 5-3. Diurnal variation in net photosynthetic rate (A) and transpiration (Tr) as a function of incident radiation (PAR) and temperature (T_{leaf}) for paired PIN_PON and PIN_ARI trees at PAL during the monsoon season (August 2005).....	186
Figure 5-4. Diurnal by seasonal needle xylem pressure potential (Ψ_p) for PIN_PON and PIN_ARI trees growing in the Santa Catalina Mountains.....	190

Figure 5-5. Variation (standard deviation, SD) in diurnal needle xylem pressure potential (Ψ_p) by season for PIN_PON and PIN_ARI trees growing in the Santa Catalina Mountains.....	192
Figure 5-6. Needle xylem pressure potential (Ψ_p) by winter (<i>top, left</i>), arid foresummer (<i>bottom</i>), and monsoon (<i>top, right</i>) for PIN_PON and PIN_ARI trees growing along an elevational gradient in the Santa Catalina Mountains.....	193
Figure 5-7. Annual variation in mean carbon ($\delta^{13}\text{C}$, <i>solid lines</i>) and nitrogen ($\delta^{15}\text{N}$, <i>dashed lines</i>) isotope composition for leaf tissue of PIN_PON and PIN_ARI trees at PAL.....	195
Figure 5-8. Annual variation in mean carbon (<i>solid lines</i>) and nitrogen (<i>dashed lines</i>) content for leaf tissue of PIN_PON and PIN_ARI trees at PAL.....	197
Figure 5-9. Carbon isotopic composition ($\delta^{13}\text{C}$) relative to carbon content in needles from PIN_PON (<i>solid line</i>) and PIN_ARI (<i>dashed line</i>) trees at PAL.....	199
Figure 5-10. Carbon isotopic composition ($\delta^{13}\text{C}$) relative to nitrogen content in needles from PIN_PON (<i>solid line</i>) and PIN_ARI (<i>dashed line</i>) trees at PAL.....	199
Figure 5-11. Nitrogen isotopic composition ($\delta^{15}\text{N}$) relative to nitrogen content in needles from PIN_PON (<i>solid line</i>) and PIN_ARI (<i>dashed line</i>) trees at PAL.....	200
Figure 5-12. Nitrogen isotopic composition ($\delta^{15}\text{N}$) relative to carbon-to-nitrogen content (C:N) in needles from PIN_PON (<i>solid line</i>) and PIN_ARI (<i>dashed line</i>) trees at PAL.....	200
Figure 5-13. Dehydration of fascicles for PIN_PON (<i>solid lines</i>) and PIN_ARI (<i>dashed lines</i>) stems from four sites in the Santa Catalina Mountains: MTL, PAL, RCL, and LIZ.....	202
Figure 5-14. Mean dehydration of fascicles for PIN_PON (<i>solid lines</i>) and PIN_ARI (<i>dashed lines</i>) stems across four sites in the Santa Catalina Mountains.....	203
Figure 5-15. Photosynthetic efficiency as a function of needle dehydration for PIN_PON (<i>solid lines</i>) and PIN_ARI (<i>dashed lines</i>) stems from four sites in the Santa Catalina Mountains: MTL, PAL, RCL, and LIZ.....	205

Figure 5-16. Photosynthetic efficiency as a function of needle dehydration for PIN_PON (<i>solid lines</i>) and PIN_ARI (<i>dashed lines</i>) stems across four sites in the Santa Catalina Mountains.....	205
Figure 5-17. Xylem vulnerability curves for PIN_PON (<i>solid lines</i>) and PIN_ARI (<i>dashed lines</i>) stems collected from three sites in the Santa Catalina Mountains: MTL, PAL, and LIZ/RCL.....	207
Figure 5-18. Xylem specific hydraulic conductivity (K_s) for PIN_PON and PIN_ARI stems collected from three sites in the Santa Catalina Mountains: MTL, PAL, and LIZ/RCL.....	208
Figure 5-19. Stomatal openings in PIN_PON (<i>left</i>) and PIN_ARI (<i>right</i>) by SEM.....	211
Figure 5-20. Chloroform-cleared stomatal openings in PIN_ARI of top and transverse views by SEM.....	212

CHAPTER 1

AN INTRODUCTION TO SOUTHWESTERN PONDEROSA PINE, ARIZONA PINE, AND THEIR ENVIRONMENT

From the time of Theophrastus (1916) some 2300 years ago, humans have been fascinated with the distribution and variation of species. Vast human and land resources have been invested in the quest to understand the biogeography of life. This information is invaluable when considering future distributions of species and their responses to global climate change patterns and other anthropogenic influences shaping the biogeography of species. A number of important questions can be posed in this regard. What restricts geographic ranges, and why does a group of organisms vary within its range and yet may be reproductively compatible across the range? How has the heterogeneous environment selected for modified and plastic features? At what point are organisms from two morphologically different populations considered different species? What effect does interspecies gene flow have on the systematics and evolution of the clade? Overall, how have the synergy of geologic processes, climate, and time interacted with ecological and evolutionary processes to produce the diversity of life around us? Finally, how have human interactions affected, or will affect, biodiversity?

The objective of this dissertation is to combine information from geographic range and ecophysiology to understand the distribution of two closely related conifers – Rocky Mountain ponderosa pine (*P. ponderosa* var. *scopulorum* Engelmann) and Arizona pine (*P. arizonica* Engelmann; formerly *P.*

ponderosa var. *arizonica* (Engelmann) Shaw) – in the Santa Catalina Mountains of southern Arizona, USA. Within the isolated mountain islands of the American Southwest, the systematics of the ponderosa pines remains unresolved (Rehfeldt 1993, 1999). Shared ancestry, dynamic climate and topography, strong selection gradients, and hybridization have contributed to the difficulties in classifying populations into species. Focusing on one geographic system – the Santa Catalina Mountains – can elucidate processes occurring across other mountain islands and species. Furthermore, following the devastating Bullock (2002) and Aspen (2003) fires, the Coronado National Forest identified the need for distribution information for improved management of the forest's genetic diversity.

This introduction serves to set the stage for the subsequent chapters on the distribution, ecophysiology, and management implications of Arizona and ponderosa pine in the Santa Catalina Mountains. Following a summary of the putative origin and current status of the systematics of these species, I will describe the geographic system in which my research was conducted. The distribution and ecological modeling of the *Ponderosae* in the Santa Catalina Mountains will be given in Chapter 2, while the ecophysiological studies that shed light on the causes of their distributions will be addressed in Chapters 3-5. Each of these chapters is intended as an individual paper without reference to the other chapters or this introduction. Last, Chapter 6 will summarize the findings and implications of this dissertation.

Origins of Ponderosa Pine

The model species for this research, Arizona and ponderosa pine, are members of the Genus *Pinus*, Subgenus *Pinus* (Diploxylon or Hard Pines), Section *Pinus*, and Subsection *Ponderosae*. Fossil evidence suggests that the common ancestor for this genus emerged in the mid-latitudes of then-contiguous northeastern United States and western Europe during the late Jurassic (Axelrod 1986, Millar 1993). At the time, the unified Laurasia was relatively homogeneous in topography and climate. Tectonic activity was low, sea levels were high, average temperatures were 10-20° C warmer than present in the middle and high latitudes, and seasonality and latitudinal gradients in the Northern Hemisphere were reduced compared to the present (Millar 1993). Subsequently, the newly emerged *Pinus* began spreading east to west (Millar 1993) toward the Western Interior seaway (Baldrige 2004).

By the end of the Cretaceous, Laurasia began to split, the Western Interior seaway began to recede (Baldrige 2004), the Laramide orogeny (tectonism) began creating new topography (e.g., elevation, dry slopes, rain shadows), and the mid-latitudes began to dry leaving the low and high latitudes more humid (Axelrod 1986, Millar 1993). This new geologic and climatic variability created the opportunity for adaptation to new environments (Axelrod and Raven 1985), and, facilitated by symbiotic associations with ectotrophic mycorrhizae, *Pinus* began speciating into the major subsections of the genus by the late Cretaceous (Axelrod 1983). Along with 5 other subsections in *Pinus*, *Ponderosae* likely originated in the Cordilleran region of Colorado south into Mexico (Axelrod 1983).

Following on the heels of the western migration and subsectional speciation of *Pinus* were the newly emerging boreotropical angiosperms in the early Tertiary (Millar 1993). Increasingly warm and humid conditions in the mid-latitudes during the Paleocene favored the more competitive and faster growing angiosperms at the expense of pines (Millar 1993). Consequently, by the early Eocene, widespread extirpation of pines in the lower elevations of the mid-latitudes as well as the first major fragmentation of remaining pines into three refugia are observed in the fossil record (Millar 1993). Some pines most closely allied to *Ponderosae* retreated north to a circumpolar high-latitude zone (65-80° N) where sufficient photosynthesis was still possible due to carbon dioxide levels higher than at present (Millar 1993). Other *Ponderosae* lineages found refugium at high elevation within the mid-latitudes (e.g., Colorado), while other lineages sought the warmer and drier Eocene climate of low latitudes (e.g., Mexico and Central America) (Millar 1993). The fragmentation of subsection *Ponderosae* during the Eocene is thought to be the most significant event leading to the speciation of *Pinus ponderosa* in the north (Axelrod and Raven 1985), with fossil evidence near British Columbia (Axelrod 1986), and other distinct species (possibly *P. arizonica*) to the south, as well as generating new centers of pine diversity (Millar 1993).

At the close of the Eocene, the evolutionary environment changed significantly. Average annual temperatures dropped 10-13° C with decreased summer rainfall and increased seasonality, while mean annual range of temperatures increased from 3-5° to 25° C (Millar 1993). Renewed tectonic

activity produced extensive volcanism and uplift producing the Rocky Mountains and Mexican Sierra Madre Occidental and Oriental (Millar 1993, Baldrige 2004). The complex climatic and geologic changes resulted in widespread extirpation of the boreotropical angiosperms and concomitant expansion of pines back into the mid-latitudes in some places in a few million years by the early Oligocene (Millar 1993). As the climate warmed and summer aridity increased through the Oligocene and into the Miocene (Axelrod and Raven 1985), pines expanded their range and abundance across latitudes, including mountainous low latitudes (Millar 1993). The former refugia served as centers of pine diversity, radiating outward to colonize the diverse environment. With at least a dozen closely related extant species of *Ponderosae* endemic to the refugia in Mexico and Central America, the events of the Eocene can still be seen through active radiation and speciation within *Ponderosae* and other subsections of *Pinus* (Millar 1993). The impact of the Eocene in forcing large latitudinal and environmental shifts in distribution, and thereby dissecting the genus into subsections, significantly contributed to the diversity in *Pinus* observed today (Millar 1993).

Climatic fluctuations following the Oligocene to the present were significantly less than those during the close of the Eocene. For example, the amplitude of average temperatures during the 2.4-million-year Pleistocene (5-10° C) was about the same as climatic cycles during the 20-million-year Eocene (Millar 1993). Pleistocene glacial events caused significant shifts in pine distributions generally from north to south or from high to low elevation. The

alternating distribution expansions and contractions (“pulsing”) allowed gene flow between formerly disjunct taxa followed by isolation over dozens of warming and cooling cycles. Through local adaptation, hybridization, and isolation, the genetic structure of Southwestern flora, including *Pinus*, has changed, or pulsed, over the last 20 million years through the present.

However, a discontinuity exists in the Quaternary fossil record for the presence of *P. ponderosa* in the Southwestern isolated mountain systems, which were generated long before by Eocene-Miocene crustal extension and tectonic uplift (Baldridge 2004). Packrat midden data from van Devender et al. (1984) extending back 40 ka did not show the presence of *P. ponderosa* in New Mexico’s mountains until the last glacial maximum (18 ka), while no such evidence appears in the Great Basin, Colorado Plateau, and current Southwest desert regions for the same period (Thompson and Anderson 2000). Yet pollen from the late Wisconsin (11.4 ka) has been detected in the Sonoran Desert (Martin and Mehringer 1965), perhaps from distant forests (Betancourt et al. 1990). Furthermore, packrat midden data from montane forests in Arizona (van Devender 1990) support the current belief that *P. ponderosa* was present at the end of the Wisconsin (14 ka) but did not extend into the Sonoran Desert nor form continuous cover between mountain systems or the high Colorado Plateau to the north (Betancourt et al. 1990). During some pre-Wisconsin glacial, *P. ponderosa* must have migrated south from the Colorado Plateau and Rocky Mountains. Likewise, *P. arizonica*, with its purported more southern origin, presumably

migrated through the lowland conifers (e.g., subsection *Cembroides*) northward into southern Arizona's mountains during a cooler but more humid glacial.

Systematics of Ponderosa Pine

Due to the inherent complexity of the topography, historical biogeography and evolution, as well as current evolutionary response to Quaternary climate changes (Axelrod 1986), the systematics of subsection *Ponderosae* is challenging and unresolved. In general, species closely related to ponderosa pine have a wide distribution ranging from British Columbia to Montana and south along the Cascade-Sierra Nevada, Rocky Mountains, isolated mountain systems of the Great Basin, Colorado Plateau, and disjunct mountain islands down into the Sierra Madre Occidental and Oriental of Mexico (Conkle and Critchfield 1988). Ponderosa pine is one of the most widely distributed *Pinus* in western North America (Oliver and Ryker 1990).

Of the many classifications of *Pinus*, Shaw (1914, 1924) placed *P. ponderosa* (Douglas ex Lawson) within the Group *Australes*, although currently the more accepted placement is within the subsection *Ponderosae* in the classification by Little and Critchfield (1969). This placement is based on morphologic features and is supported by nuclear and chloroplast phylogenies (Gernandt 2005). In 1880, Engelmann described a Rocky Mountain form (var. *scopulorum*) of *P. ponderosa* as having smaller cones, shorter needles (leaves), and 2-needed fascicles as compared to populations found in Oregon and California (Farjon and Styles 1997). The relatively low (<3%) frequency of 2-

needed fascicles (Haller 1965), significant isozyme differentiation (Conkle and Critchfield 1988), and differential growth response in range-wide provenance tests (Conkle and Critchfield 1988) of the more western populations (var. *ponderosa*) effectively segregate the Rocky Mountain populations. Later, two distinct races of var. *scopulorum* were identified: Rocky Mountain and Southwestern (Conkle and Critchfield 1988). Within var. *scopulorum*, the Southwestern trees produce higher frequency (>85% vs. 15-40%; Haller 1965) of 3-needed fascicles (average 2.7-3.2 needles/fascicle; Peloquin 1984), differential growth responses (e.g, slower early-season growth and double growth flushes; Conkle and Critchfield 1988), and more α -pinene (50% vs. 5%; Smith 1977), a monoterpene found in the xylem resin, compared to the Rocky Mountain race. While the Southwestern race is clearly recognized, the transition to the Rocky Mountain race occurs gradually and broadly over the Great Basin and Colorado Plateau (Haller 1965).

Shaw's (1914, 1924) classification of *P. ponderosa* included *P. arizonica*, *P. engelmannii*, and *P. jeffreyi*, while Little and Critchfield (1969) and The Flora of North America (Kral 1993) considered *P. arizonica* to be a variety (var. *arizonica* Engelmann) of *P. ponderosa*. However, the consensus in this field is that Arizona pine is a distinct species (*P. arizonica* Engelmann) from Southwestern ponderosa pine (Peloquin 1984, Conkle and Critchfield 1988, Price et al. 1998) due to its more southern distribution in isolated mountains of Arizona, New Mexico, and Texas south into Mexico (Farjon and Styles 1997), production of 5-

needled fascicles (4.6-5.4 needles/fascicle; Peloquin 1984), and generation of close to 100% α -pinene with no Δ^3 -carene (Peloquin 1971).

Obfuscating contemporary American classification of the species, authors more familiar with the Mexican *Pinus* redescribed *P. arizonica* with usually fewer needles per fascicle and further classified the species into additional varieties. In Perry (1991), *P. arizonica* occurs in the isolated mountains of southeastern Arizona through the Sierra Madre Occidental, produces 3 (occasionally 4-5) needles per fascicle, and has 6-10 (vs. 2-6 in *P. ponderosa* var. *scopulorum*) needle resin canals. He further describes a *P. arizonica* var. *stormiae* (Martinez) in scattered populations in west Texas and northeast Mexico with similar needle number, longer needles (20-30 cm vs. 12-22 cm), and fewer (3-8) resin canals than *P. arizonica*. Farjon and Styles (1997) split *P. arizonica* into three separate varieties: *arizonica*, *stormiae*, and *cooperi*. The first variety is distributed in southern Arizona and New Mexico through the Sierra Madre Occidental and is characterized by variable needle number (3-4, 5 closer to Sonora) and needle length (10-20 cm) (Farjon and Styles 1997). As by Perry (1991), Farjon and Styles (1997) characterized *P. arizonica* var. *stormiae* with a more eastern distribution, longer (14-25 cm) needles, and longer cones. Finally, although found in Durango and the central Sierra Madre Occidental, *P. arizonica* var. *cooperi* (Blanco) is characterized by producing 5 (4-5) needles per fascicle and shorter (6-10 cm) needles (Farjon and Styles 1997).

The great difficulty in segregating the various morphological variations (morphotypes) within subsection *Ponderosae* is in part due to environmental

clines producing geographic variation within the taxa but also their interfertility. Conkle and Critchfield (1988) summarized results of over 50 years of artificial crossing of *Ponderosae* at the Institute of Forest Genetics in Placerville, California. This work demonstrated moderate (5-40%) crossability of the Pacific race of ponderosa pine (*P. ponderosa* var. *ponderosa*) with the Rocky Mountain race, Arizona pine, Apache pine (*P. engelmannii* Carrière), and other Mexican species in the *Ponderosae*; the Rocky Mountain race of ponderosa pine and Arizona pine were not crossed. Within the Mexican species, crossability was high (>40%) (Conkle and Critchfield 1988). Based on 14 species-specific morphologic and monoterpenoid characteristics, Peloquin (1971, 1984) concluded that Southwestern ponderosa pine, Arizona pine, and Apache pine naturally hybridize in all combinations, including rare three-way hybridization. Like Arizona pine, Apache pine lacks Δ^3 -carene and has 100% α -pinene (Peloquin 1984) but produces 3 relatively long (25-35 cm; Farjon and Styles 1997) needles per fascicle.

Biogeographically, these species tend to be elevationally parapatric with Apache pine replaced by Arizona pine which is then replaced by Southwestern ponderosa pine with increasing elevation (Peloquin 1984). When grown in common gardens, genetically and environmentally controlled characteristics of the three species, as well as putative hybrids produced mostly from Arizona pine and Southwestern ponderosa pine, demonstrate the influence of geographic clines (Rehfeldt 1993). In the Southwestern mountain islands, Rehfeldt et al. (1996) identified a "Taxon X" that combined the three-needed Southwestern

ponderosa pine with trees producing a mixed (3,4, and 5) number of needles within a given year. This hypothetical Taxon X also demonstrates a strong geographic cline (i.e., spatial structure) in needle morphology (Rehfeldt 1999, Epperson et al. 2001) and growth (Rehfeldt 1999), with little spatial structure in allozymes (Epperson et al. 2003). Despite significant spatial autocorrelation, geographic clines do not necessarily signify hybridization but rather environmental influence and/or genetic differentiation. For example, Epperson et al. (unpublished data) have documented significant spatial autocorrelation in chloroplast DNA single-sequence repeats (cpDNA SSRs) from sympatric *Ponderosae* and have identified two unique populations based on cpDNA corresponding to the Arizona pine and Taxon X morphotypes. However, cpDNA is paternally inherited via pollen in *Pinus* (Wagner 1992) and since pollen flow in ponderosa pine is considered unlimited (Latta et al. 1998), this genetic structure could also be interpreted as unidirectional hybridization of Arizona pine by Southwestern ponderosa pine pollen. In Japan, Watano et al. (1995) proposed unidirectional hybridization based on cpDNA haplotype patterns within a putative hybrid transition zone between *Pinus pumila* and *P. parviflora* var. *pentaphylla*. Additionally, comparison of multiple gene markers (Watana et al. 1996, Latta and Mitton 1997, Gugerli et al. 2001, Ribeiro et al. 2002, Burban and Petit 2003), including maternally inherited mitochondrial DNA and biparentally inherited nuclear DNA (Wagner 1992), is required to detect presence and direction of hybridization. For example, in a separate paper, Watano et al. (1996) found unidirectional introgression from mitochondrial DNA haplotype patterns but in an

equal and opposite direction as the cpDNA haplotypes in their earlier paper, thereby concluding that gene exchange through both pollen and seed dispersal contribute to the formation of the hybrid zone in *P. pumila* and *P. parviflora* var. *pentaphylla*. Demonstrated strong interfertility and geographic variation within subsection *Ponderosae*, like other subsections in *Pinus* (Price et al. 1998), indicate that introgression across sympatric populations of *Ponderosae* is possible and still requires more detailed investigation.

The Santa Catalina Mountains of Southern Arizona

The origin of the contemporary topography and geology of the Santa Catalina Mountains began 35 Ma with the final subduction of the Farallon Plate beneath the North American Plate (Baldrige 2004). For 140 Ma, the Farallon Plate had been slipping beneath the North American Plate, thus fueling the extensive Laramide orogeny across the West (Baldrige 2004). By 28 Ma, the trailing end of the Farallon dipped beneath the vast continent thus fueling silicic volcanism from central Mexico through southern Arizona, New Mexico, Texas, and Colorado and forming the Sierra Madre Occidentals and many of the isolated mountain islands of the Southwest (Baldrige 2004). Furthermore, changes in the gravitational potential energy of the lithosphere of the Southwest, due in part to the Pacific Plate grinding against the North American Plate and thinner, more buoyant mantle in the Southwest, generated an extensive force that effectively structured the contemporary Southwest landscape (Baldrige 2004).

This extensional orogeny and deformation process was important in producing mountains and drop fault zones throughout the Southwest, thus forming the Basin and Range province (Baldrige 2004). The Santa Catalina Mountains were formed through one type of orogenic extension known as a metamorphic core complex (Force 1997, Baldrige 2004). As upper-crust non-metamorphic (sedimentary) rock became strained by extension, low-angle shear zones formed above the core complex of middle-crust metamorphic (gneiss; Lucchitta 2001) and plutonic rocks, which were then exposed and forced upward in elevation (Force 1997, Baldrige 2004). As the sheared upper crust thickened along the fault line, it became denser and sank ("gravitational collapse") lower in elevation than the newly exposed metamorphic rock (Baldrige 2004). The Santa Catalina Mountains are particularly complicated compared to other metamorphic core complexes due to multidirectional extension and shearing forces, intrusions, and uplifts (Force 1997). In general, since crustal tension occurred in an east-west direction, linear mountain ranges like the Santa Catalina Mountains formed perpendicular to the strain direction with broad sediment-filled valleys, or basins (i.e., Basin and Range province), separating the ranges (Baldrige 2004).

Roughly triangular in shape and extending over 510 km², the Santa Catalina Mountains rise from a basal elevation of less than 760 m in the Tucson Basin to 2,791 m (9,157 ft) on Mount Lemmon. The WNW – ESE ridgelines are separated by steep escarpments into the smaller forerange on the southwest side and the major Mount Bigelow (2608 m) and Mount Lemmon crest to the

northwest. The Samaniego, Red, and Oracle Ridges extend the crestline to the north. Shallow lithosols characterize the soil in this precipitous environment, with granitic-based soils in the south and a more complex interspersed of soils derived from various granites, argillite, quartzite, schist, andesite, slate, shale, and limestone in the northern 2/3 of the range (Whittaker and Niering 1965, 1968; Force 1997). Soil characteristics in the primarily forested zone (1830-2130 m elevation) show low fertility on diorite and limestone, respectively: bare rock 5-20 and 20-60%; pH 5.5-7.0 and 8.0; organic matter content 4.4 and 5.1%; nitrogen content 0.12 and 0.21%; carbon:nitrogen 20.0 and 14.2; and cation exchange capacity 17.1 and 25.8 m-eq/100 g (Whittaker 1968; Whittaker and Niering 1968). Minimum soil moisture is uniformly low (<5% at 15 cm) below 2000 m in elevation but increases to 28% on north slopes and 9% on south slopes near the peak (Shreve 1915). Haase (1970) likewise found the south to southwest aspects to be significantly more arid during all times of the year, while soil with southern exposure and at lower elevations experience a greater diurnal temperature range (Shreve 1924). Mature drainages with steep sides dissect the slopes and carry water and eroded crustal material downhill to the extensive bajadas of the Tucson and San Pedro Basins.

Because the topographically complex and arid Southwest is geographically close to the Pacific Ocean, Gulf of California, and Gulf of Mexico, as well as located between mid-latitude and subtropical atmospheric circulation regimes, the region experiences a unique bimodal precipitation pattern (see review by Sheppard et al. 2002). A subtropical high-pressure ridge ("Bermuda

High”) advances northward, while the predominant westerlies retreat, and high solar insolation over large upland areas bordered by lowlands generates convection for large amounts of oceanic moisture to move into the Southwest, especially Arizona. Over 60% of the total annual precipitation for the Santa Catalina Mountains falls during this North American monsoon from July through September. Much of this rain falls as intense convective storms with frequent lightning over the mountains in the late afternoon, rushes downslope as flashfloods, and evaporates from the soil surface (personal observation). Most of the remaining moisture falls during the winter months as large cyclonic storms come off the Pacific (Sheppard et al. 2002). These rain events are typically widespread with soaking rains at low elevations and snowfall at high elevations for consecutive days. Climate variability in the Southwest is strongly influenced by the interactions and synergism of the El Niño - Southern Oscillation (ENSO) and Pacific Decadal Oscillation (PDO), which acts to strengthen ENSO effects in positive years and dampen ENSO effects in negative years (Sheppard et al. 2002). For example, years of combined El Niño and positive PDO result in cool and wet winters, while negative PDO enhances the warm and dry winter effects of La Niña years (Sheppard et al. 2002). Over the last century, the Southwest has experienced low-frequency climate variability with periods of abundant moisture (1905-1930), extensive drought (1942-1964), and warm, wet winters with irregular summers since 1976 (Sheppard et al. 2002).

The influence of changing environment with elevation on vegetation patterns in the Santa Catalina Mountains has been reported in classic studies by

several well-known plant ecologists (Shreve 1915, 1922, 1924; Fuller 1916; Whittaker and Niering 1965, 1968, 1975). In the broadest sense, Shreve (1915) described four vegetation types from low to high elevation: desert, encinal (from *encina*, Spanish for evergreen oak, by J.W. Harshberger; Shreve 1915), and forest, which he further divided into pine and fir forests. In the archetypal gradient analysis, Whittaker and Niering (1965) described 9 vegetation types by elevation, aspect, aridity, and topography (i.e., canyons versus slopes) summarized by their diagram in Figure 1-1. Further work by Whittaker and Niering (1968) showed a similar transition from Desert Scrub through pine forest on limestone and granite derived soils with an upward elevational shift in species distributions on the limestone soils probably due to increased bedrock fissuring that drains available moisture, as well as a *Cercocarpus* Scrub zone below the Pine-Oak Woodland.

Whittaker and Niering's (1965) Pine Forest was dominated by ponderosa pine with interspersed western white pine (*Pinus strobiformis*). At high elevation, dense ponderosa pine stands develop and become successional to Douglas-fir (*Pseudotsuga menziesii*) (Peet 1988). Other forest components above dominant ponderosa pine include white fir (*Abies concolor*), subalpine fir (*Abies lasiocarpa*), corkbark fir (*Abies lasiocarpa* var. *arizonica*), and quaking aspen (*Populus tremuloides*) (Whittaker and Niering 1965, Peet 1988). Within mid-elevations, ponderosa pine naturally forms a woodland mosaic of interspersed grassy patches (Peet 1988). Lower in elevation, ponderosa pine is replaced by a more open woodland of encinal (*Quercus* spp.) and pygmy conifer forest

containing Chihuahuan pine (*Pinus chihuahuana*), piñon pine (*P. cembroides*), junipers (*Juniperus* spp.), and Arizona cypress (*Cupressus arizonica*) (Whittaker and Niering 1965, Peet 1988). Stand density and structure of all these forest types are strongly influenced by fire and interannual climate variability (Peet 1988).

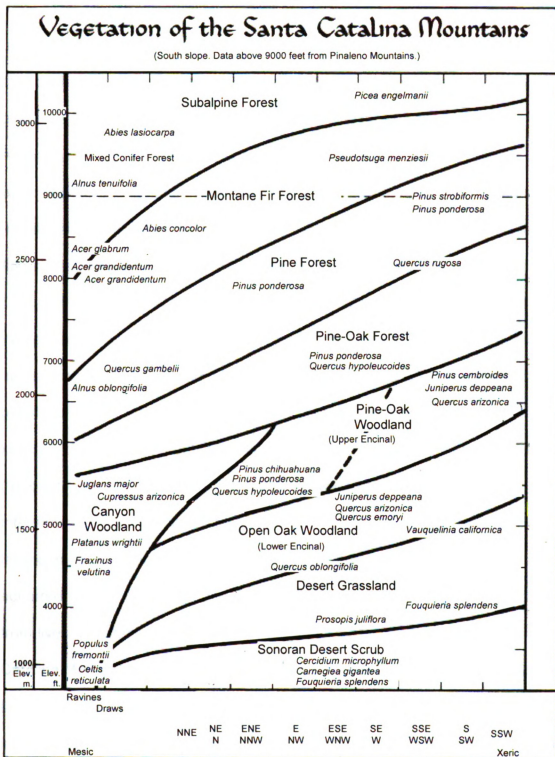


Figure 1-1. Vegetation of the Santa Catalina Mountains as drawn by Whittaker and Niering (1965) from 400 vegetation samples in a gradient analysis. Note that *Pinus arizonica* is not recognized as a species separate from *P. ponderosa* but replaces the latter species between the Pine and Pine-Oak Forests (personal observation). Also note that *Picea engelmannii* does not occur in the Santa Catalina Mountains.

The 19th-20th century changes in fire regime and widespread introduction of grazing by domestic livestock have had a profound effect on the forest structure and composition in the Santa Catalina Mountains. Due in part to a lack of knowledge of pre-European lightning frequency as well as anti-Native American bias, pre-European humans were considered to be the primary driver, while climate and lightning were secondary drivers to the past fire regime in the mountainous regions of the Southwest (Swetnam and Baisan 2003). Based on fire scar records, large fires occurred synchronously about every 7.5 years from 1700-1900 in Southwestern ponderosa pine forests (Swetnam and Baisan 2003). While prehistoric fire frequencies were generally highest during times of greatest human conflict, the understory fuel amount, which takes a few wet years of good growth to accumulate between fires, is strongly associated with large fires in the xeric ponderosa pine forests (Swetnam and Baisan 2003). Domestic livestock ("hoofed locusts;" Muir 1911) introduced in the late 19th century reduced interannual fuel accumulation by grasses and forbs. As a consequence, fire frequency significantly decreased; the last widespread fire of the 20th century occurred in 1900 (Swetnam and Baisan 2003). Due to reduced fire frequency from livestock grazing and organized fire suppression, begun in the Santa Catalina Mountains by the Forest Service during the 1910 Alder Canyon fire (Alexander 1991), stand density of Southwestern ponderosa pine in Arizona increased by several orders of magnitude through the 20th century (Moore et al. 1999). Finally, after close to a century of fire suppression, the Bullock (2002) and

Aspen (2003) Fires burned close to 470 km², or 92% of the Santa Catalina Mountain area (Coronado National Forest 2002, 2003).

Human settlement and use of the Santa Catalina Mountains has certainly had a profound effect on the system. Evidence of the Hohokam living throughout the Santa Catalina Mountains exists from 100 B.C. to 1400 A.D., after which they disappeared (Alexander 1991). Shortly afterward, Apache people occupied the northern foothills and lower slopes during the Summer (Alexander 1991). The earliest Spanish explorer was Francisco Vasquez de Coronado in the 1540s (Alexander 1991), and the 17th century arrival of Spanish settlers in the Santa Cruz Valley distressed the Apaches, whereby they raided settlers and clashed with government armies until the late 1880s (Alexander 1991). There are two stories about the European naming of the mountains: in 1697, Father Eusebio Kino called them the Santa Catarino Mountains; and, in the 1690s, a Jesuit mission in the northern foothills was called Santa Catalina de Cuitabagu, or “well where people gather mesquite beans” (Alexander 1991). The Europeans, though, recognized the potential for mineral wealth in the mountains and began exploring for gold as early as 1871 (Alexander 1991). Homesteading associated with mine claims began in 1880, and businesses to support the mining trade soon sprung up in the mountains (Alexander 1991). The highest point, Mount Lemmon, was named for Sara Plummer Lemmon, who together with botanist John Gill Lemmon and Emerson Oliver Stratton, were the first Europeans to be recognized as reaching the peak (Alexander 1991). During this trip, J.G.

Lemmon first noted the presence of Arizona pine, which he recognized as a variety of ponderosa pine (Alexander 1991).

In 1902, President Theodore Roosevelt established a 100,000-acre (404-km²) forest reserve in the Santa Catalina Mountains and, in 1908, created the Coronado National Forest, which then included the Dragoon, Rincon, Santa Rita, and Whetstone Mountains of southern Arizona (Alexander 1991). Trails to the summit begun in 1897 were improved, fire towers at Lemmon Rock Lookout (1913) and Mount Bigelow (1916) as well as numerous look-out trees aided fire detection efforts, and eventually a road was constructed to the summit (Alexander 1991). The village of Summerhaven, Boy and Girl Scout camps, and Forest Service campgrounds and picnic areas were developed from early camping sites throughout the early 20th century (Alexander 1991). In 1953, several ski runs and a lodge were constructed near the summit, bringing even more tourists to the mountain. The U.S. Air Defense Command established and operated a radar station (Semi-Automatic Ground Environment, 684th Radar Squadron) at the summit from 1959 through 1969 (Radomes, Inc. 2005). In 1962 and 1970, the University of Arizona constructed astrophysical observatories on Mount Bigelow and at the newly abandoned radar station on Mount Lemmon, respectively (Alexander 1991). Following the recent reconstruction of the 28-mile-long paved Catalina Highway, originally completed in 1949 (Alexander 1991), 22,000 vehicles per year of recreationists, homeowners, land managers, contractors, and scientists travel into the Santa Catalina Mountains (PCDOT 2007).

The nature of the Santa Catalina Mountains has changed dramatically over time, none more so than since Europeans began exploring its economic and recreational potential. While the ebb and flow of glacial climates allowed slow intermixing of Rocky Mountain and Madrean species, we are now challenged with understanding the resultant genetic diversity in the face of altered fire regimes, human uses of the mountain resources, and relatively rapid climate change. I embarked on this quest to examine ecophysiological influences on the distribution for one closely related group of species in the *Ponderosae* with the aim of contributing to a better understanding of their distribution, ecology, and genetic diversity, and with important implications for their management.

CHAPTER 2

DISTRIBUTION AND ECOLOGICAL NICHE DIFFERENTIATION OF SYMPATRIC *PONDEROSAE* TAXA IN THE SANTA CATALINA MOUNTAINS OF ARIZONA

Introduction

Phylogeographers are challenged not only with the genetic vagaries of species delimitation, especially with closely related and sympatric taxa, but also the difficulties in delineating the distribution of species. The geographic range of a species is commonly considered to be a spatial manifestation of its ecological niche (Brown and Lomolino 1998). However, one must consider the various interpretations of the niche when discussing the potential distribution of species. Early uses of the term “niche” implied a place in the environment that could support a species, thus the environment held a certain number of niches (Elton 1927). Conversely, Hutchinson (1957) proposed the n -dimensional hypervolume in which a species can persist indefinitely within the boundaries of two measured independent environmental variables and cannot exist outside of those boundaries. This fundamental, or Grinnellian, niche will be considerably larger than its realized niche, or the region between those environmental variables where the species actually exists, due to biotic interactions (Hutchinson 1957). Dispersal, whether limited or extended beyond suitable environmental conditions, can obfuscate the relationship between the geographic range and realized niche (Pulliam 2000). However, beyond the local scale, the geographic distribution of

species is largely influenced by the environment, especially climate (Woodward 1987).

The relationship between the geographic distribution and spatially structured environmental characteristics can be used to investigate the potential distribution and fundamental ecological requirements for a species. Because the influence of biotic interactions varies across a species' geographic distribution, models representing the potential distribution, or suitable habitat (Guisan and Thullier 2005), for a species are arguably more analogous to its fundamental rather than realized niche (Peterson et al. 2002). The amount of research using predictive species distribution models (SDMs) to understand the ecology and evolution of species has exploded over the last 10 years due to advances in computing technology. For example, even with few records of occurrence, the distribution of rare Madagascan geckos were successfully modeled with advanced forms of species distribution models (Pearson et al. 2007), which can then be used to focus search and conservation efforts. From comparisons of occurrences to mean climate values through simple linear and additive models, Vetaas (2002) inferred the relative role of cold versus hot temperatures on the distribution of Himalayan *Rhododendron* species from herbarium specimens and field data. The potential role of competition between closely related South American pocket mice was identified through overlapped predicted distributions as a function of relevant environmental variables (Anderson et al. 2002). Peterson et al. (1999) used reciprocal geographic distributions to demonstrate the role of geographic rather than ecologic isolation during speciation between

sister taxa of butterflies, birds, and mammals in Mexico. Environmental divergence during speciation of Andean frogs was demonstrated with principal components analysis (PCA) of environmental variables determined to be suitable habitat for different species through predictive models (Graham et al. 2004). Using an ecological niche modeling method, Costa et al. (2002) successfully identified four ecologically distinct populations of a major Chagas' disease vector in Brazil resulting in a change in monitoring and control measures. Application of a variety of ecological niche and species distribution models has resulted in advancement in the understanding of species' biogeography, ecology, evolution, and conservation.

An assortment of SDM methods have been developed that can produce successful models using only documented presence localities ("presence-only"). Sources of occurrence data, such as herbaria, museums, and field surveys, do not usually incorporate documentation of absences, especially spatially redundant for rare or cryptic species. Spatial interpolation using explanatory variables of geographic coordinates and neighborhood similarity as measured by abundance is capable of producing comparable models to those using environmental variables in a regression tree algorithm (Bahn and McGill 2007), which demonstrates the predictive value of spatially structured variables. However, most presence-only modeling methods use information about where a species is documented to occur and its associated environmental characteristics to generate a habitat suitability map (Guisan and Thuiller 2005). In these models, pseudo-absences are randomly drawn from the background to evaluate

the model's ability to correctly predict the recorded occurrences for the species. Of course, the modeled species is assumed to be in pseudo-equilibrium with its environment, thus overfitted models may conservatively underestimate the spatial extent of the potential distribution for the species (Guisan and Thuiller 2005). Another major assumption of any SDM is that an appropriate scale, both resolution and extent, is used in the modeling exercise (Maurer 2002, Guisan and Thuiller 2005; but see Guisan et al. 2007). Although each environmental variable will interact with a population at a different scale (Thomas et al. 2002), modeling algorithms usually require constant scale across explanatory variables. Despite these and other assumptions and limitations to SDM (Guisan and Thuiller 2005), the continuing advances in statistical techniques have resulted in great strides in understanding the biogeography of organisms.

The comparison of modeling algorithms, each with means to reduce autocorrelation effects and estimate goodness-of-fit, in a variety of species modeling challenges has been extensive in the literature (e.g, Segurado and Araújo 2004, Guisan and Thuiller 2005, Elith et al. 2006, Tsoar et al. 2007). Some of the more common presence-only algorithms include regression (generalized linear, additive, and multivariate models), bioclimatic envelope, boosted decision trees, artificial neural networks, classification trees, decisions made with genetic rule sets, and maximum entropy (Elith et al. 2006). The latter two methods are drawn from the machine-learning community and are considered to be the most advanced (Elith et al. 2006) at this time. As implemented in GARP (Genetic Algorithm for Rule-Set Prediction,

<http://nhm.ku.edu/desktopgarp/index.html>), the genetic algorithm uses species localities and environmental data to produce a niche-based model using conditional decision rules from a combination of approaches, including atomic, logistic regression, and bioclimatic envelope (Anderson et al. 2002). The maximum entropy algorithm, as employed by Maxent (Maximum Entropy Species Distribution Modeling, Phillips et al. 2006b), calculates a probability distribution of maximum entropy (i.e., closest to uniform) when constrained by incomplete information about the species distribution, which presents itself as species occurrences within pixels across the study area and the associated environmental variables (Phillips et al. 2006). Under the maximum entropy distribution, the expected value (probability) of each pixel is equal to its empirical average from the occurrence data (Phillips et al. 2006). Consequently, Maxent may be conservative by constraining probabilities in the environmental niche space where the species is not known to occur (Pearson et al. 2007).

The *Ponderosae* of the mountain islands in the American Southwest presents an opportunity to employ SDMs to segregate the realized niche of taxa with overlapping distributions by their association with the heterogeneous environment. These wind-pollinated conifers are extensively distributed from central Mexico through British Columbia and throughout the major mountain ranges and foothills (Little and Critchfield 1969). Despite significant outcrossing (>90%; Mitton et al. 1977), the Rocky Mountain ponderosa pine (*Pinus ponderosa* var. *scopulorum* Engelman) experiences significant intrapopulation allozyme variation associated with geographic clines, such as elevation (Hamrick

et al. 1989, Rehfeldt 1990) and slope aspect (Mitton et al. 1977, 1980). Intrapopulation genetic variation of morphological characteristics, such as needles per fascicle, needle length, shoot length, and height:diameter ratio (Rehfeldt 1999), are also associated with geographic clines. Factors varying with geographic clines such as elevation and slope aspect and that seem to influence genetic variation center on length of the frost-free season and patterns of precipitation (Rehfeldt 1990). For example, years with prolonged drought are linked to decreased number of needles per fascicle in the following year (Haller 1965). Ecological response surface models produced by Humphries and Bourgeron (2003) identified maximum January temperature, annual solar radiation, and maximum July temperature as important predictors for presence of mature ponderosa pine in granite-based soils. Limited pollen dispersal (Latta et al. 2001) and limited seed-bearing trees (Linhart and Mitton 1985), in combination with strong environmental selection gradients in mountainous areas (Rehfeldt 1986, 1990), generates considerable genetic and morphologic spatial structure at local scales in ponderosa pine (Epperson et al. 2001). Although less work has been done on the closely related Arizona pine (*P. arizonica* Engelman; formerly *P. ponderosa* var. *arizonica* Engelman) (except see Barton et al. 2001), its mating system and interactions with the environment are expected to produce similar genetic structures.

Due to extensive geographic variation, the systematics of the ponderosa pine and its closely related species in the Southwest's mountain islands has not been resolved (Kral 1993). The Southwestern race (Conkle and Critchfield 1988)

of the Rocky Mountain ponderosa pine reaches its southernmost distribution in these disjunct habitats, while the Sierra Madrean Arizona pine extends northward into southern Arizona, New Mexico, and Texas (Farjon and Styles 1997). Putative hybrids with varying needle number are reported by Peloquin (1971, 1984) to occur where the species distributions come into contact; artificial hybridization between closely related *Ponderosae* has been demonstrated by Conkle and Critchfield (1988). Alternatively, based on allometric, needle, and phenologic properties expressed in a common garden, Rehfeldt (1996) suggests that a nonhybrid "Taxon X," identifiable in the field by producing variable needle number (range 3-5, mean 3.3, standard deviation 0.4; Rehfeldt et al. 1996) in comparison to the mean 3- and 5-needled fascicles of Southwestern ponderosa and Arizona pine, respectively (Peloquin 1984), replaces the commonly identified ponderosa pine of the Southwest. In the Santa Catalina Mountains of southern Arizona, Epperson et al. (2001, 2003) demonstrated a very strong elevational cline in number of needles per fascicle (0.55-0.64% heritable; Rehfeldt 1993) with little differentiation in allozymes across a contact zone between Arizona and Southwestern ponderosa pine. Unpublished work on the same trees by Epperson et al. shows strong spatial structure in chloroplast DNA single-sequence repeats (cpDNA SSRs) with two unique populations with regard to cpDNA heritage: trees corresponding to Arizona pine and the Taxon X morphotype.

The objectives for this paper are to document the geographic distribution and determine if there is any detectable ecological niche differentiation between

the closely related *Ponderosae* taxa in the Santa Catalina Mountains. These taxa form a relatively continuous cover interrupted only by uninhabitable rock from about 1760 m to the summit of Mount Lemmon at 2791 m, depending on aspect and associated changes in forest cover; on the north slope of the peak, ponderosa pine becomes a minor component of a mixed subalpine forest community. Populations producing a mean of 3 needles per fascicle at the summit and on the north slope of Mount Lemmon, 5 needles per fascicle below 2438 m, and 3-5 needles per fascicle with high intratree variance ("Taxon X" of Rehfeldt et al. (1996), or "mixed") between these two elevations have been reported by Dodge (1963) and observed by others (F. Telewski and T. Harlan, personal communication). Following the Bullock (2002) and Aspen (2003) fires, the Coronado National Forest (W. Hart, personal communication) identified a need to recognize the genetic diversity of the *Ponderosae* in the Santa Catalina Mountains and to delineate their distributions for reforestation and conservation efforts.

Given the close genetic relatedness within *Ponderosae*, I expect distributions for all of the taxa to be associated with similar climatic factors, including minimum winter and maximum arid foresummer temperatures, and monsoonal precipitation. However, I expect that the 3- and 5-needled trees should have little overlap in ecological niche space. Under the hybridization hypothesis, the mixed-needled trees should have an intermediate ecological distribution, or niche overlap, and be less sensitive or intermediate in response to relevant climatic factors than the other taxa (Anderson and Stebbins 1954).

Assuming Taxon X (Rehfeldt et al. 1996), the 3- and mixed-needled trees should have the same distribution, occupied niche space, and climatic sensitivity.

Methods

Study area

The Santa Catalina Mountains are located within the Basin and Range Province of the American Southwest (Figure 2-1). These isolated mountains were formed from a metamorphic core complex uplifted as strong crustal extension forces sheared the overlying sedimentary rock (Force 1997, Baldrige 2004). Multidirectional extension, shearing, intrusions, and uplifts have produced a ruggedly complex landscape in this system (Force 1997). The resulting mountainous area is roughly triangular in shape, extends over 510 km², and rises from a basal elevation of less than 760 m in the Tucson Basin to 2,791 m (9,157 ft) on Mount Lemmon. Soils are shallow lithosols derived largely from acidic granites and local outcrops of sedimentary rock (Whittaker and Niering 1965, 1968; Force 1997). Mature drainages with steep sides dissect the slopes and carry water and eroded crustal material downhill.

The semiarid climate is characterized by the Southwestern bimodal precipitation pattern with an arid foresummer (May-June) followed by summer monsoon (Sheppard et al. 2002). Annual precipitation is about 820 mm at Palisade Ranger Station (2426 m elevation) near the observed transition zone between the 3- and 5-needled trees (Western Regional Climate Center 2007), with approximately half falling during the summer (Whittaker and Niering 1965).

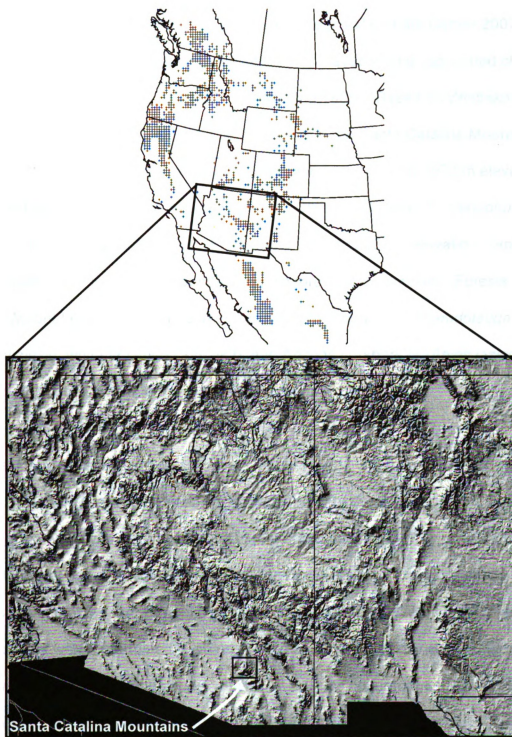


Figure 2-1. General distribution of ponderosa pine (top, *Pinus ponderosa*, Thompson et al. 1999), and location of study region in the Santa Catalina Mountains in southeastern Arizona (bottom, USGS 2004).

The minimum January, maximum June, and annual temperatures at this location are -4, 23, and 15° C, respectively (Western Regional Climate Center 2007).

The vegetation is strongly influenced by elevation and associated changes in climate (Shreve 1915, Whittaker and Niering 1965). Based on Whittaker and Niering's classic study using gradient analysis in the Santa Catalina Mountains, the first "ponderosa pine" trees at low elevation occur around 1500 m elevation mixed with piñon pine, (*Pinus cembroides*), Chihuahuan pine (*P. chihuahuana*), and oak scrub (*Quercus* spp.). From about 1900 to 2500 m elevation, depending on aspect and topography, ponderosa pine forests are dominant. Forests near the Mount Lemmon peak become dominated by Douglas-fir (*Pseudotsuga menziesii*), white fir (*Abies concolor*), and Arizona corkbark fir (*Abies lasiocarpa* var. *arizonica*), with interspersed ponderosa pine

Field data collection

Georeferenced species occurrence (presence-only) and needle samples were derived from several sources. Most of the data (n=671 samples, "SCAT;" data in Appendix, Table A-1) were collected with the intent to examine the spatial distribution of the three morphotypes in the Santa Catalina Mountains. Sampling locations were determined in an arbitrary manner to efficiently capture the spatial variation of these morphotypes. Based on species cover maps (Terri Austin, CNF, personal communication), institutional knowledge (William Hart, CNF, personal communication), and past observations (Frank Telewski, and Thomas Harlan, University of Arizona, personal communication), sampling locations were

located prior to entering the field so as to confirm centers of and transitions in distribution between the three morphotypes. Accessibility was limited to proximity of road and trail due to the rugged terrain, thus some geographical bias was introduced by the sampling methods. At each predetermined location, over 300 geographic positioning system (GPS; GPSMAP 60CS, Garmin International, Inc., Olathe, Kansas, USA) readings were averaged to increase georeferencing accuracy. The point-centered quarter method was used to select the four closest *Ponderosae* trees. This method was used to increase the efficiency of species data per effort in a less subjective manner (Cottam and Curtis 1956) and was employed by Dodge (1963) when examining biogeographic patterns of *Ponderosae* in Arizona. From each tree, diameter at breast height (1.37 m) and distance to the GPS unit were recorded, and 1-4 needle-bearing branches from the most southern accessible side were cut with 23-ft pole pruners and stored in labeled paper bags; the more xeric southern exposure was expected to force variable production of needle number per fascicle, but a subsequent examination by aspect from trees across a transition zone (Epperson et al. 2001) yielded no difference (two-sample t-test, $p > 0.12$, $n = 62$ trees (19713 fascicles)). In some cases, the closest tree had been recently killed by fire (CNF 2002, 2003) or branches were completely inaccessible, so the next closest tree in the quadrant was sampled. Predominant cover type and other notes were also recorded. From August 2004 to October 2006, 671 georeferenced samples were collected from 176 locations (Figure 2-2).

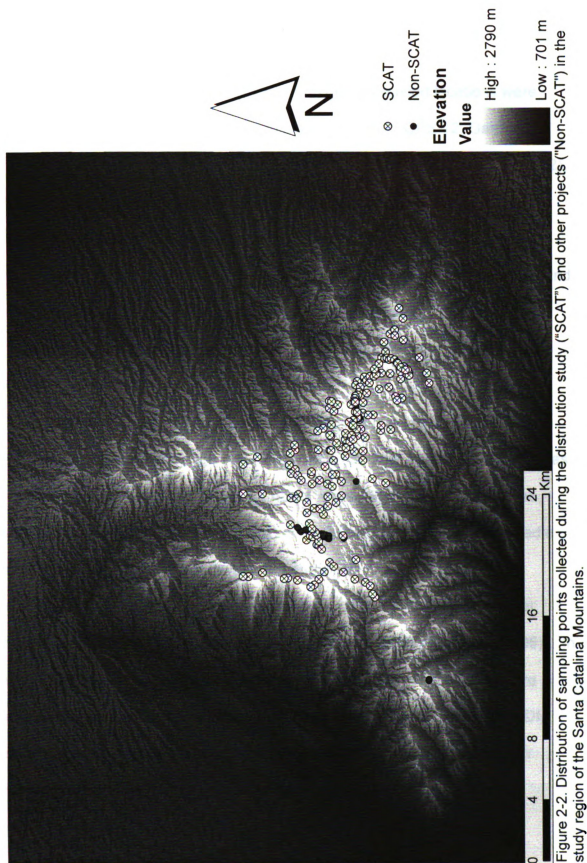


Figure 2-2. Distribution of sampling points collected during the distribution study ("SCAT") and other projects ("Non-SCAT") in the study region of the Santa Catalina Mountains.

Samples were also collected in association with other components of this research program ("Non-SCAT," Figure 2-2). Needles from at least the south side of each tree were similarly collected, and georeferenced locations were recorded by GPS at Kimball Peak Saddle (n=10 in 2001; GPS 12, Garmin International, Inc., Olathe, Kansas, USA), Bear Canyon (n=15 in 2002; GPS 12), Wilderness of Rocks (n=10 in 2002; GPS 12), and Mount Lemmon (n=183 in 2004; GS20 Personal Data Mapper, Leica Geosystems AG, St. Gallen, Switzerland). I identified the coordinates for additional trees (n=23) sampled and intensively studied at Palisade Rock with the aid of field notes and an online mapping program (Google Earth, URL: <http://earth.google.com>, accessed May 2007).

Needles from each sample were examined by year to determine the average needle number for the tree (Epperson et al. 2001). Needle number was calculated both by year and across sampled years. Species, or morphotype, determination was by Peloquin's (1984) classification: trees with mean needle number less than 3.2 are Southwestern ponderosa pine, greater than 4.6 needles per fascicle are Arizona pine, and between 3.2 and 4.6 needles per fascicle are Mixed (hybrids (Peloquin 1984) or Taxon X (Rehfeldt et al. 1996)). In sum, 75,083 fascicles from 671 trees in the distribution study ("SCAT") were individually examined. The species occurrence data files (.csv) used for SDM contained a combination of geographic coordinates (WGS 1984) with either mean needle number or morphotype, depending on the model.

Environmental data

The explanatory variables used in the species distribution modeling were derived from on-line sources. Digital elevation data were downloaded from the National Elevation Dataset ("NED," 1/3 arc-second, or ~10-m resolution; USGS 2004). Annual and monthly average minimum temperature, maximum temperature, and precipitation data (30 arc-second, or 800-m resolution) for 1971-2000 were downloaded from PRISM (2006). The data were projected to a geographic coordinate system using the WGS 1984 datum in ArcCatalog (ESRI 2006). I imported the raster coverages into ArcView (ESRI 2006) as grids, clipped the grids to a rectangular polygon surrounding the Santa Catalina Mountains (32.6181481469°N, -110.984166666°W to -110.564629628°N, 32.2984259247°W) using Hawth's Analysis Tools (Beyer 2006), and then converted the clipped grids into ascii format in ArcCatalog (ESRI 2006). Both NED (USGS 2004) and PRISM (2006) data are globally available and commonly used in the SDM literature.

Modeling algorithm

The SDM software called Maxent (Version 2.3, Phillips et al. 2006b) was the only method selected to focus less on modeling techniques and more on the ecophysiological relevance of the output. Maxent is proven useful in conservation planning, easy to use, freely downloadable from the internet, and successful at predicting species distributions in comparative studies (e.g. Elith et al. 2006), even with small (<25) sample sizes (Hernandez et al. 2006). In

addition, Maxent does not explicitly require absence data, incorporates interactions between variables, minimizes model overfitting through regularization, and produces spatially continuous output for comparative interpretation (Phillips et al. 2006a). Furthermore, model complexity can be controlled by selecting from a combination of linear, quadratic, product, binary, and hinge mathematical functions ("features"). Recommended user-specified parameters included: 30% of the occurrence data set aside for model validation ("testing"); maximum iterations = 500; convergence threshold = 10^{-5} ; regularization multiplier = 1.0; automatically select mathematical features depending on sample size; and remove duplicate occurrences within an environmental pixel, except for comparisons (see Results). The major drawbacks are its use of an exponential distribution, which is inherently unbounded above, and its recent development in terms of fully understanding the implications of regularization, sample size, and spatial extent as well as its performance when extrapolating to environmental features outside the model's calibration (Phillips et al. 2006a).

Model selection

The number of occurrences for a given species affects the predictive potential for any statistical procedure, including SDM. The asymptote of maximum predictive power depends not only on the sample size, or number of occupied pixels across the study region, but also the quality of and heterogeneity within the explanatory variables, the strength and shape of the species response,

and the spatial resolution of the analysis (Hernandez et al. 2006). However, due to the sampling structure, multiple trees for a given species will share a geographic coordinate, thus spatially pseudoreplicating that species' occurrence at that location. In addition, the useful sample size can be reduced due to the resolution of the explanatory variables. Any duplicate occurrences for a species within the 0.64-km² PRISM pixel would also constitute spatial pseudoreplication in the modeling algorithm. Consequently, in the SCAT dataset, the number of occurrences for the 3-needed morphotype decreased from 146 to 31, with similar reductions for the other morphotypes. This sample size should be adequate given machine-learning methods, such as Maxent, correctly predict occurrences around 90% of the asymptote with 10 sample points and near maximum with 50 data points (Stockwell and Peterson 2002).

Most algorithms allow inclusion of multiple environmental variables to use as explanatory variables for species distribution modeling. With extensive data freely available on-line, the modeler is tempted to include as many variables as the algorithm can tolerate to increase the precision and accuracy of predicting the spatial extent and probability of species occurrence within the region of study. However, ecological theory must be part of the model building exercise or else the output will have little relevance or application (Austin 2002). For example, in most models and ecology textbooks, species response to environmental gradients is assumed to be unimodal and symmetric. Unlike earlier algorithms like GLM, Maxent incorporates a number of mathematical functions (e.g., linear,

quadratic, threshold, and hinge) that can be combined into a response to each variable.

The selection of explanatory variables depends in part on the ultimate application or hypotheses to be tested by the model. Conservation biologists interested in parameterizing occupied habitat for projection to potentially suitable habitat elsewhere will likely utilize a larger suite of environmental variables to capture and better transfer the multidimensional niche space for the species with more concern on successful prediction and less concern with the direct physiological implications of the variables. When the objective is to understand more about the environmental constraints on the distribution of a species, fewer but ecophysiological important variables should be used to reduce interaction effects. In addition, decreasing the number of spatially and temporally autocorrelated variables, such as precipitation in July and August ($r=0.92$ for the Santa Catalina Mountains; Appendix, Table A-2), to those representing seasonally important features of the habitat further reduces potentially complex interaction effects.

In this research, physiologically relevant variables representing the amount and pattern of precipitation and temperature (PRISM 2006) were used to parameterize the SDMs because of their demonstrated relation to the distribution of ponderosa pine across the Rocky Mountains of the American West. Daubenmire (1943) showed experimentally that soil drought during the summer is the primary determinant of lower elevation in seedlings, and thus adults, of Rocky Mountain conifers, including ponderosa pine. Although lower elevationally

distributed conifers had a higher tolerance for high summer temperatures, the ability to access moist soil (i.e., rate of root growth) during summer drought was most important (Daubenmire 1943). In California, Haller (1959) showed that lower elevational distribution in ponderosa pine was determined by drought, while the upper limit was determined by cold temperatures. He also noted that occupied elevational bands decrease in elevational range with decreasing latitude due to more rapid altitudinal climb in isohyets than isotherms further south (Haller 1959), thus the effects of summer drought and cold winter temperatures should be less spatially distal in the Santa Catalina Mountains. Independently, Yeaton et al. (1980) showed that summer drought stress limits the ability of ponderosa pine seedlings to grow below their lower elevation distributional limit in the Sierra Nevada; he also demonstrated unimodal mortality along an elevational gradient. Tree-ring data from *P. ponderosa* var. *scopulorum* suggest that summer drought becomes more important with decreasing elevation (Adams and Kolb 2005). At larger spatial scales, Oliver and Ryker (1990) surmised that precipitation in May and June were most associated with ponderosa pine distributions, and Thompson et al. (1999) showed that a combination of annual precipitation, January and July precipitation, and January and July temperature could effectively contain the realized niche for ponderosa pine across the American West. Similarly, Norris et al. (2006) demonstrated the importance of temperature in January and July, as well as growing season precipitation, in characterizing the realized niche space for *P. ponderosa* var. *scopulorum*. Further support for the importance of maximum January and July

temperature, in addition to the overall solar radiation, in predicting presence of ponderosa pine growing on granite in the Southwest is provided by Humphries and Bourgeron (2003).

Consequently, the variables selected for this research in the Santa Catalina Mountains characterize winter cold and summer drought (Table 2-1). Models using variables suggested by the literature ("Lit") focus on the influence of cold temperatures in restricting upper elevational distributions via the mean minimum and maximum January temperature variables (PRISM 2006). The influence of growing season drought, combining warm temperatures and soil moisture, was encapsulated by mean maximum June temperature ("arid foresummer") and mean July precipitation ("monsoon") (PRISM 2006). Models using the full set and various combinations of climatic (PRISM 2006) or topographic (USGS 2004) variables were generated to compare predictive versus physiological tolerance types of output. Topographic variables were not combined with climatic variables due to expected correlation between the variables.

As mentioned earlier, spatial considerations influence the model outcome. For example, the spatial extent of the species' range with regard to the environment can influence the success of the predictive model. Wide-ranging species will be less associated with certain environmental characteristics and thus could result in reduced predictive potential (Stockwell and Peterson 2002). On the other hand, McPherson et al. (2004) conclude that effects of range size may be statistically artifactual. Although *Pinus ponderosa* has a large

geographic range (Little 1971), its horizontal range within the craggy Santa Catalina Mountains relative to the scale of the explanatory variables is considerably smaller.

Table 2-1. Models and environmental variables used in the modeling of species distributions, or suitable habitat (Phillips et al. 2006a), using Maxent (Phillips et al. 2006b). Climate data are either mean annual or monthly normals for 1971-2000 at 800-m resolution (PRISM 2006). Topographic data are 10-m resolution (USGS 2004).

Model	Variables
Full	Annual temperature Minimum January-December temperature Maximum January-December temperature Annual precipitation January- December precipitation
Win.Sum	Minimum December, January, February temperature Maximum June temperature January, February, July, August precipitation
Lit	Minimum January temperature Maximum January, June temperature July precipitation
Lit.Thresh	Minimum January temperature Maximum January, June temperature July precipitation
Lit.Red1	Maximum January, July temperature
Lit.Red2	Maximum January, June temperature
NED.Asp	Elevation Aspect

The extent of the explanatory variables used in training (calibrating) the model has received much less attention in the SDM literature. Restricting the spatial extent of the environmental data to a species' likely habitat reduces the number of "pseudo-absent" background points and thus affects the tails of the response curves (Thuiller et al. 2004). However, higher probabilities are given for the restricted versus complete environmental data range, thus the complete range is more conservative. R. Pearson (personal communication) has stated that the influence of the spatial extent of the explanatory variables on model

outcome for different species is currently attracting much attention by SDM modelers.

Model evaluation

Successful models depend on their objective and two types of statistics – threshold-dependent and -independent – against which competing models can be compared. Similar to the Type I/II error matrix from hypothesis testing, predictive models can be evaluated based on their ability to correctly predict occurrences and absences from real data, whether apportioned from the existing data set (“test data”) or validated against independent data. Sensitivity and specificity are successful positive and negative (absent, or “pseudo-absent”) predictions, respectively (Phillips et al. 2006a). The analogous Type II error is the omission rate which is the fraction of actual observations (by pixel) predicted absent, while the commission index measures the fraction of predicted occurrences where no observation was made (Anderson et al. 2003). A threshold-dependent evaluation includes comparison of the omission rate and proportional predicted suitable area at a particular threshold across the models with a binomial probability calculated to determine if each model is better than random (Phillips et al. 2006a). At an arbitrarily determined cumulative threshold, t , $t\%$ of resampled pixels will have cumulative probability of t or less, or $t\%$ omission of test localities, and some minimum (correctly) predicted background area (Engler et al. 2004, Phillips et al. 2006a). Put another way, to measure one model output's ability to discriminate between occupied and unoccupied sites

against another model's output, a threshold of predicted probability of occurrence must be selected at which sensitivity and specificity will be calculated (Pearce and Ferrier 2000). A higher decision threshold will have lower sensitivity (proportion of correct positive predictions) but higher specificity (proportion of correct negative or absent predictions).

A variety of thresholds can be selected depending on known rarity of the species and the model application (Pearce and Ferrier 2000, Anderson et al. 2003, Liu et al. 2005). To focus on identifying differences in suitable habitat between the taxa in the Santa Catalina Mountains, I will use the "minimum training presence" (Phillips et al. 2006b), or "lowest presence threshold" (Pearson et al. 2007). This conservative approach will identify pixels where the environment (based on the explanatory variables) is at least as suitable as where the species was recorded with zero omission rate (Pearson et al. 2007), and thus will constrain the potentially suitable niche space for each species.

The threshold-independent approach measures model performance by plotting the sensitivity against 1-specificity for all possible thresholds and then calculating the area under the curve (AUC). An AUC value of 1.0 indicates the model (or Maxent distribution) fits randomly selected recorded presences and absences perfectly, while an AUC equal to 0.5 indicates that a random model fits just as well (Phillips et al. 2006a, b). Due to using presence-only data, and thus Maxent generating pseudo-absences, the AUC must remain less than 1.0 (Phillips et al. 2004). The use of AUC on such plots, called receiver operating characteristic (ROC) curves, has a long history in medical research, and its

significance is approximated by the nonparametric Wilcoxon statistic (Hanley and McNeil 1982).

Ecological niche space

Ecological niche differentiation was measured by the ability of one species' model to predict the occurrence of another species. Species occurrences were overlain onto the Maxent output (.asc) for each of the species in ArcView (ESRI 2006), and then Hawth's Analysis Tools (Beyer 2006) was used to identify the output pixel's value (probability) for each occurrence locality. Summary statistics for each combination were calculated in R (R Development Core Team 2007). Visualization of occupied ecological niche space was accomplished by plotting species occurrence points as a function of two-dimensional climate space (Thompson et al. 1999, Norris et al. 2006). The pixel value for the environmental variable on which an occurrence was located was determined as in the previous analysis.

Results

Spatial distribution of morphotypes

The distribution of mean needle number per fascicle across all trees from the distribution study was bimodal (Figure 2-3). Of these 671 trees, 145 (22%) were classified as Southwestern ponderosa pine (PIN_PON), 136 (20%) were classified as mixed-needle (Mixed), 281 (42%) fall into Taxon X (Rehfeldt et al. 1996), and 390 (58%) were classified as Arizona pine (PIN_ARI). Within tree

variability in needle production peaked at a mean needle number around 4.0 (Figure 2-4), but 41 PIN_PON and 35 PIN_ARI trees had zero intratree variance in needle number. Intrannual and interannual variability in needle number was minimal for PIN_PON and PIN_ARI, while Mixed trees had 1.8-5.4 times the intrannual variation as the other morphotypes (Figure 2-5). More needles per fascicle were produced by Mixed trees in 2003 than either in 1999-2002 or 2004-2006 (two-sample *t*-test, $p < 0.01$), and more needles per fascicle were produced in 2003-2006 than in 1999-2002 (two-sample *t*-test, $p < 0.01$).

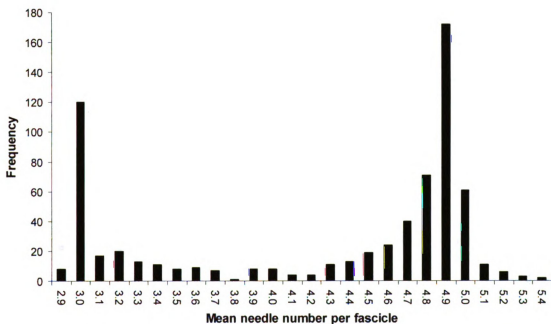


Figure 2-3. Frequency of trees (n=671) by mean needle number per fascicle. Data are from the distribution study ("SCAT").

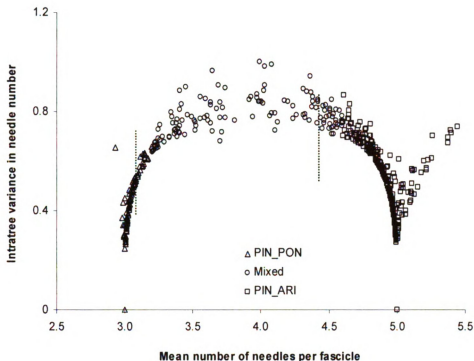


Figure 2-4. Variability in needle number within a tree as a function of its mean needle number. Hashed lines indicate breaks between one morphotype and another (Peloquin 1984). Forty-one PIN_PON and 35 PIN_ARI have no intratree variance. Data are from the distribution study ("SCAT").

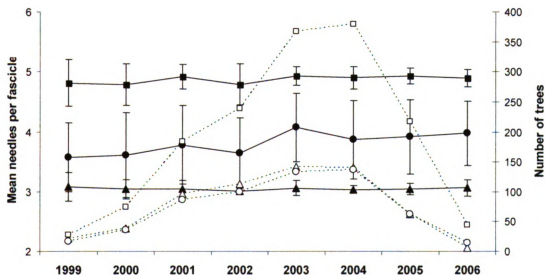


Figure 2-5. Mean annual needle number (solid, \pm SD) and sample size (hollow) for the PIN_PON (Δ), Mixed (\circ), and PIN_ARI (\square) morphotypes (Peloquin 1984). Data are from the distribution study ("SCAT").

The *Ponderosae* morphotypes as described by Pelouquin (1984) have visible differences in their distribution (Figure 2-6). The occurrences of PIN_PON hug the high-elevation ridgelines, with three visible exceptions – Romero Pass in the southwest (n=3 trees, average needle number equal to 3.05, mean elevation 2041 m), Catalina Camp in the north (n=4 trees, average needle number equal to 3.00, elevation 1745 m), and near Lizard Rock in the southeast (n=1 tree, needle number equal to 3.10, 2125 m). These anomalous trees are located either below or at the lowest extent of the local distribution of PIN_ARI, but they are retained in the modeling and analysis, unless noted. In general, PIN_ARI were found along slopes and lower elevation ridges. The spatial distribution of Mixed trees overlapped both of the other taxa. Factors linked with elevation were positively and significantly associated with production of fewer needles per fascicle at high elevation within Mixed, Taxon X, and PIN_ARI, as well as when all occurrences are combined (Figure 2-7, Table 2-2); however, the correlation for PIN_ARI was weak ($R^2=0.04$).

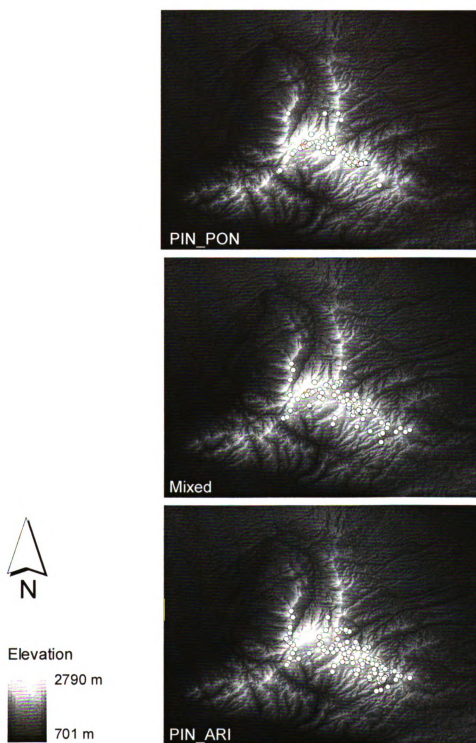


Figure 2-6. Distribution of occurrences for the three morphotypes in the region using the distribution study ("SCAT") data.

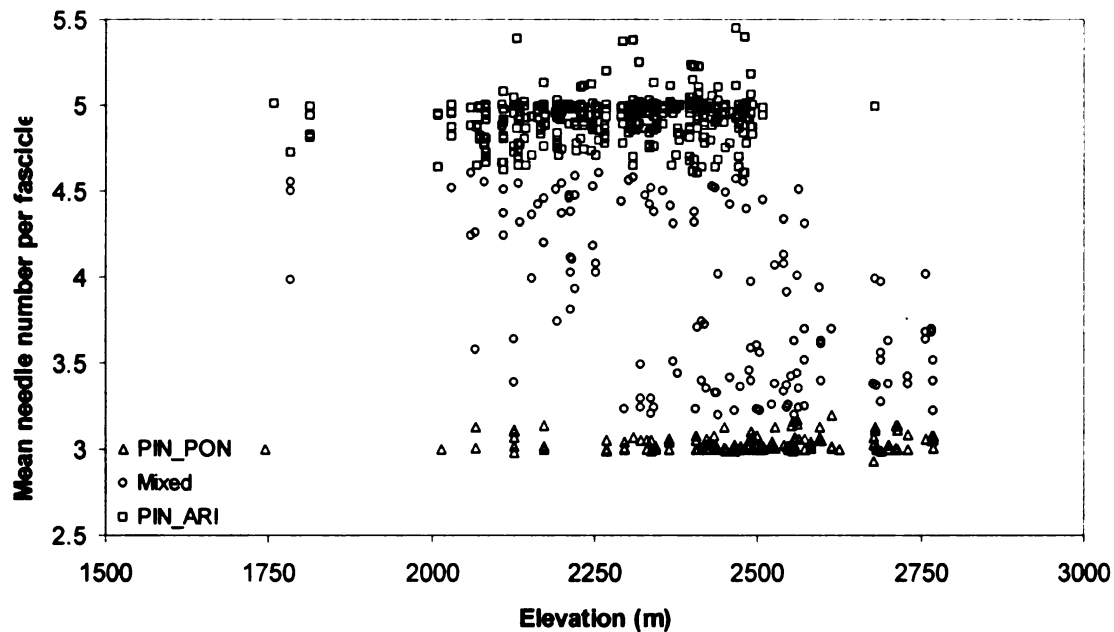


Figure 2-7. Mean number of needles per fascicle as a function of elevation for each morphotype. Data are from the distribution study ("SCAT").

Table 2-2. Summary statistics for regression of mean number of needles per fascicle per tree by morphotype and combined species against elevation at which the tree was located. Data are from the distribution study ("SCAT"). All trees within each sampling plot are included in the regression.

Morphotype	N	Mean Elevation (m)	Stdev Elevation (m)	R ²	P-value
PIN_PON	146	2405.2	214.7	0.02	0.08
Mixed	137	2469.1	207.4	0.26	2.28E-10
Taxon X	283	2438.2	213.0	0.11	1.09E-08
PIN_ARI	388	2286.0	143.7	0.04	1.80E-04
All	671	2350.2	191.5	0.19	7.29E-33

Ecological distribution of morphotypes

The distributions of morphotypes in climatic space show not only the clear overlap among the taxa but also the limiting climatic influences. The three morphotypes occupy the coldest portions of the study region with little apparent differentiation between distributions (Figure 2-8). The warmest monthly minimum

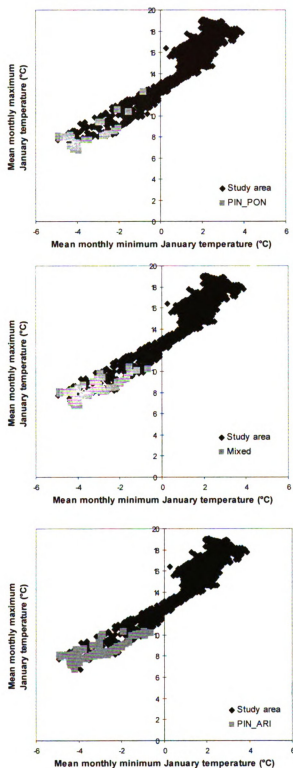


Figure 2-8. Distribution of the three morphotypes in climatic space with regard to mean monthly minimum and maximum January temperatures. Data are from the distribution study ("SCAT").

and maximum January temperatures where Mixed and PIN_ARI were found were -0.6 and 10.4 °C, and -0.6 and 10.3 °C, respectively. If the anomalous 3-needled trees are removed, then the warmest minimum and maximum January temperature where PIN_PON were found were -2.0 and 9.5 °C, respectively; otherwise, these temperatures are -0.8 and 12.3 °C, respectively.

For summer climate space, the three morphotypes were found in the coolest and wettest portions of the study region (Figure 2-9). Excluding the anomalous trees, PIN_PON was located in areas with no warmer maximum June temperature than 26.6 °C, while Mixed and PIN_ARI were found in areas as warm as 28.6 °C. Although overlapping in the wettest areas of the study region, Mixed and PIN_ARI were found in drier areas (down to 89.2 mm of July precipitation) than PIN_PON (down to 96.0 mm of July precipitation). Including the anomalous PIN_PON trees in these bivariate plots suggests that this taxon would occupy a larger climatic niche space than the other taxa.

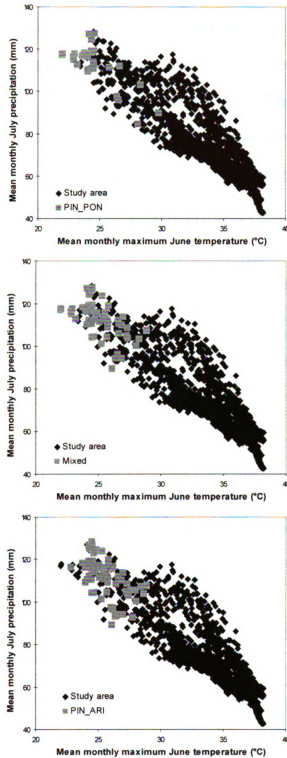


Figure 2-9. Distribution of the three morphotypes in climatic space with regard to mean monthly maximum June temperature and monthly July precipitation. Data are from the distribution study ("SCAT").

Model comparison

The Maxent modeling algorithm does not appear to be sensitive to the spatial extent of calibration (“training”) data (Figure 2-10). The rasters for environmental explanatory variables of maximum June temperature and annual precipitation were clipped in either rectangular or irregular polygon shapes around the Santa Catalina Mountains, in both cases excluding much of the lower elevation desert and foothills from the modeled area. Models were generated for each polygon shape using the PIN_PON data, excluding duplicate occurrences in the same pixel, from the distribution study (“SCAT”). Based on both threshold-dependent and -independent statistics, models generated from the rectangular-shaped environmental data performed better than the polygon-shaped data (Table 2-3). Consequently, all further models were based on environmental data conforming to the former shape.

Table 2-3. Comparison of influence of spatial extent by shape of calibration area on model output. Species data are PIN_PON from SCAT; environmental data are maximum June temperature and annual precipitation. Threshold-dependent statistics are based on the lowest presence threshold as described in the Methods: cumulative threshold (“cum.thr”), fractional predicted area (“fr.prd.ar”), and binomial probability (“*P*-value”). The threshold-independent statistics are based on the area under the receiver operating (ROC) curve (AUC) (see Methods).

Shape	Lowest presence threshold			AUC from test data		
	Cum.thr	Fr.prd.ar	<i>P</i> -value	N	AUC	Std dev
Polygon	3.689	0.198	4.589E-07	9	0.974	0.009
Rectangle	3.656	0.140	3.036E-08	9	0.982	0.006

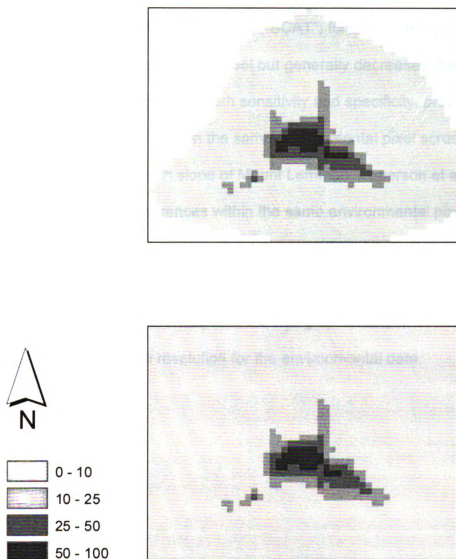


Figure 2-10. Distribution of cumulative probability of suitable habitat for PIN_PON relative to maximum June temperature and annual precipitation in two spatial extents ("polygon" and "rectangle") for Maxent model calibration. Data are from the distribution study ("SCAT").

Fourteen models using the Maxent algorithm were generated for comparison for each morphotype, with all but one model being highly statistically significant (Table 2-4). Incorporating the occurrence data from finer spatial scaled studies with the distribution data ("SCAT") for the modeling often increased the significance of the model but generally decreased the AUC, or ability of the model to maximize both sensitivity and specificity, probably due to increasing the overlap of taxa in the same environmental pixel across steep transition zones (e.g., south slope of Mount Lemmon, Epperson et al. (2001)). Removing duplicate occurrences within the same environmental pixel, or spatial pseudoreplication, generally decreased the model's ability to fit the data but also decreases the likelihood of model overfitting. Understandably, the models with the highest AUC were generated with the topographic data at 10-m resolution, in comparison to the 800-m resolution for the environmental data.

Table 2-4. Performance characteristics and statistics for prediction models generated by Maxent for the rectangular study region. Species names are described in the text. Species data include either all recorded occurrences ("All") within the study region or those collected for the distribution study ("SCAT"). Spatial replication of occurrences within an environmental pixel is either included or removed. Environmental data are described in Table 2-1. Threshold-dependent and -independent statistics are described in Table 2-3. Important variables are those contributing the largest coefficients to the final probability distribution.

Species	PIN_PON	Species data	Remove dupl.?	Environ. data	Lowest presence threshold			AUC from test data			Important variables	
					cum.thr	fr.prd.ar	P-value	n	AUC	Std dev		
		All	N	Full	0.401	0.153	0.00E+00	68	0.993	0.002	MJuneT+ MMayT + MAprT + MJJulyT	
		All	Y	Full	2.878	0.131	1.51E-09	10	0.955	0.013	MJuneT + MMarT + MJJulyT + MAugT	
		SCAT	Y	Full	3.696	0.12	5.22E-09	9	0.979	0.010	MJuneT + mAprT + pptJuly	
		All	Y	Win.Sum	1.893	0.144	3.91E-09	10	0.959	0.013	MJuneT + pptJuly + pptFeb	
		SCAT	Y	Win.Sum	2.592	0.145	2.89E-08	9	0.980	0.009	MJuneT + pptJuly	
		All	N	Lit	1.236	0.131	0.00E+00	68	0.992	0.002	MJuneT	
		All	Y	Lit	1.853	0.145	4.05E-09	10	0.959	0.012	MJuneT + mJanT + MJanT	
		SCAT	N	Lit	4.662	0.089	0.00E+00	43	0.986	0.004	MJuneT + MJanT	
		SCAT	Y	Lit	2.55	0.145	2.89E-08	9	0.980	0.009	MJuneT + MJanT	
		SCAT	Y	Lit.Thresh	0	1	1.00E+00	9	0.974	0.011	MJuneT + MJanT	
		SCAT	Y	Lit.Red1	2.572	0.148	3.47E-08	9	0.980	0.009	MJuliT	
		SCAT	Y	Lit.Red2	2.568	0.145	2.89E-08	9	0.980	0.009	MJunT	
		All	Y	NED.Asp	3.266	0.07	0.00E+00	43	0.987	0.004	NED	
		SCAT	Y	NED.Asp	0.877	0.135	2.83E-17	19	0.990	0.003	NED	

Table 2-4. (Continued)

Species Mixed	Species data	Remove dupl.?	Environ. data	Lowest presence threshold			AUC from test data			Important variables
				cum.thr	fr.prd.ar	P-value	n	AUC	Std dev	
Mixed	All	N	Full	1.821	0.071	0.00E+00	64	0.983	0.003	MJanT + pptMar + MJunT + MMarT
	All	Y	Full	3.686	0.094	3.50E-18	17	0.966	0.006	MJanT + MDecT + mJanT
	SCAT	Y	Full	7.143	0.082	4.56E-18	16	0.968	0.006	MJanT + pptMar+ MDecT + mJunT
	All	Y	Win.Sum	5.867	0.093	4.47E-16	17	0.965	0.007	MJuneT + pptJuly + pptJan
	SCAT	Y	Win.Sum	4.685	0.112	6.23E-16	16	0.976	0.005	MJuneT + pptJan + pptAug + mFebT
	All	N	Lit	1.062	0.1	0.00E+00	64	0.982	0.003	MJanT+ MJuneT
	All	Y	Lit	3.54	0.098	7.14E-18	17	0.964	0.006	MJuneT + MJanT + mJanT
	SCAT	N	Lit	1.516	0.103	0.00E+00	41	0.971	0.004	MJanT + MJuneT
	SCAT	Y	Lit	5.295	0.098	6.71E-17	16	0.975	0.005	MJanT + MJuneT
	SCAT	Y	Lit.Thresh	6.802	0.094	3.42E-17	16	0.976	0.005	MJanT + MJuneT
	SCAT	Y	Lit.Red1	5.619	0.099	7.91E-17	16	0.978	0.005	MJanT
	SCAT	Y	Lit.Red2	5.733	0.098	7.28E-17	16	0.978	0.005	MJanT
	All	Y	NED.Asp	23.883	0.042	0.00E+00	48	0.987	0.002	NED
	SCAT	Y	NED.Asp	2.686	0.115	1.34E-45	26	0.985	0.003	NED
PIN_ARI	All	N	Full	0.275	0.12	0.00E+00	140	0.983	0.002	MJanT + MNovT+ MDecT + mJulyT
	All	Y	Full	7.543	0.074	2.37E-17	22	0.955	0.007	MJanT + MDecT + mFebT + pptJuly
	SCAT	Y	Full	4.97	0.094	2.74E-22	21	0.969	0.006	MJanT + MDecT + pptMar + mFebT
	All	Y	Win.Sum	5.64	0.095	2.89E-23	22	0.956	0.007	MJuneT + mFebT + pptJuly
	SCAT	Y	Win.Sum	5.004	0.108	8.14E-19	21	0.968	0.006	MJuneT + mFebT + pptFeb
	All	N	Lit	1.642	0.09	0.00E+00	140	0.980	0.003	MJanT + MJuneT
	All	Y	Lit	3.057	0.102	3.05E-20	22	0.954	0.007	MJuneT + MJanT + mJanT
	SCAT	N	Lit	0.986	0.091	0.00E+00	116	0.980	0.003	MJanT + MJuneT
	SCAT	Y	Lit	5.411	0.096	3.82E-22	21	0.968	0.006	MJanT + MJuneT
	SCAT	Y	Lit.Thresh	4.72	0.095	6.88E-20	21	0.959	0.009	MJanT + MJuneT
	SCAT	Y	Lit.Red1	6.28	0.096	4.27E-22	21	0.969	0.006	MJanT + MJulyT
	SCAT	Y	Lit.Red2	6.291	0.096	4.27E-22	21	0.969	0.006	MJanT
	All	Y	NED.Asp	1.891	0.129	0.00E+00	59	0.978	0.004	NED
	SCAT	Y	NED.Asp	2.153	0.104	9.90E-62	36	0.971	0.005	NED

Excluding climate-based models with spatial pseudoreplication, the simplest models in terms of number of variables were the most significant and had highest AUC values (Table 2-4). When available in the suite of explanatory variables, maximum June and January temperatures had the highest coefficients and individually contributed most to the models. As the number of variables were reduced, maximum June temperature became the most important for PIN_PON, while maximum January temperature became the most important for Mixed and PIN_ARI. Monsoonal precipitation was consistently less important than maximum June and winter temperatures in predicting suitable habitat for all three morphotypes. Although statistically very close, models using only maximum January and June (or July) temperatures had highest success in correctly predicting the test data.

Two models from each morphotype were more closely analyzed for differences in predicted suitable habitat, or niche differentiation, between the taxa. The Lit model, whose output in Figure 2-11 is shown with large class breaks to highlight coarse patterns, demonstrated marked differences between morphotypes. Suitable habitat (>50% cumulative probability) for PIN_PON was restricted to 1728 ha in the two high-elevation regions within the Santa Catalina Mountains: Mount Lemmon and Mount Bigelow/Kellogg complex. Suitable habitat for PIN_ARI included 3456 ha and was located on the west and south slopes of Mount Lemmon and Mount Bigelow/Kellogg complex, and southeast of Palisade Ranger Station. Suitable habitat for Mixed included 3008 ha, overlapped that for PIN_PON, and overlapped the southeastern portion of

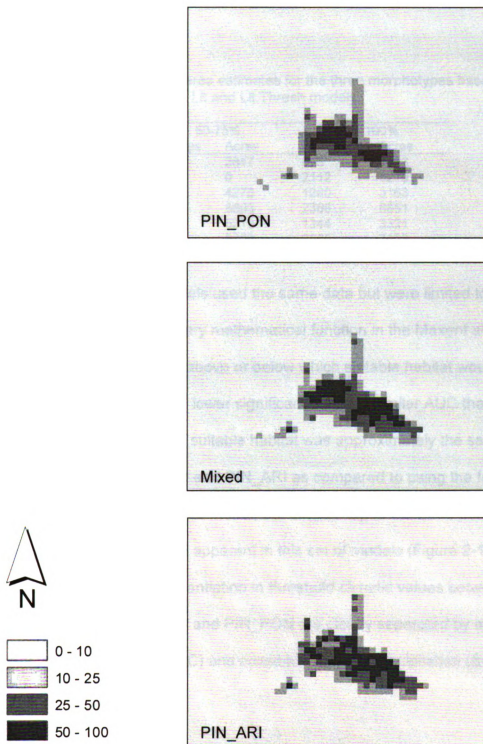


Figure 2-11. Distribution of cumulative probability of suitable habitat for the three morphotypes in the region for the Lit model by Maxent. Data are from the distribution study ("SCAT").

PIN_ARI's predicted distribution. Area estimates for finer class breaks are shown in Table 2-5.

Table 2-5. Climatically suitable area estimates for the three morphotypes based on cumulative probabilities from the Lit and Lit.Thresh models.

Morphotype	Model	50-75%		75-100%	
		Hectares	Acres	Hectares	Acres
PIN_PON	Lit	1152	2847	576	1423
	Lit.Thresh	0	0	2112	5219
Mixed	Lit	1728	4270	1280	3163
	Lit.Thresh	2304	5693	2368	5851
PIN_ARI	Lit	2112	5219	1344	3321
	Lit.Thresh	2816	6958	3008	7433

The second set of models used the same data but were limited to the threshold ("Lit.Thresh") or binary mathematical function in the Maxent algorithm to identify climatic thresholds above or below which suitable habitat would not be predicted. These models had lower significance and/or similar AUC than the Lit models. The spatial extent of suitable habitat was approximately the same for PIN_PON but larger for Mixed and PIN_ARI as compared to using the full suite of mathematical functions in the Lit model, but the overlap of the other taxa's niche space by Mixed is much more apparent in this set of models (Figure 2-12). Although there was little differentiation in threshold climatic values between PIN_ARI and Mixed, the latter and PIN_PON are clearly separated by minimum January temperature ($\Delta=8.1$ °C) and possibly even July precipitation ($\Delta=1.6$ mm) (Table 2-6).

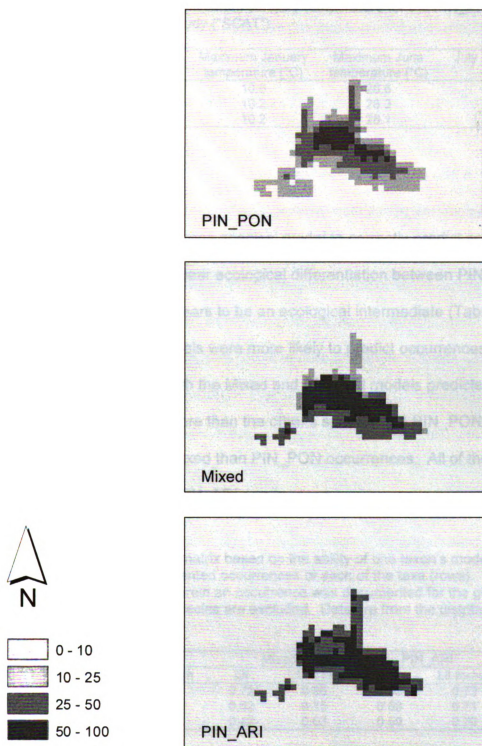


Figure 2-12. Distribution of cumulative probability of suitable habitat for the three morphotypes in the region for the Lit.Threshold model by Maxent. Data are from the distribution study ("SCAT").

Table 2-6. Thresholds for the three morphotypes based on the Lit.Thresh model. No coefficients were generated for minimum January temperature for the PIN_ARI model. Data are from the distribution study ("SCAT").

Morphotype	Minimum January temperature (°C)	Maximum January temperature (°C)	Maximum June temperature (°C)	July precipitation (mm)
PIN_PON	-20.1	10.6	26.6	11.0
Mixed	-12.0	10.2	28.3	9.4
PIN_ARI	n/a	10.2	28.1	9.3

Model prediction

Based on the ability of one species' model to correctly predict occurrences of each of the taxa, there is clear ecological differentiation between PIN_PON and PIN_ARI, but Mixed appears to be an ecological intermediate (Table 2-7). In all cases, the Lit.Thresh models were more likely to predict occurrences than were the Lit models. Although the Mixed and PIN_ARI models predicted their own species' occurrences more than the other's species, the PIN_PON models were more likely to predict Mixed than PIN_PON occurrences. All of the models had similar ability to predict PIN_ARI occurrences.

Table 2-7. Ecological similarity matrix based on the ability of one taxon's model (columns) to predict the documented occurrences of each of the taxa (rows). Values are mean probabilities of pixels wherein an occurrence was documented for the given model; duplicate locations by species are excluded. Data are from the distribution study ("SCAT").

Model	PIN_PON		Mixed		PIN_ARI	
	Lit	Lit.thresh	Lit	Lit.thresh	Lit	Lit.thresh
PIN_PON	0.64	0.80	0.73	0.86	0.53	0.73
Mixed	0.50	0.64	0.62	0.75	0.53	0.71
PIN_ARI	0.33	0.51	0.49	0.63	0.59	0.70

Discussion

The data and analyses presented in this paper give biogeographic and ecological evidence for possible hybridization between the 3-needled Southwestern Rocky Mountain ponderosa pine (PIN_PON) and the 5-needled Arizona pine (PIN_ARI). Close to 90% of the trees sampled in the distribution study produce fascicles intermediate to pure ($s^2=0.0$) PIN_PON and PIN_ARI. While PIN_PON generally occupied a cooler and moister climatic niche, the same bivariate plots showed mixed-needle (Mixed) trees overlapping PIN_ARI. The Maxent models demonstrated the limiting influence of winter temperature on Mixed and PIN_ARI, while PIN_PON was more limited by temperature during the arid foresummer. Furthermore, PIN_PON appears to tolerate areas with an 8° C colder minimum January temperature than the Mixed trees. However, because of the broader distribution for the Mixed trees, suitable habitat predicted for this taxon overlapped the other species. The interpretation for these results must be tempered by a number of factors, including quality of data entering the models, model assumptions and selection, and ecophysiological considerations.

Data quality

The original intent for collecting species occurrence data was to characterize the distribution for the three taxa, and thus a particular subjective sampling strategy was employed. It was understood that their distributions varied across elevation (Dodge 1963, Epperson et al. 2001), but that elevation was not the sole factor determining location for each taxon (Telewski

unpublished data). For example, in March 2000, Telewski (unpublished data) located a tree producing mean 3.02 needles per fascicle at low elevation (~1800 m) near Bear Canyon, while the rest of the trees were mixed and 5-needed. Within my distribution study, I located 8 (“anomalous”) trees that also unexpectedly produced less than mean 3.2 needles per fascicle: Romero Pass, Catalina Camp, and near Lizard Rock. Interestingly, the climate at these lower elevation sites could be moderated by cold-air drainage patterns (Adams 2007): Mule Ears is adjacent to a northerly exposed pass through Samaniego Ridge; Romero Pass is located at the origin to a large canyon draining northwest to Romero Canyon and southeast to Upper Sabino Canyon; Catalina Camp is situated in the valley between two prominent ridges extending north from the main Santa Catalina ridgeline; and the Lizard Rock site is situated in a low-lying pocket with a substantial watercourse. These disjunct PIN_PON trees could simply be remnants of a once larger population at these elevations, surviving but lacking a suitable regeneration niche. The Maxent models included these and potentially other disjunct low-elevation trees, thus interpretations of the observed differences between distributions of the taxa are strengthened.

In retrospect, the sampling strategy did not prove to be efficient for characterizing and modeling the distribution of the taxa. All of the trees to be sampled were selected by various, usually subjective, means. For example, at Palisade Rock, PIN_PON and PIN_ARI were selected as pairs in close proximity for ecophysiological studies. Along the south and north face of Mount Lemmon, as well as for Kimball Peak Saddle, Bear Canyon, and Wilderness of Rocks,

trees were selected either for accessibility, reproductive status, or systematically for spatial analyses (Epperson et al. 2001, 2003). Each of these trees had a unique set of geographic coordinates.

In an effort to maximize efficiency in species data collection, up to four trees per point-location were sampled for the distribution study. These points were located within centers and expected edges (Telewski unpublished data) of each taxon's distribution. At each predetermined point-location, four trees from a point-centered quarter could be represented by one to three taxa, which results in spatial pseudoreplication for this point-location. This error is compounded by the fact that multiple sampling points were located within a given pixel of environmental data, thus removing such duplication due to relatively low resolution of the explanatory variables resulted in drastic reduction of the sample sizes for each taxon in the modeling. For example, including duplicate samples in the modeling consistently increased the predictive performance of the models and likely produced overfitted models. Furthermore, I believe that performance statistics were consistently lower for models using all of the occurrence data (SCAT and non-SCAT), even with larger sample sizes, as compared to just the distribution study data (Table 2-4) because the former includes data from the very steep transition zones of PIN_PON to PIN_ARI on Mount Lemmon (Epperson et al. 2001) and Palisade Rock (Kilgore unpublished data), yet each case occurs within a single environmental pixel. The resultant smaller sample sizes, even with 30% of the occurrences allocated to model verification, are not expected to have had a significant effect on the model output (Stockwell and

Peterson 2002, Engler et al. 2004, and Pearson et al. 2007). Overall, the distribution study data were more dispersed, thus allowing better discrimination between their distributions across the field of environmental data.

Additional bias in the sampling strategies was introduced due to geography and two major disturbance events. The Santa Catalina Mountains are treacherously rugged but have a major paved road to the summit as well as extensive hiking trails. All of the sampled trees were close to primary and secondary roads or hiking trails. With the exception of the Front Range and the north slope of the Mount Bigelow-Kellogg ridge, most of the potential habitat for the three taxa was sampled, relative to the dimensions of the environmental pixels. However, the Bullock Fire (2002) extensively burned the forests on the north slope, while the Aspen Fire (2003) burned through most of the remainder of the forests in the Santa Catalina Mountains, except for the extreme southwest side of the Front Range (CNF 2002, 2003). Consequently, in most areas (especially Samaniego Ridge, north slope of Mount Lemmon, Wilderness of Rocks, Box Camp Ridge, and north of Mount Bigelow), live or dead trees with accessible needles were sometimes difficult or impossible to locate. Distribution data for some of these areas are functionally lost but can be inferred from the habitat suitability models.

The parametric assumption of randomly sampling the entire study region for distribution modeling is unrealistic and unfeasible. Hirzel and Guisan (2002) found that random sampling was the least accurate and robust method as compared to regular and environmentally-informed systematic sampling in

correctly predicting presences of a virtual species. Instead, Araújo and Guisan (2006) argue that a model-based environmental stratification approach be used to direct additional sampling, assuming that the abiotic range of the taxon has been preliminarily sampled. Increasing sampling-effort at the extremes of a range, or tails of the unimodal species response curve, increases the accuracy in estimating species distributions (Mohler 1983). Fortuitously, this was the approach taken for the distribution study, given the limitations of accessibility and living forest. In the case of the Santa Catalina Mountains, the model outputs suggest that sampling effort be focused on the Front Range where suitable habitat for all three morphotypes is predicted (Figures 2-11 and 2-12).

Although the Maxent model output provided additional support to the literature for the limiting influence of summer drought and winter cold on the distribution of ponderosa pine, the relatively large resolution of the environmental data restricted the full use of species data, as explained earlier. As expected, models using the 10-m resolution topographic data produced much finer scaled predictions (Figure 2-13), but a species' association to elevation in the Santa Catalina Mountains is not transferable outside this system (Phillips et al. 2006). Instead, climate constrains the macroscale distribution of species (Woodward 1987), reducing historical contingencies, and associations with climate can be projected to another system. Furthermore, the objective here is to determine if any difference exists between species in their response to limiting climatic factors.

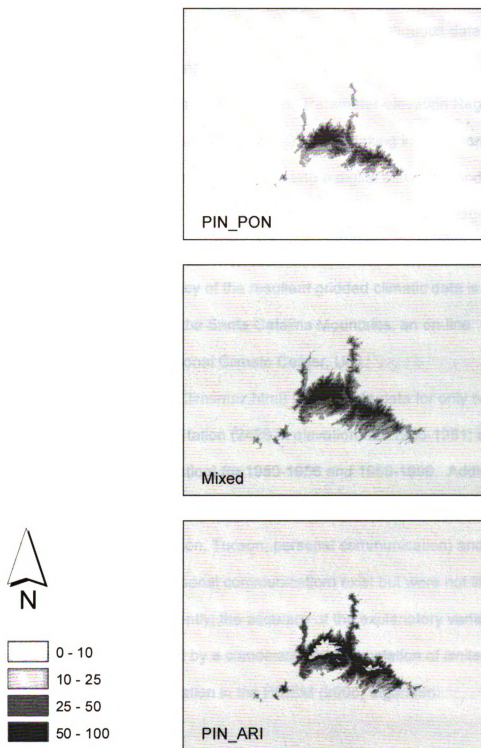


Figure 2-13. Distribution of cumulative probability of suitable habitat for the three morphotypes in the region for the NED.Asp model by Maxent. Data are from the distribution study ("SCAT").

Unfortunately, the highest resolution climatic data available for the study region is 30-arcsec, or 800-m, resolution (PRISM 2006). These continuous data were generated by interpolating climatic data from monitoring stations using an algorithm developed for mountainous terrain: Parameter-elevation Regressions on Independent Slopes Model (PRISM 2006). While taking into account spatial scale and pattern of orographic processes using a digital elevation model (PRISM 2006), which should detect topographically depressed drainageways, the climatic data are scaled up to 800-m resolution and thereby lose much of that information. Also, the accuracy of the resultant gridded climatic data is limited to the actual data collected. In the Santa Catalina Mountains, an on-line clearinghouse (Western Regional Climate Center, URL: www.wrcc.dri.edu/summary/Climsmaz.html) lists climate data for only two locations: Palisade Ranger Station (2426 m elevation) for 1965-1981; and Mount Lemmon (2344-2374 m elevation) for 1950-1956 and 1958-1996. Additional “unofficial” data from Mount Lemmon Ski Valley (A. Corona, National Oceanic and Atmospheric Administration, Tucson, personal communication) and Green Mountain (W. Hart, CNF, personal communication) exist but were not likely used by PRISM (2006). Consequently, the accuracy of the explanatory variables used in the modeling is determined by a combination of interpolation of limited climatic data and orographic extrapolation in the PRISM (2006) algorithm.

Model assumptions and selection

A fundamental assumption of species distribution models (SDMs) is that they accurately approximate the species' ecological niche from known occurrences and their association with particular values of climatic variables. In general, ecological niches are highly conserved, at least since the last glacial maximum (Peterson et al. 1999, Martínez-Meyer and Peterson 2006), so projecting the models to other locations should be informative. The output to such correlative models is a map of potential suitable habitat and, in fact, not potential geographic distribution because the models do not take into account spatially explicit features such as dispersal (Araújo and Guisan 2006). Other factors such as competition, historical contingency, and human fragmentation of populations and habitat can also alter the potential geographic distribution for a species. For example, Brown et al. (1996) suggest that species are limited along a key environmental gradient by abiotic stresses at one extreme and biotic stresses at the other extreme. Vetaas (2002) supported this theory with cold temperatures as an absolute boundary, while a mixture of competition and warm temperature forms the other boundary in Himalayan *Rhododendron* species. However, the Maxent models suggested that primarily warm temperatures during a particularly dry period (arid foresummer) for PIN_PON and cold temperatures during winter for PIN_AR1 explain a sufficient amount of the variability in each taxon's distribution to geographically segregate their distribution based on potential suitable habitat. Consequently, competition between these taxa may occur but does not need to be included in the models to differentiate their

ecological niches. Like PIN_ARI, the upper elevation distribution of the Mixed trees appears to be limited by winter temperatures, but its distribution overlaps both taxa. If the Mixed trees represent hybridization between PIN_PON and PIN_ARI (Peloquin 1984) and if hybrid trees possess “new adaptive systems” as suggested by Anderson and Stebbins (1954), then the Mixed trees in this system may have absorbed adaptive features such as greater cold tolerance from PIN_PON and higher heat tolerance from PIN_ARI. Competition between for limited resources during establishment of these sympatric taxa and their offspring is therefore expected.

Input data can be processed to remove areas where a species cannot occur for one reason or another despite climatic suitability, but, in general, Maxent models approximate Hutchinson’s (1957) realized niche on a coarse climatic scale (Phillips et al. 2006). As a consequence, Maxent and other SDMs will predict suitable habitat larger than a species’ actual distribution (Phillips et al. 2006). Species are often absent from suitable habitat, and vice versa (Pulliam 2000). However, predicting larger potential ranges proves useful in targeting future sampling efforts and identifying potential restoration locations.

A second fundamental assumption of SDMs is that modeled populations or species are in equilibrium with their environment (Guisan and Thuiller 2005). Alternatively, modelers are interested in how distant from equilibrium are current distributions (Araújo and Pearson 2005). Natural dispersal ability, landscape barriers, human fragmentation of habitat, and species interactions are factors that can restrict the ability of a species to track climate change (Davis et al. 1998,

Pearson and Dawson 2003). For example, Leathwick (1998) found that the distribution of disjunct *Nothofagus* species in New Zealand corresponds more to suboptimal habitat due to slow dispersal ability. Due to producing wind-borne pollen and winged seeds, ponderosa pine can disperse relatively long distances (Conkle and Critchfield 1988, Epperson et al. 2001). However, trees greater than 1.5 m in height were selected for the distribution study, which may bias the climatic interpretation of the model output toward conditions present at the time of their establishment rather than current conditions. Ponderosa pine are long-lived trees; for example, most of the trees cored on Green Mountain were around 300 years old, but one dated back to 1460 (Graybill 1986). On the other hand, dendrochronologists usually seek out the oldest trees for extending chronologies, while the nearest tree to the point-center was selected for this study. The trees sampled for the distribution study (n=671, mean diameter at breast height = 34.4 cm, range = 0.9-399.0 cm, standard deviation = 22.4 cm) more likely represent climatic conditions from the last 20-250 years. Given the 2° C rise in mean temperature over the last century in this region (USEPA 1998), which translates to an elevational shift of 267 m (Shreve 1915), focusing on presence and taxonomy of young trees would bring the model predictions closer to equilibrium with current climatic conditions.

The Santa Catalina Mountains present numerous physical challenges to surmount for non-vagile organisms to migrate in response to climate change. The steep canyon walls, xeric southern exposures, and shallow lithosols reduce the ability for seeds to disperse and establish higher in elevation. Conversely,

the deeply etched valleys that bear floodwaters from higher elevations provide mesic refugia, sometimes from fire as well, for trees left behind in the march upward. Since larger surviving individuals produce a disproportionately large number of pistillate cones, these disjunct trees receive pollen from the invading lower elevation pines which produce pollen in all mature age classes (Conkle and Critchfield 1988). Assuming vigorous offspring, the stage for hybridization is prepared in part due to the landscape structure, whose complex topography allows for disequilibrium in distribution at the landscape scale.

Nevertheless, at the available spatial resolution, certain climatic variables consistently gained larger coefficients than other variables across the variety of models for each species. Surprisingly, precipitation variables were always at least secondary in importance to either summer (all taxa) or winter (PIN_ARI and Mixed) temperature. Use and examination of the most parsimonious models (Lit and Lit.Thresh) supported by physiological tolerances indicated in the literature appears to be appropriate for these taxa. Winter temperature was likely not limiting to PIN_PON because little of the study region existed above the upper elevation distribution for this taxon; of the Southwestern mountain islands, only the Pinalenos and Chiricahua Mountains have substantial habitat above the ponderosa pine zone. Because of the bimodal distribution of precipitation in the Southwest, early summer (June) is the most xeric period of the growing season. Spring-germinating seeds are thus quickly exposed to drought conditions, an interaction of high temperature and low soil moisture. Consequently, cold winter temperatures constrain upward migration of Mixed and PIN_ARI and warm

temperatures prevent establishment of PIN_PON at its lower elevation distribution. These hypotheses could easily be tested by establishing climatically monitored common gardens at different elevations (*sensu* Clausen et al. 1940).

Exclusive use of the binary, or threshold, mathematical function (Lit.Thresh model) for detecting differences in cutoffs in species distribution appears to be unique in this study. Physiological tolerance for variation in a climatic variable is not expected to be binary, in fact the response is typically close to unimodal, but forcing the coefficients in the Maxent algorithm into binary mode seems to have allowed quantification of ecological niche differentiation between taxa with overlapping distributions. In this study, suitable (or at least occupied) habitat differed between PIN_PON and the other taxa by -8.1° C in January, -1.5° C in June, and 1.6 mm precipitation in July (Table 2-6), implying that cold temperatures in winter restrict PIN_ARI and Mixed from PIN_PON habitat, and that the warm arid foresummer restricts PIN_PON from growing in PIN_ARI and Mixed habitat. These conclusions are supported by the other models, but now a quantified difference can be related to other studies examining ecophysiological differences between the taxa and incorporated into models examining the effects of climate change on species distribution.

Distribution and ecological differentiation

The spatial distribution of occurrences (Figure 2-6), climatic niche space (Figures 2-8 and 2-9), and predicted suitable habitat maps (Figures 2-11 through 2-13) are all based on a single morphologic character (Peloquin 1984) with high

heritability (~ 0.6 , Rehfeldt et al. 1996): mean needles per fascicle. In addition, elevation (Dodge 1963) and previous year's July-August precipitation (Haller 1965) are correlated to the number of needles per fascicle in trees producing variable numbers of needles. Despite these confounding factors, the separation of distribution and ecological niche space is apparent for those trees classified as PIN_PON and PIN_ARI, even when the intratree variation in mean needle number (Figure 2-4) is relatively high. Ecophysiologic results support the ecological differentiation between PIN_PON and PIN_ARI. Dodge (1963) monitored radial expansion and reported tree-ring characteristics from sympatric PIN_PON and PIN_ARI trees near Mount Bigelow. Although both taxa ceased radial expansion simultaneously, PIN_ARI lagged initiation by 6 weeks yet produced significantly larger ring-widths over time. Furthermore, PIN_PON chronologies had higher autocorrelation (0.65 versus 0.24), and PIN_PON produced twice as many intra-annual rings, which was interpreted to be a genetic expression of adaptation to more consistent precipitation patterns during the growing season typical of the Rocky Mountains (Dodge 1963) or greater sensitivity to drought at the lower edge of its distribution (Fritts 1974). Besides needle number, Pelouquin (1971) also noted significant differences between PIN_PON and PIN_ARI in number of resin canals in the needles and monoterpene ratios from sap. Morphologic, phenologic, and growth responses are clearly differentiated between PIN_PON and PIN_ARI.

The biogeographic and phylogenetic quandary are the trees classified as Mixed, or those producing 3.2 to 4.6 needles per fascicle (Pelouquin 1984).

Dodge (1963) found a needle cline, implying mixed-needle trees, in the Santa Catalina, Rincon, Chiricahua, Huachuca, and Santa Rita Mountains, but not in the nearby Galiuro or Pinaleno Mountains, which had only 3-needled trees. Based on community associations, Lowe (1961) describes the more southern mountains (Chiricahua, Huachuca, and Santa Rita Mountains) as outlying Sierra Madreal systems, while the other more northern mountains are extensions of the Rocky Mountains. Based on the distribution of needle and cone morphologies, Dodge (1963) concluded that the Santa Catalina and Rincon Mountains express the junction of the Rocky Mountain – Sierra Madreal flora more than the other mountains. Consequently, these mountains will have the highest likelihood for populations of Southwestern ponderosa and Arizona pines to interact and produce the needle number cline (Dodge 1963). From monoterpenoid analysis, as well as needle and cone morphologies, Peloquin (1971) concluded that trees producing mixed-needled fascicles, even those sampled below Mount Bigelow, were F_1 and advanced hybrids between Southwestern ponderosa and Arizona pines. Dodge (1963) reported that dendrochronological characteristics for Mixed trees at the Mount Bigelow site were intermediate but more similar to PIN_PON than to PIN_ARI. Furthermore, Conkle and Critchfield (1988) point out the moderate crossability of *Ponderosae*, in general, and especially across species that shared glacial refugia. Supporting Peloquin's (1971) results with a common garden approach, Rehfeldt (1993) concluded that introgression between the *Ponderosae* in southern Arizona is common. However, Rehfeldt partially recanted with the development of a novel Taxon X (Rehfeldt et al. 1996) and

ascribed the geographic cline in needle number to within population genetic variability (Rehfeldt 1999). In the Santa Catalina Mountains, spatial structuring of needle number could indicate hybridization (Epperson et al. 2001), while the lack of allozyme structure and differentiation support either advanced introgression or insufficient time since isolation for differentiation to have occurred (Epperson et al. 2003). Unpublished cpDNA data (Epperson et al.) indicate either unidirectional cytoplasmic hybridization (Watano et al. 1995) between Arizona and Southwestern ponderosa pines or genetic barriers to unlimited pollen flow between Arizona pine and Taxon X.

The hybridization hypothesis is supported by the results of this study. Despite arbitrary divisions between continuous needle numbers, the spatial extent of predicted suitable habitat for Mixed trees was similar at high elevation but visibly extended lower in elevation than suitable habitat for PIN_PON (Figures 2-11 through 2-13). Although Rehfeldt (1999) aligned the Mixed trees with PIN_PON, they in fact appear to be more climatically associated with PIN_ARI than PIN_PON (Table 2-6). Therefore, PIN_PON and Mixed do not share climatic tolerances, despite their sympatry. Given the results of prior work with these taxa (Dodge 1963, Peloquin 1971, Conkle and Critchfield 1988, Rehfeldt 1993, and Epperson et al. 2001), as well as similar patterns of hybridization in other *Pinus* (e.g., Watano et al. 1996), and the biogeographic evidence provided in this study, I deduce that the Mixed trees represent hybridization between PIN_PON and PIN_ARI (*sensu* Anderson and Stebbins 1954). Modeling the spatial variability of characteristics distinguishing PIN_PON

and PIN_ARI, such as monoterpenoid ratios and genetic markers (e.g., cp/mt/nuclear DNA), would lead to greater understanding of the historical progression of migration and putative introgression of the *Ponderosae* in the Santa Catalina Mountains.

Projection

A natural extension of SDMs is to spatially or temporally project the habitat, or climate, suitability model derived for each species (Guisan and Thuiller 2005, Hijmans and Graham 2006). Spatial projection to other mountain islands in the Southwest would identify areas to sample for not only validating the model but also conservation purposes. Although the Galiuro and Pinaleno Mountains are close to the Santa Catalina Mountains, Dodge (1963) did not find any PIN_ARI despite seemingly suitable habitat. Projection of the models derived in the Santa Catalina Mountains to these other systems can identify climatically limiting conditions and contribute to the understanding of biogeographic patterns. Conversely, such projection would highlight the importance of other factors, such as historical contingency in the lack of migration during the last glacial maximum to these systems from the Sierra Madrean PIN_ARI. Projecting to a geographically proximal and climatically similar but independent location could improve the model through validation and subsequent fine-tuning of variable selection and parameterization. This process could also be used to assess the ability of the model to project to different climate scenarios (Guisan and Thuiller 2005). In both cases, biotic interactions may differ and thus the projected

“realized niche” may vary depending on the parameterization of the original model. Since these models do not currently incorporate spatially explicit processes like dispersal, their output is potential suitable habitat, not potential geographic distribution. However, in comparison to a mechanistic model and other niche modeling algorithms, Maxent consistently performs well in predicting current, past, and future ranges in response to climate change (Hijmans and Graham 2006). Such an approach would be useful in predicting the potential response by taxa isolated on mountain islands to climate change, as well as identifying potential habitat for climatically induced plant migration.

CHAPTER 3

INFLUENCE OF SEED GERMINATION ECOLOGY ON THE DISTRIBUTION OF *PONDEROSAE* IN THE SANTA CATALINA MOUNTAINS OF ARIZONA

Introduction

The realized distribution for any species is determined by the establishment of seedlings, thus germination and survival through establishment are critical life history stages (Bazzaz 1979). Steep environmental gradients, such as those found in montane systems, present particular challenges for seeds dispersed beyond a relatively narrow bioclimatic window. At higher elevation, seeds are faced with more mesic conditions, such as colder air and soil temperatures, higher litter depth, higher soil moisture, and lower light due to shading from the more productive canopy (Whittaker and Niering 1975, Barton 1993). Seeds dispersed below the current range are faced with more xeric conditions than those of its seed-producing parent. In addition, biotic interactions, such as competition from shallow-rooted forbs, and disturbance regime (e.g., fire frequency) different from a seed-tree's locally adapted habitat could affect eventual establishment. On the contrary, dispersal and establishment outside of a species' current distribution could suggest that the species is not in equilibrium with its environment. However, due to restricted species niches in mountains, potential species migration here is sensitive to variations and change in climate (Tranquillini 1979), and thus the germination ecology for a species will influence the outcome of potential species migration.

Most montane tree seeds exhibit some sort of physiological dormancy, likely selected to avoid germination at a time with unfavorable environmental conditions for seedling establishment (Baskin and Baskin 1998). This dormancy is normally manifested as a chilling requirement, or cold stratification, before seed germination occurs. In some cases, such as the Carices (Schutze and Rave 1999), germination occurs regardless of stratification but is higher with colder stratification. Given that most seeds mature and disperse by the end of a growing season (Young and Young 1992, Baskin and Baskin 1998), a chilling requirement in cold, or higher elevation, conditions should increase the likelihood of seedling establishment in the subsequent growing season(s). Even after a year's growth, though, disruption of the delicate root system of the seedling through frost-heaving can lead to high mortality (Heidmann 1987).

The timing of germination during the growing season relative to local climate conditions, as well as irregular disturbances such as fire or logging, can also influence germination and establishment. For example, Larson (1961, as referenced by Howard 2003b) noted that Southwestern ponderosa pine seedling mortality is highest in regions with a bimodal precipitation pattern, which is characterized by winter precipitation, an arid foresummer drought (May-June), summer monsoon precipitation (July-August), and a moderate fall drought (Sheppard et al. 2002). Barton (1993) showed that the early summer drought limits pine seedling establishment lower in elevation, as higher elevation species germinated but did not survive the first year. In contrast, lower elevation pines germinated and survived for at least two years above their distributional limit

(Barton 1993). The fall drought also affects ponderosa pine seedling mortality (Jones 1967, Larson and Schubert 1970, cited in Howard 2003b). In Arizona, Schmid and Mitchell (1986, cited in Howard 2003b) measured highest first-year survivorship (13-19%) by seedlings that germinated during the early part of the monsoon, with lower (2-7%) survivorship by those germinating later in August. Like the climatic niche, the temporal window for germination and successful establishment confines opportunities for species migration.

The closely related *Ponderosae* are roughly segregated, but sympatric in places, by elevation and factors contributing to more or less xeric conditions in the Santa Catalina Mountains of southern Arizona. Southwestern ponderosa pine (*Pinus ponderosa* var. *scopulorum* Engelmännii) co-occurs with Arizona corkbark fir (*Abies lasiocarpa* var. *arizonica*) at high elevation (>2650 m) and with Douglas-fir (*Pseudotsuga menziesii* Franco) and Southwestern white pine (*Pinus strobiformis*) throughout most of its elevational distribution (Whittaker and Niering 1965). At its steep (Epperson et al. 2001) xeric boundary (~2430-2530 m elevation), Southwestern ponderosa pine ("PIN_PON") transitions to Arizona pine (*Pinus arizonica* Engelmännii), which extends down to ~1760 m elevation. This narrow boundary suggests that abiotic conditions may be limiting the upward migration of Arizona pine ("PIN_ARI") and downward migration of PIN_PON. Since prechilling is required to germinate stored (i.e., over-wintered) seed from PIN_PON, but notably not PIN_ARI (Krugman and Jenkinson 1974), the lack of cold conditions at low elevation could also prevent germination of PIN_PON seeds. Further, putative hybrids ("Mixed") between PIN_PON and PIN_ARI have

been reported throughout the range of both species as producing an intermediate number of needles per fascicle (Dodge 1963, Peloquin 1984, Rehfeldt et al. 1996, Epperson et al. 2001). If a product of hybridization, then the ability of this morphotype to overcome the lower and upper elevational barriers experienced by the other taxa (Kilgore, unpublished data) suggests that differences in germination ecophysiology that may exist between the parental taxa may have been reduced through hybridization.

The principal aim for this study is to determine if there is a genetic difference in seed germinability and response to stratification by PIN_PON and PIN_ARI, and to relate these expected differences to potential species migration beyond current distributions. Given the close genetic relatedness of these taxa, little difference in total germination is expected. Although prechilling is not necessary for PIN_ARI seed (Young and Young 1992), stratification is expected to increase germination rate of seeds from both taxa (Baskin and Baskin 1998). Further, if lower elevation conifers can establish at high elevation, but not conversely (Barton 1993), then PIN_ARI germinants should have high survivorship at high elevation, and PIN_PON germinants should have relatively low survivorship at low elevation.

Methods

Seeds used in these experiments were collected from mature trees in the Santa Catalina Mountains in September-October 2005. In general, PIN_PON cones mature and seeds disperse in August-September, while PIN_ARI cone

ripening and seed dispersal are delayed by a month (Krugman and Jenkinson 1974). The PIN_PON trees near the summit of Mount Lemmon have been studied for needle number production for at least 10 years and are part of a larger research program (Epperson et al. 2001, 2003). Cones from PIN_ARI were collected from Rose Canyon, an area previously considered to be composed of "pure" 5-needled trees (F. Telewski, personal communication). The site effect will be reduced by collecting seed from all three morphotypes at a transition zone near Palisade Rock; at least maternal genetic contribution will be determined by known morphotype. Annual variability in seed lots will be controlled by using seed from one cone production year.

With the aid of a 23-ft pole-pruner, branches containing abundant needles and multiple ripe cones were harvested from the mid- to upper-crown of each tree. Even for trees of known species, needles were counted to determine species designation (Peloquin 1984, Epperson et al. 2001). Cones were air-dried at room temperature in paper bags, and seeds were removed from the cones by shaking and removing cone bracts in early January 2006. Unopened cones were heated 14-27 h at 40° C to encourage opening (Young and Young 1992). Empty, parasitized, or otherwise unhealthy appearing seeds were discarded, while whole seeds were dewinged by hand, inventoried (Table 3-1), and stored in labeled small manila envelopes at room temperature.

Cold stratification experiment

The controlled seed germination test as a function of cold stratification treatments was conducted in the laboratory at Michigan State University. The experimental design was a factorial with three sites, three taxa, and three stratification periods (0, 15, and 30 days). For each stratification period, an equal number ($n=115$) of seeds from 3-8 trees from each site and needle type were selected based on number of trees and seeds available (Table 3-1).

Table 3-1. Seeds inventoried from cones collected from the Santa Catalina Mountains in September-October 2005. Site refers to south slope of Mount Lemmon (MTL), south slope between Palisade Rock and Mount Bigelow (PAL), northeast of Lizard Rock (LIZ), and entrance drive to Rose Canyon Lake (RC). Morphotype refers to producing mean 3- (PIN_PON), mixed, or 5-needed (PIN_ARI) fascicles (Peloquin 1984). Tree refers to specific tree sampled as part of other research or specifically for this experiment. The first number in the last column refers to the number of seeds used from each tree per cold stratification treatment, while a second number refers to seeds used in the reciprocal transplant experiment (see Methods).

Site	Morphotype	Tree	Number of seeds	Number of seeds per treatment
MTL	PIN_PON	MTL 9	296	15 / 20
		MTL 5	388	15 / 20
		MTL 24	800	15 / 20
		MTL 23	722	15 / 20
		MTL 15	31	10
		MTL 132	458	15 / 20
		MTL 11	2388	15 / 20
		MTL 104	282	15
		MTL 1.5m behind junction	911	0
		MTL junction of MTL+MeadowTrail	481	0
		MTL 9.2m@280° from MTL 104	554	0
		MTL 20m@210° from 60"dome	360	0
		MTL 23m@330° from RadioTowerFence	299	0
PAL	PIN_PON	PAL 1	133	41
		PAL 41	53	17
		PAL 3	62	20
		PAL 12	74	24
		PAL 40	40	13
PAL	Mixed	PAL 28	270	87
		PAL 32	48	16
		PAL 30	36	12
PAL	PIN_ARI	PAL 14	332	30 / 20
		PAL 2	104	30 / 10
		PAL 10	366	32 / 20
		PAL 16	71	23
		PAL 49	11	0 / 10
RC	PIN_ARI	RC PINARI GroupPicnic 29.5cm dbh	214	37 / 20
		RC Tree#15	28	0 / 20
		RC Tree#16	n/a	0 / 20
LIZ	PIN_ARI	LIZ 1	43	14
		LIZ 3	17	5
		LIZ PINARI 10cm dbh	3	0
		LIZ PINARI 353° from LIZ 2	71	23
		LIZ PINARI 61.5cm dbh	155	36
		LIZ PINARI	5	0

Seed handling and stratification methods for ponderosa pine vary widely in the literature (e.g., Stefferud 1961, Smith 1986, Weber and Sorensen 1990,

Young and Young 1992, Evans et al. 2001, Wenny and Dumroese 2001, Dreesen 2003), while little is published on germination characteristics for Arizona pine (except see Young and Young 1992). In general, seeds are rinsed with a fungicide, soaked for some period of time to induce imbibition and reduce germination inhibitors (Evans et al. 2001), placed into media or plastic bag, and stored (2-8 wk) at a constant cool temperature (0-5° C). Smith (1986) reported no effect of pregermination fungicides on germination success of ponderosa pine seeds. A contract grower for the Coronado National Forest and Trees for Mount Lemmon stores ("cold stratifies") ponderosa pine seeds from southern Arizona at 1-2° C for variable lengths of time, rinses the seeds with 10% bleach solution for 5 minutes before rinsing and soaking the seeds for 12-24 h, and then immediately plants seeds into soil with ~85% germination success (B. Blake, Northern Arizona University, personal communication).

The seed handling methods used in this paper combine elements from the literature, especially Weber and Sorensen (1990), with practices in use by CNF growers. In mid-January 2006, seeds from each tree by stratification treatment (see Table 3-1) were placed into a perforated and labeled 4-mL Whirl-Pak Write-On Bag (Nasco, Fort Atkinson, Wisconsin, USA); perforation of the plastic bag walls was accomplished with a wallpaper removing tool to allow water and air infiltration to the seeds. Approximately 25 h before each stratification treatment, or sowing for the no stratification treatment, the seeds were surface-sterilized in 10% bleach solution for 30 min, rinsed with distilled water, and soaked in a running distilled water bath at room temperature for 24 h. The seeds were air-

dried on individually labeled paper towels, while the bags were oven-dried at 40° C. The dry seeds were returned to their appropriate bags, which were pooled into a 1-gal Zip-Loc (SC Johnson, Racine, WI, USA) bag containing 1 L perlite moistened by 200 mL distilled water. The Zip-Loc bag containing the Whirl-Pak bags of seeds was stored in a standard refrigerator kept at 2-4° C. Each stratification treatment was temporally staggered so that all seeds would begin incubation at the same time; the seeds for the 0- and 15-day treatments were stored in Whirl-Pak bags at room temperature before surface sterilization.

In mid-February 2006, stratified seeds were removed from refrigeration, and the no-stratification seeds were surface sterilized in preparation for incubation and germination; no seeds germinated prior to sowing. Following Weber and Sorensen (1990), seeds from each Whirl-Pak bag were sown into polystyrene Petri plates (100mm Not TC-Treated Culture Dish, Product #430591, Corning Life Sciences, Corning, NY, USA) containing 15 mL fine (#4) vermiculite saturated with 13 mL deionized (DI) distilled water (NANOpure ultrapure water system, Model D4741, Barnstead International, Dubuque, IA, USA) and covered by a 90-mm round filter paper (Whatman Grade 1; Whatman, Inc., Florham Park, New Jersey, USA). Appropriately labeled lids allow gas exchange by design. The plates containing seeds were randomly arranged within an aerated growth chamber (Model E-15, Environmental Growth Chambers, Chagrin Falls, OH, USA) and kept in the dark at 20° C; Li et al. (1994) report no effect of light on germination of stratified ponderosa pine seed. DI water was added to plates as

necessary to maintain moist (but not saturated) filter papers, and plates were regularly shifted in the growth chamber to avoid chamber effects.

Germinated seeds were assessed more frequently (e.g., twice daily) early in the experiment and then at least daily as the number of new germinants curtailed. Germination was counted when the radicle reached ~1 mm in length (Weber and Sorensen 1990). Seeds covered by fungi were not removed because many of them germinated even when infected. As temporally feasible, germinated seeds were removed with forceps sterilized with ethanol and planted into individual pots with soil for another component of this dissertation research. Ungerminated seeds were counted at the end of the experiment and considered functionally nonviable in the analyses.

The time to initial germination, total percent, and time to complete actual germination were determined from each tree within each stratification treatment. Effects of site on the response variables within 3-needle (MTL and PAL sites) and 5-needle (PAL and RC/LIZ sites) were estimated by two-factor analysis of variance (ANOVA), then effects of species and stratification were similarly estimated for the PAL site. All response data were transformed by natural logarithm to normalize residuals. Finally, the pooled effects of species and stratification were estimated with two-factor ANOVA. Given the unbalanced design, Type II sums of squares (SS; Langsrud 2003) were used to test hypotheses using the 'car' (Companion to Applied Regression; Fox 2006) package in R (R Development Core Team 2007). Means were compared at each factor level using Tukey's Honest Significant Difference (HSD) in R, which

incorporates an adjustment for unbalanced designs (R Development Core Team 2007).

Reciprocal germination experiment

Two sites were selected for the reciprocal germination experiment: the top of a ridge extending off the north slope of Mount Lemmon (32.445°N 110.789°W, ~2720 m elevation), and the top of a small west-facing ridge near Willow Canyon (32.387°N 110.694°W, ~2185 m elevation). These sites represent the top of the mountain beyond the known distribution of PIN_ARI and below the known distribution of PIN_PON, respectively. The soil at the Mount Lemmon site is derived from micaceous sandstone and sandy phyllite, while the soil around Willow Canyon is derived from muscovite-garnet leucogranite (Force 1997). The vegetation at the Mount Lemmon site is dominated by Douglas-fir (*Pseudotsuga menziesii*) and PIN_PON; the 2003 Aspen Fire eliminated regeneration and killed most of the overstory at this site. Willow Canyon vegetation is dominated by PIN_ARI, Arizona madrone (*Arbutus arizonica*), and oaks (*Quercus* spp.); the Aspen Fire eliminated ground vegetation, soil organic matter, and small-diameter trees at this site but little of the overstory was killed. In January 2006, canopy openness measured by spherical densiometer (Lemmon 1957) was not significantly different between the two sites (Mount Lemmon: \bar{x} = 16.6%, s = 2.6%; Willow Canyon: \bar{x} = 22.9%, s = 12.2%; Wilcoxon Rank Sum Test, W = 38.5, p -value = 0.4055; R Development Core Team 2007).

Seeds from six PIN_PON (mean 2752 m elevation) and seven PIN_ARI (Palisade Rock – mean 2526 m elevation; Rose Canyon – mean 2159 m

elevation) trees were selected for the reciprocal germination experiment (Table 3-1). In late January 2006, a total of twelve seeds, one from each contributing tree, were sown on a prepared seedbed free from litter within each of ten predator-exclusion cages. Six aluminum nails centered longitudinally and spaced by 10 cm were pushed into the soil to serve as sowing and monitoring guides (Figure 3-1). Each seed was placed 5 cm above or below the nail in a predetermined randomized pattern. Seeds were covered with 1 cm of light duff before cages were placed over the seeds (Figure 3-2). The cages were constructed from 0.5-in (1.3-cm) hardware cloth to provide a 20-cm wide x 61-cm long seedbed with 15 cm of space for vertical growth and 3 cm of cloth folded back under the soil. Landscape pins and tags listing cage number and contact information were installed at two opposing corners of the cage.





Figure 3-1. Prepared seedbed within the predator-exclusion cage at the Willow Canyon site. Note the six aluminum nails either side of which seeds were sown.

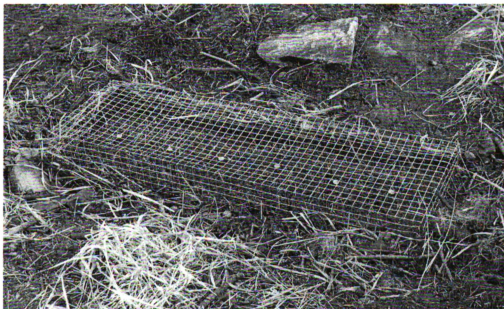


Figure 3-2. Predator-exclusion cage after placement over sown seeds at the Willow Canyon site (January 2006).

Seed germination was assessed at both sites in June 2006 and mid-October 2006. No germinants were observed in any cage at either site in June 2006 (G. Friedlander, personal communication), thus no documentation was required. In October 2006, the germinants in each cage were digitally photographed from above, and live and dead pine germinants within each cage were mapped relative to the aluminum nails and sides of the cage. Patterns of erosion evidenced by lack of duff were also mapped. The roofs of two cages at the Mount Lemmon site were bent and repaired in the field; substantial force from a round object (e.g., bear paw) was required to create the pattern along the crease of the roofs and corners. No germinants appeared to have been damaged.

Without referring to the identity of seeds arranged within each cage, probable planted (versus naturally sown) germinants were identified on the maps and then color-coded by species of seed. Each cage was considered to be a replicate in a balanced, two-factor (site and species) design, and thus percent germination was calculated for each species in each cage. Differences in germination resulting from site, species, and their interaction effects were summarized and analyzed by two-factor ANOVA, and means were compared at each factor level by Tukey's HSD in R (R Development Core Team 2007).

Results

Cold stratification experiment

Seed coats began cracking two days after incubation began, and the first germinants appeared by the third day. Most of the germination occurred within the first 8 days with a number of seeds germinating for another 12 days; the experiment was terminated after day 22. No trend in total percent germination across site, species, or stratification was observed (Figure 3-3); range in values was 75% (PIN_ARI from PAL site in 0-day stratification) to 93% (PIN_ARI from RC/LIZ site in 15-day stratification). Stratification increased the mean time to first and last germination events for all morphotypes; values ranged from 77.6 h (3.2 d; PIN_PON from MTL site in 0-day stratification) to 111.4 h (4.6 d; PIN_ARI from RC/LIZ site in 30-day stratification). There was a large amount of variability in time to last seed germination for PIN_ARI, especially in the shorter stratification treatments. Mean time to last germination ranged from 99.7 (4.2 d; PIN_PON from MTL site in 0-day stratification) to 271.1 h (11.3 d; Mixed from PAL site in 30-day stratification).

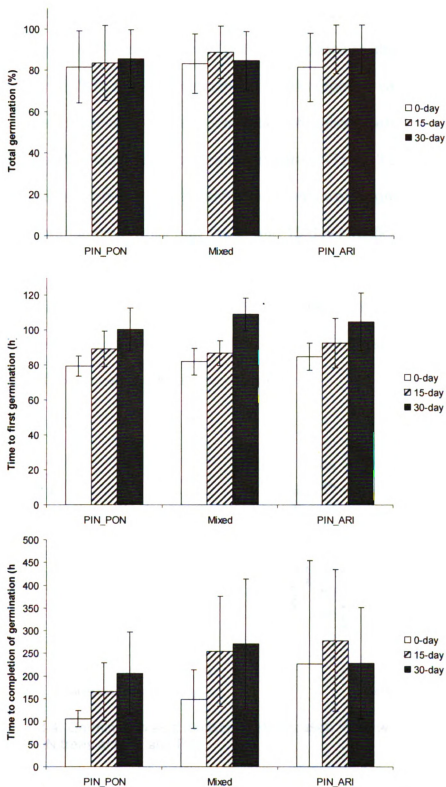


Figure 3-3. Mean seed germination (*top*), time to first germination (*middle*), and elapsed time to the last seed germination (*bottom*) for the full data set. Species data are pooled across sites. Data are mean values; bars are one standard deviation.

Site effects within each of the PIN_PON and PIN_ARI groups were either not significant. In the PIN_PON group, responses to stratification treatments by seeds from MTL and PAL overlapped for all response variables (Figure 3-4). However, the time to first and completion of realized germination were significantly affected by stratification treatment (Table 3-2); all pairwise comparisons between stratification treatments were significant ($p < 0.05$) for time to first germination, while only the 0- and 15-day stratification treatments were not different for time to completion of germination. Removing the non-significant interaction term, as in all of the analyses presented in this section, had no effect on identifying significant model terms, but rather only slightly affected their level of significance, which will not be reported.

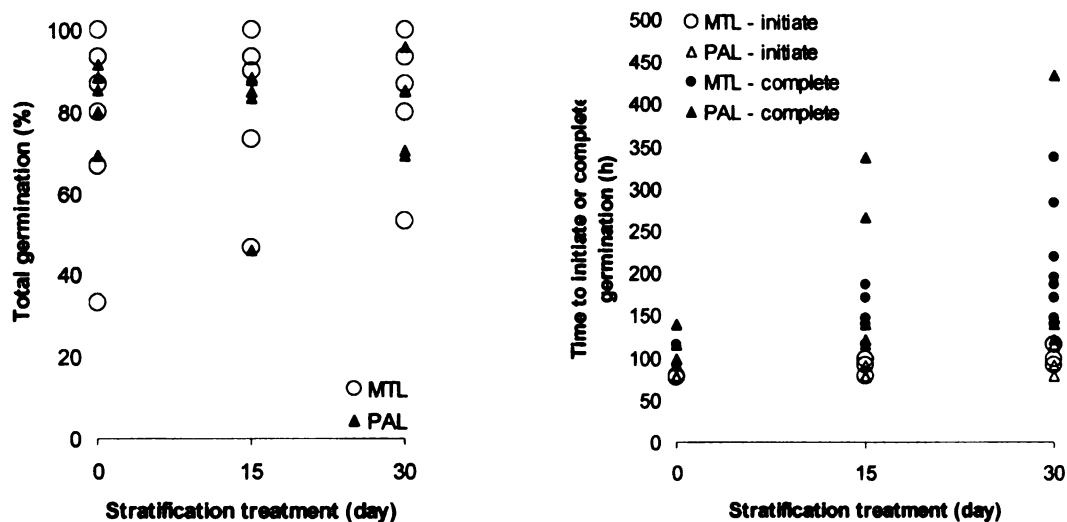


Figure 3-4. Germination as a function of stratification treatment for seeds from PIN_PON trees at MTL and PAL.

Table 3-2. Type II tests of 2-factor ANOVA of percent germination (pergerm), time to first germination (initiate), and time to last realized germination (complete) for PIN_PON seed as a function of site (MTL and PAL), stratification (strat; 0-, 15-, and 30-day), and their interaction. Determination of site effect was made by Tukey's HSD. Adjusted R^2 for the three models are -0.1029, 0.4235, and 0.4122, respectively. Significant ($\alpha < 0.05$) terms are bolded.

Response	Site effect Adj- <i>p</i>	Term	Df	SS	F-value	P-value
Ln(pergerm)	0.6454	Site	1	0.01405	0.2156	0.6454
		Strat	2	0.02647	0.2031	0.8172
		Site*strat	2	0.05426	0.4163	0.6629
		Residuals	33	2.15052		
Ln(initiate)	0.7028	Site	1	0.00088	0.0797	0.7794
		Strat	2	0.35205	15.9125	1.451E-05
		Site*strat	2	0.01119	0.5060	0.6075
		Residuals	33	0.36505		
Ln(complete)	0.3221	Site	1	0.08894	1.0103	0.3221
		Strat	2	2.48218	14.0971	3.756E-05
		Site*strat	2	0.21532	1.2229	0.3074
		Residuals	33	2.90527		

In the PIN_ARI group, responses were similarly distributed, but stratification appeared less important across the dependent variables (Figure 3-5). Site and stratification were not significant ($p > 0.05$) effects on percent germination or time to completion of germination, but both were significant ($p = 0.043$ and 0.010 , respectively) for time before initiation of germination (Table 3-3). The response of the seeds from RC/LIZ in the 30-day cold stratification treatment influences these results more than any of the other relevant pairwise comparisons; the 0- and 30-day stratification treatments within RC/LIZ was slightly less than significant ($p = 0.084$) and across both sites was highly significant ($p = 0.008$). Interestingly, the Type-III test reports nonsignificant p -values for site ($p = 0.450$) and stratification ($p = 0.198$) in the model for initiation of germination. Furthermore, a one-way ANOVA test of site on time to initial

germination was minimally significant ($\ln(\text{initiate}) \sim \text{site}$, $p=0.071$). Due to the sole influence of the 30-day stratified seed from RC/LIZ, site effects between PAL and RC/LIZ are considered to be inconsequential for the analysis of the full data set.

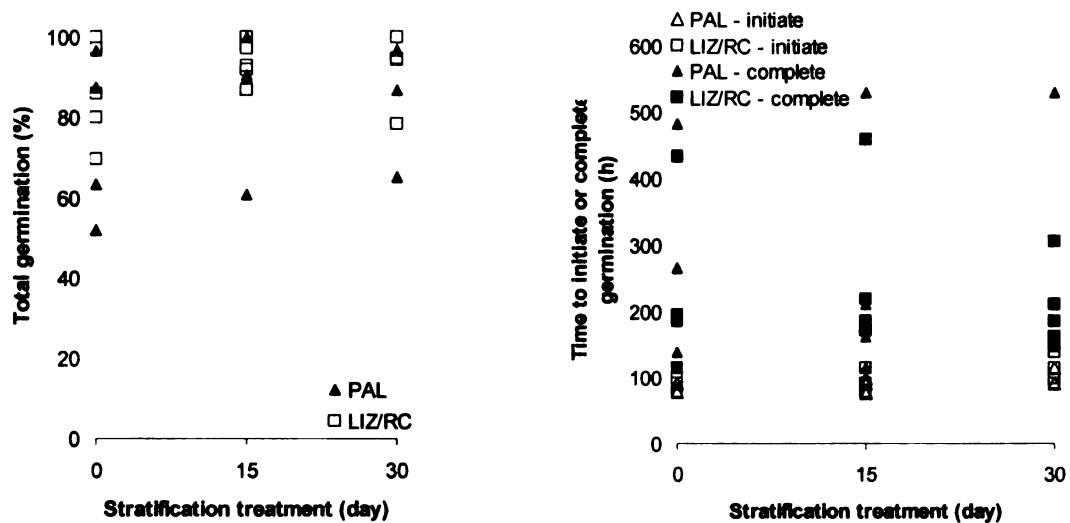


Figure 3-5. Germination as a function of stratification treatment for seeds from PIN_ARI trees at PAL and RC/LIZ.

Table 3-3. Type II tests of 2-factor ANOVA of percent germination (pergerm), time to first germination (initiate), and time to last realized germination (complete) for PIN_ARI seed as a function of site (PAL and RC/LIZ), stratification (strat; 0-, 15-, and 30-day), and their interaction. Determination of site effect was made by Tukey's HSD. Adjusted R^2 for the three models are 0.0396, 0.3054, and -0.1518, respectively. Significant ($\alpha < 0.05$) terms are bolded.

Response	Site effect Adj- <i>p</i>	Term	Df	SS	F-value	<i>P</i> -value
Ln(pergerm)	0.0871	Site	1	0.09728	3.2220	0.08706
		Strat	2	0.07894	1.3073	0.29169
		Site*strat	2	0.00712	0.1178	0.88943
		Residuals	21	0.63405		
Ln(initiate)	0.0427	Site	1	0.07790	4.6543	0.04271
		Strat	2	0.19128	5.7141	0.01044
		Site*strat	2	0.00587	0.1754	0.84031
		Residuals	21	0.35149		
Ln(complete)	0.9280	Site	1	0.0024	0.0084	0.9280
		Strat	2	0.2285	0.3962	0.6778
		Site*strat	2	0.2228	0.3863	0.6843
		Residuals	21	6.0550		

Within the PAL site containing all three morphotypes, there were no effects of species on any of the response variables (Table 3-4). Time to initiation was influenced by stratification, especially the 30-day treatment; the mean difference between the 0- and 30-day and the 15- and 30-day treatments were significant ($p=0.001$ and 0.033 , respectively; Figure 3-6).

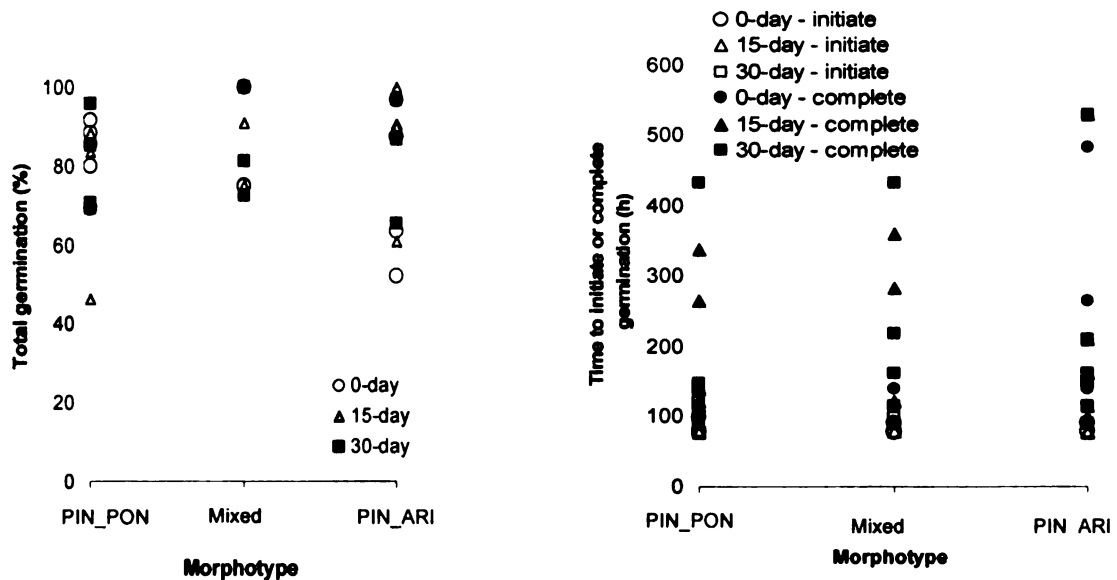


Figure 3-6. Germination as a function of stratification treatment for combined morphotypes at the PAL site.

Table 3-4. Type II tests of 2-factor ANOVA of percent germination (pergerm), time to first germination (initiate), and time to last realized germination (complete) for the PAL site as a function of morphotype (PIN_PON, Mixed, and PIN_ARI), stratification (strat; 0-, 15-, and 30-day), and their interaction. Pairwise comparison of PIN_PON and PIN_ARI (3-5 effect) was made by Tukey's HSD. Adjusted R^2 for the three models are -0.1774, 0.2311, and 0.0015, respectively. Significant ($\alpha < 0.05$) terms are bolded.

Response	3-5 effect Adj- <i>p</i>	Term	Df	SS	F-value	P-value
Ln(pergerm)	0.9909	Morphotype	2	0.02273	0.2831	0.7556
		Strat	2	0.01380	0.1719	0.8430
		Site*strat	4	0.07290	0.4540	0.7686
		Residuals	27	1.08392		
Ln(initiate)	0.9028	Morphotype	2	0.01074	0.3453	0.7111
		Strat	2	0.25405	8.1721	0.0017
		Site*strat	4	0.02307	0.3711	0.8271
		Residuals	27	0.41969		
Ln(complete)	0.2327	Morphotype	2	0.8094	1.5417	0.2323
		Strat	2	0.9196	1.7516	0.1926
		Site*strat	4	0.3844	0.3662	0.8305
		Residuals	27	7.0872		

Because site effect was not significant, the data were pooled across sites (Figure 3-3) and analyzed by morphotype and stratification treatments. None of the terms, including interaction, explained a significant ($p > 0.05$) portion of the variance in percent germinated seed (Table 3-5). For time to initiation of germination, stratification was highly significant ($p < 0.001$), but the effect of morphotype was not significant ($p = 0.28$; PIN_ARI versus PIN_PON pairwise comparison $p = 0.26$). Time to complete germination was significantly affected by both species and stratification (both $p = 0.001$). Pairwise comparisons in this model between PIN_ARI and PIN_PON ($p = 0.001$), 15- and 0-day stratification ($p = 0.010$), and 30- and 0-day stratification ($p = 0.002$) were highly significant; the Mixed-needled trees were only marginally different ($p = 0.106$) from PIN_PON. However, PIN_PON and PIN_ARI were only significantly different in the 0-day stratification treatment (Table 3-6). Although there was no significant interaction

($p=0.28$), morphotype and stratification treatment affected the time to completion of germination.

Table 3-5. Type II tests of 2-factor ANOVA of natural-log-transformed percent realized germination (pergerm), time to first germination (initiate), and time to last germination (complete) for pooled sites as a function of morphotype (PIN_PON, Mixed, and PIN_ARI), stratification (strat; 0-, 15- and 30-day), and their interaction. Pairwise comparison of PIN_PON and PIN_ARI (3-5 effect) was made by Tukey's HSD. Adjusted R^2 for the three models are -0.0666, 0.388, and 0.2657, respectively. Significant ($\alpha<0.05$) terms are bolded.

Response	3-5 effect Adj- p	Term	Df	SS	F-value	P-value
Ln(pergerm)	0.5939	Morphotype	2	0.04697	0.4984	0.6098
		Strat	2	0.08355	0.8867	0.4169
		Morphotype*strat	4	0.02873	0.1525	0.9613
		Residuals	66	3.10959		
Ln(initiate)	0.2598	Morphotype	2	0.03384	1.3004	0.2793
		Strat	2	0.66130	25.4099	6.56E-09
		Morphotype*strat	4	0.01932	0.3712	0.8283
		Residuals	27	0.85883		
Ln(complete)	0.0011	Morphotype	2	2.5232	7.5459	0.0011
		Strat	2	2.4268	7.2575	0.0014
		Morphotype*strat	4	0.8651	1.2935	0.2816
		Residuals	27			

Table 3-6. Pairwise comparisons (Tukey's HSD) of PIN_PON and PIN_ARI seeds for natural-log-transformed percent realized germination (pergerm), time to first germination (initiate), and time to last germination (complete) as a function of stratification treatment for pooled sites. Data are reported as adjusted p -values; significant values are bolded.

Stratification	pergerm	initiate	complete
0-day	1.0000	0.9168	0.0212
15-day	0.9860	0.9993	0.2557
30-day	0.9993	0.9974	0.9999

Reciprocal germination experiment

Approximately one-half of the PIN_PON seeds germinated the first growing season at both sites, while only around one-fourth of the PIN_ARI seeds germinated between the two sites (Figure 3-7). Consequently, site was not

significant but species was significant in the ANOVA (Table 3-6). The overall interaction term was not significant (Table 3-7), but a significant difference exists between germination of PIN_PON and PIN_ARI seeds at the high elevation site on Mount Lemmon (Table 3-8). There was no difference in germination of PIN_ARI seeds from Palisade Rock and Rose Canyon ($\chi^2=1.6897$, $df=1$, p -value=0.1936; R Development Core Team 2007).

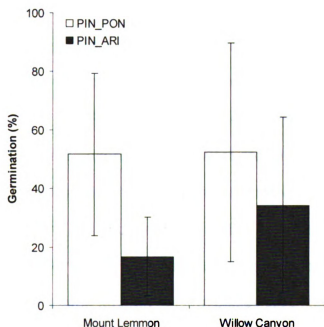


Figure 3-7. Germination of PIN_PON and PIN_ARI seeds planted at high (Mount Lemmon) and low (Willow Canyon) elevation. Values are mean percent germination; bars are one standard deviation.

Table 3-7. ANOVA for germination success of PIN_PON and PIN_ARI seeds at the Mount Lemmon and Willow Canyon sites (adjusted $R^2=0.1625$). Significant ($\alpha<0.05$) terms are bolded.

Term	Df	SS	MS	F-value	P-value
Site	1	837.2	837.2	1.0287	0.3172
Morphotype	1	7049.0	1049.0	8.6613	0.0057
Site*morphotype	1	714.0	714	0.8773	0.3552
Residuals	36	29298.7	813.9		

Table 3-8. Multiple comparisons between site (Mount Lemmon - MTL and Willow Canyon - WC), morphotype, and interactions by Tukey's HSD. Significant ($\alpha < 0.05$) comparisons are bolded.

Group 1	Group 2	Mean difference	P-value
WC	MTL	9.15	0.3172
PIN_ARI	PIN_PON	-26.55	0.0057
WC PIN_PON	MTL PIN_PON	0.7	0.9999
WC PIN_ARI	MTL PIN_ARI	17.6	0.5200
WC PIN_ARI	WC PIN_PON	-18.1	0.4962
MTL PIN_ARI	MTL PIN_PON	-35.0	0.0445

Discussion

Effects of stratification on germination success and rate

In the controlled cold stratification experiment, a similar percentage (75-93%) of PIN_PON and PIN_ARI seeds germinated across stratification treatments. Although molds were present in some Petri dishes, seeds continued to germinate and thus were not considered to be affected by the molds. Seeds from PIN_ARI appeared (Figure 3-3) to have higher germination rates than PIN_PON with longer stratification periods, but this difference was not significant due to a large amount of intraspecies variation.

In contrast to the stratification experiment, more PIN_PON than PIN_ARI seeds from the same seed lots used in the laboratory experiment (Table 3-1) germinated at both high (Mount Lemmon site; 52 vs. 13%, $p=0.0445$) and low (Willow Canyon site; 52 vs. 34%, $p=0.4962$) sites, although the difference at the latter site was not significant (Figure 3-7). Since the seeds in the present study were sown into the field in January, approximately the coldest time of year, "natural" cold stratification is assumed. In October, a large number of germinants were growing around the predator-exclosure cages at the Willow Canyon site

(personal observation), likely due to release of seeds by overlying trees during the winter. Consequently, selection of germinants from seeds sown for this experiment was highly conservative; i.e., I included only those germinants falling exactly in the expected location, which ostensibly led to a lower perceived germination rate for both taxa. Also, runoff appeared to have removed the light duff over the seeds in portions of two cages at the Willow Canyon site; expected seeds from these portions were removed from the calculations. No ponderosa pine germinants were observed outside of the cages at the Mount Lemmon site; instead, forbs had sprouted within and around the cages, possibly shading or displacing seeds away from the expected location. Like the stratification experiment, there was a large amount of intraspecies variability in total germination (Figure 3-7).

In the controlled laboratory experiment, cold stratification significantly increased the amount of elapsed time after sowing before seeds began to germinate as well as the length of time before the last seeds germinated (Figure 3-3). There seemed to be no species difference in time to first germination, while PIN_ARI generally took longer to complete germination than PIN_PON in all stratification treatments and noticeably longer than Mixed in the 0-day control treatment. Distinct from all other patterns of stratification effects, PIN_ARI seeds in the longest stratification treatment actually completed germination in less time than those in the 15-day treatment and about the same amount of time as those in the 0-day control treatment (Figure 3-3). This idiosyncrasy is due to seeds from 2 of the 5 PIN_ARI trees from RC/LIZ completing their (100% actual)

germination relatively early (162 h; 6.7 d) in the incubation period and thus biasing the mean and trend observed in the other morphotypes.

The effects of stratification on germination success and rate in ponderosa pine seeds varies, as was demonstrated in the present experiments. In laboratory tests, Barton (1930) also found higher initial but similar final germination by stratified and unstratified ponderosa pine seed. Smith (1986) also reported higher initial rate but found lower overall germination of stratified (\bar{x} = 25% over 30-90 days) versus unstratified (\bar{x} = 38%) ponderosa pine seed from New Mexico and Colorado. The effects of stratification were supported by a second test of the same seed batch conducted at a production greenhouse (\bar{x} = 7% over 31-55 days versus \bar{x} = 12% for unstratified seed; Smith 1986); the significantly lower germination at the greenhouse as compared to the laboratory could not be explained. Weber and Sorensen (1990) found that stratification increased germination rate but also uniformity and total percentage, especially at lower incubation temperatures, in ponderosa pine (*Pinus ponderosa* var. *ponderosa*) from central Oregon. All whole seeds germinated after 30 days of stratification followed by incubation at 20° C, the same temperature used in this study, with fewer days before the majority of seeds germinated in longer stratification periods (Weber and Sorensen 1990). Following sowing of ponderosa pine seed in Fort Valley Experimental Forest of northern Arizona, Schmid and Mitchell (1986, cited by Howard 2003b) found 61-90% germination beginning 12-37 days after sowing.

From the controlled stratification experiment, I conclude that there is no difference in germinability between any of the morphotypes tested in this study. In addition, stratification by itself did not appear to affect germination success as demonstrated in the cold stratification experiment. The difference in observed germination success between PIN_PON and PIN_ARI in the field must be due to some other factor, such as timing of germination (see below). However, emergence is only the first critical threshold in seedling establishment; germinant survival through the first arid foresummer (May-June 2007) has not been determined. In Barton's (1993) study of elevational distribution of desertic pines in nearby Chiricahua Mountains, the species with the lowest elevational distribution (*Pinus discolor*) had higher emergence and first-year survival at high than low elevation, which is an opposite trend to PIN_ARI in the present study. However, all of the germinants of the higher elevation species (*P. engelmannii* and *P. leiophylla* var. *chihuahuana*) had died at lower elevation by the end of the first arid foresummer (Barton 1993). In the present study, the PIN_PON germinants, then, are expected to have lower survivorship at the Willow Canyon site as compared to the Mount Lemmon site. The long-term implication of survival by young seedlings through multiple seasons of drought is the determination of the community composition.

Implications of variable germination period

Seed germination is affected by a multitude of abiotic factors influencing the seed physiology, including temperature, water potential, light, smoke, and soil

chemistry (Bewley and Black 1985, Baskin and Baskin 1998). The survival of the resultant seedling is highly dependent on the narrow temporal congruence of these factors, especially temperature and water potential, or moisture content. Given that most montane trees produce and disperse mature seeds in the fall, it is no surprise that physiological dormancy is induced at maturity to endure the winter (Kozlowski et al. 1991, Baskin and Baskin 1998). Germinants would have precious few weeks to establish root systems and store photosynthates before the onset of freezing conditions. Where snow cover is absent, freezing injury severely reduces seedling survivorship (Germino et al. 2002). In pines, populations that are adapted to colder temperatures (i.e., higher in elevation) tend to have deeper dormancy and longer chilling requirements (Weber and Sorensen 1990, Skordilis and Thanos 1995, Allen and Meyer 1998). However, dormancy will vary within a given seed lot (Kozlowski et al. 1991) and even within mother plants (Andersson and Milbert 1998). Ponderosa pine is known for producing mature seeds in the fall that can germinate under light but that generally require prechilling for maximum (dark) germination (Li et al. 1994). However, more slowly drying seeds could become more dormant than those that dry fast (Baskin and Baskin 1998); in other words, seeds from more xeric habitats at low elevation could be less dormant than those from higher elevation. Although there was no species difference in time to initial germination in this study, PIN_PON did complete germination faster (i.e., more dormant and thus more influenced by the stratification effect) than PIN_ARI, the lower elevation species.

Physiological dormancy is usually broken in seeds by imbibing water during the stratification process (Baskin and Baskin 1998). Once the minimum cardinal temperature for germination is reached (Bewley and Black 1985), ponderosa pine germinants begin to appear in the spring through epigeal germination (Oliver and Ryker 1990). Since there is no innate soil seed bank in pines (Keeley and Zedler 1998; except for *Pinus albicaulis* in Tomback et al. 2001), all viable seeds should germinate when minimum moisture content and thermal loads coincide (Alvarado and Bradford 2002). However, pine seeds that germinate in the spring in the Santa Catalina Mountains and similar mountain islands of the semiarid Southwest will face the arid foresummer with little growing time to establish root systems that can access deeper water. Schubert (1974, cited in Oliver and Ryker 1990) noted that water potentials more negative than 0.7 MPa significantly reduced seed germination, as well as root penetration, root dry weight, and cotyledon length in southwestern ponderosa pine germinants. If seeds were to germinate during this cooler, moist period followed by the arid foresummer, drought stress would ultimately kill them. In fact, by 27 June 2006, there were no pine germinants observed around or in any of the predator-exclusion cages at either Mount Lemmon or Willow Canyon site (G. Friedlander, personal communication); this observation indicates that no pine seeds had yet germinated.

Consequently, despite more northern Rocky Mountain ponderosa pine populations producing seed that germinate in the spring (Young and Young 1992), the Southwestern race (Conkle and Critchfield 1987) as well as Arizona

pine trees produce seed that undergo a secondary conditional dormancy. Baskin and Baskin (1998) describe primary dormancy as that which a seed possessed when freshly mature, while secondary conditional dormancy occurs when primary dormant seeds become partially or fully nondormant but then are induced into a second conditional dormancy under certain environmental conditions. The moist stratified seeds of PIN_PON and PIN_ARI are exposed to sufficiently warm but inconsistent (i.e., frequent night frosts) spring temperatures but do not germinate. Instead, as their water potential increases (i.e., the seeds lose moisture) with the coming arid foresummer, they undergo an induced secondary conditional dormancy. This secondary dormancy is then broken by the summer monsoon precipitation when the soil temperatures are consistently warm and soil is moist. Figure 3-8 illustrates the hypothesized path through secondary conditional dormancy and subsequent successful germination relative to the hydrologic seasons.

We should then not be surprised that the species found at higher elevation, and thus presumably more sensitive to drought (Barton 1993), completes the entire germination process more rapidly and uniformly than lower elevation species. As the summer monsoon subsides, air and soil temperatures remain high, and soon the fall drought will impose stress on the young seedlings. Therefore, there is strong selection for rapid initiation and completion of germination in the narrow window of adequate soil moisture and consistently warm temperatures before both the fall drought ensues and winter delivers freezing conditions. Conversely, total loss of a year's regeneration efforts could

occur as a result of precipitation events before the arid foreshummer concludes, while species whose seeds take longer to germinate may endure the remaining drought prior to monsoon.

Ponderosa pine seedlings rapidly grow tap roots, which enables them to survive in xeric soils (Howard 2003b), yet seedling mortality is highest in the arid Southwest (Howard 2003b). Ponderosa pine seedlings in Arizona that germinated earlier in the monsoon were more likely to survive the first year than those that germinated in August (Schmid and Mitchell 1986, cited by Howard 2003b). Given that there is greater selection for extreme conditions than for the mean (Ledig 1998) and that PIN_PON are faced with more limiting conditions as the growing season is shorter at high elevation, it is sensible that the germination and competition for soil-water resources occurs more rapidly for PIN_PON than for PIN_ARI, which is shown in part by the more rapid completion of germination after stratification by PIN_PON in this study.

evapotranspiration, are difficult to ascertain, especially when complex topography and elevation are considered. However, the projections do suggest that the *Ponderosae* in Arizona may experience a warming climate, especially during the winter and summer, and the bimodal precipitation pattern characteristic of southeastern Arizona may be somewhat more smoothed across the seasons, especially by reducing the intense monsoonal precipitation and severity of the fall drought. However, the projections are based on the entire state of Arizona, of which the southeastern portion that contains the mountains islands of *Ponderosae* is most affected by the rising subtropical high-pressure ridge ("Bermuda High") and its associated intense convective storms (Sheppard et al. 2002). Consequently, I can only suggest with some confidence that all seasonal temperatures are expected to increase ("global warming") and that precipitation patterns may be shifted toward a wetter fall and winter.

In other parts of the world, global warming has already resulted in altitudinal shifts of over 100 m in treeline and over 300 m in advanced regeneration of tree species (e.g., Kullman 2002). In colder climates, the milder winters reduce freezing-related injuries and extend the growing season, especially important to germination (Hobbie and Chapin 1998) and resultant seedlings (Kullman 2002). In the Santa Catalina Mountains and other mountain islands of the Southwest, the overall warmer climate but wetter fall may extend the temporal window for germination and successful establishment for both PIN_PON and PIN_ARI. Dodge's (1963) observation of dead trees and stumps of "ponderosa pine" below the current elevation of both PIN_PON and PIN_ARI

in the Santa Catalina Mountains indicates that at least one of the two species is migrating upward in elevation, likely in response to climate change. In fact, the annual average temperature has increased by 2 °C and the annual precipitation has increased by at least 15% in the Tucson area over the last century (USEPA 1998). Given the presumed strong influence of drought in limiting the more xeric lower elevational distribution for both species and that more humid fall conditions are projected for the next century, both taxa may be able to expand their overall range in the mountain islands. However, if the additional moisture is not physiologically useful (i.e., increased storm intensities), then drought will become even more severe in limiting their lower elevations. Given the low soil-water holding capacity of the shallow lithosols overlying steep bedrock gradients in the Santa Catalina Mountains, as well as the other mountain islands of the Southwest, though, distribution expansion is likely only to occur toward more mesic conditions at high elevation.

CHAPTER 4

DIFFERENTIAL COLD TOLERANCE SEGREGATES DISTRIBUTION OF *PONDEROSAE* IN THE SANTA CATALINA MOUNTAINS OF ARIZONA

Introduction

Cold conditions restrict the upper boundary, whether high latitude or elevation, of plant distribution through negative carbon balance (or inability to process acquired carbon; Hoch and Körner 2003), interrupted phenological cycle, and poor resistance to secondary factors, such as wind force, snow abrasion, parasites, and high heat (Tranquillini 1979). Since closely related species (Sutinen et al. 1992, Lindgren and Hällgren 1993, Hawkins et al. 2003, Nippert et al. 2004), populations within species (DeHayes 1977, Kolb et al. 1985, Schaberg et al. 1995), and even hybrid species (Lu et al. 2007) vary in their cold tolerance, their upper elevational limit should vary accordingly. Seedlings, in particular, are more sensitive to the severe abiotic conditions present at upper elevation limits (Cui and Smith 1991, Johnson et al. 2004) and should thus present stronger signals of differential interspecific cold tolerance.

The development of cold tolerance, or hardening, is related to genetic endogenous rhythms and enhanced by exposure to environmental conditions that limit metabolism and carbon acquisition (Havranek and Tranquillini 1995). The endogenous control is observed when dormant plants recover little under favorable conditions until later in winter (Pisek and Schiessl 1947, cited by Havranek and Tranquillini 1995). The initiation of predormancy is triggered by shorter day lengths, which is associated with lower daily temperatures.

Consequently, chemical reaction rates (i.e., metabolism), biosynthesis, gas exchange, water and nutrient acquisition, and carbon assimilation decrease, with primary growth finally terminating at the end of the season (Larcher 2003). Even before freezing temperatures are experienced by plants, lower temperatures induce changes in cellular structures in preparation for hardening. The changes occur at different rates in different organs of the plant; e.g., cold hardiness develops slower and to higher temperatures in roots than in other organs (Kozlowski et al. 1991). Protoplasmic osmotic potential increases, and thus intracellular freezing point decreases, from accumulation of sugars, amino acids, and ions, the vacuole fissions, and intracellular water moves to extracellular wall spaces, which also increases the osmotic potential and translocates initial (“extracellular”) ice crystal formation outside the cellular wall barrier (Larcher 2003). Exposure to near-zero freezing temperatures induces production of cold-stable phospholipids and stress proteins that stabilize biomembranes (Larcher 2003). Cellular survival is dependent on the ability to prevent ice crystal formation within the cell; not only do the crystals destroy membrane integrity, but they increase cellular dehydration due to the higher vapor pressure above the ice than the supercooled cytoplasm. As cytoplasmic desiccation increases, as in drought conditions, the concentration of salt ions and organic acids reach a toxic level which results in enzyme inactivation, biomembrane phospholipid deterioration, protein disassociation, and ATPase inactivity (Larcher 2003).

During dormancy, conifer leaves continue to absorb light, even though low temperatures inhibit the enzyme-mediated rate of carbon assimilation (Berry and

Björkman 1980). Consequently, the light energy in excess of that used for photochemistry must be dissipated lest oxidized radicals damage the photosynthetic machinery. In fact, conditions where the amount of absorbed light energy is greater than biochemically useful can occur during other stressful times of the growing season (e.g., drought) or day (e.g., midday solar peak), as well. In photosynthetic leaves, light energy is absorbed by accessory pigments (e.g., carotenoids, chlorophyll b and c) and chlorophyll (chl) a in the thylakoid membrane of the chloroplast. When the pigment molecule absorbs a photon of light, an electron is elevated to an excited state; this energy is transferred by resonance to chl a and then to a specialized chl a ("trap") molecule in one of two thylakoid membrane-bound photosystems (Nobel 2005). Production of a variety of pigments increases the ability to absorb photons from a broader range of the electromagnetic spectrum, but this can be harmful under limitation of electron sinks, such as during dormancy.

Light energy absorbed by chl a can be dissipated via excitation transfer through photochemistry or through nonphotochemical quenching (NPQ), such as fluorescence, phosphorescence, or radiationless transfer (i.e., heat; Nobel 2005). During noncyclic electron flow in photosynthesis, energy from an excited electron is transferred by resonance to photosystem I (PSI) or II (PSII) to drive electron transport and eventually reduce NADP^+ (Larcher 2003). Under high light conditions, some of the energy is lost by deexcitation of the electron to its ground state with concomitant production of radiation slightly lower in energy ($\Delta=1 \text{ KJ mol}^{-1}$), or longer wavelength ($\Delta=4 \text{ nm}$), than the 662-nm absorption peak (Nobel

2005). This radiation, fluorescence, originates largely from the antennae pigments associated with PSII (Larcher 2003). Phosphorescent radiation is emitted when a pigment molecule deexcites from a triplet state; the probability of an excited electron reversing its orbital spin (i.e., "triplet state) is low, thus phosphorescence is rare (Nobel 2005). Last, excess absorbed light energy can be dissipated by heat in a variety of ways. Higher-energy photons, such as those in the 430-nm absorption peak of chl a, excite electrons to a higher but unstable energy level; the electron quickly transitions to a lower-energy excited state with the energy difference resulting in production of heat (Nobel 2005).

Another energy-dissipating mechanism through heat is by downregulating photosynthesis (Öquist and Huner 2003, Adams et al. 2004). When the thylakoid lumen acidifies from a buildup of protons due to reduced rate of proton pumping by electron transport, the carotenoid violaxanthin (V) is de-epoxidised to antheraxanthin (A) and then zeaxanthin (Z) (Björkman and Demmig-Adams 1994). This occurs when the electron transport chain becomes sink limited; i.e., environmental conditions reduce ATP consumption and photosynthate production. Normally, violaxanthin transfers absorbed light energy to pigments associated with chl a, while zeaxanthin thermally dissipates the energy (Adams et al. 2004). In a review by Öquist and Huner (2003), decreased total chlorophyll content, increased VAZ pool, and increased ratio of V to A+Z are concluded as the primary means of NPQ in lodgepole pine (*Pinus contorta*). As the plastoquinone pool becomes more reduced from photochemically excessive light, transcription of genes coding for the light-harvesting polypeptides and reaction-

center D1 protein in PSII is repressed, while the chlorophyll-binding PsbS protein from PSII becomes involved in the de-epoxidation of V to A+Z (Öquist and Huner 2003). The reverse reaction, Z+A to V, can occur within minutes in nondormant leaves or hours in fully hardened leaves (e.g., 100 h for *Pinus ponderosa*; Verhoeven et al. 1999).

Damage by cold, or lack of cold tolerance, can be measured by a number of destructive and non-invasive methods following natural (e.g., Nippert et al. 2004) or controlled (e.g., Burr et al. 1990) freezing events, and different methods are often used complementarily (Burr et al. 2001). The non-destructive measurement of chlorophyll fluorescence yields an indicator of quantum efficiency, or efficiency of the photosynthetic apparatus. In dark-acclimated leaves, all reaction-centers in the ETC are oxidized, thus the steady-state fluorescence (F_o) can be measured with a fluorometer. A rapid pulse, or series of pulses, of saturating light then reduces all reaction-centers (i.e., Q_A in PSII), and photochemically excess light energy is reradiated as fluorescence, which is recorded as F_m . The ratio of $(F_m - F_o)/F_m$, or F_v/F_m , is a measure of the potential maximum PSII quantum yield, or efficiency of PSII (Schreiber et al. 1994). During the daytime, the quantum yield of open (oxidized) PSII centers, also phrased as the excitation capture efficiency of PSII, can be determined by first reducing Q_A with a weak far red light source that exclusively drives PSI and thus drains electrons from PSII, measuring steady-state fluorescence (F_o'), flashing a saturation pulse to measure F_m' , and calculating F_v'/F_m' as for dark-acclimated leaves (Schreiber et al. 1994). Both measures of variable fluorescence give an

indication of injury or reduction in function at the photosystem-level in the chloroplast as a function of cold or other stress.

Another method commonly used to assess cold damage and hardiness is by visual inspection of tissues after an incubation period (7-10 days) following the freezing event (Burr et al. 2001). While survival into future years following freezing at certain temperatures is a better test of cold hardiness, industry and researchers demand more rapid results. Once-frozen tissues, such as needles, buds, and cambia, are examined, and injury is quantified as percent 'browning' or mortality. This method requires expertise to accurately gauge existence and extent of tissue damage, but it can produce results consistent with other methods (e.g., Lindgren and Hällgren 1993). Furthermore, survival after freezing is an integrated response to cold damage and recovery. However, this method requires destruction of stems and/or roots to examine cambial damage.

Measurement of electrolyte leakage following cellular membrane disruption by ice formation is another destructive method for assessing damage by freezing temperatures. Prepared tissue samples normally release some amount of cellular electrolytes into a solution; after membrane destruction by freezing, the electrical conductivity (EC_o) of the prepared tissue samples in solution increases. Cells are lysed by heating to release the remaining electrolytes, and the solution is remeasured (EC_f). Relative conductivity is calculated variably as EC_o/EC_f (Ritchie 1991) or $(EC_o-B_1)/(EC_f-B_2)$ where B_1 and B_2 are EC values for blanks before and after heating (Burr et al. 2001). This method is relative fast, inexpensive, but does not produce a measure of mortality

(Burr et al. 2001). Also, the results can vary significantly by variation in plant health status (Burr et al. 2001).

Other methods for assessing cold injury include differential thermal analysis (DTA) and electrical impedance spectroscopy (EIS). DTA is useful for identifying the extent to which supercooling has been employed by various tissues by measuring the exothermic spike in response to spontaneous nucleation of extra- and intracellular supercooled water (Burr et al. 2001). A carefully controlled block or chamber contains both the tissue sample and an inert reference material against which tissue temperature is compared as block temperature decreases. DTA is less useful for some plant organs, especially during early and late dormancy, and must be standardized to another method (Burr et al. 2001). EIS works on the principle that different structures within the plant, or even cell, pose impedance to an applied electrical current. Currently, the biological meaning of EIS values is not well understood, but technological advances in interpreting results from this method have eliminated an actual freezing test (Burr et al. 2001).

Populations of the closely related Southwestern ponderosa pine (*Pinus ponderosa* var. *scopulorum* Engelmännii) and Arizona pine (*Pinus arizonica* Engelmännii) are known to segregate along an elevational gradient that varies in range and absolute value depending on topographic features and local climate conditions in the Santa Catalina Mountains of southern Arizona (Dodge 1963, Whittaker and Niering 1965, Barton 1993). At higher elevation (2430-2650 m), Southwestern ponderosa pine is codominant to Douglas-fir (*Pseudotsuga*

menziesii Franco) and Southwestern white pine (*Pinus strobiformis*) (Whittaker and Niering 1965). Around 2430-2550 m elevation (Epperson et al. 2001), the dominant *Ponderosae* transitions to Arizona pine, which extends down to ~1760 m elevation (personal observation). This differential distribution suggests that cold winter conditions could limit the upward migration of Arizona pine. While cold tolerance tests have been conducted on 'ponderosa pine' (e.g., Burr et al. 1989, 1990), no such tests have been reported for Arizona pine.

The goal for this study was to determine if there is a genetic difference in cold tolerance between Southwestern ponderosa and Arizona pine in the Santa Catalina Mountains that could lead to differences in elevational distribution. Intraspecific variation in cold tolerance has been noted in *Pinus* (Hawkins et al. 2003), so local source of plant material was used in this study; however, extrapolation to other mountains with this or other pairs of *Ponderosae* taxa should be relevant. Given that Southwestern ponderosa pine has a higher elevational distribution than Arizona pine, I hypothesized that the former species will have higher resistance, or lower critical temperature values (LT_{50} , temperature at which 50% mortality or failure is detected), to freezing conditions. This study incorporates three separate experiments involving 1-year-old potted seedlings in highly controlled laboratory conditions, 4-year-old potted seedlings exposed to Michigan's climate, and small trees in the Santa Catalina Mountains.

Methods

Controlled whole-seedling freezing test

In September-October 2005, multiple ripe cones were harvested from trees considered to be located within “pure” Southwestern ponderosa pine (“PIN_PON”) or Arizona pine (“PIN_ARI”) populations in the Santa Catalina Mountains. PIN_PON trees were located near the summit of Mount Lemmon (“MTL,” 32.4396°N, 110.7871°W (NAD83/WGS84), 2770 m elevation), while PIN_ARI trees were located either near Rose Canyon (“RC,” 32.3964°N, 110.6932°W (NAD83/WGS84), 2175 m elevation) or northeast of Lizard Rock (“LIZ,” 32.3844°N, 110.6930°W (NAD83/WGS84), 2135 m elevation). Cones were air-dried at room temperature in paper bags, and seeds were removed from the cones by shaking and removing cone bracts in early January 2006.

Unopened cones were heated 14-27 h at 40° C to encourage opening (Young and Young 1992). Empty, parasitized, or otherwise unhealthy appearing seeds were discarded, while whole seeds were dewinged by hand, inventoried, and stored in labeled small manila envelopes at room temperature. Seeds were germinated in February-March 2006 as part of another component of this dissertation. Germinants were carefully transferred to ShortOne TreePots (9.5 cm wide, 24 cm tall, 1.64 L volume; Stuewe & Sons, Inc., Corvallis, OR) containing a 1:1:3 (v/v) mix of perlite, steam-sterilized loamy sand, and Fafard52 (33% bark, 18% peat, 6% perlite, and 3% vermiculite; Conrad Fafard, Inc., Agawam, MA). After planting, 50 mL (~5 mm) of medium-grit crushed granite was spread onto the soil. Seedlings were grown for 10 months in greenhouses

(17-30° C daily) at Michigan State University (East Lansing, MI; 42.7225°N, 84.4763°W (NAD83/WGS84), 259 m elevation) with natural light (~9 h in December), regular watering, and two applications (19 May and 8 October 2007) of slow-release granular fertilization (Osmocote Classic, 14-14-14, 3-4 mo release at 70° C; The Scotts Company, Marysville, OH). From the available stock, 68-70 healthy seedlings of uniform size (i.e., similar number of fully expanded fascicles) from each species were selected for this experiment, which will use 60 seedlings per species. There were 8 mother trees for PIN_PON and 5 mother trees for PIN_ARI, and 8-9 PIN_PON and 14 PIN_ARI seedlings were selected from each seed source (Table 4-1). The proportion of trees coming from each germination treatment (see Chapter 3) did not differ (PIN_PON, $\chi^2=1.4412$, $df=2$, p -value=0.4865; PIN_ARI, $\chi^2=1.9143$, $df=2$, p -value=0.384).

Table 4-1. Seedlings and source trees from the Santa Catalina Mountains used in the controlled whole-seedling experiment.

Site	Morphotype	Source tree	No. trees available	No. trees used
Mount Lemmon	PIN_PON	MTL 9	35	9
		MTL 5	38	9
		MTL 24	42	9
		MTL 23	38	9
		MTL 15	24	8
		MTL 132	16	6
		MTL 11	35	9
		MTL 104	34	9
Rose Canyon	PIN_ARI	RC PINARI GroupPicnic	90	8
Lizard Rock	PIN_ARI	LIZ 1	24	8
		LIZ 3	20	14
		LIZ PINARI 353 from LIZ 2	40	19
		LIZ PINARI 61.5cm dbh	53	19

Measurement of cold-induced injury throughout the acclimation and deacclimation process would yield a complete picture of differential seasonal

susceptibility to cold, or cold tolerance. However, in ponderosa pine, Burr et al. (1990) observed little difference in tissue hardness prior to acclimation and large differences during deacclimation. Due to limited numbers of seedlings available for this experiment, investigation of cold-induced injury was restricted to three periods corresponding to the hardening, full acclimation, and deacclimation stages.

The seedlings underwent simulated field conditions for hardening, winter, and dehardening (Table 4-2) following the methods of Burr et al. (1989). Seedlings were hardened for 7 weeks on short-days (SD, 10-h light, $300 \mu\text{mol m}^{-2} \text{s}^{-1}$) at $10^{\circ}/3^{\circ} \text{C}$ in a standard walk-in growth chamber (TC2 controller, Environmental Growth Chambers, Chagrin, OH). Winter conditions were imposed at $5^{\circ}/-3^{\circ} \text{C}$ SD ($280\text{-}340 \mu\text{mol m}^{-2} \text{s}^{-1}$) for 4 weeks in a controlled growth chamber (Model GC-20 BDAF, ENCONAIR, Ecological Chambers, Inc., Winnipeg, Manitoba). Dehardening occurred under long-days (16-h natural light extended by sodium vapor bulbs) at $16^{\circ}/25^{\circ} \text{C}$ in a greenhouse. When needed, seedlings were equally watered at all stages with distilled water.

Table 4-2. Conditions for hardening, acclimating, and deacclimating PIN_PON and PIN_ARI seedlings for the whole-seedling freezing test. Relative timing and date for the freezing tests in each period are noted in the last two columns.

Stage	Length (wk)	Date	Day		Night temp (° C)	Freezing test	
			Length (h)	Temp (° C)		Week	Date
Hardening	7	22Dec-9Feb	10	10	3	5.4	29Jan
Winter	4	9Feb-9Mar	10	5	-3	10	23Feb
Deacclimation	2	9-23Mar	16	25	16	14	23Mar

Cold injury was inflicted by whole-plant freezing at 5.4, 10, and 14 weeks (Tables 4-2), and response to freezing was measured by before-and-after dark-adapted chlorophyll fluorescence (DACF), freezing-induced electrolyte leakage (FIEL), and visual scoring of needles, buds, and cambia. Twelve hours prior to starting each test, 20 randomly selected seedlings from each species were watered to field capacity to reduce effects of different plant-water status (J. Flore, personal communication), and attached needles from 3-4 fascicles from every plant were carefully marked with small pieces of tape at the fascicle sheath. PSII quantum efficiency, or DACF, was measured from the taped needles with a pulse-amplitude modulated fluorometer (6400-40 Leaf Chamber Fluorometer, LI-COR Biosciences, Inc., Lincoln, Nebraska, USA) attached to the base LI-COR 6400 Portable Photosynthesis System. The fluorometer was calibrated before the first set of measurements, zero-ed before each set, and adjusted to recommended settings: Saturating pulse (flash) - 0.8 s saturating multiple flash of $\sim 8800\text{--}9000 \mu\text{mol m}^{-2} \text{s}^{-1}$, 20KHz modulation, and 50 Hz averaging filter; no Dark pulse since dark-acclimated needles were measured; and Measurement light – intensity 2, 0.25 KHz modulation, 1Hz averaging filter, and 10 gain factor (LI-COR 2005a). Taped needles were then scored under fluorescent lighting for color (hue, value, and chroma; Munsell Tissue Color Chart, 1977 ed.) as in Boorse et al. (1998). Afterward, the seedlings were moved from the growth chamber (or greenhouse for the deacclimation treatment) to a completely dark room (20 °C) for at least 30 minutes before DACF was remeasured from the same taped needles to determine if DACF is a function of temperature or

photosynthetic down-regulation associated with physiological acclimation (B. Pratt, personal communication). In both the Hardening and Acclimation stages (Table 4-2), DACF was significantly (paired t-test, $df=19$, $p<0.05$) higher when measured at room temperature, thus all analyses use values recorded at room temperature.

The 20 selected seedlings from each species were then moved directly to a programmable (Model CN-2042 TC, Omega Engineering, Inc., Stamford, Connecticut, USA) large-capacity freezer. The freezing rate, duration at test temperature, and rate of thaw were meant to simulate conditions experienced by rooted seedlings in the field during extreme cold events. Sixteen of the seedlings per species were randomly arranged within the freezer, a fan at each end of the freezer circulated air, and at least 10 thermocouples were distributed in the seedling crowns throughout the freezer to monitor temperature distribution and level; four seedlings per species served as controls and were moved to a cold room (1°C). The ambient freezer temperature was lowered rapidly to 0°C and then at a rate of 5°C h^{-1} (Cannell and Sheppard 1982, Burr et al. 1989) to each test temperature. The same amount of damage is incurred between 1 and 4 h at a given freezing temperature (Cannell and Sheppard 1982); consequently, after the average crown temperature stabilized for 2 h at each of four test temperatures (Table 4-3), four seedlings of each species were quickly removed from the freezer, placed in a cooler with ice packs, and immediately transported to the cold room (1°C) to thaw (Burr et al. 1989).

Table 4-3. Temperature profiles for each of the freezing tests outlined in Table 4-2. The bolded steps are those times after which four seedlings from each species were removed from the freezer.

Step	Hardening Stage		Winter Stage		Deacclimation Stage	
	Duration (h)	Temp (°C)	Duration (h)	Temp (°C)	Duration (h)	Temp (°C)
00	~1:30	Down to 0	~1:30	Down to 0	~1:30	Down to 0
01	1:00	0	1:00	0	1:00	0
02	3:00	-15	2:00	-10	0:36	-3
03	2:10	-15	2:10	-10	2:10	-3
04	1:00	-20	1:00	-15	0:36	-6
05	2:10	-20	2:10	-15	2:10	-6
06	1:00	-25	1:00	-20	0:36	-9
07	2:10	-25	2:10	-20	2:10	-9
08	1:00	-30	1:00	-25	0:36	-12
09	2:10	-30	2:10	-25	2:10	-12

After thawing for 12-21 h, depending on relative time of removal from the freezer, the seedlings were moved to the laboratory (~20° C) for the FIEL measurements. Two-four healthy-appearing and non-taped fascicles from each tree were excised at the base of the fascicle sheath with a razor blade and then cut into 1-cm segments on a dry glass plate. The seedlings were moved to the greenhouse (described above). The cut segments were quickly rinsed in deionized (DI) distilled water (NANOpure Ultrapure Water System, Model D4741, Barnstead International, Dubuque, IA, USA) in a Petri dish, and then 40 segments were carefully removed with forceps and placed into a 55-mL culture tube (25x150 mm, Pyrex No. 9826, Corning Incorporated Life Sciences, Lowell, MA) containing 10 mL of DI water. A pilot test of seedlings frozen down to -15° C indicated that 20 segments produced an electrical conductivity (EC) reading 3.7 times lower than the EC meter's calibration setting (447 μ S), thus doubling the number of segments would safely increase the absolute range and precision of EC measurements. The tubes were capped, vortexed, incubated for 12 h in 20°

C distilled water, vortexed again, and measured for initial EC (CON 410, Oakton Instruments, Vernon Hills, IL). The EC meter was recalibrated using standard calibration (447 μ S) solution before every set of measurements. With caps loosened 45° to prevent explosion, the tube were incubated at 90° C in an oven for 2 h to lyse the cells and then for 12 h in 20° C water before the maximum EC (Ritchie 1991) was measured. Marked tubes did not lose any noticeable solution to evaporation during the incubation. The relative conductivity (RC) of the solution was calculated as the initial conductivity value divided by the maximum conductivity value (Ritchie 1991).

The seedlings in the greenhouse were evaluated at both 3 and 7 days following the freezing test by DACF and visual scoring to assess any recovery of photosynthetic function. Bud and cambium were evaluated for visible tissue injury 7 days following the freezing test (Burr et al. 1989). In natural light conditions, apical buds were removed by razor and cut longitudinally to determine if the bud were live (bright green) or dead (dull green or brown); percent mortality was calculated to compare against freezer temperature. Seedlings were measured for length from root-collar to base of apical bud, and most of the stem was shaved with a razor to expose cambium. Live cambium, using the control trees as a standard, was very bright green, while functionally dead cambium was dull green or brown. The length of stem with dead cambium was measured and converted to percent injury relative to the total length of stem. Determination of live or dead bud and cambium requires close inspection, expertise, and conference with an experienced person; L. Sage (Department of Horticulture,

MSU) provided the initial calibration, while F. Telewski assisted with every bud and cambial scoring test.

PSII quantum efficiency (DA CF), freezing-induced electrolyte leakage (RC, relative conductivity), cambial and bud mortality, and change in Munsell value after freezing were modeled using analysis of variance (ANOVA) in R (R Development Core Team 2007). The full models included the main factors of species and freezing treatment, as well as their interaction. For each phase, the critical temperature (LT_{50}) was estimated for each response variable, except change in Munsell value, by visual interpolation from plots of the fitted values from the full model ('predict' function; R Development Core Team 2007). The y-axis value for estimating LT_{50} was determined as one-half of the mean species response in the control trees at 3° C for DA CF and RC, while 50% was used for cambial and bud mortality.

Observational whole-seedling freezing test

In fall 2004, the nongovernmental organization named Trees for Mount Lemmon (contact: Barbara Eisele) donated 391 two-year-old "ponderosa pine" seedlings for our research purposes. The seeds were originally collected within the Santa Catalina Mountains (exact locations not recorded) by a private contractor for Coronado National Forest to replant areas affected by the Catalina Highway reconstruction (B. Eisele, personal communication) and grown in greenhouses near Flagstaff (W. Hart, personal communication). In early November 2004, I retrieved the potted (n=3-7 seedlings per small pot) seedlings

from outdoor storage at high elevation (Summerhaven School and Radio Ridge), counted the number of needles in every fascicle (2003-2004), labeled each seedling with morphotype (*sensu* Peloquin 1984) and a unique identifying number, and barerooted all seedlings with roots covered by moist paper toweling and packed into plastic bags in cardboard boxes. The 6 wardrobe boxes were shipped ground freight to Michigan State University. All seedlings were then potted within 2 days of arrival in a standard conifer soil mix (Fafard52, Conrad Fafard, Inc., Agawam, MA) in 2-gal plastic pots.

The seedlings were kept outdoors for about one week and then moved to a greenhouse heated sufficiently through the winter to prevent ice formation in the water pipes. Daytime temperatures inside the greenhouse during the winter were usually 4-10° C, but high solar radiation raised the temperature to ~20° C on occasion. Through spring, daytime temperatures inside the greenhouse reached 32° C; trees were generally watered as needed, but high seedling mortality in the greenhouse suggested that watering had been insufficient and/or daytime temperatures had been too high. On 21 May 2005, all seedlings were moved outside the greenhouse, with supplemental watering as needed; survival was high during the summer. Temperatures remained above freezing until mild frost on 27-29 October and 14 November (NCDC 2007). Beginning 22 November, nighttime (except 29 November) and daytime (except 28-29 November) temperatures stayed below 0° C, even reaching -11° C on 25 November (NCDC 2007). Consequently, soil water in the pots had frozen

diurnally for about a week and then likely remained frozen for at least 2 days before measurements of PSII excitation capture efficiency began.

Light-acclimated chlorophyll fluorescence (LACF; F_v'/F_m') was measured from every living seedling as they were moved into the heated ($\bar{x}=13^{\circ}\text{C}$) greenhouse from 2-5 December 2005. Seedling selection was determined by a disinterested assistant, thus the order of moving trees into the greenhouse for measurement was not advertently biased by morphotype. LACF was measured by the LI-COR fluorometer, as described in the first experiment, but a 6-s dark pulse was added to measure F_o' with the following additional settings: far red intensity of 8 turned on 1 s before and remain on for 1 s beyond actinic light off, 0.25 KHz modulation, and 1 Hz averaging filter (LI-COR 2005a). As before, the fluorometer was calibrated with a standard before the first set of measurements and zero-ed before each set. After securely clamping a sufficient number of non-overlapping healthy needles to completely cover the aperture in the fluorometer, measurements were initiated after base fluorescence had stabilized ($dF/dT < 5$; LI-COR 2005a). Temperature inside the cuvette was simultaneously measured by a thermocouple.

LACF was modeled with morphotype as a fixed effect and temperature as a covariate by analysis of covariance (ANCOVA) in R (R Development Core Team 2007). Afterward, temperature was removed from the model and LACF was fitted to morphotype in a one-way analysis of variance (ANOVA). Given the unbalanced design, Type II sums of squares (SS; Langsrud 2003) were used to

test hypotheses using the 'car' (Companion to Applied Regression; Fox 2006) package in R (R Development Core Team 2007).

Small trees on the mountain

Response to natural variations in cold temperatures was measured for small PIN_PON and PIN_ARI trees in the Santa Catalina Mountains in January 2006. Since the small-diameter trees would have been severely damaged by coring, their ages were not determined; size does not correlate well with age for semiarid mountainous trees (T. Harlan, personal communication). However, standardizing for size across sites (elevation) should reduce effects related to ability to acquire water and to tolerate above-ground climate conditions.

Trees selected for winter measurements at the MTL (n=3 PIN_PON), Palisade Rock ("PAL," 32.4138°N, 110.7149°W (NAD83/WGS84), 2475 m elevation; n=4 per species), and LIZ (n=3 PIN_ARI) sites were part of ongoing research discussed elsewhere in this dissertation. Trees at each site were measured within one day over 24-27 January. For each tree at both predawn and midday, the ratio of variable to maximum chlorophyll fluorescence (F_v/F_m and F_v'/F_m' , respectively) was measured from the same attached 2005 needles (recently taped at the fascicle sheath) on the lowest living branch with a LI-COR fluorometer calibrated with a standard before the first set of measurements, adjusted to settings used in the previous experiment, and zero-ed before each set of measurements. Net photosynthesis (A) was simultaneously measured during the midday fluorescence measurements (LACF). At predawn, DACF was

measured once per tree, while LACF and A were measured 3-4 times from the same needles and averaged. Predawn and midday xylem water pressure potentials (Ψ_p) were measured from detached 2005 needles from the same branch as the fluorescence measurements. Ψ_p give an accurate estimate of plant water status (Kaufmann 1968, Ritchie 1975), especially diurnal changes in status, and has been used to assess cell rupture by freezing (Brown et al. 1972). Five-ten fascicles per tree were cut at the base of the fascicle sheath with a razor blade, immediately placed in a small resealable plastic bag containing moist paper toweling, and stored in a cooler with ice packs prior to measurements. Within 2-6.5 h, each fascicle was cleanly cut with a razor ~1 cm from the basipetal end of the fascicle sheath, inserted into a rubber grommet, and pressurized with N_2 gas in a pressure chamber (Model 1000, PMS Instruments, Corvallis, Oregon, USA) to determine the xylem pressure potential. Measurements were taken from 3-6 fascicles from each tree and averaged by observer and replicates to obtain a mean Ψ_p per tree.

DACF and LACF were modeled with site and species as fixed factors and temperature as a covariate by ANCOVA in R (R Development Core Team 2007). Afterward, temperature was removed from the models, and DACF, LACF, Ψ_p , and A were modeled using two-factor ANOVA in R (R Development Core Team 2007). The full models included the main fixed factors of site and species, but interaction was not included due to the small sample size at MTL and LIZ. Given the unbalanced design, Type II SS (Langsrud 2003) were used to test the ANOVA hypotheses using the 'car' (Companion to Applied Regression; Fox

2006) package in R (R Development Core Team 2007), while the default Type I SS were used for the ANCOVA tests.

Results

Controlled whole-seedling freezing test

Freezing caused significant damage to the seedlings, especially beyond threshold temperatures (Figures 4-1 and 4-2). The threshold was most obvious during the Hardening stage when the difference between the controls (3° C) and the first freezing treatment (-15° C) was greater than for the other stages; this difference is likely due to a lack of temperature treatments closer to zero during the Hardening freezing test. In the ANOVAs, the temperature treatments were significant ($p < 0.0004$, but $p < 0.002$ for change in Munsell value) for all response variables, but the interaction of temperature treatment and species was not significant ($p > 0.523$, but $p > 0.3306$ for change in Munsell value). Given the lack of pattern and precision in the change in Munsell value, these data will not be reported.

Little difference in response by species was observed within the Hardening and Deacclimation phases, except for a larger degree of cambial mortality in PIN_ARI seedlings from the -15° C treatment during the Hardening stage (Figure 4-2). The largest apparent species difference occurred during the Winter stage. In this stage, PIN_PON had higher DACF in every temperature treatment group (Figure 4-1) and lower cambial and bud mortality in the -15° and -20° C freezing treatments (Figure 4-2). With the exception of the -3° C

treatment, PIN_ARI also had higher cambial and bud mortality in the -15° and -20° C freezing treatments during the Deacclimation stage (Figure 4-2). However, the ANOVAs indicated that the only significant ($p < 0.05$) difference between species is the amount of cambial mortality during the Winter stage (Table 4-4).

Table 4-4. ANOVA results for dark-acclimated chlorophyll fluorescence (DACF), relative conductivity (RC), and cambial (Camb) and bud (Bud) mortality for PIN_PON and PIN_ARI seedlings exposed to freezing treatments (Tx) during the acclimation phase. Significant ($\alpha < 0.05$) terms are bolded.

Response	Adj R ²	F(p-value)	Term	Df	SS	F-value	P-value
DACF	0.7111	1.96E-10	Species	1	0.0904	2.3771	0.1319
			Tx	1	3.6766	96.6332	9.80E-12
			Species*Tx	1	0.0001	0.0037	0.9517
			Residuals	36	1.3697		
RC	0.708	4.36E-10	Species	1	0.0113	0.9321	0.3409
			Tx	1	1.1360	94.0674	1.88E-11
			Species*Tx	1	0.0015	0.1202	0.7309
			Residuals	36	0.4227		
Camb	0.6135	3.48E-08	Species	1	0.4655	5.4571	0.0252
			Tx	1	5.0310	58.9809	4.3E-09
			Species*Tx	1	0.0401	0.4707	0.4971
			Residuals	36	3.0708		
Bud	0.3182	0.0007	Species	1	0.2250	1.2903	0.2635
			Tx	1	3.4490	19.7786	8.02E-05
			Species*Tx	1	0.0234	0.1343	0.7162
			Residuals	36	6.2776		

Seasonal effects, or differences between acclimation stages, on response to freezing temperatures can be demonstrated by comparing the regressions of the response variables against treatment temperature for all stages (Figure 4-3). Although the expected response is sigmoidal, the R² for the linear regressions were generally high ($\bar{x} = 0.81$, $s = 0.12$). The interpretation of these plots is simpler when summarized by plots of slope and intercept against time during the acclimation process (Figure 4-4); no standard errors are associated with these

plots, thus significance testing was not performed. In general, slope values are related to the degree of hardening, or sensitivity to freezing; larger absolute values of slopes indicates a stronger response to freezing. In other words, slopes should converge to zero when the plant tissue has thoroughly hardened. Intercepts indicate the degree of injury expected at 0° C; i.e., the difference between intercepts suggests the (genetic) difference in cold tolerance between species.

Slope values were similar for both species across the Hardening and Winter stages but were steeper during Deacclimation (Figure 4-4). This suggests that both species were close to the degree of hardening during the first stage as compared to the second stage, but both species were functionally deacclimating during the third stage and thus becoming more sensitive to freezing temperatures. There was no species difference in sensitivity to freezing as measured by DACF and RC, but cambium in PIN_PON appeared to be more sensitive across stages than in PIN_ARI. However, PIN_ARI buds were more sensitive than PIN_PON buds during the Winter and Deacclimation stages.

As for the slope values, the intercepts for the two species in the DACF and RC plots were similar, with PIN_PON having slightly higher PSII quantum efficiency and vaguely lower electrolyte leakage than PIN_ARI during the Hardening and Winter stages (Figure 4-4). The hump-shaped DACF curve for PIN_PON is considered anomalous because 2 seedlings had relatively high DACF following the -10° C during the Winter stage and thus biased the regression curve (Figure 4-3). With significance ($p=0.025$) calculated by ANOVA

(Table 4-4), PIN_ARI seedlings had much higher cambial mortality than PIN_PON seedlings; furthermore, mortality increased through the acclimation process, peaking during the Deacclimation stage, like PIN_PON. Bud mortality also increased for both species through the acclimation process, with PIN_ARI seedlings experiencing higher bud mortality during the Winter stage than PIN_PON seedlings.

Table 4-5 shows the results of the second approach to examining species differences in cold tolerance, with LT_{50} 's interpolated from the fitted values from the ANOVAs. The mean LT_{50} 's for whole PIN_PON seedlings across the three stages were -12.6, -12.9, and -9.6° C, while the mean LT_{50} 's for PIN_ARI seedlings were -11.1, -8.4, and -7.6° C. PIN_PON was consistently more cold tolerant across measured variables than PIN_ARI, especially during the Winter ($\Delta=-4.4^{\circ}$ C) when both species should have been fully hardened. The rank-order of variables according to their insensitivity to freezing (i.e., lower LT_{50}) changed from buds, cambia, and needles (DACF/RC) during Hardening and Winter to buds, needles (DACF/RC), and cambia during Deacclimation. The species differences are generally supported by the previous method. PIN_PON had lower LT_{50} 's for loss of PSII quantum efficiency during Hardening and Winter, for electrolyte leakage and cambial mortality during all stages, and for bud mortality during the Winter stage.

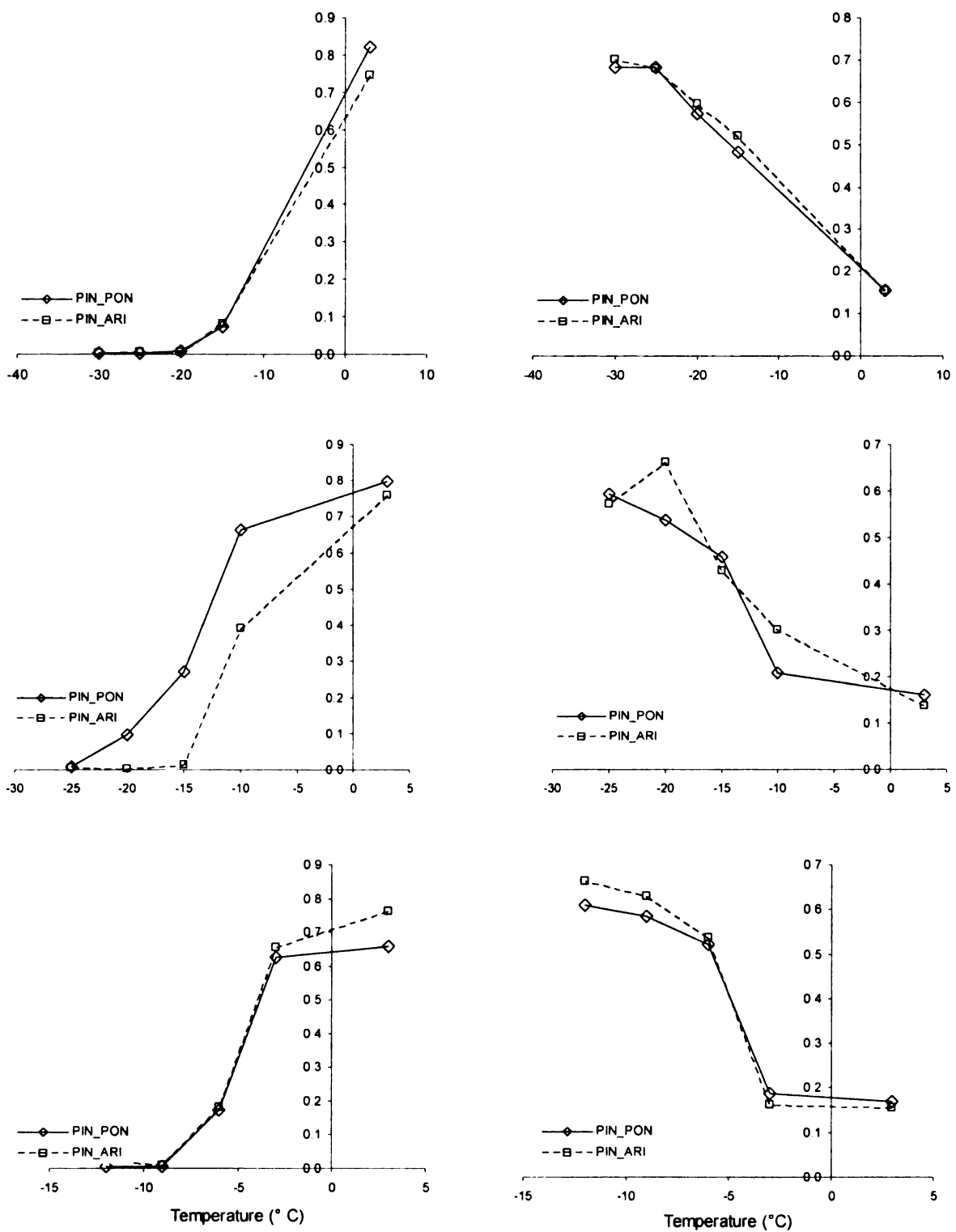


Figure 4-1. Dark-acclimated chlorophyll fluorescence (*left*) and relative conductivity (*right*) for PIN_PON and PIN_ARI after different freezing treatments across three stages of cold acclimation: Hardening (*top*), Acclimation (*middle*), and Deacclimation (*bottom*). Note the varying temperature scale between phases.

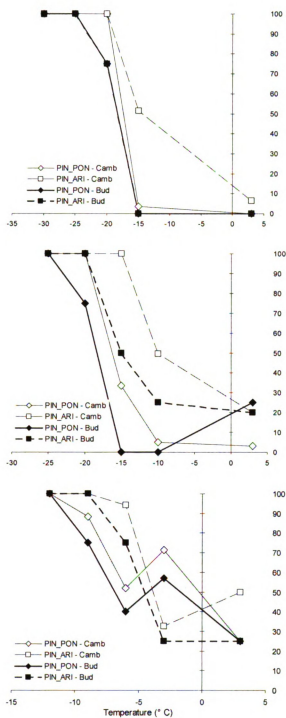


Figure 4-2. Cambial and bud mortality for PIN_PON and PIN_ARI after different freezing treatments across three stages of cold acclimation: Hardening (*top*), Winter (*middle*), and Deacclimation (*bottom*). Note the varying temperature scale between phases.

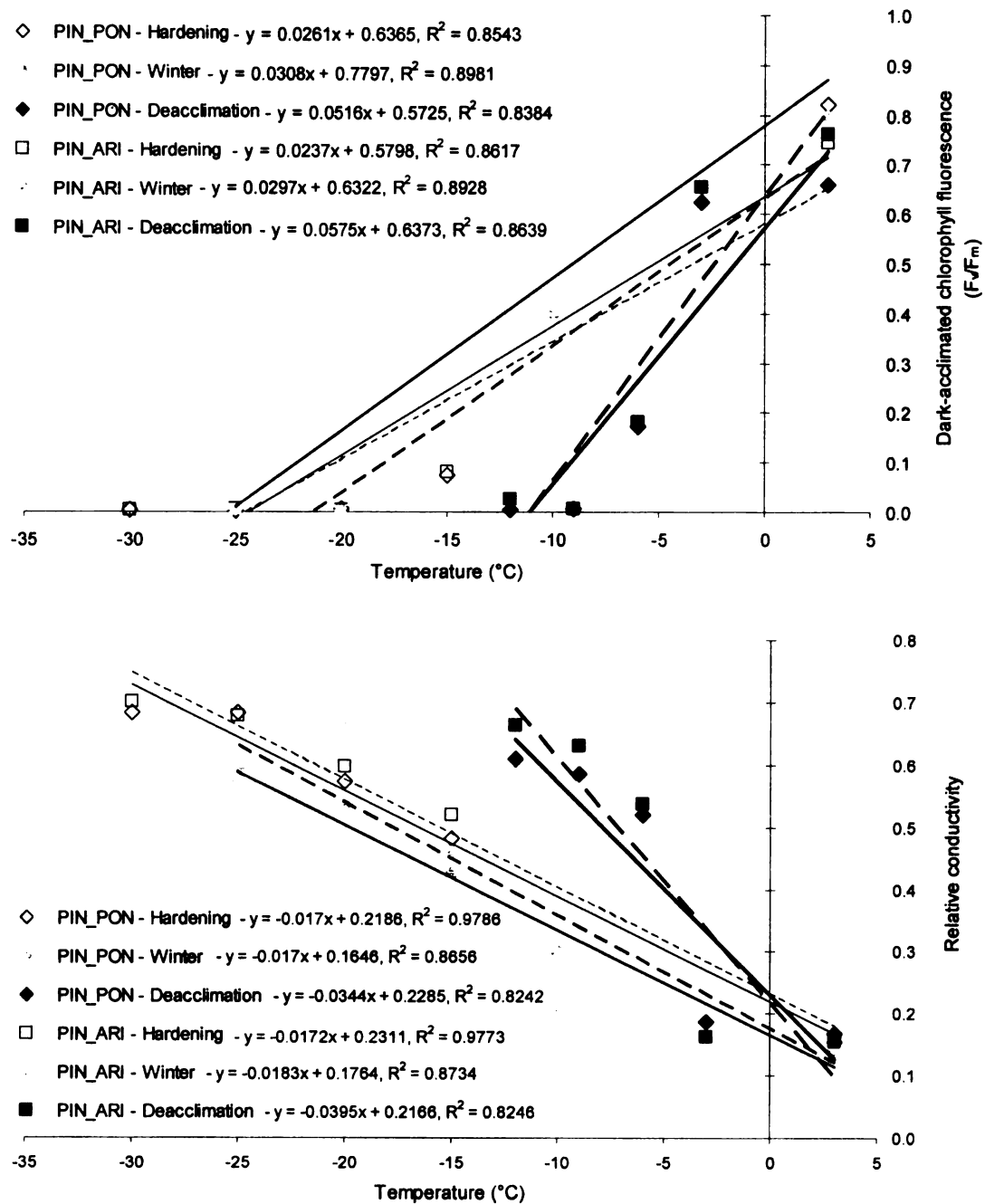


Figure 4-3. Linear regression of dark-acclimated chlorophyll fluorescence, relative conductivity, and cambial and bud mortality against treatment temperature for PIN_PON (solid line) and PIN_ARI (dashed line) across three stages of cold acclimation: Hardening (thin line), Winter (normal line), and Deacclimation (thick line). Note the varying temperature scale between phases.

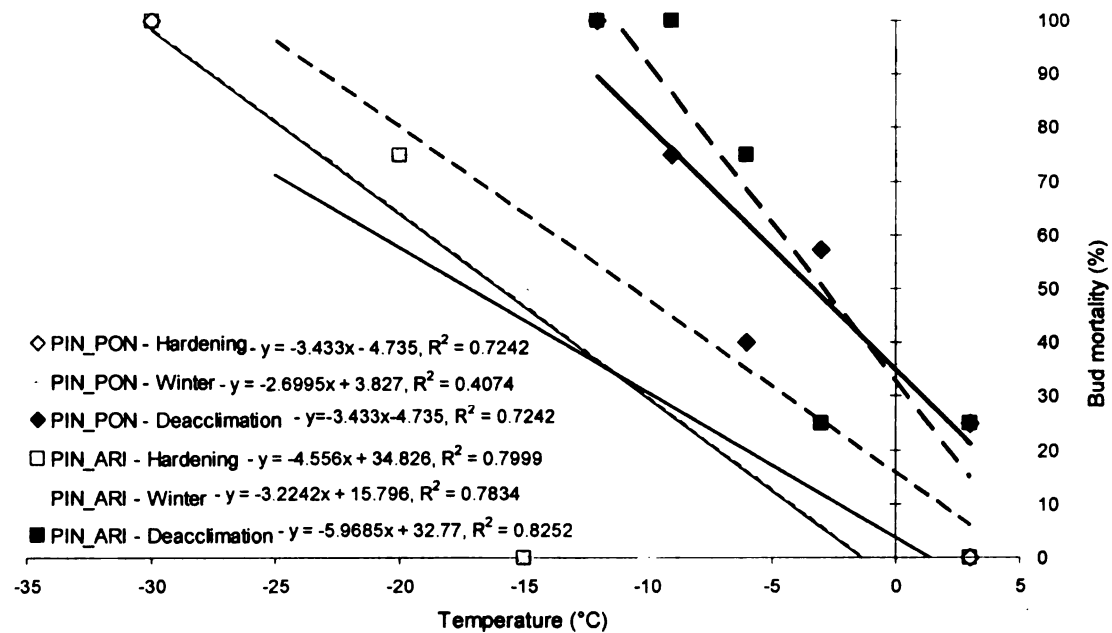
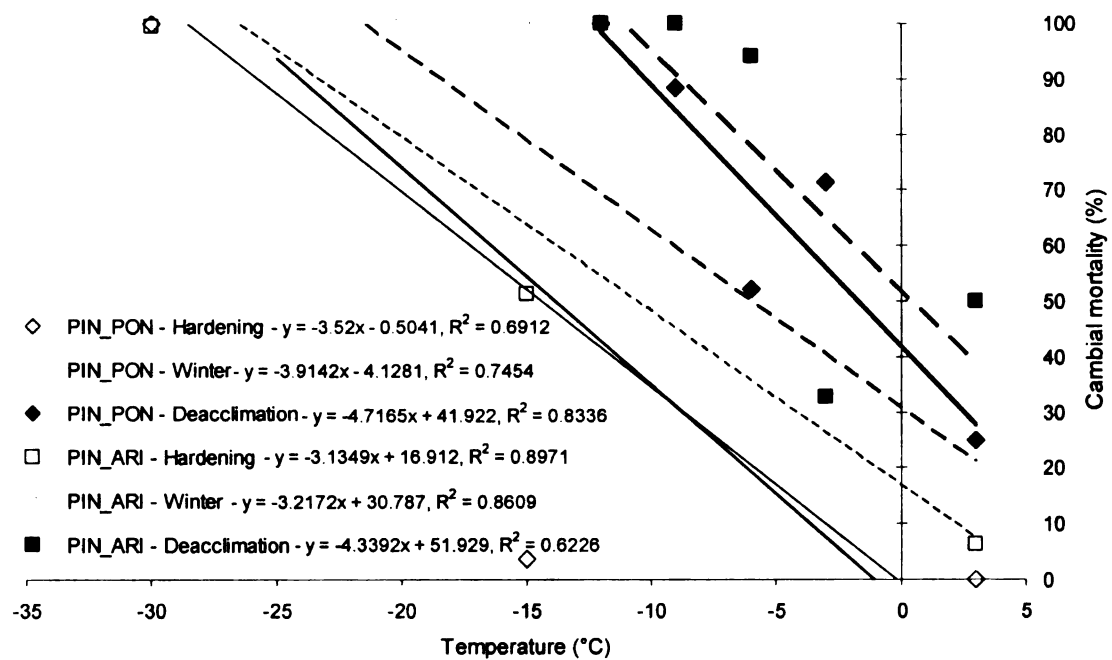


Figure 4-3. *Continued.*

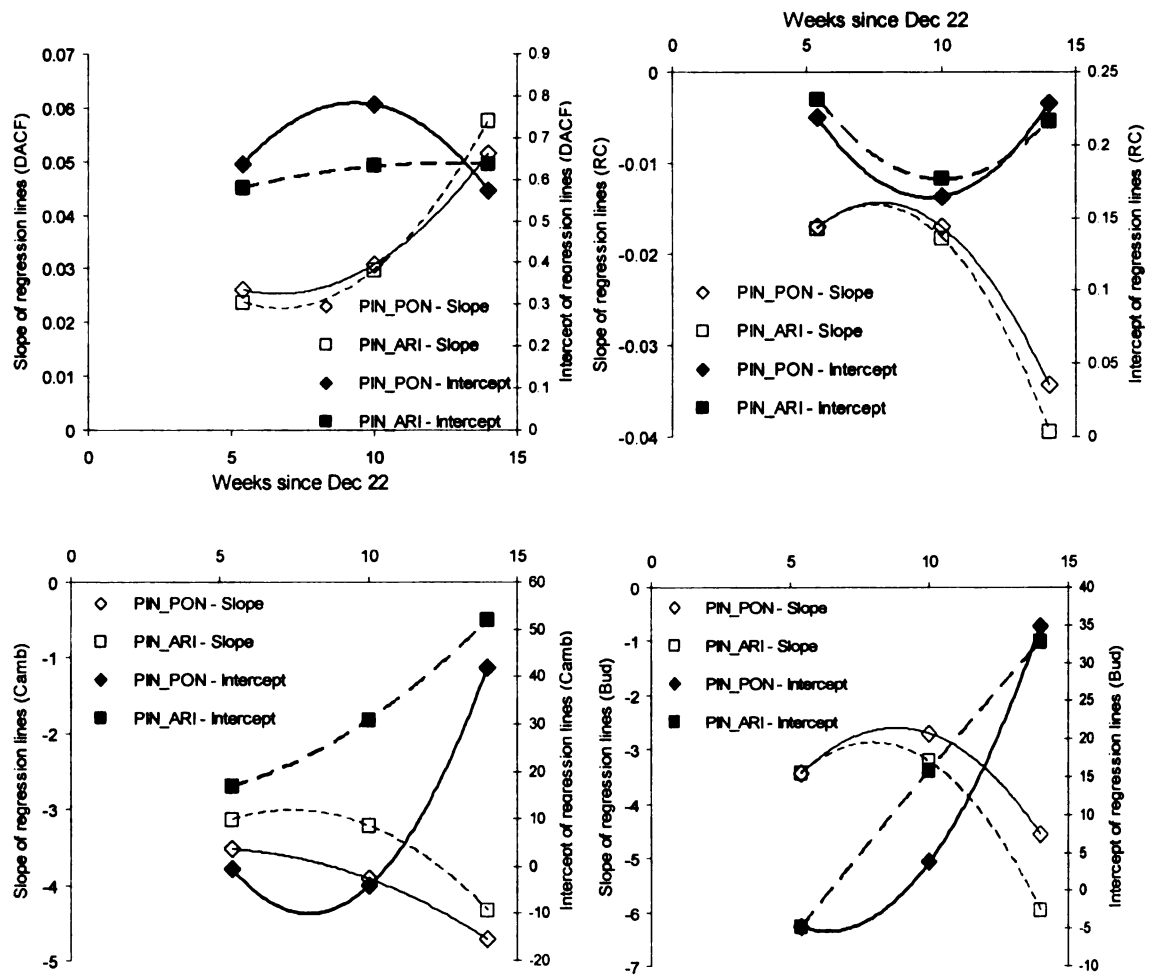


Figure 4-4. Slope (*thin line*) and intercept (*thick line*) for regressions of dark-acclimated chlorophyll fluorescence, relative conductivity, and cambial and bud mortality against treatment temperature for PIN_PON (*solid line*) and PIN_ARI (*dashed line*) across weeks of cold acclimation. Note the varying axis scales across graphs.

Table 4-5. Cold tolerance (LT_{50}) of PIN_PON and PIN_ARI estimated as a function of needle dark-acclimated chlorophyll fluorescence (ndl - DnCF), needle relative conductivity (ndl - RC), and cambium and bud mortality across three stages of cold acclimation: Hardening, Winter, and Deacclimation.

Response	Hardening		Winter		Deacclimation	
	PIN_PON	PIN_ARI	PIN_PON	PIN_ARI	PIN_PON	PIN_ARI
Ndl - DnCF	-11.25° C	-10.0° C	-12.25° C	-8.5° C	-12.5° C	-12.25° C
Ndl - RC	-9.0	-8.0	-8.5	-7.25	-9.25	-6.0
Cambium	-14.25	-10.5	-13.75	-6.75	-6.25	-2.5
Bud	-16.0	-16.0	-17.0	-11.25	-10.5	-9.75

Observational whole-seedling freezing test

The quantum yield of open PSII reaction centers, measured by LACF (F_v'/F_m'), varied from 0.07 to 0.399 with a mean of 0.270 ($s=0.053$) across all seedlings ($n=163$) (Figure 4-5). Most of the data are slightly lower than the theoretical overall quantum yield of unstressed plants under incident light ($F_v'/F_m'=0.3-0.35$; Schreiber et al. 1994). Mean (\pm SD) quantum yields for PIN_PON, Mixed, and PIN_ARI were 0.282 (± 0.051), 0.255 (± 0.051), and 0.241 (± 0.057), respectively. Air temperature when the seedlings were measured ($p=0.105$) and its interaction with morphotype ($p=0.524$) did not significantly affect LACF in the ANCOVA (Table 4-6). However, there was a highly significant ($p=0.0009$) effect of seedling morphotype on the quantum yield. Pairwise comparison across morphotypes using Tukey's HSD from a one-way ANOVA of morphotype indicated that LACF measured from PIN_PON seedlings was significantly higher than from both Mixed ($p=0.023$) and PIN_ARI ($p=0.001$), but LACF measurements from Mixed and PIN_ARI were not significantly different ($p=0.569$).

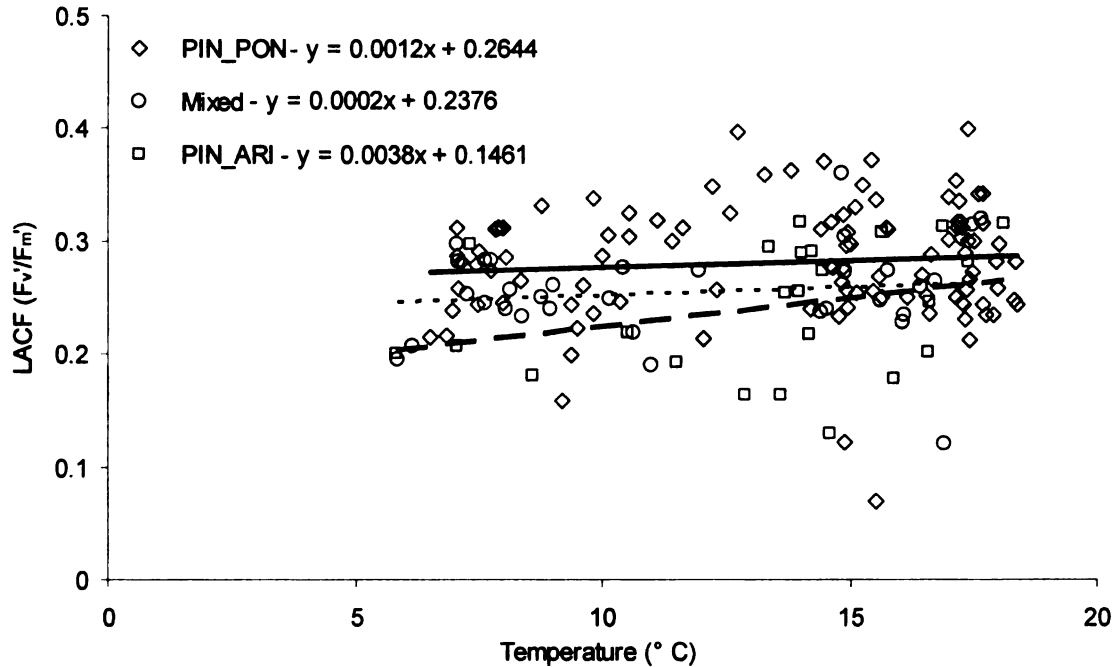


Figure 4-5. PSII quantum yield (LACF) as a function of air temperature when measured from 3-year-old potted seedlings with frozen soil water: PIN_PON (*solid line*), Mixed (*dotted line*), and PIN_ARI (*dashed line*). Coefficients are from full ANCOVA model.

Table 4-6. Type II tests of ANCOVA for PSII quantum yield (LACF) fitted to morphotype and the covariate air temperature (Temp) for 3-year-old potted seedlings with frozen soil water. Significant ($\alpha < 0.05$) terms are **bolded**.

Adj R ²	F(p-value)	Term	Df	SS	F-value	P-value
0.0876	0.0016	Morphotype	2	0.0372	7.3279	0.0009
		Temp	1	0.0067	2.6570	0.1051
		Morphotype *Temp	2	0.0033	0.6481	0.5244
		Residuals	157	0.3980		

Small trees on the mountain

The potential maximum PSII quantum yield, measured as DACF (F_v/F_m), varied from 0.555-0.746 across all sites, with the highest means recorded at MTL and LIZ, while the realized PSII quantum yield under incipient light, measured as LACF (F_v'/F_m'), ranged from 0.300-0.509, with the trees at the intermediate PAL site exhibiting the highest F_v'/F_m' readings (Figure 4-7). The values of DACF

were larger than of LACF because the PS reaction-centers are not fully oxidized thus increasing the relative minimal yield (F_o) and heat dissipation, which reduces maximum fluorescence (Schreiber in Larcher 2005). Consequently, the ratio of the difference between F_o and F_m over F_m decreases accordingly.

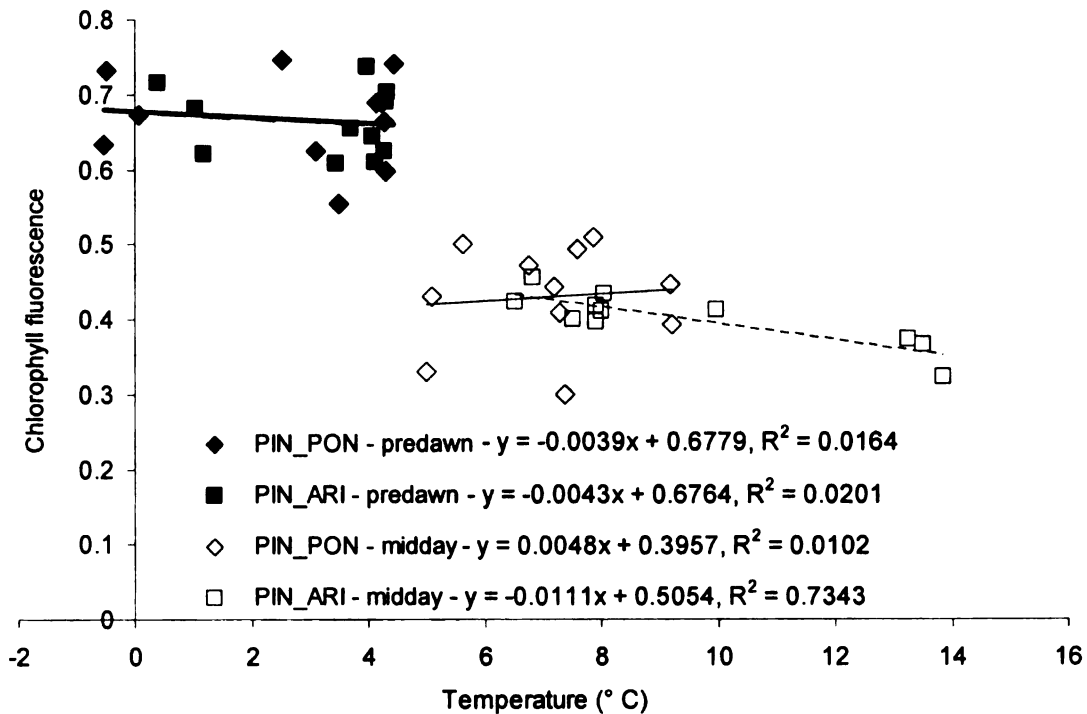


Figure 4-7. Variable chlorophyll fluorescence (F_v/F_m , solid; F_v'/F_m' , empty) as a function of leaf temperature for PIN_PON and PIN_ARI trees combined across sites in January 2006.

As a function of temperature, little difference in the ratio of variable to maximum chlorophyll fluorescence is apparent between species within time periods (Figure 4-7). However, the three midday measurements taken from PIN_ARI trees at LIZ at lower elevation (and thus higher temperature) bias the linear regression toward a negative slope (-0.0111) and larger intercept ($\Delta=0.1097$). Consequently, temperature was a significant ($p=0.038$) covariate for the midday variable fluorescence measurements (Table 4-7). The interaction of

temperature and site were also significant terms for the midday xylem pressure potential (Ψ_p) and net photosynthesis (A) models. However, temperature varied consistently by site, which generated 5-56 times higher SS than temperature across all of the ANCOVA models, and was thus confounded site; consequently, temperature was dropped from all further analyses.

Table 4-7. ANCOVA results for predawn dark-acclimated chlorophyll fluorescence (pDACF), midday light-acclimated chlorophyll fluorescence (mLACF), predawn (ppsi) and midday (mpsi) xylem pressure potential, and midday net photosynthesis (mphoto) for PIN_PON and PIN_ARI trees at three sites (MTL, PAL, and LIZ) in the Santa Catalina Mountains in January 2006. Significant ($\alpha < 0.05$) terms are bolded.

Response	Adj R ²	F(p-value)	Term	Df	SS	F-value	P-value
pDACF	-0.3344	0.9644	Species	1	0.0001	0.0332	0.8580
			Site	2	0.0010	0.1353	0.8746
			Temp(covariate)	1	0.0000	0.0103	0.9206
			Species*Temp	1	0.0000	0.0010	0.9747
			Site*Temp	2	0.0053	0.7112	0.5079
			Residuals	14	0.0518		
mLACF	0.5936	0.0037	Species	1	0.0045	3.6257	0.0777
			Site	2	0.0331	13.3687	0.0006
			Temp(covariate)	1	0.0065	5.2417	0.0381
			Species*Temp	1	0.0009	0.7450	0.4026
			Site*Temp	2	0.0016	0.6595	0.5324
			Residuals	14	0.0173		
ppsi	0.5209	0.0106	Species	1	0.4541	9.3342	0.0086
			Site	2	0.9304	9.5616	0.0024
			Temp(covariate)	1	0.0412	0.8477	0.3728
			Species*Temp	1	0.0097	0.1999	0.6616
			Site*Temp	2	0.0158	0.1627	0.8514
			Residuals	14	0.6811		
mpsi	0.7777	0.0003	Species	1	0.4700	20.9632	0.0006
			Site	2	0.9589	21.3854	0.0001
			Temp(covariate)	1	0.0170	0.7583	0.4001
			Species*Temp	1	0.0004	0.0167	0.8992
			Site*Temp	2	0.2008	4.4782	0.0352
			Residuals	14	0.2690		
mphoto	0.6589	0.0012	Species	1	12.2521	13.8766	0.0023
			Site	2	16.9186	9.5810	0.0024
			Temp(covariate)	1	0.3441	0.3897	0.5425
			Species*Temp	1	3.3358	3.7781	0.0723
			Site*Temp	2	9.1430	5.1777	0.0207
			Residuals	14	12.3610		

Since the interaction of species and site was not calculated by R due to the small number of trees ($n=3$) measured at each site, the resultant ANOVA models contained only the fixed factors of species and site. Using all of the data, the effect of species was not significant ($p<0.05$) in any model (Table 4-8). The significant effect of site on Ψ_p and A are apparent in Figures 4-8 and 4-9, with trees at lower elevation having lower Ψ_p and A . Predawn and midday Ψ_p varied significantly (paired t-test, $t=5.1532$, $df=19$, $p=5.65E-05$) across all sites, with the largest difference observed within both species at PAL (Figure 4-8). However, analysis of the midday LACF and A models indicated a few major outliers. An MTL tree had 36% higher F_v'/F_m' than the other two trees, while a different MTL tree had 53% lower A than the other two, and one LIZ tree had 4% of the A as the other two trees. Despite consistent F_v'/F_m' readings, this LIZ tree had highly variable A ($\bar{x}=0.253$, $s=0.759$). When these data points were removed, the species effect shifted slightly toward significance for both models (Table 4-8).

Table 4-8. Type II ANOVA results for predawn dark-acclimated chlorophyll fluorescence (pDACF), midday light-acclimated chlorophyll fluorescence (mLACF), predawn (ppsi) and midday (mpsi) xylem pressure potential, and midday net photosynthesis (mphoto) for PIN_PON and PIN_ARI trees at three sites (MTL, PAL, and LIZ) in the Santa Catalina Mountains in January 2006. The numeral "2" following a response name indicates removal of outlier data points. Significant ($\alpha < 0.05$) terms are bolded.

Response	Adj R ²	F(p-value)	Term	Df	SS	F-value	P-value
pDACF	-0.1441	0.9483	Species	1	0.0001	0.0215	0.8851
			Site	2	0.0010	0.1578	0.8852
			Residuals	18	0.0571		
mLACF	0.5189	0.0009	Species	1	0.0062	4.2386	0.0543
			Site	2	0.0331	11.2944	0.0007
			Residuals	18	0.0264		
mLACF2	0.6782	4.892e-05	Species	1	0.0062	6.0578	0.02484
			Site	2	0.0421	20.5039	2.95E-05
			Residuals	17	0.0174		
ppsi	0.5908	0.0002	Species	1	0.0084	0.2027	0.6579
			Site	2	0.9304	11.1955	0.0007
			Residuals	18	0.7479		
mpsi	0.6981	5.13E-05	Species	1	0.0051	0.1668	0.6884
			Site	2	0.9589	15.7453	0.0002
			Residuals	18	0.4872		
mphoto	0.4595	0.0026	Species	1	3.9908	2.8524	0.1085
			Site	2	16.9186	6.0462	0.0098
			Residuals	18	25.1839		
mphoto2	0.4673	0.0042	Species	1	3.9908	5.9438	0.0268
			Site	2	3.9617	2.9502	0.0812
			Residuals	18	10.7429		

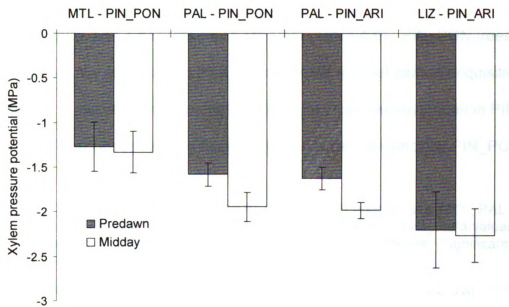


Figure 4-8. Xylem pressure potential (Ψ_p) from excised needles of PIN_PON and PIN_ARI trees at three sites (MTL, PAL, and LIZ) in the Santa Catalina Mountains in January 2006. Values are means; bars are ± 1 standard deviation.

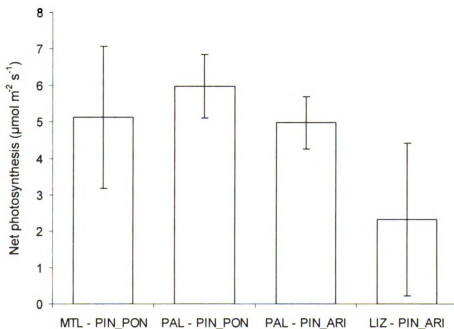


Figure 4-9. Midday net photosynthesis (A) results for PIN_PON and PIN_ARI trees at three sites (MTL, PAL, and LIZ) in the Santa Catalina Mountains in January 2006. Values are means; bars are ± 1 standard deviation.

Following removal of the outlying data points, the species difference in midday LACF and A become more apparent (Table 4-9). PIN_PON trees had higher potential and realized PSII quantum yield and net carbon acquisition, while leaf water status was more favorable (i.e., less negative) than in PIN_ARI trees. All responses indicate higher light and water efficiency by PIN_PON.

Table 4-9. Mean responses by PIN_PON and PIN_ARI trees by site (MTL, PAL, and LIZ) and across sites (Combined) following removal of three outlying data values. Responses listed in Table 4-8. Standard deviations in parentheses. Significant ($p < 0.05$) responses (Table 4-8) are bolded.

Response	PIN_PON			PIN_ARI		
	MTL	PAL	Combined	PAL	LIZ	Combined
pDACF	0.68 (0.49)	0.66 (0.07)	0.68 (0.06)	0.67 (0.05)	0.66 (0.05)	0.66 (0.05)
mLACF2	0.32 (0.02)	0.46 (0.04)	0.43 (0.07)	0.35 (0.03)	0.42 (0.02)	0.40 (0.04)
ppsi	-1.3 (0.3)	-1.6 (0.1)	-1.5 (0.2)	-2.2 (0.4)	-1.6 (0.1)	-1.8 (0.3)
mpsi	-1.3 (0.2)	-1.9 (0.1)	-1.8 (0.3)	-2.3 (0.3)	-2.0 (0.1)	-2.1 (0.2)
mphoto2	6.2 (0.6)	6.0 (0.9)	6.0 (0.8)	3.4 (1.2)	5.0 (0.7)	4.7 (1.0)

Discussion

Controlled whole-seedling freezing test

Differential cold tolerance of organs across the three “seasons” of cold hardiness was expected (Sakai and Larcher 1987). In this study, needle tissue was less cold tolerant than cambial and bud tissue during the Hardening and Winter stages, while cambium became the least cold tolerant during Deacclimation (Table 4-10). Bud tissue was the most hardy until Deacclimation when its LT_{50} was similar to that of needle tissue. In fact, little difference in needle cold hardiness across seasons was observed, with species differences only during the Winter stage (Table 4-5). In contrast, Burr et al. (1990) calculated much lower LT_{50} values as well as a 3° C increase in needle cold tolerance from

hardening through simulated winter, and a subsequent 8° C decrease in cold tolerance during deacclimation (Figure 4-10). Their LT₅₀ was estimated by interpolating 50% index of injury from an inverted, modified Gauss sigmoid model of electrolyte leakage against test temperature (Burr et al. 1990), while this study estimated LT₅₀ for needles by interpolating the temperature from a linear regression at 50% of the mean control (3° C) response. Low response values at higher test temperatures increase the (-) slope (Figure 4-3), thus increasing the interpolated LT₅₀ value, which could contribute to the higher LT₅₀'s observed in this study in comparison to Burr et al. (1990). Consequently, tissue and species differences in LT₅₀'s are more informative than their absolute values.

Table 4-10. Cold tolerance (LT₅₀) of combined PIN_PON and PIN_ARI tissues from this study and from Burr et al. (1990) across three stages of cold acclimation: Hardening, Winter, and Deacclimation. The Winter value for Southwestern ponderosa pine needles for Burr et al. (1990) was interpolated between two values.

Response	Hardening	Winter	Deacclimation
Needle	-9.6° C	-9.1° C	-10.0° C
Needle (Burr et al. 1990)	-18.7	[-22]	-13.6
Cambium	-12.4	-10.2	-4.4
Bud	-16.0	-14.1	-10.1

The lower cold tolerance of needle tissue by both PIN_PON and PIN_ARI during the Hardening and Winter stages suggests that hardening, and thus photosynthetic downregulation, had not fully occurred. The PSII quantum efficiency for the combined species (0.78) in the control treatments was close to the theoretical optimum of 0.832 for healthy plants (Björkman and Demmig 1987); the mean value dropped to 0.71 during deacclimation. However, PIN_PON had 4-6% higher PSII quantum efficiency in the first two stages and

then 10% lower efficiency during deacclimation than PIN_ARI in the control groups (Figure 4-1).

Photosynthetic downregulation in conifers is induced by a combination of environmental influences, including day length, temperature, and radiation, in concert with respiratory demand for processed carbon. If the plant remains metabolically active, then reduction in photosynthesis becomes less sink regulated. While the temperature and photoperiod in this study closely followed Burr et al. (1990), I was unable to maintain the same light level. Consequently, leaf-level light was $\sim 300 \mu\text{mol m}^{-2} \text{ s}^{-1}$ for the Acclimation and Winter stages, with natural lighting exceeding this level during Deacclimation; in contrast, Burr et al. (1989, 1990) sustained $518 \mu\text{mol m}^{-2} \text{ s}^{-1}$, which is closer to the light saturation value ($600 \mu\text{mol m}^{-2} \text{ s}^{-1}$) reported by Helms (1972) for mature ponderosa pine trees. Although pigment analysis was not conducted, I would expect little conversion of V to A+Z. Instead, the seedlings in this study were photosynthetically active to maintain respiratory carbon demand, thus the rate of hardening relative to other tissues was delayed with slow recovery during deacclimation (Table 4-5).

Resistance to freezing temperatures by the bud tissue was consistently higher than by the cambium across all stages of cold tolerance (Tables 4-5 and 4-9). The method for examining but not measuring injury was the same across these two tissues; response was continuous for cambium and binary for bud. Consequently, the error distribution should have varied, yet the data were parallel within species (Figure 4-2), suggesting only a difference in tissue cold tolerance

and not a problem with data analysis. Sakai and Larcher (1987) note that bud resistance develops slightly later than needle resistance; this study found a 3-5° C increase in resistance by needles than buds, again suggesting that photosynthesis was not fully downregulated. Cambial tissue of PIN_ARI had successively more injury across acclimation stages even in the control groups, suggesting that sustained cold growing conditions can impose substantial mortality in PIN_ARI seedlings.

Observational whole-seedling freezing test

Despite having severely reduced water supply due to the frozen soil, and likely frozen stem storage, the 3-year-old seedlings had remarkably high PSII quantum efficiency (\bar{x} = 0.270, s = 0.053). On a colder day (-8 to -10° C versus mean maximum -2° C), Verhoeven et al. (1999) measured F_v'/F_m' for detached ponderosa pine needles between 0.15-0.20. PSII quantum efficiency should decrease with temperature, and ponderosa pine has been noted to retain some photosynthetic capacity through winter (Marshall et al. 2001). However, given the duration (week) of subfreezing maximum temperatures preceding this test, extracellular and xylem freezing was expected to have reduced PSII quantum efficiency beyond that observed in this study. Incipient light levels were not measured, but the seedlings were exposed to at least diffuse bright to sunny days. The “leaf temperature” plotted in Figure 4-5 represents that measured by the thermocouple inside the fluorometer’s cuvette, which was representative of air temperature inside the greenhouse. Seedlings were measured immediately

(i.e., within 1.5 min) as they were transferred to the lower-light greenhouse (13° C); the time between outdoor and greenhouse temperature did not likely raise inner leaf temperatures sufficiently to affect PSII efficiency. This supposition is borne out by the lack of significance of the temperature term (Table 4-6).

Verhoeven et al. (1999) recorded an increase in the ratio F_v/F_m of 0.23 15 min after moving samples from -23° C to room temperature, a much larger change in temperature of approximately 43° C. Consequently, temperature likely had little effect on PSII quantum efficiency observed in this study.

The significant finding from this test is that PIN_PON seedlings exhibited higher PSII quantum efficiency than the Mixed and PIN_ARI seedlings (Table 4-6). In addition, the Mixed trees, which may be hybrids between PIN_PON and PIN_ARI (Peloquin 1984, Rehfeldt et al. 1996, Epperson et al. 2001), had a mean PSII quantum efficiency intermediate to the two purported parent species, although the difference to PIN_ARI was not significant ($p=0.569$). Intermediate cold tolerance has also been observed in white x Himalayan blue pine hybrids (Lu et al. 2007).

Small trees on the mountain

Removal of three significant outlier data points improved the demonstration of differential realized PSII quantum yield and net carbon acquisition by 'small' PIN_PON and PIN_ARI trees growing in the Santa Catalina Mountains. Although the sample sizes were small ($n=2-3$) at the elevational

extremes, sufficient number of sympatric trees were present at PAL to detect a species effect.

The pattern of net photosynthesis, in combination with the xylem pressure potential and chlorophyll fluorescence data, across sites suggests different limiting factors to survival during the winter in these mountains. The mean maximum PSII quantum yields for both species were lower than recorded by the hardening and acclimated seedlings in the controlled laboratory experiment, but similar to the deacclimating seedlings. This suggests that the Santa Catalina Mountain trees were more innately hardened but yet able to utilize light resources during the day. The PIN_ARI trees at LIZ had higher net photosynthesis but also larger change in needle water status than the PIN_ARI trees at PAL; the higher temperatures lower in elevation stimulate higher rates of respiration and thus demand for carbon gain, despite the more xeric conditions at LIZ. The PIN_PON trees at the high-elevation MTL site also exhibited higher net photosynthesis than those at PAL but had much lower realized PSII quantum efficiency with no change in needle water status; these trees are likely much more hardened than those at PAL, suggesting a strong site effect (Table 4-7). However, gas exchange is occurring, as evidenced by substantial net photosynthesis and diurnal increases in xylem pressure potential (Table 4-9). Most obvious when compared at PAL, PIN_PON trees have higher PSII excitation capture efficiency, higher net photosynthetic rates, and smaller changes in needle water status, a critical component to surviving winter desiccation (Sakai and Larcher 1987), than do PIN_ARI trees.

Implications of differential cold tolerance on distribution

All of the experiments in this study have demonstrated that PIN_PON is more cold tolerant than PIN_ARI, while only the controlled laboratory experiment quantified differences in cold tolerance. Using the most sensitive (i.e., highest LT_{50}) tissues to calculate species differences, one finds a 1°, 1.25°, and 0.75° C difference across the three acclimation stages for needle electrolyte leakage for the first two values and bud mortality for the third value. Given that needle and bud primordia in *Pinus* are similarly tolerant to cold (Sakai and Larcher 1987), a mean of 1° C difference can be assumed from this experiment. This seemingly minor temperature differential translates to 133 m in elevation, using Shreve's (1915) data of an adiabatic lapse rate of 7.5° C per 1000 m elevation for the Santa Catalina Mountains. Given a current upper elevational boundary for PIN_ARI of 2548 m on the south face of Mount Lemmon (Epperson et al. 2001) and the 133-m differential predicted by differences in cold tolerance in this study, then the upper boundary for PIN_PON should be ~112 m below the very peak of the mountain. In fact, on this aspect, PIN_PON extends to the top and north side of the mountain, suggesting that the difference in cold tolerance estimated by this experiment is conservative. Instead, assuming that the top of the mountain is the upper elevational boundary for PIN_PON, then the differential cold tolerance would be 1.8° C, based on Shreve's (1915) model. This difference is not very large nor far from the species differences estimated from the controlled laboratory experiment (Table 4-5). In fact, the difference in cold tolerance as related to elevational difference will become moot if winter temperatures in the

region increase by the projected 2.8° C by 2100 (USEPA 1998). Kupfer et al. (2005) predict an upward migration of communities with a 53% loss in montane forest on Madrean mountain islands such as the Santa Catalina Mountains given projected local climatic changes (USEPA 1998). Consequently, assuming minimal dispersal limitation and disturbance (or lack of disturbance), winter conditions at the top of the Santa Catalina Mountains will become suitable for PIN_ARI within this century.

CHAPTER 5

THE ROLE OF DROUGHT TOLERANCE IN STRUCTURING *PONDEROSAE* DISTRIBUTION IN THE SANTA CATALINA MOUNTAINS OF ARIZONA

Introduction

While tolerance to cold conditions in determining high latitude or elevation limits in pine distribution is well known, the cause of the lower elevation boundary is less well understood (Rundel and Yoder 1998). The tacit assumption is that intolerance to more xeric conditions, or drought, constrains regeneration at lower elevation (Barton 1993). Daubenmire (1943) showed that soil drought is the primary determinant for lower elevation distribution for Rocky Mountain conifer seedlings, while Haller (1959) and Yeaton et al. (1980) demonstrated the lethal effect of drought stress on ponderosa pine (*Pinus ponderosa*) seedlings. However, the extensive range of habitats in which ponderosa pine can be found implies that a suite of genetically controlled and phenotypically plastic mechanisms have evolved that allow survival in a variety of soil-water conditions (Rundel and Yoder 1998).

Plants must trade-off the maintenance of whole-plant water status for the requirement of the carbon substrate for photosynthesis. The entry of carbon into the plant requires concomitant loss of water through transpiration at the stomata. As air temperature increases, the water vapor gradient increases at the stomata, thereby increasing stomatal conductance (g_s), or loss of water through the stomata. This increases the tension (negative pressure, Ψ_p) of water within the root-stem-leaf pathway, which is exacerbated by low soil water availability.

When Ψ_p becomes sufficiently negative, cavitation, or air infusion into the xylem, occurs and an embolism is formed (Sperry and Tyree 1990). Cavitation results in a sustained increased resistance to water transport in those vessels or tracheids and, if sufficient amount of hydraulic conduits cavitate, wilting with eventual plant death (Tyree and Sperry 1988). The most direct means of preventing cavitation is by stomatal closure (Sperry et al. 1993) and recovery of plant water status through water uptake in the roots. It is thought that stomatal closure is stimulated by negative feedback from cells surrounding the stomatal complex in response to cell water potential (Hubbard et al. 2001) and/or root signaling via abscisic acid (Jackson et al. 1995).

Plants have evolved a number of other mechanisms by which water loss relative to carbon acquisition is balanced. Rooting architecture varies genetically and depending on soil characteristics in ways to help access available soil water. For example, ponderosa pine can develop very deep roots (24 m; Stone and Kalisz 1991) to access deep water sources and interstitial bedrock water (Rundel and Yoder 1998). Roots also vary in their ability to extract available water; Fowells and Kirk (1945) reported ponderosa pine seedlings extracting water from soil below the wilting point of sunflowers. Pines also maintain a significant portion of functional xylem sapwood with storage of reserve water (Rundel and Yoder 1998). In comparison to populations growing in more mesic sites, genetically undifferentiated populations of ponderosa pine have reduced total leaf surface area (A_L) relative to sapwood area (A_S), even with higher whole-tree leaf specific hydraulic conductance (K_L), thereby buffering total water loss (Maherali

et al. 2002). The anatomical properties of xylem also contribute to cavitation resistance. For example, larger conduits reduce overall hydraulic resistance, but larger diameter vessels are more susceptible to irreparable cavitation than tracheids. Stronger pit membranes are less porous and thus cause higher resistance to both water flow and air infusion (Piñol and Sala 2000). At the leaf-level, higher water-use efficiency (WUE), whether by increasing photosynthetic rate (A), decreasing g_s , or effectively dissipating heat, results in better maintenance of whole-plant water status relative to carbon gain (Monson and Grant 1989, Rundel and Yoder 1998). In contrast, Zhang et al. (1997) found no relationship between drought tolerance and high WUE, measured by instantaneous gas exchange and carbon isotope ratio ($\delta^{13}\text{C}$), a measure of integrated WUE (Farquhar et al. 1989), in highly controlled ponderosa pine seedlings. Furthermore, in greenhouse studies, ponderosa pine seedlings from geographically variable sources differed in biomass allocation patterns but not in g_s , A , or needle Ψ_p (Cregg 1994).

The combination of anatomical and ecophysiological attributes contributing to drought tolerance, especially the apparent trade-off between K_L and resistance to cavitation, is an active area for research. Recent evidence indicates that ponderosa pine is highly plastic (Maherali 2002), reduces $A_L:A_S$ in xeric habitats (Carey et al. 1998), maintains high Ψ_p in drought conditions (Hubbard et al. 2001), and has similar vulnerability to cavitation across habitats and climates (Maherali and DeLucia 2000) but increased stomatal control (Piñol and Sala 2000) and sapwood water storage (Stout and Sala 2003) relative to

codominant Douglas-fir (*Pseudotsuga menziesii*). These combinations of adaptations to low soil-water and high vapor pressure deficit contribute to differential survival across environmental gradients. For example, within a group of Southwestern montane conifers distributed along an elevational gradient, seedlings from lower elevation species suffered less photosynthetic depression yet maintained higher plant water status under imposed drought (Barton and Teeri 1993). Mechanistically linking distribution limits to ecophysiological responses should improve our understanding of species responses to climate.

In the Santa Catalina Mountains of southern Arizona, populations of the Southwestern ponderosa pine (*Pinus ponderosa* var. *scopulorum* Engelmännii) exhibit a discontinuous lower elevational boundary suggesting an abiotic influence. Although located in the Sonoran Desert, the forests in the Santa Catalina Mountains experience reduced frostfree seasons (17 weeks at 2438 m; Shreve 1915) due to high elevation (2793 m peak). In addition, the climate is characterized by a bimodal distribution of precipitation as a result of an infusion of subtropical high pressure from the south during the summer months (Sheppard et al. 2002); consequently, a pronounced drought (“arid foresummer”) occurs through late spring until the mid-summer rains (“monsoon”) arrive. At the lower elevational boundary for Southwestern ponderosa pine, a closely related *Ponderosae*, Arizona pine (*Pinus arizonica* Engelmännii), overlaps in distribution forming a transition zone at approximately 2430-2550 m in elevation on a south aspect (Epperson et al. 2001). This transition zone has been noted in Santa Catalina Mountains (Whittaker and Niering 1965) and other mountain islands of

the Southwest (Dodge 1963, Barton 1993), but only Barton and Teeri (1993) have sought an ecophysiological explanation for the lower elevational limits. Arizona pine was included in Barton's dissertation work but was not represented by sufficient replicates for analysis (A. Barton, personal communication).

The objective for this study was to determine if critical measures of drought tolerance indicated a genetic difference between Southwestern ponderosa pine and Arizona pine. If evidence suggests that the higher elevation Southwestern ponderosa pine ("PIN_PON") were less drought tolerant than Arizona pine ("PIN_ARI"), then the correlation of their differential distribution by elevation would be supported by physiological (mechanistic) differences. In one series of experiments, I measured diurnal A , transpiration (Tr), and Ψ_p from coincident 'small' PIN_PON and PIN_ARI trees across three hydrologically important seasons: winter (January-February), arid foresummer (June), and monsoon (August); Ψ_p was compared to trees from other elevations, as well. A second experiment tested for differences in integrated WUE ($\delta^{13}C$) and nutrient dynamics in needle (leaf) tissue of coincident PIN_PON and PIN_ARI. The third experiment investigated photosynthetic function, measured as Photosystem II (PSII) excitation capture efficiency (F_v'/F_m' ; Schreiber et al. 1994), relative to dehydrating needles of PIN_PON and PIN_ARI. In the final experiment, xylem vulnerability to cavitation was measured from PIN_PON and PIN_ARI stems across an elevational gradient; the laboratory work for this portion of the study was conducted by Anna Jacobsen (MSU, Michigan State University).

Methods

Tree and site selection

At three locations across an elevational gradient, I selected “small” PIN_PON and PIN_ARI trees for the ecophysiological experiments in this study (Table 5-1). Small trees were chosen because they are more sensitive to changes in soil water availability and temperature than larger trees with more developed root systems and larger stem storage capability (Rundel and Yonder 1998). The Aspen fire (CNF 2003) eliminated most of the small-diameter trees and virtually all seedlings from most of the *Ponderosae* forest in the Santa Catalina Mountains (personal observation). Consequently, I attempted to standardize the size by diameter across sites. A second criterion was to locate similarly sized PIN_PON and PIN_ARI trees as close as possible to each other (“paired”) without other nearby trees influencing potential soil water availability. At each site, species designation was determined by calculating the mean number of needles per fascicle across 5 years of needles in one terminal shoot; a mean less than 3.2 was considered to be PIN_PON, and a mean greater than 4.6 needles per fascicle was a PIN_ARI tree (Peloquin 1984). Trees with mean needle number between 3.2 and 4.6 were not used in this study because they may represent hybrids between PIN_PON and PIN_ARI (Peloquin 1984, Rehfeldt et al. 1996, Epperson et al. 2001).

Table 5-1. Characteristics of 'small' trees used for gas exchange and xylem pressure potential measurements in 2005-06 at the Mount Lemmon (MTL), Palisade Rock (PAL), and Lizard Rock (LIZ) sites.

Site	Location (NAD83)	Elev (m)	Tree	Species	DBH (cm)	Height (m)
Mount Lemmon	32.4396°N, 110.7871°W	2770	MTL 221	PIN_PON	19.3	6.2
			MTL 222	PIN_PON	5.1	2.3
			MTL 223	PIN_PON	6.8	3.0
Palisade Rock	32.4138°N, 110.7149°W	2475	PAL 1	PIN_PON	12.9	4.4
			PAL 2	PIN_ARI	13.0	3.9
			PAL 3	PIN_PON	19.3	5.3
			PAL 4	PIN_ARI	12.4	4.1
			PAL 5	PIN_PON	17.0	2.4
			PAL 6	PIN_ARI	8.1	3.4
Lizard Rock	32.3844°N, 110.6930°W	2135	LIZ 1	PIN_ARI	17.7	3.6
			LIZ 2	PIN_ARI	12.2	3.1
			LIZ 3	PIN_ARI	7.0	2.7

I selected three major sites for this study: Mount Lemmon (MTL), Palisade Rock (PAL), and Lizard Rock (LIZ). The MTL site is located on a gentle slope just south of the summit of Mount Lemmon. Three PIN_PON trees at the north edge of the forest cover were selected; PIN_ARI has not been documented at this elevation. The PAL site is located downslope of the Mount Bigelow radio towers and upslope from the Palisade Ranger Station (Coronado National Forest). Brown (1968) and Budelsky (1969) measured gas exchange from “ponderosa pine” at this site, but they did not differentiate between PIN_PON and PIN_ARI. This site was not selected due to this previous work but rather because it was identified as a possible steep transition zone between the two taxa; Epperson et al. (2001) documented the steep transition on the south face of Mount Lemmon at similar elevation. Three “pairs” of PIN_PON – PIN_ARI trees growing closely (<3 m) were located and chosen for this study. Another 44 trees were identified, with 5 from each species used to increase sample size for the Ψ_p

measurements. The LIZ site is located along a small ridge northeast of Lizard Rock and across the Catalina Highway. The xeric ridge is bare bedrock with pockets of disintegrated granite, while the valleys on both sides of the ridge receive floodwater and are thus much more mesic. Three PIN_ARI trees were selected from this site; PIN_PON has not been documented in this area. All of the trees were labeled with both aluminum write-on and nailed disc tags. Additional PIN_ARI trees for the xylem vulnerability study were selected from a ridge south of Rose Canyon Lake (RC, 32.3964°N, 110.6932°W (NAD83), 2175 m elevation) but were not labeled.

Seasonal gas exchange and xylem pressure potential

Diurnal net photosynthetic (A) and transpiration (Tr) rates were measured from PIN_PON and PIN_ARI needles to investigate relative changes in gas exchange through the course of the day and across seasons. Needles from three “pairs” of PIN_PON – PIN_ARI trees were selected for measurements from the terminal shoot on the lowest living branch with southern exposure. Within an hour prior to measurements, three PIN_PON fascicles (9 needles) and two PIN_ARI fascicles (10 needles) were taped at the fascicle sheath so as to prevent needle crossing within the cuvette, but the needles remained attached to the branches; this number of needles per species covered the entire cuvette with no overlap. One pair of trees was measured per day for the arid foresummer (14/16/18 June 2005) and monsoon (2/4/6 August 2005) seasons, while all three pairs were measured in the same day during the winter (31 January 2006).

Consequently, except for winter, species comparisons are limited to measurements from the paired trees. Frequency of measurements varied but were approximately hourly, with 10 points taken per tree, while measurements were taken from predawn through afternoon during the monsoon and through dusk during winter and the arid foreshummer; regular afternoon thunderstorms (and even funnel clouds) during the monsoon prevented many opportunities for data collection.

Gas exchange was measured using the standard 2x3-cm sensor head in a LI-COR 6400 Portable Photosynthesis System (LI-COR Biosciences, Inc., Lincoln, Nebraska, USA). The actinic light, infrared gas analyzer (IRGA), and CO₂ mixer were calibrated prior to measurements each day, and the IRGAs were matched prior to each set of paired measurements within a time period. Carbon dioxide concentration was maintained at approximately 400 $\mu\text{mol CO}_2 \text{ mol}^{-1}$, which was usually the ambient concentration, with CO₂ gas cartridges (6400-01 CO₂ Injector, LI-COR Biosciences, Inc.). Relative humidity was stabilized across measurements from the paired trees within a time period. A constant block temperature was used to stabilize leaf temperature across trees within a set of paired measurements. Incident light (6400-02B, LI-COR Biosciences, Inc.) for paired measurements was selected based on maximum light intensity (9901-013 External Quantum Sensor, LI-COR Biosciences, Inc.) under full sky prior to each set of measurements. Leaf temperature was measured by contact thermocouple (6400-04 Leaf Temperature Thermocouple, LI-COR Biosciences, Inc.) inside the

cuvette. Power was supplied by a number of rechargeable batteries (6400-03 Rechargeable Battery, LI-COR Biosciences, Inc.).

Diurnal patterns in gas exchange are difficult to statistically compare across trees, species, days, and seasons because changes in instantaneous gas exchange occur rapidly in response to highly variable conditions, such as solar radiation, temperature, and wind (Jarvis 1976). Consequently, analysis of this experiment is limited to intrapair comparisons of patterns in response to mean climatic fluctuations (e.g, incident light and temperature). The rate of change (i.e., slope) in A and T_r in response to leaf temperature was compared by species and season with paired t-test in R (R Development Core Team 2007), assuming species within a day's measurements represents the before-and-after treatment.

Coincident with the diurnal gas exchange measurements, xylem pressure potential (Ψ_p) was measured from PIN_PON and PIN_ARI fascicles to assess whole-tree water relations. At predawn, midday, and dusk (arid foresummer only), fascicles were harvested from the trees used for the gas exchange experiment, as well as 5 additional trees of each species to increase sample size. On other days, diurnal Ψ_p was also measured from PIN_PON trees at MTL and PIN_ARI trees at LIZ (Table 5-1). Fascicles were selected from a different branch but same whorl number as that from which diurnal gas exchange was being measured. Each of 5-10 fascicles was excised at the base of the fascicle sheath with a razor blade, immediately placed into a prelabeled resealable plastic bag with moist paper toweling, and then placed in a small cooler containing ice

packs. Within 2.5 h, Ψ_p was measured from up to 7 fascicles per tree with a pressure chamber (PMS Instruments, Inc., Corvallis, Oregon, USA) and averaged for each tree. Seasonal differences in predawn and midday Ψ_p across sites were compared by the Welch two-sample t-test, while species differences by season and time of day were examined with univariate ANOVA; site effects were nested within species. All statistical analyses were conducted in R (R Development Core Team 2007).

Integrated water-use efficiency and nitrogen dynamics

Needle tissue harvested from sympatric PIN_PON and PIN_ARI trees in the Santa Catalina Mountains was analytically measured for species and annual differences in integrated water-use efficiency (WUE), as measured by carbon isotope composition ($\delta^{13}\text{C}$; Farquhar et al. 1989). Given the physiological relationships between foliar nitrogen content (%N) and $\delta^{13}\text{C}$ (Sparks and Ehleringer 1997) and nitrogen isotope composition ($\delta^{15}\text{N}$; Hobbie et al. 2000), these parameters were also measured in the same analysis to investigate potential differences in potential photosynthetic capacity (Reich et al. 1995) and nitrogen acquisition (%N, $\delta^{15}\text{N}$). Amount of structural carbon (%C) in the samples was analyzed as a signal for differences in carbon-to-nitrogen (C:N) allocation.

Needle tissue was collected in the late afternoon through early evening of 26 October 2005 for both this and the following experiment (*Photosynthetic function during dehydration*). I harvested one healthy lower branch ~0.8-m in

length from each of 11 PIN_PON trees near the summit of Mount Lemmon, 12 PIN_PON trees and 8 PIN_ARI trees at PAL, 6 PIN_ARI trees from ridges surrounding Rose Canyon Lake (RCL), and 4 PIN_ARI trees at LIZ. Sampled trees included those listed in Table 5-1. Immediately after removal from the tree, each branch was placed in a separate plastic bag containing moist paper toweling inside a large cooler with ice packs. To reduce the effect of differential soil water availability, the base of the branches were submersed in water in a 5-gal bucket, ~1 cm was cut off from each end to restore sapflow into the branch, and the base of the branches remained in water for ~ 7 h before being sealed with instant cyanoacrylate adhesive (All Purpose Instant Krazy Glue Gel, Krazy Glue, Columbus, Ohio, USA). Sealed branches were returned to the plastic bags with moist toweling, placed into the cooler with ice packs, and shipped by air to MSU. Approximately 20 h after the branch ends were sealed, the branch ends were recut under water in a 5-gal bucket and rehydrated in a humid walk-in cooler room (4° C) for ~58 h. After removing and processing fascicles for the next experiment (see *Photosynthetic function during dehydration*), the remaining fascicles on the terminal shoot were excised by razor blade at the base of the fascicle sheath, separated by year of production, and placed into prelabeled envelopes (No. 10 28-lb Heavy-Duty Brown Kraft Envelope, Columbian, Stamford, Connecticut, USA) to dry at room temperature.

In early June 2006, I selected samples from 10 trees from each species growing at the PAL site based on trees having the largest range of annual production (e.g., 2001-2005 fascicles) in sampled fascicles; needles from an 11th

PIN_PON tree were also included, but, at the time, there was some doubt as to its taxonomic nature because of finding more >3-neededled fascicles in the samples than when in the field. All of the samples within their envelopes were placed into the drying oven (60° C) for at least 24 h before processing (CPSIL 2006). At least 5 (up to 12) fascicles with the appropriate number of complete, uninjured, and consistently colored needles (e.g., PIN_PON fascicles had to have 3 needles) were selected from each year for each tree, trimmed by razor 1 cm from the terminus of the fascicle and from the distal portion of the needle, and cut into ~1-cm pieces on a dry glass plate. The pieces were poured into a small stainless steel canister containing a small stainless steel rod, both of which were thoroughly cleaned, rinsed with deionized distilled water (NANOpure Ultrapure Water System, Model D4741, Barnstead International, Dubuque, IA, USA), and dried between samples. The tissue was pulverized within the covered canister by a ball-mill grinder (Model 6, WIG-L-BUG Amalgamator, Crescent Dental Manufacturing Company, Lyons, Illinois, USA) for 5-10 min per sample until becoming a fine powder (CPSIL 2006). [Milling with a standard hand-held coffee grinder and UDY Cyclone Sample Mill (0.5- and 1.0-mm screens; Seedburo Equipment Company, Chicago, Illinois, USA), even for 15+ min, produced visibly heterogeneous tissue particles unsuitable for isotopic analysis (CPSIL 2006).] The pulverized tissue was stored in new 1-dram glass vials (Gerresheimer Glass, Inc., Vineland, New Jersey, USA) that were color-taped by needle-year and labeled by tree, species, and year. The capped vials were stored at room temperature.

The powdered samples were prepared for laboratory analysis by removing and packaging ~4.000-mg aliquots into 5x9-mm pressed tin capsules (COSTECH Analytical Technologies, Inc., Valencia, California, USA). The capsules were weighed before and after adding a sample followed by crimping with a microanalytical balance (Model CP2P, Sartorius AG, Goettingen, Germany). Sterile technique was used to prevent sample contamination since the entire capsule is consumed in a mass spectrometer. Crimping was accomplished by placing the preweighed capsule in one of three depressions in an aluminum block (10 x 5 cm) and carefully pinching and then shaping the capsule to a tight ball with two pairs of sterile forceps (CPSIL 2006). Eighty-five capsules, in addition to a number of duplicates to check the analysis, containing pulverized needle tissue from 21 trees were placed into a 96-well cell plate (Greiner Bio-One North America, Inc., Monroe, North Carolina, USA) and shipped overnight on 20 June 2006 for analysis at the Colorado Plateau Stable Isotope Laboratory (CPSIL, Northern Arizona University, Flagstaff, Arizona, USA). The samples were processed on 5 August 2006 by a continuous-flow gas isotope-ratio mass spectrometer (Thermo-Finnigan Delta^{plus} Advantage, Thermo Fisher Scientific, Inc., Waltham, Massachusetts, USA) interfaced with an elemental analyzer (ECS4010, COSTECH Analytical Technologies, Inc., Valencia, California, USA); specifications can be found at CPSIL (2006). CPSIL used a variety of standards to check raw isotope data (NIST peach leaves, pine needles, apple leaves, tomato leaves, bovine liver, and mussel tissue; and caffeine - Aldrich), normalize raw isotope data (NAEA CH6, CH7, N1, and N2), and correct raw %C and %N

data (acetanilide, BBOT, cystine, methionine, sulfanilamide, cyclohexanone, and nicotinamide). Their external precision from the standards is reported as $\pm 0.10\text{‰}$ or better for $\delta^{13}\text{C}$ and $\pm 0.20\text{‰}$ or better for $\delta^{15}\text{N}$; $\delta^{13}\text{C}$ and $\delta^{15}\text{N}$ are expressed relative to VPDB and air, respectively (CPSIL 2006).

The analysis of $\delta^{13}\text{C}$, $\delta^{15}\text{N}$, %C, %N, and C:N could be approached by assuming independence in the variables across years within a given tree or by assuming that they represent repeated measures from the same individuals across years. The physiological questions relate to the relationship of timing of current-year needle production to current-year nitrogen and carbon acquisition, and the lability of nitrogen and carbon from one year's needles to another year. Budelsky (1969) showed that ponderosa pine needles at the PAL site begin slowly elongating in mid-May, have the highest rate of elongation during July and early August, and complete extension by the end of August. Consequently, I will assume that current-year needle structural carbon was acquired during the growing season. There is no *a priori* reason to assume that structural carbon is labile; Billow et al. (1994) report strong seasonal differences in foliar starch and sugar concentration, but no difference from August-October in New Mexican Douglas-fir. Total nitrogen shifts seasonally, at least in Douglas-fir (Billow et al. 1994), and purportedly translocates from older to younger foliage (Rundel and Yoder 1998). Consequently, both %N and $\delta^{15}\text{N}$ are expected to show some degree of temporal autocorrelation. Potvin and Lechowicz (1990) demonstrated complex approaches to modeling repeated measures from individuals in ecophysiological experiments. However, the simplest statistical approach to

recognize repeated measures is to compare mean responses by species within a given year by one-way ANOVA, with species as the fixed factor, which was achieved using R (R Development Core Team 2007). Another approach is to conduct an ANOVA on each response by nesting individual tree responses in year, which in turn is nested in species: response ~ species (year (individual tree)); this approach was also calculated in R. In addition, relationships between isotopic composition and nutrient content by species were assessed in two-factorial ANCOVAs with nutrient content as a continuous covariate to trees nested in species. All of the nested analyses indicated no significant ($p>0.26$) effects of individual trees on patterns observed across years and species (Table 5-5), thus the nested approach was considered satisfactory for investigating species x year responses.

Photosynthetic function during dehydration

Needles collected from PIN_PON and PIN_ARI trees across an elevational gradient in the Santa Catalina Mountains were slowly dehydrated with concomitant measurement of PSII excitation capture efficiency to determine the relationship of photosynthetic capacity during severe drought. PSII excitation capture efficiency was estimated by the ratio of variable to maximum chlorophyll fluorescence when acclimated to light. I used a pulse-amplitude modulated fluorometer (6400-40 Leaf Chamber Fluorometer, LI-COR Biosciences, Inc., Lincoln, Nebraska, USA) attached to the base LI-COR 6400 Portable Photosynthesis System. The fluorometer was calibrated before the first set of

measurements, zero-ed before each set, and adjusted to recommended settings: Saturating pulse (flash) - 0.8 s saturating multiple flash of $\sim 8800\text{-}9000 \mu\text{mol m}^{-2} \text{s}^{-1}$, 20KHz modulation, and 50 Hz averaging filter; a 6-s pulse of far red (“dark”) intensity of 8 turned on 1 s before and remain on for 1 s beyond actinic light off, 0.25 KHz modulation, and 1 Hz averaging filter; and Measurement light – intensity 2, 0.25 KHz modulation, 1Hz averaging filter, and 10 gain factor (LI-COR 2005a).

Needles from branches harvested on 26 October 2005 were used in this experiment; see *Methods* in previous experiment for collection, processing, and transport details. After hydrating overnight in the walk-in cooler (4° C), the buckets of branches were moved to the laboratory. At room temperature, one 2005 fascicle per branch (i.e., tree) was excised from the terminal shoot with a razor blade at the base of the fascicle sheath, weighed using an analytical balance (Model AJ100, Mettler Instrument Corporation, Hightstown, New Jersey, USA), immediately sealed with instant cyanoacrylate adhesive, and lightly marked at the base with colored typographic correction fluid (Liquid Paper, Sanford, Oak Brook, Illinois, USA) by species and relative elevation. After all fascicles (n=41) were processed (~ 1.7 h), PSII excitation capture efficiency (F_v'/F_m') was measured twice with the fluorometer, with a weight measurement between readings, and averaged for the initial value. Over the next 16 days, fascicle mass and F_v'/F_m' were remeasured 30 times. Laboratory conditions were monitored 2-3 times within each measurement period with a porometer (LI-1600 Steady State Porometer, LI-COR Biosciences, Inc., Lincoln, Nebraska,

USA). Needles were exposed to fluorescent lighting ($\bar{x}=9.5\pm1.1\text{SD } \mu\text{mol m}^{-2} \text{ s}^{-1}$) during normal laboratory hours; air temperature was relatively high ($\bar{x}=26.7\pm8.7\text{SD } ^\circ\text{C}$), and relative humidity varied with Michigan's weather ($\bar{x}=29.2\pm14.8\text{SD } \%$). After the last mass and F_v'/F_m' measurements, fascicles were dried in individual paper envelopes (No. 10 28-lb Heavy-Duty Brown Kraft Envelope, Columbian, Stamford, Connecticut, USA) for 6 days at 60° C in a ventilated drying oven (Model 637G Isotemp Oven, Fisher Scientific, Inc., Pittsburgh, Pennsylvania, USA) and then weighed to determine if all nonlabile water had been removed from the needles.

Relative loss of fresh (wet) mass and PSII excitation capture efficiency were modeled using 3-factor ANCOVA in R (R Development Core Team 2007). The former model used site and species as fixed factors and time since excision from the branch as a (continuous) covariate. The latter model also used site and species as fixed factors but included percent loss of fresh mass as the covariate. Nonstructural water remaining after the last mass and F_v'/F_m' measurements was tested against final mass by paired t-test (R Development Core Team 2007).

Xylem conductivity and vulnerability

Branch stems were collected from mature PIN_PON and PIN_ARI trees in the Santa Catalina Mountains on 20 October 2005 for determination of stem xylem vulnerability to cavitation and xylem specific conductivity. Throughout the morning, stem sections approximately 0.5 m in length were cut from the lowest living branch from trees at the MTL (n=11 trees), PAL (n= 9 trees per species),

RCL (n=7 trees), and LIZ (n=3 trees) sites. Stems with few curves, diameter between 5 and 10 mm, and no branches for at least 15 cm were selected. The cut stems were immediately double-bagged (Zip-Loc) with a moist paper towel, placed on ice, and transported via overnight shipping to Anna Jacobsen at MSU. Stems were refrigerated until measured, and all stems were measured within 3 days of collection. A. Jacobsen performed all sample preparation, conductivity measurements, methods documentation, and conductivity calculations for this experiment.

Each stem was prepared for conductivity measurements by trimming under water from each end until a straight, unbranched segment 6-9 mm in diameter and 14 cm in length was obtained. Stems were connected to a tubing system and flushed with low pH degassed water (pH 2 HCl) that had been passed through a 0.1 μm filter to remove gas emboli from stems. Stems were flushed for 1 h at 30 kPa. This relatively low pressure was used in order to avoid aspiration of tori in pit membranes. Hydraulic conductivity (K_h) of stems was then measured, and stems were flushed for additional 20 min intervals until a constant maximum hydraulic conductivity ($K_{h\text{max}}$) was obtained (usually less than 2 h). Hydraulic conductivity of stems was measured gravimetrically (Sperry et al. 1988) using an analytical balance (Model BP 121 S, Sartorius AG, Goettingen, Germany). Following determination of $K_{h\text{max}}$, stems were spun in a centrifuge (Sorvall RC-5B, DuPont Instruments, Wilmington, Delaware, USA) using a custom built rotor to generate known negative pressures (Alder et al. 1997). Stems were then reconnected to the tubing system and the new hydraulic

conductivity (K_h) determined. This process was repeated with successive spins generating more negative pressures until stems experienced >80% loss in hydraulic conductivity. Percent loss in hydraulic conductivity (PLC) was calculated as $[K_{hmax} - K_h] / K_{hmax}$. Vulnerability-to-cavitation curves were constructed by plotting the PLC against the water potential generated using the centrifuge. For each stem, curves were fit with a second-order polynomial model (Jacobsen et al. 2007) to predict the water potential at 50% loss in hydraulic conductivity (Ψ_{50}). Xylem specific hydraulic conductivity (K_s) of stems was determined using the K_{hmax} and the cross-sectional xylem area. Cross-sectional xylem area was measured using a dissecting microscope and digital calipers. The xylem diameter (without bark) and pith diameter were measured in two perpendicular directions, and the area of the calculated pith area (an oval defined by the radii in two directions) was subtracted from the xylem area (also calculated as an oval defined by the radii in two directions). The K_{hmax} was then divided by this area for each stem to yield the xylem specific conductivity ($\text{kg m}^{-1} \text{MPa}^{-1} \text{s}^{-1}$).

Ψ_{50} and K_s were modeled using two-factor ANOVA in R (R Development Core Team 2007). The full models included the main fixed factors of site and species, as well as their interaction. Given the unbalanced design, Type II sums of squares (SS; Langsrud 2003) were used to test hypotheses using the 'car' (Companion to Applied Regression; Fox 2006) package in R (R Development Core Team 2007). Means were compared at each factor level using Tukey's Honest Significant Difference (HSD) in R, which incorporates an adjustment for

unbalanced designs (R Development Core Team 2007).

Results

Seasonal gas exchange and xylem pressure potential

Species differences in diurnal gas exchange during the winter were similar during the morning and evening but highly variable during the midday (Figure 5-1). Incident radiation (PAR) peaked at $3000 \mu\text{mol m}^{-2} \text{s}^{-1}$ at midday, while leaf temperature (T_{leaf}) varied from -1°C at dusk to 14°C at midday (Figure 5-1). Transpiration (T_r) values were negative around dawn and after sunset, suggesting either that needles were absorbing moisture from the air or that the instrument calibration was in error. At cold temperature, condensation of water vapor on the warmer-than-ambient IRGA sensors could have generated erroneous measurements of reference versus sample water vapor; this error is not expected for CO_2 given its much lower freezing point. T_r values were highly variable within and across species during the midday. Net photosynthesis (A) was negative at predawn and dusk, indicating respiration. A increased rapidly for all trees following daybreak and decreased rapidly in the late afternoon; like T_r , A was highly variable across all trees during the midday. The rate of change in A as a function of T_{leaf} was the same for the two species (paired t-test, $t=0.971$, $\text{df}=2$, $p\text{-value}=0.434$).

The paired trees demonstrated different responses in gas exchange through the course of the day during the arid foresummer (Figure 5-2). PAR across all three days was consistently $\sim 2000 \mu\text{mol m}^{-2} \text{s}^{-1}$ by early morning and

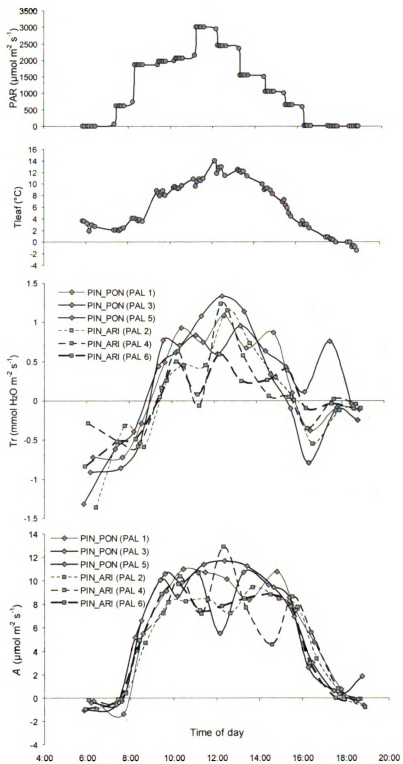


Figure 5-1. Diurnal variation in net photosynthetic rate (A) and transpiration (Tr) as a function of incident radiation (PAR) and temperature (Tleaf) for paired PIN_PON and PIN_ARI trees at PAL during winter (January 2006).

to late evening before sunset; once the sun broke the horizon at ~5:45, intensity increased rapidly. T_{leaf} was consistently 11-16° C in early morning, increased to ~22° C by midday, and then decreased to ~17° C by dusk. Both species experienced active Tr and A in the early morning, followed by a midday depression before renewal of limited gas exchange in the later afternoon. In particular, the PIN_PON tree labeled PAL 1 precipitously dropped Tr and A before 10:00, indicating almost complete closure of stomata (Figure 5-2, first page). Its paired PIN_ARI tree also decreased gas exchange by almost 75% of its early morning rate but did continue losing water through transpiration. Under similar climatic conditions, though, another PIN_PON tree (PAL 3) decreased Tr and A through the afternoon but did not demonstrate the severe midday depression. Likewise, its paired PIN_ARI tree steadily decreased gas exchange through the afternoon. The third pair of trees demonstrated a great deal of variability in gas exchange throughout the day but did peak at around the same time (~9:00) as the other pairs of trees. As during the winter, the two species did not differ in the rate of change in A as a function of T_{leaf} ($t=0.9375$, $df=2$, $p\text{-value}=0.4475$).

Changes in gas exchange for the same three pairs of trees tracked climatic conditions independent of species during the monsoon season (Figure 5-3). PAR was higher than during the arid foresummer but lower than during winter, but it was highly variable throughout each day and peaked near 2010, 2290, and 2620 $\mu\text{mol m}^{-2} \text{s}^{-1}$ across the three days of measuring the paired trees, respectively. T_{leaf} was higher than during the arid foresummer, with temperatures

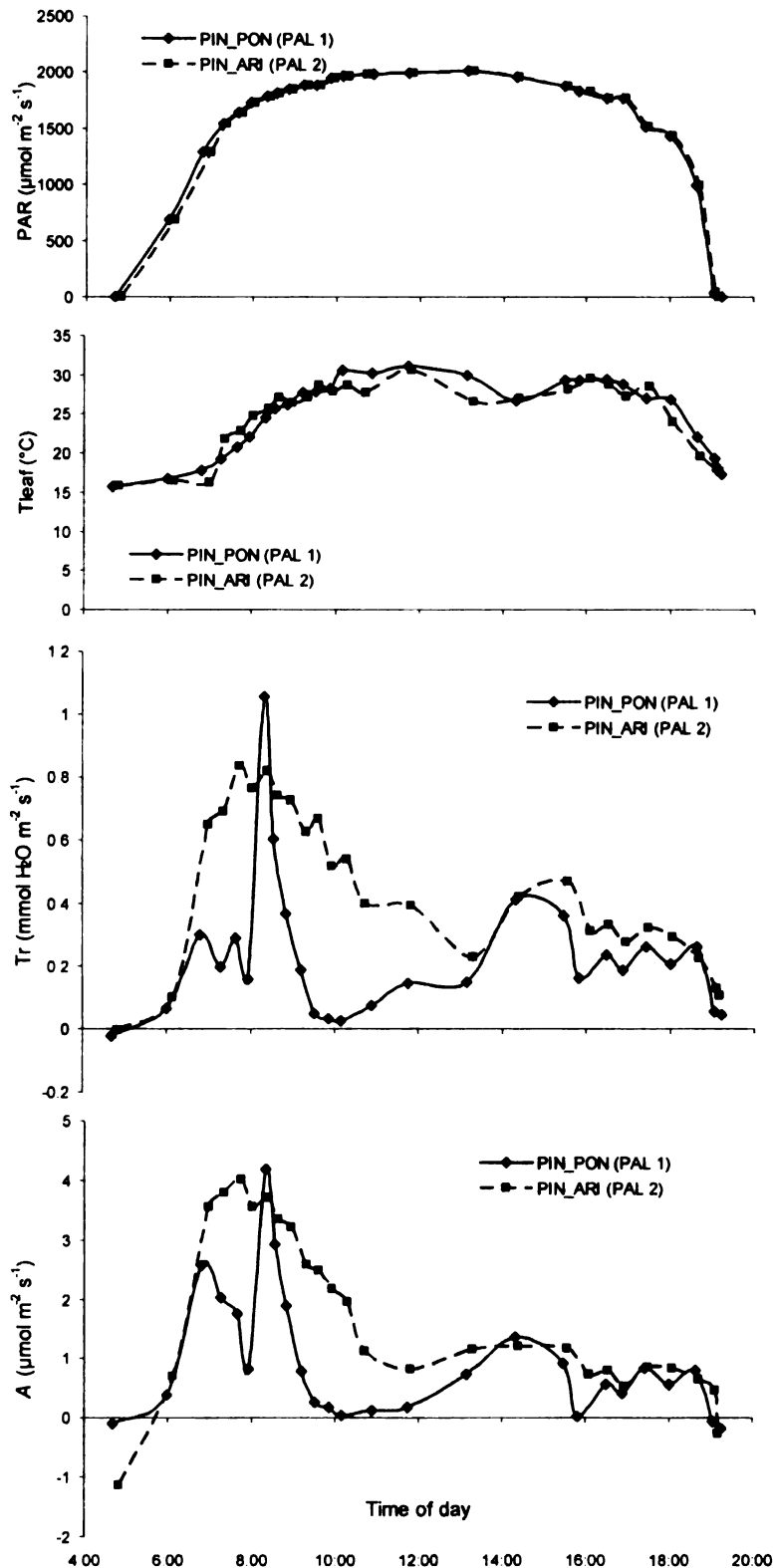


Figure 5-2. Diurnal variation in net photosynthetic rate (A) and transpiration (Tr) as a function of incident radiation (PAR) and temperature (T_{leaf}) for paired PIN_PON and PIN_ARI trees at PAL during the arid foresummer (June 2005). Note that the ordinate scales for A and Tr vary across pages.

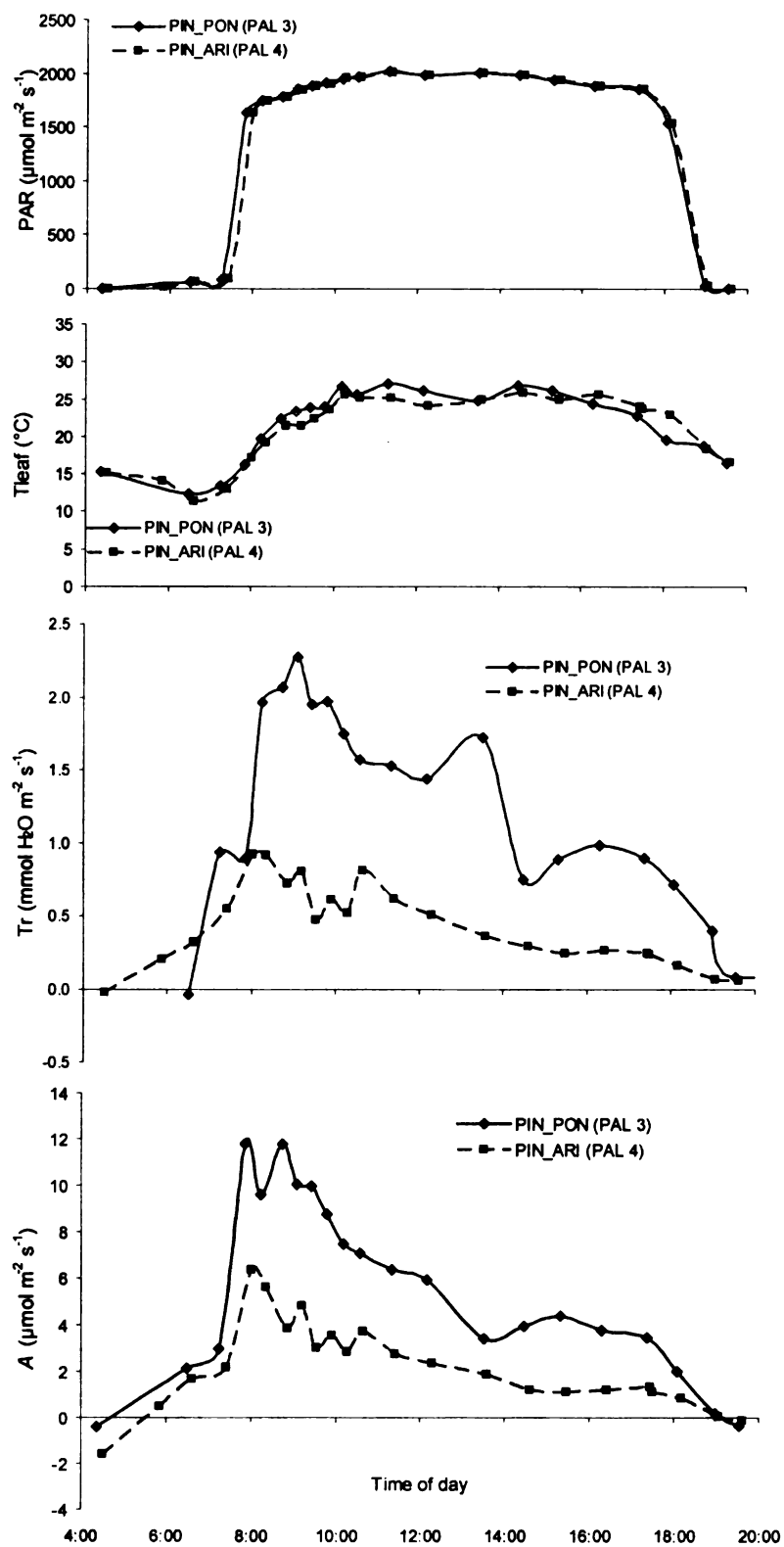


Figure 5-2. *Continued.*

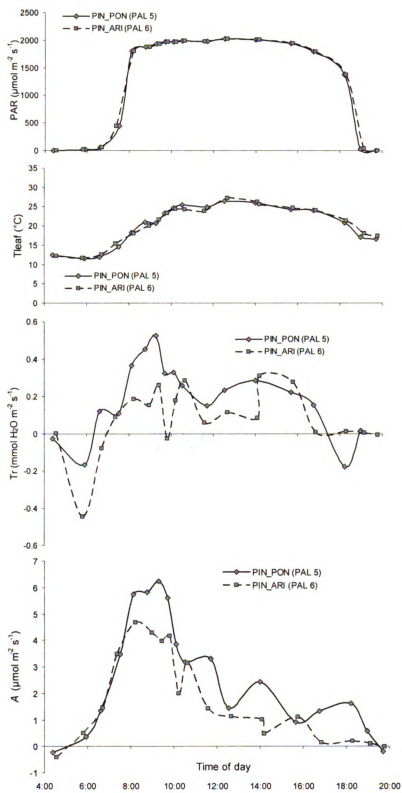


Figure 5-2. *Continued.*

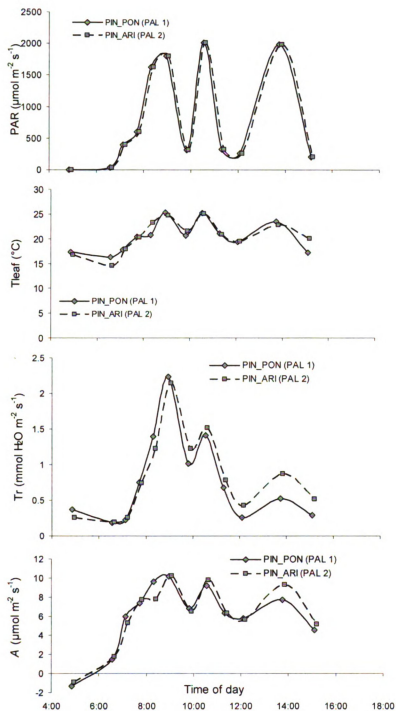


Figure 5-3. Diurnal variation in net photosynthetic rate (A) and transpiration (Tr) as a function of incident radiation (PAR) and temperature (T_{leaf}) for paired PIN_PON and PIN_ARI trees at PAL during the monsoon season (August 2005). Note that the ordinate scales for A and Tr vary across pages.

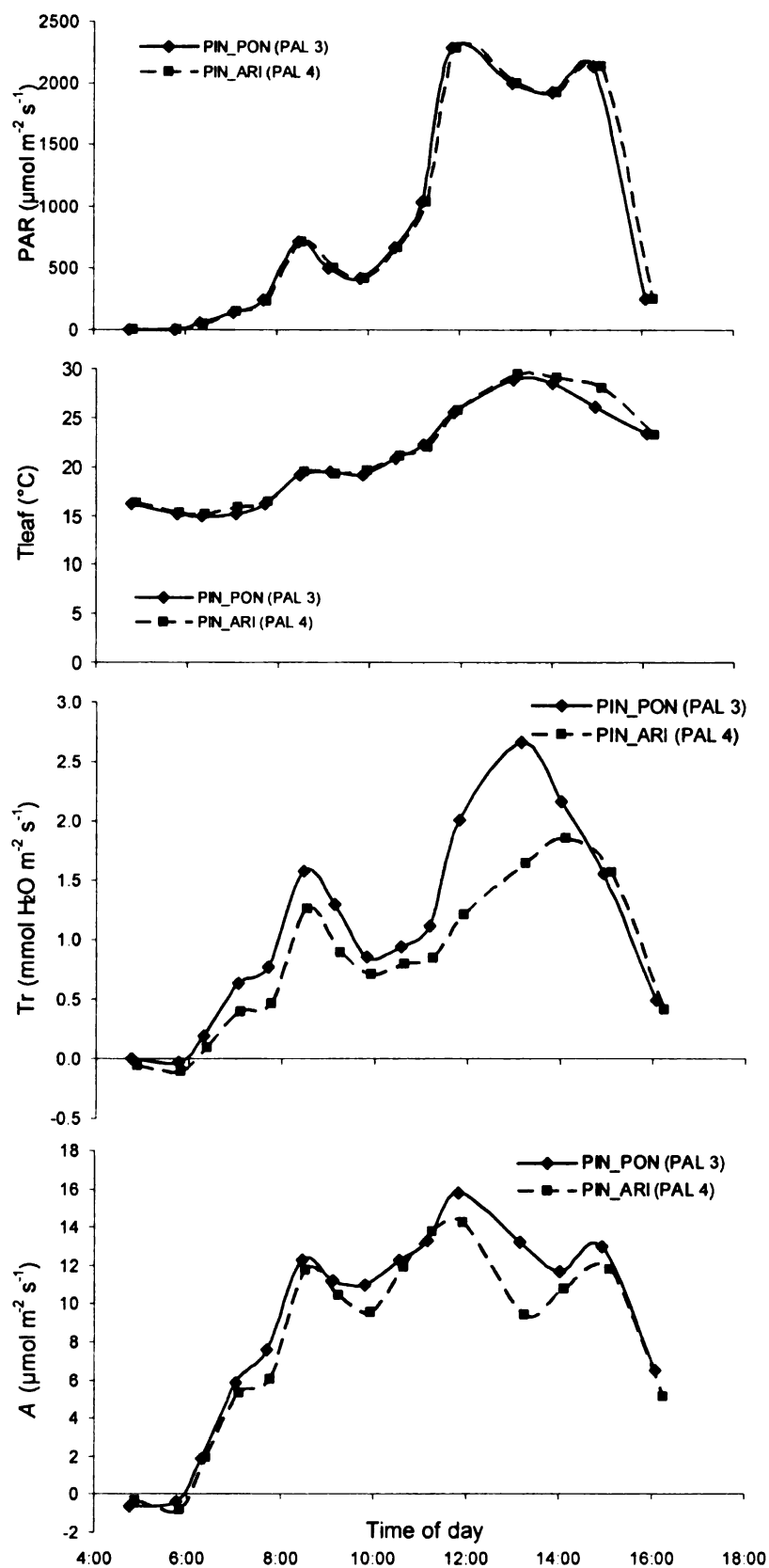


Figure 5-3. *Continued.*

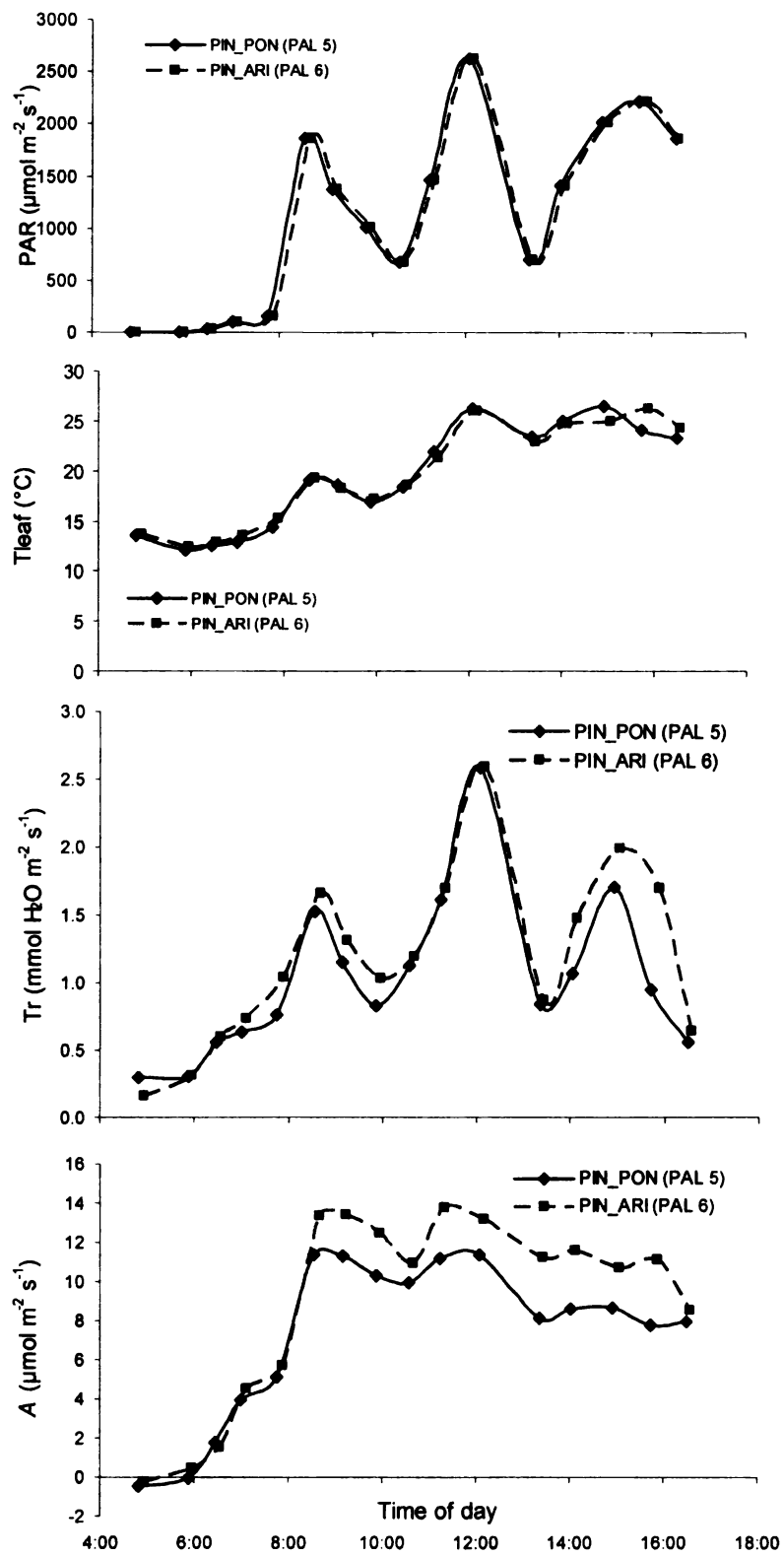


Figure 5-3. Continued.

varying from 14-17° C in the morning to peak readings of 25-29° C later in the day. T_r and A for both species paralleled changes in PAR; T_r and A increased when PAR increased. Given this very strong apparent relationship of gas exchange with PAR, and no visible evidence of such a relationship with T_{leaf} , the rate of change in A to T_{leaf} by species is not given.

Across all seasons, needle xylem pressure potential (Ψ_p) from PIN_PON and PIN_ARI trees became more negative from predawn to midday and then partially recovered by evening (PIN_PON, $t=-1.9774$, $df=14.239$, $p\text{-value}=0.068$; PIN_ARI, $t=-2.3072$, $df=19.79$, $p\text{-value}=0.032$), at least during the arid foresummer (Figure 5-4). Ψ_p was most negative for both species in winter and least negative during the monsoon season, with significant ($p<0.04$) differences at each time period across every season (Table 5-2). For both individual species, there was no significant ($p<0.05$) difference in predawn Ψ_p between the arid foresummer and monsoon, indicating similar soil water availability during these two seasons; however, the difference for PIN_ARI was marginally significant ($p=0.087$), suggesting a lower ability to acquire soil water relative to PIN_PON. The differences in midday Ψ_p for PIN_PON trees across winter to the arid foresummer and across the arid foresummer to monsoon were marginally significant ($p=0.076$ and 0.063 , respectively); relatively large variation in winter and monsoon Ψ_p prevented finding a significant difference, although the trend remains. Across the elevational gradient, these data suggest that the order of “drought” conditions was winter > arid foresummer > monsoon.

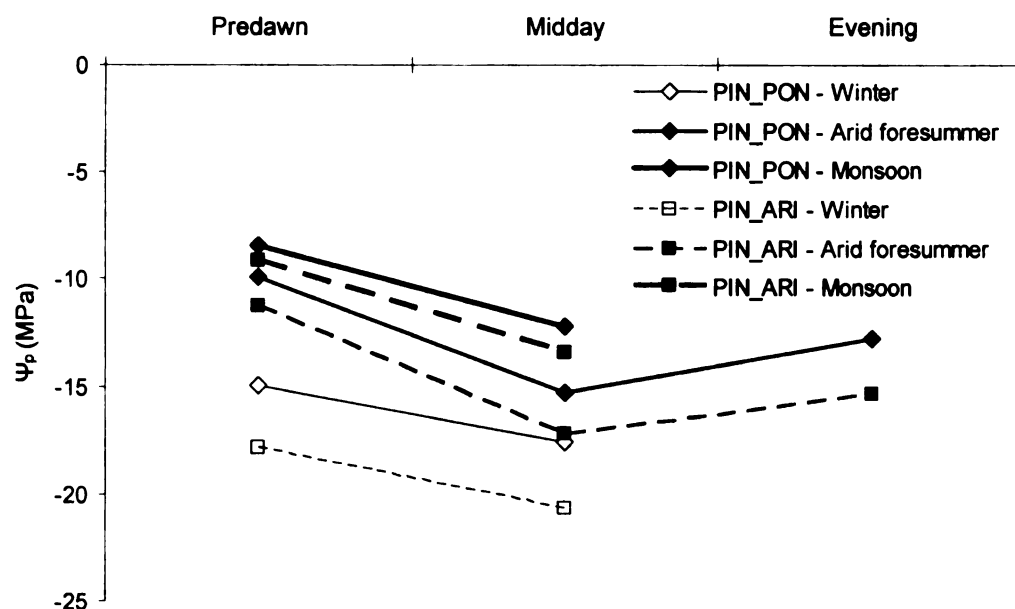


Figure 5-4. Diurnal by seasonal needle xylem pressure potential (Ψ_p) for PIN_PON and PIN_ARI trees growing in the Santa Catalina Mountains.

Table 5-2. Comparison of seasonal xylem water potential (Ψ_p) of combined (both), PIN_PON, and PIN_ARI fascicles harvested at predawn, midday, and evening across an elevational gradient. Significant ($p < 0.05$) terms are bolded.

Season 1	Season 2	Time	Species	t-value	df	p-value
Winter	Arid Foresummer	Predawn	Both	-6.5491	40.973	7.2E-08
		Predawn	PIN_PON	-4.1688	17.22	0.0006
		Predawn	PIN_ARI	-5.6791	14.742	4.7E-05
Winter	Arid Foresummer	Midday	Both	-3.5004	31.469	0.0014
		Midday	PIN_PON	-1.9242	13.234	0.0761
		Midday	PIN_ARI	-4.0673	17.900	0.0007
Winter	Monsoon	Predawn	Both	-8.6737	40.420	9.1E-11
		Predawn	PIN_PON	-7.9012	18.309	2.6E-07
		Predawn	PIN_ARI	-5.9794	19.991	7.6E-06
Winter	Monsoon	Midday	Both	-8.6737	40.420	9.1E-11
		Midday	PIN_PON	-3.0359	18.207	0.0070
		Midday	PIN_ARI	-4.4044	13.659	0.0006
Arid Foresummer	Monsoon	Predawn	Both	-2.2027	41.931	0.0332
		Predawn	PIN_PON	-1.2752	14.332	0.2225
		Predawn	PIN_ARI	-1.8300	14.919	0.0873
Arid Foresummer	Monsoon	Midday	Both	-3.1052	28.169	0.0043
		Midday	PIN_PON	-2.0384	12.813	0.0627
		Midday	PIN_ARI	-2.3528	12.552	0.0357

The diurnal pattern of intraspecies variation in Ψ_p within each season gives an indication of individual tree variation in water loss (Figure 5-5). In winter, more variation is observed from predawn to midday in PIN_PON but not PIN_ARI, which in fact demonstrated less variability by midday; this result could be due to cold conditions limiting photosynthesis for PIN_PON trees at the highest elevation while milder conditions at PAL allowed photosynthesis, and thus transpiratory water loss. During the arid foresummer, variation in Ψ_p decreased for PIN_PON midday but increased by evening, while PIN_ARI trees were quite consistent in their response throughout the day. In the monsoon season, midday variation increased substantially for both species relative to predawn variation. During winter and arid foresummer, less variation is expected by midday as trees respond to the drought conditions; conversely, when soil (liquid) water availability is high such as during the monsoon, variation is expected to be greater during the midday as both species are actively photosynthesizing. Intraspecies variation in recovery of water status during the evening of the arid foresummer was larger for PIN_PON than PIN_ARI trees.

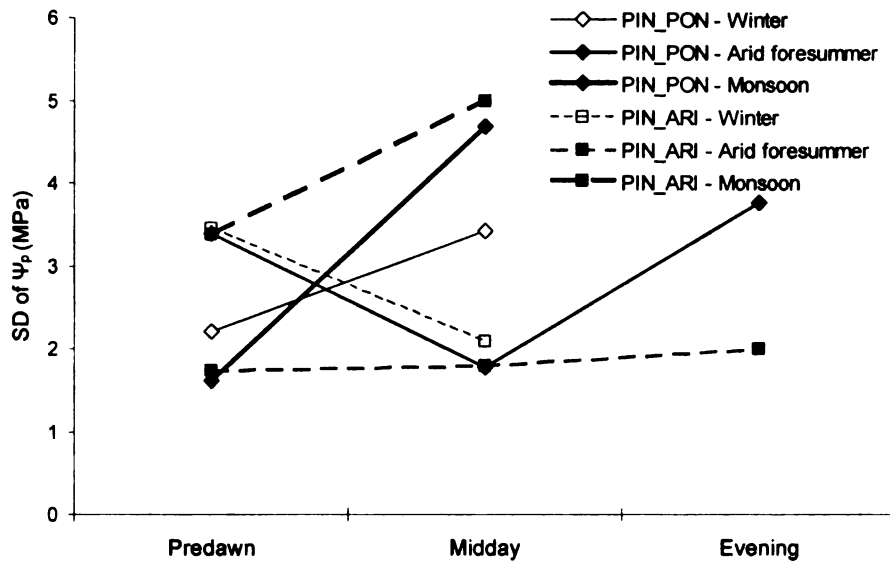


Figure 5-5. Variation (standard deviation, SD) in diurnal needle xylem pressure potential (Ψ_p) by season for PIN_PON and PIN_ARI trees growing in the Santa Catalina Mountains.

Separation of Ψ_p measurements by site (i.e., nesting) allows consideration of species \times site interactions (Figure 5-6). During winter, needles from trees growing at higher elevation site had consistently lower (i.e., less negative) Ψ_p than those from lower elevation; the diurnal change in Ψ_p was largest at PAL ($\Delta = -3.6$ MPa), considered to be the intermediate site in terms of cold at high and aridity at low elevation. Both species and site effects were significant ($p < 0.004$) in explaining variation in Ψ_p (Table 5-3). The same pattern of diurnal Ψ_p was observed during the arid foresummer, with higher elevation correlated with lower Ψ_p , but the needles at the highest elevation site had the largest amount of diurnal variation ($\Delta = -8.2$ MPa). While site effects were significant ($p < 0.005$) across predawn, midday, and evening periods, species differences were only significant at midday and evening ($p < 0.005$); large variation in predawn Ψ_p for PIN_PON trees at PAL reduced the species effect (Figure 5-5). During the monsoon

season, predawn Ψ_p was unexpectedly highest at the lowest elevation site (LIZ, $\Psi_p = -6.5$ MPa), followed by trees from MTL and PAL (mean $\Psi_p = -8.8$ MPa), and then the negative elevation-to- Ψ_p pattern developed by midday as all Ψ_p increased substantially (mean $\Delta = -4.8$ MPa). However, Ψ_p did not significantly vary by species ($p > 0.50$) nor site ($p > 0.09$) at predawn or midday.

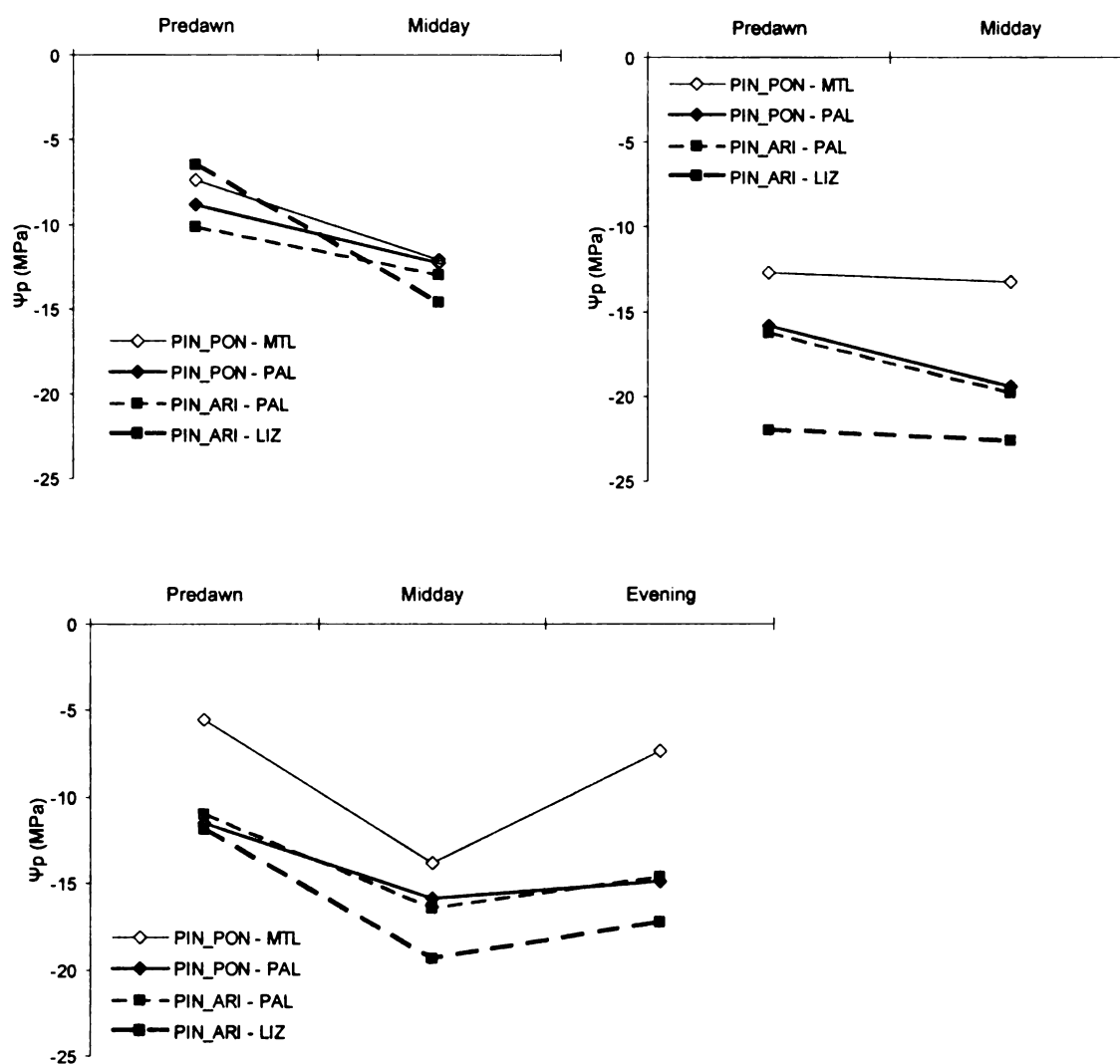


Figure 5-6. Needle xylem pressure potential (Ψ_p) by winter (*top, left*), arid foresummer (*bottom*), and monsoon (*top, right*) for PIN_PON and PIN_ARI trees growing along an elevational gradient in the Santa Catalina Mountains.

Table 5-3. Nested ANOVA results xylem pressure potential (Ψ_p) in needles from PIN_PON and PIN_ARI trees across an elevation gradient, 3 seasons ("Arid" is arid foresummer), and 2-3 daytime periods. Significant ($\alpha < 0.05$) models and terms are bolded.

Season	Period	Adj R ²	F(p-value)	Term	df	SS	F-value	P-value
Winter	Predawn	0.591	0.0002	Species	1	45.413	10.929	0.0039
				Species(site)	2	93.039	11.195	0.0007
				Residuals	18	74.794	4.155	
Winter	Midday	0.698	5.1E-05	Species	1	46.997	15.434	0.0012
				Species(site)	2	95.887	15.745	0.0002
				Residuals	16	48.719		
Arid	Predawn	0.506	0.0012	Species	1	10.128	2.7815	0.1127
				Species(site)	2	79.278	10.8861	0.0008
				Residuals	18	65.542		
Arid	Midday	0.511	0.0011	Species	1	20.119	10.2943	0.0049
				Species(site)	2	28.687	7.3389	0.0047
				Residuals	18	35.180		
Arid	Evening	0.767	1.6E-06	Species	1	35.112	14.587	0.0013
				Species(site)	2	138.178	28.703	2.5E-06
				Residuals	18	43.326		
Monsoon	Predawn	0.126	0.1491	Species	1	2.756	0.4635	0.5047
				Species(site)	2	33.049	2.7786	0.0888
				Residuals	18	107.047		
Monsoon	Midday	-0.132	0.9071	Species	1	8.30	0.3226	0.5770
				Species(site)	2	5.76	0.1119	0.8948
				Residuals	18	463.18		

Integrated water-use efficiency and nitrogen dynamics

Carbon isotopic composition ($\delta^{13}\text{C}$) varied strongly across years, while nitrogen isotopic composition ($\delta^{15}\text{N}$) was relatively more stable (Figure 5-7). Mean $\delta^{13}\text{C}$ was -25.7‰ ($s=0.8\text{‰}$) across years for both species, with a mean increase of 0.8‰ in 2004-05 relative to the previous two years. There was no significant species effect on $\delta^{13}\text{C}$ within each year ($p>0.52$, Table 5-4) nor across years ($p=0.94$, Table 5-5). Mean $\delta^{15}\text{N}$ was -4.4‰ ($s=0.8\text{‰}$) across years for both species, but PIN_PON needles discriminated against ^{15}N more than PIN_ARI

needles ($\Delta=18\%$) for the years 2003-05, with significant ($p>0.05$) differences only for 2003 ($p=0.013$) and 2005 ($p=0.047$) (Table 5-4).

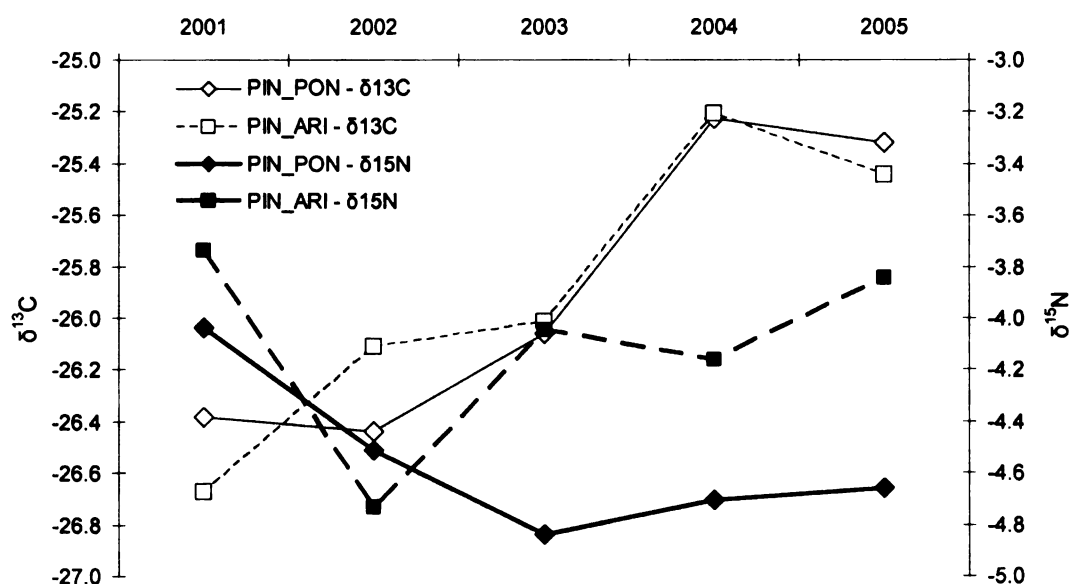


Figure 5-7. Annual variation in mean carbon ($\delta^{13}C$, *solid lines*) and nitrogen ($\delta^{15}N$, *dashed lines*) isotope composition for leaf tissue of PIN_PON and PIN_ARI trees at PAL. Note the different ordinate scales.

Table 5-4. Univariate ANOVA results for carbon isotope ($\delta^{13}C$), nitrogen isotope ($\delta^{15}N$), carbon (%C), nitrogen (%N), and carbon-to-nitrogen (C:N) content in needles for each year from PIN_PON and PIN_ARI trees at PAL. Responses with significant ($\alpha<0.05$) differences between species for at least one year and significant terms are **bolded**.

Response	Year	Adj R ²	Term	Df	SS	F-value	P-value
$\delta^{13}C$	2001	-0.1096	Species	1	0.1280	0.5061	0.5161
			Residuals	4	1.0114		
	2002	-0.1161	Species	1	0.2022	0.2719	0.6207
			Residuals	6	0.7439		
	2003	-0.0503	Species	1	0.0113	0.0418	0.8401
			Residuals	19	5.1448		
	2004	-0.0525	Species	1	0.0011	0.0027	0.9588
			Residuals	19	7.5773		
	2005	-0.0435	Species	1	0.0847	0.1668	0.6875
			Residuals	19	9.6468		

Table 5-4. *Continued.*

Response	Year	Adj R ²	Term	Df	SS	F-value	P-value
$\delta^{15}\text{N}$	2001	-0.0199	Species	1	0.1368	0.9023	0.3960
			Residuals	4	0.6066		
	2002	-0.1402	Species	1	0.0901	0.1391	0.7220
			Residuals	6	3.8848		
	2003	0.2428	Species	1	3.3051	7.4131	0.0135
			Residuals	19	8.4710		
	2004	0.0815	Species	1	1.5587	2.7744	0.1122
			Residuals	19	10.6746		
	2005	0.1501	Species	1	3.4746	4.532	0.0466
			Residuals		14.5671		
%C	2001	-0.1146	Species	1	0.0977	0.4861	0.5241
			Residuals	4	0.8043		
	2002	-0.1627	Species	1	0.0044	0.0203	0.8913
			Residuals	6	1.2857		
	2003	0.1251	Species	1	1.4059	3.8610	0.0642
			Residuals	19	6.9183		
	2004	0.1217	Species	1	1.3576	3.7714	0.0671
			Residuals	19	6.8397		
	2005	-0.0375	Species	1	0.0305	0.2778	0.6043
			Residuals	19	2.0843		
%N	2001	0.7836	Species	1	0.0109	19.1010	0.0120
			Residuals	4	0.0022		
	2002	0.0788	Species	1	0.0102	1.5988	0.2530
			Residuals	6	0.0382		
	2003	-0.0294	Species	1	0.0052	0.4294	0.5201
			Residuals	19	0.2318		
	2004	0.1217	Species	1	1.3576	3.7714	0.0671
			Residuals	19	6.8397		
	2005	0.0626	Species	1	0.0586	2.3361	0.1429
			Residuals	19	0.4764		
C:N	2001	0.8096	Species	1	27.8548	22.2640	0.0092
			Residuals	4	5.0045		
	2002	0.0654	Species	1	27.9230	1.4902	0.2680
			Residuals	6	112.2470		
	2003	-0.0082	Species	1	14.8900	0.8367	0.3718
			Residuals	19	338.1900		
	2004	-0.0422	Species	1	3.6900	0.1906	0.6673
			Residuals	19	367.7400		
	2005	0.0599	Species	1	27.4190	2.2751	0.1479
			Residuals	19	228.9850		

Like $\delta^{13}\text{C}$, needle tissue carbon content (%C) was relatively stable for both species in the years 2001-03 but then dropped ~2% in the years 2004-05, which correspond to years with higher precipitation than the drought years of 2000-02

in the Santa Catalina Mountains (personal observation) (Figure 5-8). In 4 of 5 years, PIN_ARI needles had higher %C than PIN_PON needles. Consequently, both year and species were significant (Table 5-5). Conversely, nitrogen content (%N) was ~36% lower in the older (3-4 year-old) foliage relative to the 2005 needles; nonetheless, the difference was not significant ($p=0.571$). However, PIN_PON needles had consistently (Figure 5-8) higher %N than PIN_ARI needles across years.

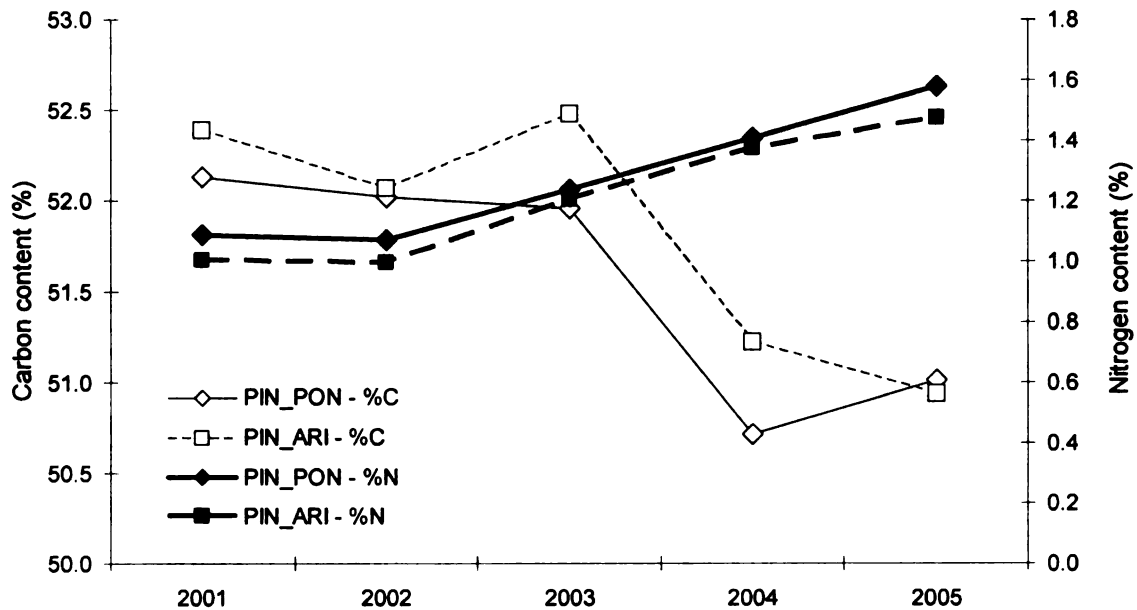


Figure 5-8. Annual variation in mean carbon (*solid lines*) and nitrogen (*dashed lines*) content for leaf tissue of PIN_PON and PIN_ARI trees at PAL. Note the different ordinate scales.

Table 5-5. Nested ANOVA results for carbon isotope ($\delta^{13}\text{C}$), nitrogen isotope ($\delta^{15}\text{N}$), carbon (%C), nitrogen (%N), and carbon-to-nitrogen (C:N) content in needles from PIN_PON and PIN_ARI trees at PAL. Individual tree (tree) is nested in year, which is nested in species. Significant ($\alpha < 0.05$) models and terms are bolded.

Response	Adj R ²	F(p-value)	Term	Df	SS	F-value	P-value
$\delta^{13}\text{C}$	0.1989	0.0236	Species	1	0.0023	0.0049	0.9445
			Species(year)	8	17.0604	4.5055	0.0003
			Species(year(tree))	10	0.8642	0.1826	0.9969
			Residuals	57	26.9792		
$\delta^{15}\text{N}$	0.1071	0.1286	Species	1	6.9880	12.1216	0.0010
			Species(year)	8	3.8800	0.485	0.5706
			Species(year(tree))	10	5.3420	0.9266	0.5160
			Residuals	57	32.8620		
%C	0.5774	1.91E-08	Species	1	1.3775	5.0514	0.0285
			Species(year)	8	29.7354	13.6303	8.24E-11
			Species(year(tree))	10	2.3886	0.8759	0.5604
			Residuals	57	15.5436		
%N	0.5964	6.08E-09	Species	1	0.0482	2.4496	0.1231
			Species(year)	8	2.3547	14.9629	1.53E-11
			Species(year(tree))	10	0.1798	0.9142	0.5267
			Residuals	57	1.1212		
C:N	0.6964	4.15E-12	Species	1	54.0200	3.5350	0.0652
			Species(year)	8	2718.7100	22.2391	6.28E-15
			Species(year(tree))	10	181.32	1.1866	0.3191
			Residuals	57	871.02		

Nutrient content in leaf tissue was related to $\delta^{13}\text{C}$ but not to $\delta^{15}\text{N}$. $\delta^{13}\text{C}$ was significantly negatively associated with %C (Figure 5-9; $p=0.0001$), positively associated with %N (Figure 5-10; $p=6.79\text{E}-05$), and negatively associated with C:N ($p=1.51\text{E}-05$); nutrient dynamics of PIN_PON and PIN_ARI relative to $\delta^{13}\text{C}$ did not differ ($p>0.45$). Conversely, $\delta^{15}\text{N}$ was not significantly ($p>0.17$) associated with nutrient content, but the species effect was significant for all models (%C, $p=0.0009$; %N, Figure 5-11, $p=0.0003$; and C:N, Figure 5-12, $p=0.0003$).

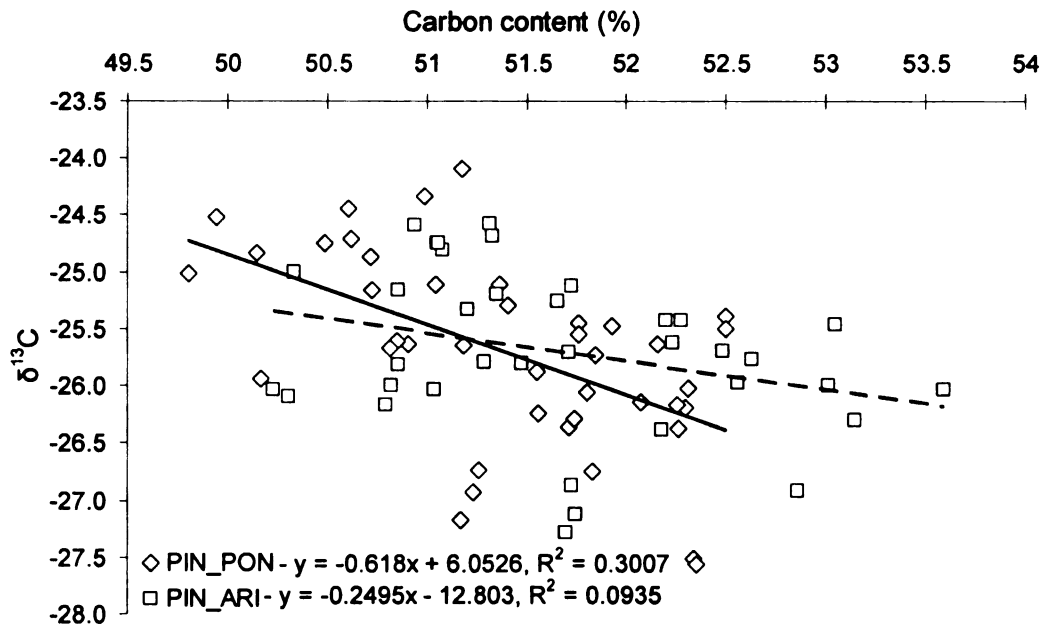


Figure 5-9. Carbon isotopic composition ($\delta^{13}\text{C}$) relative to carbon content in needles from PIN_PON (solid line) and PIN_ARI (dashed line) trees at PAL.

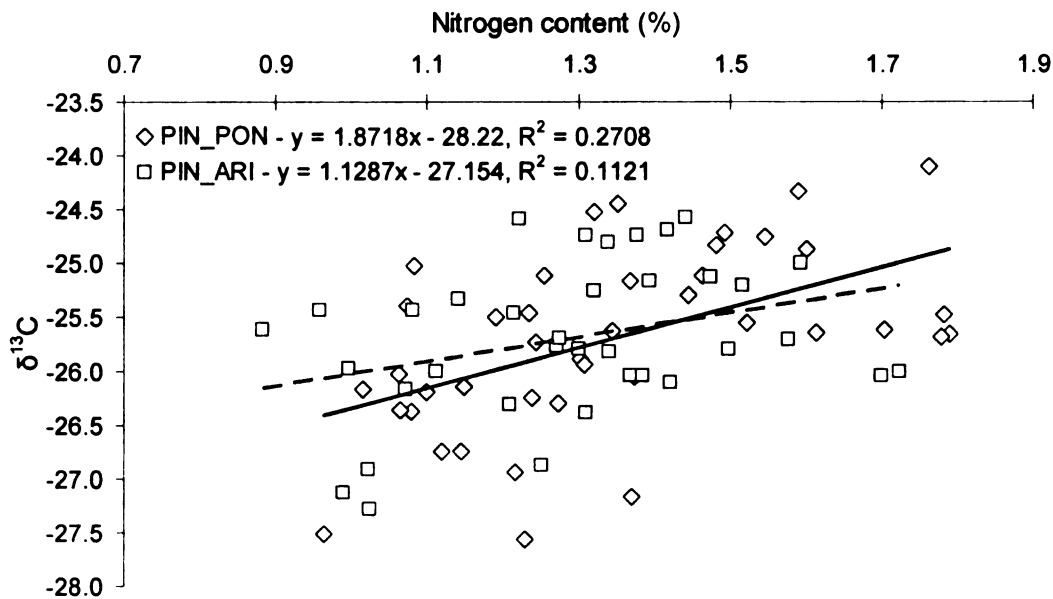


Figure 5-10. Carbon isotopic composition ($\delta^{13}\text{C}$) relative to nitrogen content in needles from PIN_PON (solid line) and PIN_ARI (dashed line) trees at PAL.

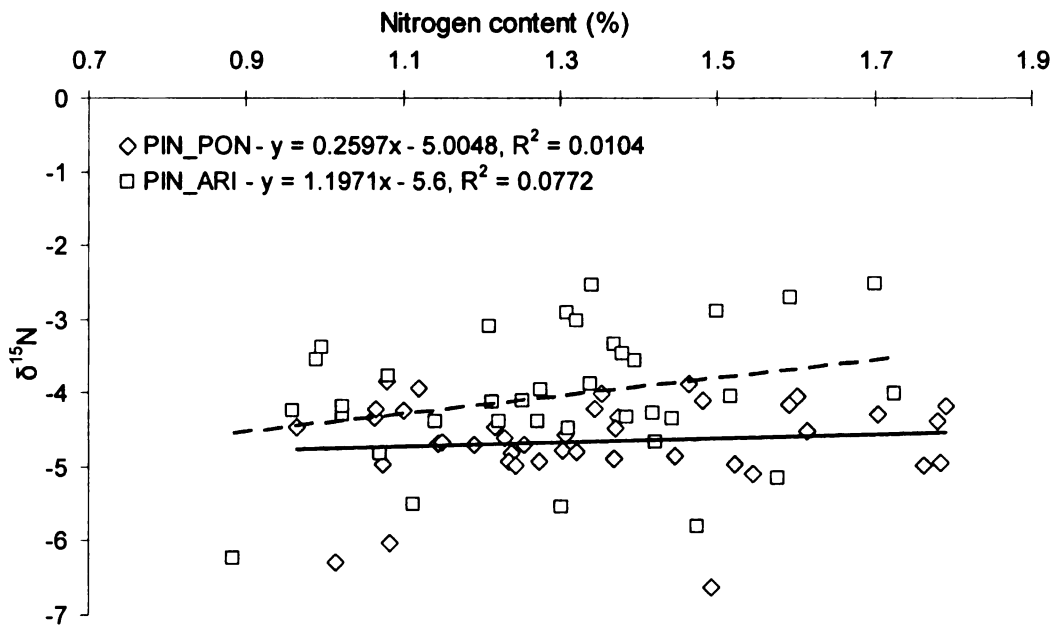


Figure 5-11. Nitrogen isotopic composition ($\delta^{15}\text{N}$) relative to nitrogen content in needles from PIN_PON (solid line) and PIN_ARI (dashed line) trees at PAL.

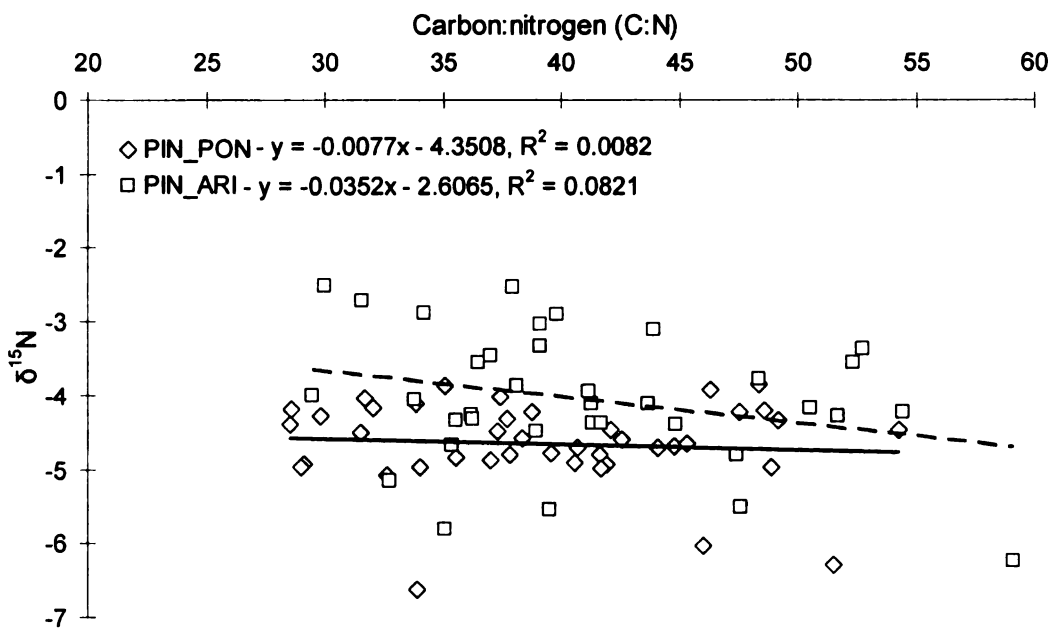


Figure 5-12. Nitrogen isotopic composition ($\delta^{15}\text{N}$) relative to carbon-to-nitrogen content (C:N) in needles from PIN_PON (solid line) and PIN_ARI (dashed line) trees at PAL.

Photosynthetic function during dehydration

Needles from PIN_PON and PIN_ARI trees across the elevational gradient lost a similar amount of water mass across the first 8 d, but mass loss asymptoted earlier for PIN_ARI than PIN_PON needles consistently across sites (Figure 5-13). All measurements from one tree (LIZ 1) were removed due to exceptionally low initial F_v'/F_m' (0.035); resultant sample sizes for PIN_PON and PIN_ARI were 23 and 18, respectively. There was a significant decrease in water loss following the final drying (paired t-test, $t=5.7051$, $df=40$, $p\text{-value}=1.27\text{E-}06$), indicating that some intracellular water remained after the final measurements.

The species difference becomes more apparent when trees are grouped across sites by species (Figure 5-14). Two-way ANOVA ($\text{Adj-}R^2=0.507$, $F(p\text{-value})=4.85\text{E-}06$) of mass loss at the final (31st) measurement indicates a significant species ($p=1.81\text{E-}07$) effect but no site effect ($p=0.309$). However, when analyzed as a function of time since excision from the hydrated branch, almost twice the amount of variation in mass lost is accounted for by site differences than species differences, although both terms were highly significant in the ANCOVA (Table 5-6). Attempts to reduce the right skewness of the otherwise normally distributed residuals through square, square-root, reciprocal, natural-log, natural-log of reciprocal, and arc-sine transformation of the response variable were not successful; i.e., skew remained and the adjusted- R^2 decreased. Because all transformations identified the same significant terms, only the level of significance varied, the linear model was retained. The

significant interaction of site by time elapsed since branch excision is unfortunate and related to the order imposed to prevent measurement error; no difference in measurements as a function of elapsed time was expected due to the rapid rate in taking F_v'/F_m' measurements at each time period ($\bar{x}=1.23$ h, $s=0.25$ h).

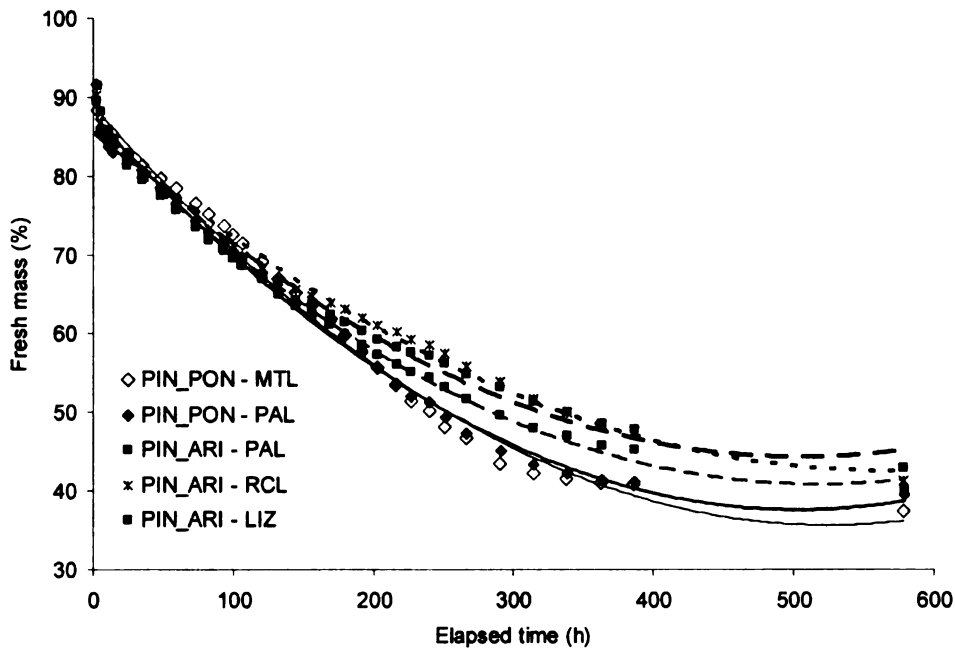


Figure 5-13. Dehydration of fascicles for PIN_PON (*solid lines*) and PIN_ARI (*dashed lines*) stems from four sites in the Santa Catalina Mountains: MTL, PAL, RCL, and LIZ. Fitted curves are second-order polynomials.

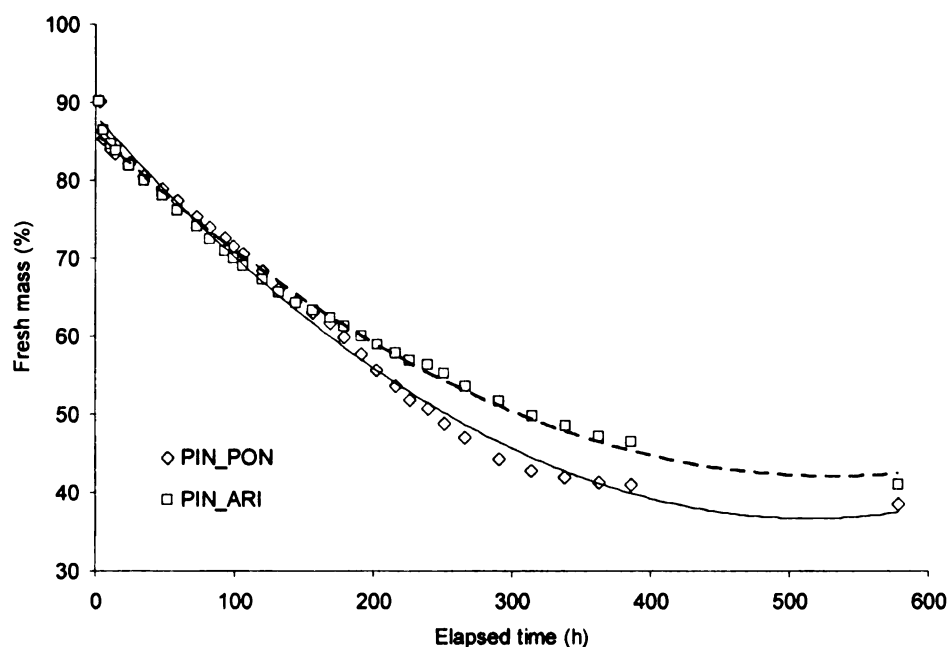


Figure 5-14. Mean dehydration of fascicles for PIN_PON (solid lines) and PIN_ARI (dashed lines) stems across four sites in the Santa Catalina Mountains. Fitted curves are second-order polynomials.

Table 5-6. ANCOVA results for fresh mass loss (pmass) and PSII excitation capture efficiency (F_v'/F_m') of dehydrating needles for PIN_PON and PIN_ARI stems from four sites in the Santa Catalina Mountains: MTL, PAL, RCL, and LIZ. Covariates for the two models are elapsed time (Etime) and pmass, respectively. Significant ($\alpha < 0.05$) terms are bolded.

Response	Adj R^2	F(p-value)	Term	Df	SS	F-value	P-value
pmass	0.8059	<2.2E-16	Site	1	1145	25.7966	4.36E-07
			Species	3	640	4.8117	0.0025
			Etime	1	230338	5191.3640	<2.2E-16
			Site*Etime	1	2097	47.2516	9.79E-12
			Species*Etime	3	210	1.5805	0.1923
			Residuals	1261	55950		
F_v'/F_m'	0.7939	<2.2E-16	Site	1	0.1145	19.9976	8.45E-06
			Species	3	0.1520	8.8483	8.33E-06
			pmass	1	27.7698	4848.7223	<2.2E-16
			Site*pmass	1	0.0002	0.0272	0.8689
			Species*pmass	3	0.0352	2.0491	0.1052
			Residuals	1261	7.2221		

PSII excitation capture efficiency relative to progression of dehydration was consistently higher for needles from PIN_PON trees than from PIN_ARI trees, while site differences were only apparent for PIN_ARI (Figure 5-15). While very close, PIN_PON needles from PAL had higher F_v'/F_m' for a given relative loss in water mass, while higher elevation PIN_ARI clearly had higher retention of photosynthetic function through dehydration. Grouping by site increased the apparent species difference (Figure 5-16) that is supported by the ANCOVA results (Table 5-6). In contrast to rate and extent of dehydration, both site and species are equally significant ($p=8E-06$) in contributing to variation in PSII excitation capture efficiency; no interactions with the covariate in this model were significant (Table 5-6). Although statistical pairwise comparison by site within species is not possible due to the significance of the covariate relative mass, the overall site effect was significant (Table 5-6). In Figure 5-16, the difference in photosynthetic function for a given relative amount of water loss appears minimal across sites for PIN_PON but clear for PIN_ARI, hence the overall significant site effect.

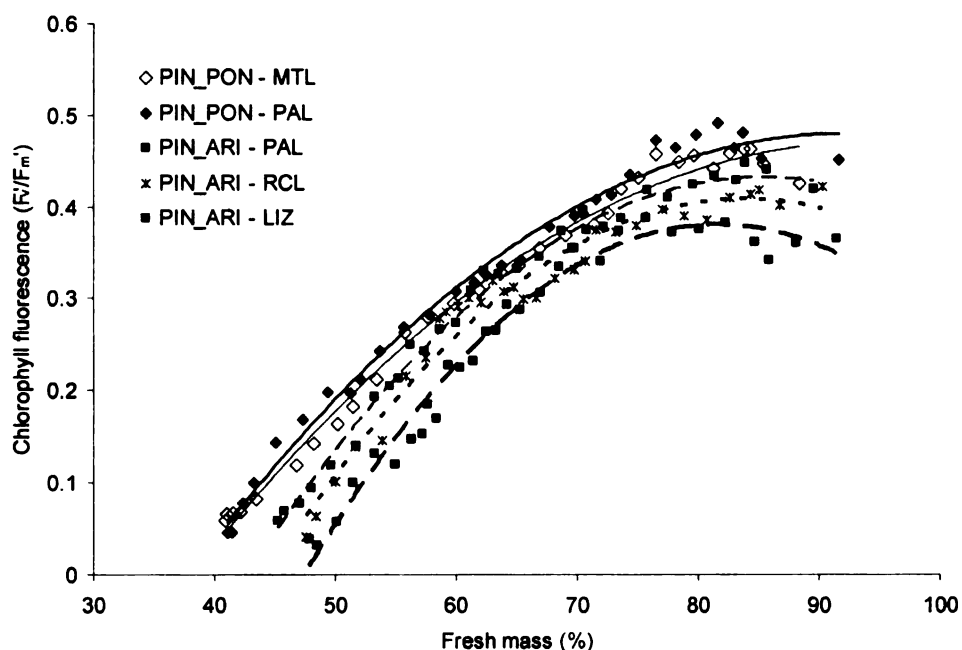


Figure 5-15. Photosynthetic efficiency as a function of needle dehydration for PIN_PON (solid lines) and PIN_ARI (dashed lines) stems from four sites in the Santa Catalina Mountains: MTL, PAL, RCL, and LIZ. Fitted curves are second-order polynomials.

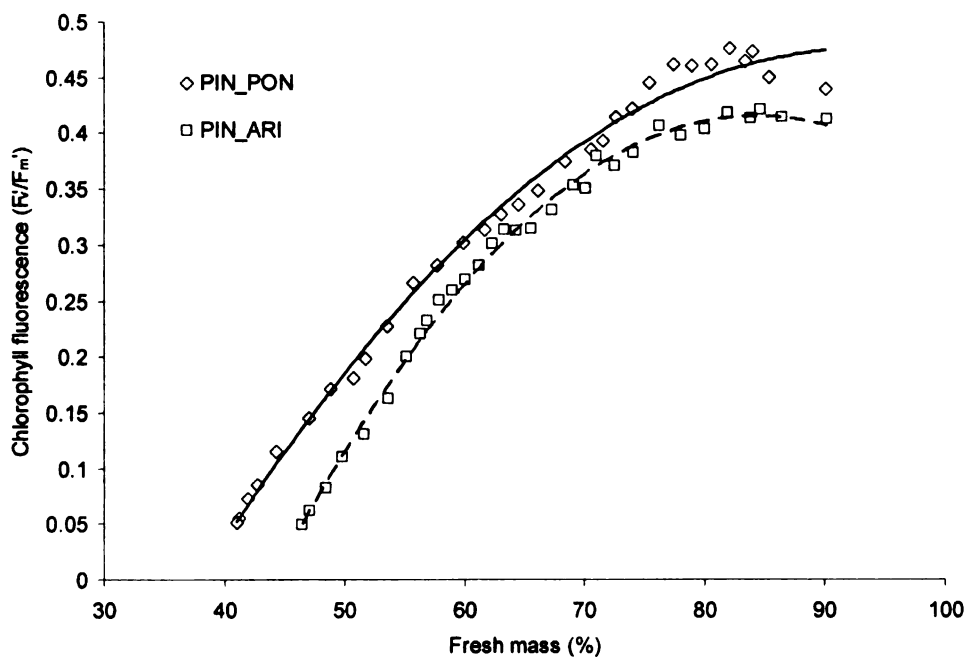


Figure 5-16. Photosynthetic efficiency as a function of needle dehydration for PIN_PON (solid lines) and PIN_ARI (dashed lines) stems across four sites in the Santa Catalina Mountains. Fitted curves are second-order polynomials.

Xylem conductivity and vulnerability

Stems from trees lower in elevation (i.e., more xeric) had consistently higher loss of xylem conductivity for a given imposed xylem tension (Figure 5-17). PIN_ARI stems were also more vulnerable to cavitation than PIN_PON stems, but neither site nor species was significant in the ANOVA (Table 5-7). The interaction term was not calculated due to the extremely small sample size at the LIZ (n=1) and RCL (n=2) sites; stem disintegration (i.e., explosion) inside the centrifuge at moderate tensions ($\Psi = -2.5$ MPa) prevented completion of individual vulnerability curves for a number of trees. One-way ANOVA of species effect at PAL only was also not significant ($p=0.3527$).

Xylem specific hydraulic conductivity was likewise not different between species, but there was a clear (Figure 5-18) and significant ($p=0.005$) site effect (Table 5-7). Sample sizes for non-PAL sites were substantially larger, but the non-significant interaction term was removed from the final model. Based on Tukey's HSD comparison of means, K_s of MTL stems was significantly higher than those from PAL ($p=0.041$) and RC/LIZ ($p=0.005$), while there was no difference in K_s between stems at PAL and RC/LIZ ($p=0.348$). Increased sample size could have reduced the substantial variation in K_s found within the PIN_ARI trees and thereby separate the lower elevation sites.

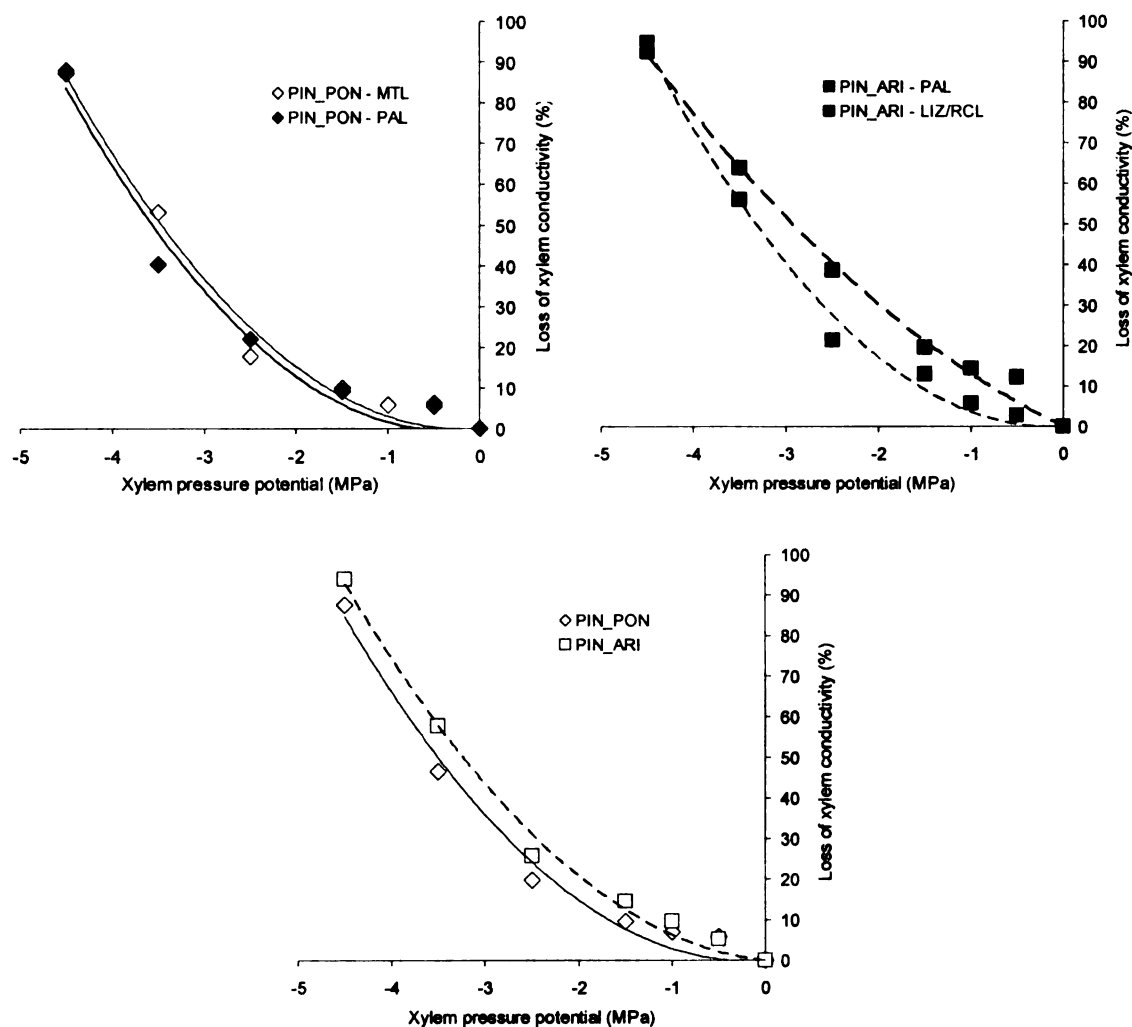


Figure 5-17. Xylem vulnerability curves for PIN_PON (*solid lines*) and PIN_ARI (*dashed lines*) stems collected from three sites in the Santa Catalina Mountains: MTL, PAL, and LIZ/RCL. The bottom curve combines sites by species.

Table 5-7. ANOVA results for xylem pressure potential at 50% loss of hydraulic conductivity (Ψ_{50}) and xylem specific hydraulic conductivity (K_s) for PIN_PON and PIN_ARI stems collected from three sites in the Santa Catalina Mountains: MTL, PAL, and LIZ/RCL. Significant ($\alpha < 0.05$) terms are **bolded**.

Response	Adj R ²	F(p-value)	Term	Df	SS	F-value	P-value
Ψ_p	0.0053	0.3924	Site	2	0.4493	1.0180	0.3777
			Species	1	0.2424	1.0984	0.3060
			Residuals	22	4.8543		
K_s	0.2383	0.0121	Site	2	2.27E-05	6.4777	0.0047
			Species	1	9.70E-08	0.0553	0.8157
			Residuals	29	5.08E-05		

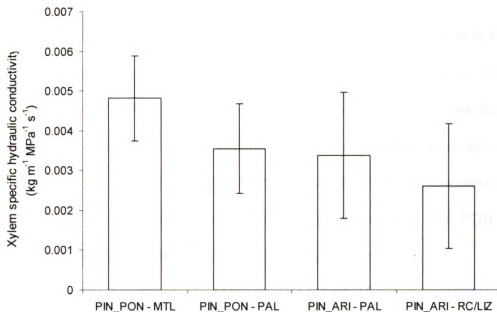


Figure 5-18. Xylem specific hydraulic conductivity (K_s) for PIN_PON and PIN_ARI stems collected from three sites in the Santa Catalina Mountains: MTL, PAL, and LIZ/RCL. Values are means; bars are ± 1 sd.

Discussion

Seasonal gas exchange and xylem pressure potential

The results from this experiment support the hypothesis (Brown 1968, Barton and Teeri 1993) that ponderosa pine, in this case Southwestern ponderosa pine, avoids drought effects by maintaining positive water balance during periods of low moisture availability and actively photosynthesizing during favorable conditions. The relative species differences, especially from the Ψ_p results, suggest that PIN_PON is more drought tolerant than PIN_ARI. These differences are most evident during the winter and less obvious during the arid foresummer. The 3-needled PIN_PON had consistently less negative Ψ_p than 5-needled PIN_ARI across all seasons, sites, and periods during the day (Figure 5-

4). These results support Haller's (1965) findings that ponderosa pine with fewer needles are associated with drought conditions, but they contrast with Malusa (1992) who found that single-needled fascicles in hybrid pinyon pine (*Pinus californiarum* x *P. edulis*) had more negative Ψ_p than the double-needled fascicles and concluded that needle number did not affect water relations. This experiment found a significant difference in Ψ_p , with the fewer-needled species having lower Ψ_p , thus these data support the conclusion that PIN_PON is more drought tolerant than PIN_ARI based on differences in Ψ_p .

Given the hypothesis by Monson and Grant (1989) that ponderosa pine has adapted to drier habitats by lowering g_s at the expense of reduced maximum A , the more drought tolerant of the two species in this study should have lower A and g_s , or Tr as measured here. Conclusions about absolute differences in gas exchange should not be made from the limited number of paired diurnal measurements in this experiment, but patterns and variation in these values can be discussed. The Ψ_p data suggest that winter leaf desiccation is more severe than during the arid foresummer (Figure 5-4); however, both species showed positive A and Tr at the intermediate-elevation site (PAL) during the high-PAR winter (Figure 5-1). On the other hand, Ψ_p did not change through the day for high-elevation PIN_PON and low-elevation PIN_ARI, suggesting no change in water status (i.e., no Tr) and possibly no A . Osmotic adjustment from cold hardening can increase total leaf xylem water potential by around -2 MPa (Abrams 1988), which is insufficient to compensate for differences observed here between winter and the other seasons at any of the sites. Consequently, we can

assume that both species are photosynthetically active during the winter at the intermediate PAL but less so at MTL and LIZ. Ascertaining the degree of photoinhibition and photosynthetic down-regulation, measured partly by ratio and total pool sizes of leaf violaxanthin-antherxanthin-zeaxanthin (Björkman and Demmig-Adams 1994), during winter across the three sites would contribute to understanding more about cold temperature influences on the distributions of these species.

While gas exchange during the monsoon appeared to be directly linked to PAR, thus soil water was not considered to be limiting, gas exchange during the arid foresummer was not related to PAR or T_{leaf} , but instead was likely related to soil moisture (Bassman 1987). In ponderosa pine, Tr rates are typically higher than other western conifers until a threshold soil Ψ (-0.2 MPa) is reached, after which Tr for ponderosa pine decreases immediately, long before other conifers (Bassman 1987). Greater stomatal control, or sensitivity to leaf water status, leading to higher overall WUE, is considered the mechanism by which ponderosa pine survive in more xeric habitats than expected given its higher Tr . In this study, Ψ_p was similar for coincident PIN_PON and PIN_ARI at predawn and midday, but PIN_PON had an average 42% higher standard deviation in daily A measurements and average 62% higher standard deviation in daily Tr than did PIN_ARI at PAL during the arid foresummer. These data support the conclusion that PIN_PON is more drought tolerant than PIN_ARI based on more rapid stomatal control of transpiration.

Density and architecture of stomata also exert considerable control over gas exchange (Bassman 1987, Rundel and Yoder 1998). Increased stomatal density, as well as increased needle surface area, should lead to increased Tr . Stomatal density was compared for a limited number of needles from PIN_PON and PIN_ARI; no significant ($p>0.05$) difference in density on any side of the needle was found. Hadley (1986) found that epicuticular waxes had a profound influence on stomatal conductivity. In a limited inspection of scanning electron microscopy (SEM) images (courtesy of Anna Jacobsen, MSU) from PIN_PON and PIN_ARI needles from PAL, abundant epicuticular wax is produced by both species, with little observed difference (Figure 5-19). Removal of the waxes with chloroform revealed a deeply sunken stomatal aperture (Figure 5-20).

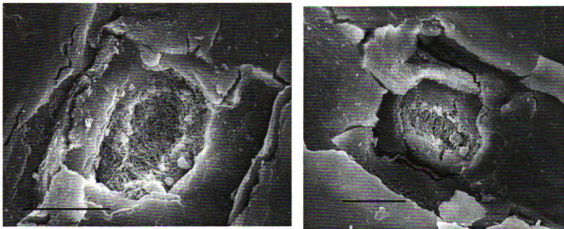


Figure 5-19. Stomatal openings in PIN_PON (*left*) and PIN_ARI (*right*) by SEM. Note the abundant epicuticular waxes surrounding the stomatal pit, as well as the network of waxes above the aperture. Scale bar equal to 20 microns. Photos courtesy of Anna Jacobsen.

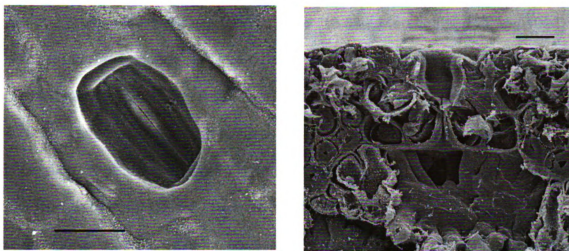


Figure 5-20. Chloroform-cleared stomatal openings in PIN_ARI of top and transverse views by SEM. Scale bar equal to 20 microns. Photos courtesy of Anna Jacobsen.

Integrated water-use efficiency and nutrient dynamics

Discrimination against heavier isotopes occurs in plants due to physical properties of the heavier isotope and ecophysiological responses through fractionation (Fry 2006). Less discrimination of ^{13}C is associated with higher WUE because plants that produce photosynthate with relatively higher ^{13}C close their stomata during stressful conditions, thereby increasing the intercellular-to-atmospheric CO_2 concentration (c_i/c_a) and increasing relative ^{13}C concentration inside the leaf (Dawson et al. 2002). Under normal conditions, the higher diffusivity (Melander and Saunders 1979) and reactivity with ribulose-1,5-bisphosphate carboxylase (Park and Epstein 1961) of ^{12}C results in discrimination of ^{13}C . When stomata close, c_i decreases, relative concentration of ^{12}C decreases, more ^{13}C is processed, and photosynthates are produced without losing water; hence, plants with greater stomatal control should have higher

WUE and less negative $\delta^{13}\text{C}$. In this experiment, $\delta^{13}\text{C}$ values were low (-25.2 to -26.6 ‰) relative to ponderosa pine in Idaho (18.6‰; Marshall and Zhang 1994) but comparable to ponderosa pine in northern Arizona (-24 to -25.5‰ at low and high elevation; Adams and Kolb 2004). There was no significant difference in $\delta^{13}\text{C}$ between species across years at the coincident PAL site (Table 5-4), but inspection of the values from 2001 and 2002 lead to some speculation (Figure 5-7). The years 2000 and 2002 were considered drought years; the manifestation of drought was observed in the substantially shorter needles from these years than from 2001 and 2003. In 2001, the PIN_PON needles had relatively less ^{13}C than the PIN_ARI needles, while the converse was true in 2002, the drought year. These data suggest that, with a larger sample size, PIN_ARI may in fact have higher WUE than PIN_PON, but the data are sparse to make such an inference. This conclusion departs from the supposition made after analyzing the Ψ_p and gas exchange results. Comparison of $\delta^{13}\text{C}$ and %N for both species across the elevational gradient would lead to greater insight on differential response to drought (Adams and Kolb 2004).

Carbon (%C) and nitrogen (%N) content varied by year, while species differences were observed only for %C (Figure 5-8). PIN_ARI had greater allocation of mass to structural C across most years; the higher leaf surface area to volume ratio for this 5-needled pine should increase the relative amount of C allocated to structural than photosynthetic cells. The increase in %N in younger needles likely represents N reallocation within the plant rather than less N produced and stored in 2001-02 relative to later years. Foliar nitrogen is strongly

correlated to maximum *A* on a leaf mass (not area) basis for conifers (Reich et al. 1995). Although not significant, PIN_PON needles had higher %N than PIN_ARI needles, suggesting a slightly higher potential photosynthetic capacity by PIN_PON.

The nitrogen isotope discrimination ($\delta^{15}\text{N}$) results suggest differential nitrogen resource dynamics between PIN_PON and PIN_ARI. Interestingly, $\delta^{15}\text{N}$ decreased during the drought year 2002 for both species, but more discrimination against ^{15}N occurred in PIN_ARI trees in subsequent years (Figure 5-8). Discrimination of ^{15}N in plants is much more complex than ^{13}C (Dawson et al. 2002). Nitrogen is normally acquired by plants through the soil. While physical discrimination against the heavier isotope does not occur across living membranes, enzyme-mediated processes can lead to discrimination (Dawson et al. 2002). Low nitrogen availability, osmotic stress, or drought can lead to N isotopic fractionation, but the mechanism remains unclear (Dawson et al. 2002). Hobbie et al. (2000) suggest that fractionation occurs during transfer of nitrogen from mycorrhizal fungi to plants, especially at low-nitrogen sites. Given the significant effect of ectomycorrhizal fungi in the establishment, survival, and nutrient acquisition for *Pinus* (Read 1998), the results of this experiment suggest that these fungi may be influencing the nitrogen dynamics, and thus photosynthetic capacity, of PIN_PON and PIN_ARI trees at PAL. Although highly speculative, increased fractionation of ^{15}N (i.e., more negative $\delta^{15}\text{N}$) by PIN_PON trees may suggest lower accessibility to N and thus lower potential growth.

Photosynthetic function during dehydration

Needles of trees from lower in elevation lost less mass from dehydration, or conversely had a lower relative water content, even when potentially fully hydrated, than needles from trees higher in elevation within a species (Figure 5-13). Furthermore, needles from lower elevation trees, especially PIN_ARI, had lower PSII excitation capture efficiency than those originating from higher elevation (Figure 5-15). Given the identical pretreatment conditions, these results suggest a plastic response in total potential needle water storage and photosynthetic function during extreme dehydration (i.e., drought) across the elevational gradient.

PIN_PON needles lost a larger portion of their initial mass through dehydration, suggesting that, despite full opportunity for hydration prior to the experiment, PIN_PON needles had a higher storage capacity for water than do PIN_ARI needles. Furthermore, for a given relative loss of water mass, PIN_PON trees had higher PSII excitation capture efficiency through the dehydration period (Figure 5-16). However, needle morphology was not characterized. Higher-needled fascicles for a given fascicle diameter and length have a geometrically higher surface area to volume ratio. The difference in total stored water mass per fascicle, and thus water available for photosynthesis, observed in this experiment could be accounted for by the difference in potential storage volume due to area:volume relationships, hence these results should be cautiously interpreted.

Xylem conductivity and vulnerability

Vulnerability of the xylem to cavitation has been suggested to be the primary driver for drought tolerance in plants (Tyree and Ewers 1991), but plants have evolved alternative avoidance strategies that are also important. For example, Piñol and Sala (2000) showed that increased stomatal control of water loss compensated for lower resistance to cavitation by ponderosa pine than by codominant species. In this study, the lower elevation species, PIN_ARI, was more vulnerable to cavitation than PIN_PON as determined by 50% loss of conductivity as a function of imposed negative xylem pressure (Figure 5-17); mean Ψ_{50} for PIN_PON was -3.44 MPa and for PIN_ARI was -3.16 MPa. The difference of -0.24 MPa is not substantial nor significant (Table 5-7). A mild site effect was also discernible but not significant.

In a study of desert versus montane ponderosa pine populations, vulnerability to cavitation did not differ, but xylem specific hydraulic conductivity (K_s) was higher for the more xeric trees (Maherali and DeLucia 2000). In this study, K_s was highest for PIN_PON stems from the highest elevation site (MTL), similar across species at PAL, and lowest for PIN_ARI at low elevation (Figure 5-18). High K_s implies an increased capability to transport water due to lower conductive resistance, whether due to larger tracheids, more porous pit membranes, or fewer cavitated tracheids. Standardizing for xylem area allows interspecies comparisons in potential hydraulic conductance. However, K_s did not differ for PIN_PON and PIN_ARI when coincident, while K_s was positively correlated with elevation. Maherali et al. (2002) also found K_s to be

phenotypically plastic in ponderosa pine across a climatic gradient. The results from this experiment indicate that K_s is similar for PIN_PON and PIN_ARI, that the ensemble of traits contributing to K_s is sufficiently plastic to acclimate across a steep climatic gradient within a species, and that drought stress is negatively associated with elevation.

Implications of drought tolerance to distribution

The balance of evidence from this study, composed of four experiments, suggests that PIN_PON is more drought tolerant than PIN_ARI. With only the exception of PIN_ARI trees at LIZ during the monsoon season, PIN_PON trees had less negative Ψ_p at all periods of the day and across major seasons (Figure 5-6). PIN_PON trees exhibited greater variation in A during the arid foresummer than did PIN_ARI trees (Figure 5-2); this result could be interpreted as PIN_PON stomata responding more closely to fluctuations in soil Ψ or as PIN_PON trees being closer to the drought threshold at that time of year. However, the less negative Ψ_p for PIN_PON trees suggests the former interpretation. Neither species appears to be water-limited during the monsoon season; rather light is limiting to A (Figure 5-3). When exposed to severe drought (i.e., dehydration), PIN_PON needles retain a higher level photosynthetic function than do PIN_ARI needles (Figure 5-16). Although not significant, PIN_PON trees had higher %N, which is correlated with maximum A and therefore growth potential. Conversely, PIN_PON needles contain a relatively higher concentration of ^{15}N , suggesting a larger amount of fractionation (or processing) occurs before N reaches the leaf;

this could indicate drought stress or, alternatively, different access to soil N pools than experienced by PIN_ARI trees. However, in sum, the results from this study suggest that PIN_PON trees are more drought tolerant than PIN_ARI trees.

If drought tolerance is not limiting the lower elevational distribution of PIN_PON, then what factors are limiting its range? This study did not examine potential competition nor the role of drought tolerance on seedlings, which are more susceptible to low soil water availability due to their developing root systems. In controlled greenhouse conditions as well as reciprocal *in situ* plantings, Barton and Teeri (1993) investigated drought tolerance of Southwestern conifers, excluding Arizona pine, and found that lower elevational distributions were determined by drought tolerance of seedlings. A similar approach with the taxa from this study would allow for standardized comparisons among these and other Southwestern species. Likewise, Daubenmire (1943) saw soil water availability as the limiting factor to Rocky Mountain conifers. Grasses and forbs are significant competitors against ponderosa pine seedlings for belowground resources, especially water and available nitrogen (White 1985, Elliott and White 1987, Riegel et al. 1992, and Kolb and Robberecht 1996). Seedling mortality due to moisture stress, in part from competition for water by all plants, can be over 90% within the first year (Elliott and White 1987). Relative differences in seedling root growth rates significantly affect survival (Kolb and Robberecht 1996). Although seedlings in the field were preferred subjects for this study, extensive recent ground fires, especially through the transition zone in the Santa Catalina Mountains, eliminated all small diameter seedlings and many

saplings, but the fires also created more habitat for grass, forb, and pine regeneration (personal observation).

Stomatal control of water relations appear key to separating ponderosa pine from other conifers of the Rocky Mountains. Given the purported warm, humid origins of Arizona pine (Millar 1993) relative to the cooler, drier evolutionary origin for ponderosa pine (Axelrod and Raven 1985, Millar 1993), investigations into differences in stomatal control may shed insight on how the two species control water loss, especially during the predictable arid foresummer. Since roots directly acquire water and since ponderosa pine are known for extensive root systems, differential rooting architecture, water uptake, and nutrient absorption may be important in segregating species distribution across the shallow soils of the Santa Catalina Mountains. The intriguing nitrogen isotope data suggest that differential mycorrhizal relationships may influence nitrogen uptake (Perry et al. 1989) and consequent photosynthetic capacity and WUE. The value of the elevational gradient and transition zone in this region should not be overlooked when examining distributions of related species. As indicated by this study, a number of responses to drought can be integrated to contribute to an understanding of species distributions; for example, spatial analysis of indicators, including integrative measures like $\delta^{13}\text{C}$ and tree-rings, can yield models to predict expected changes in distribution from climate change.

CHAPTER 6

GENERAL CONCLUSIONS

The objectives for this dissertation research were to characterize the spatial distribution and examine ecophysiological responses that could affect the respective distributions of the *Ponderosae* in the Santa Catalina Mountains of southern Arizona. *A priori* expectations were that Southwestern ponderosa pine were distributed higher in elevation than the evolutionarily close and spatially overlapping Arizona pine because the former species is less drought tolerant and the latter taxon is less cold tolerant. Differences in distribution and cold tolerance met these expectations, while results from the drought tolerance work demonstrated the opposite expectation. In general, Southwestern ponderosa pine was better able to maintain positive net photosynthesis and water balance during periods of low soil water availability, both during winter and the arid foresummer.

Most Southwestern ponderosa pine were indeed located at higher elevation than Arizona pine trees, with a few low-elevation occurrences by the former species. As expected, spatial modeling of sampled trees by species, or morphotype to avoid taxonomic debate, suggested that Arizona pine and the Mixed morphotype are limited in upper and lower range by cold temperatures and climatic variables contributing to drought during the arid foresummer, respectively. Because the upper elevational range was not reached by Southwestern ponderosa pine in the Santa Catalina Mountains, its distribution

was understandably limited most by arid foresummer conditions. However, Southwestern ponderosa pine and the Mixed morphotype had higher probability of occurrence at higher elevation as compared to the distribution predicted for Arizona pine, while both Arizona pine and the Mixed morphotype had higher probability of occurrence at lower elevation as compared to the distribution predicted for Southwestern ponderosa pine. Since lower elevational limits were based on the same climatic factors, the higher placement of Southwestern ponderosa pine suggests a decreased ability to establish at its lower margin, where drought is more severe and Arizona pine is sympatric. Furthermore, the presence of the Mixed morphotype above the upper margin for Arizona pine and below the lower margin for Southwestern ponderosa pine suggests that this group possesses unique genetic adaptations to a broader climatic range than the other taxa.

The ecophysiological experiments indicate that Southwestern ponderosa pine is undoubtedly more cold tolerant than Arizona pine. Arizona pine seed had much lower germination rate, especially at high elevation, while Southwestern ponderosa pine seed germinated equally well across elevations. Survival of germinants at both sites through the first full arid foresummer (2007) has yet to be determined. Sapling Southwestern ponderosa pine had higher photosynthetic function and rate and less negative leaf xylem pressure potential during the winter than did Arizona pine saplings, demonstrating less cold tolerance of Arizona pine trees; in one experiment, seedlings of the Mixed morphotype in frozen soil water exhibited photosynthetic function intermediate to Southwestern

ponderosa and Arizona pine seedlings. Additionally, fully hardened Arizona pine seedlings had higher threshold freezing temperatures than did similarly hardened Southwestern ponderosa pine seedlings, thereby further supporting the conclusion of greater genetic cold tolerance by Southwestern ponderosa pine.

The studies examining indicators of drought tolerance offered no clear sign of Arizona pine being more drought tolerant than Southwestern ponderosa pine; in fact, most evidence suggested the opposite trend. Southwestern ponderosa pine had less negative leaf xylem pressure potentials across all times of day and seasons, lower vulnerability to xylem cavitation in branches, higher immediate response to variations in climatic conditions during the arid foresummer, and higher photosynthetic function during dehydration. These indications suggest that Southwestern ponderosa pine is *more* drought tolerant than Arizona pine. Although not statistically significant, Southwestern ponderosa pine had higher foliar nitrogen across all drought and non-drought years, possibly indicating a higher maximum photosynthetic capacity. No difference in integrated water-use efficiency, as measured by carbon isotopic discrimination, was found between sympatric species; however, sample sizes were small, and application of this technique across the elevational gradient may detect species x site differences. Differential leaf nitrogen isotope composition suggests that these species differ in their nitrogen uptake pathway, and, although nitrogen dynamics are highly complex, combining this type of analysis with studies of rooting architecture and mycorrhizal associations may contribute more to understanding

lower elevational distribution of these taxa in the nitrogen-poor granitic soils of the Santa Catalina Mountains.

The rapidly developing field of species distribution modeling offers tools for inferring evolutionary processes, tracing population migration, and predicting responses to climate change. Heretofore unseen in the literature, a thorough spatial analysis of genetically linked morphological traits and combined cytoplasmic and nuclear DNA of the *Ponderosae* would contribute to an understanding of the systematics and evolution of this complex in the Southwest. In this dissertation, the unique spatial and modeled niche of trees producing intermediate needle numbers ("Mixed") relative to Southwestern ponderosa and Arizona pine do not support the Taxon X hypothesis; instead, these results support the accepted taxonomy of the parent species (Conkle and Critchfield 1988, Price et al. 1998) and putative introgression (Peloquin 1984, Rehfeldt et al. 1996, Epperson et al. 2001). Further, the high intratree variance in the highly heritable morphologic feature of number of needles per fascicle (Rehfeldt et al. 1996) draws attention to intermediate, or putative hybrid, morphotypes. Population migration can be traced, for example, by back-calibrating models without the outlying low-elevation 3-needled trees to determine the likelihood of their being part of, or date of last contact with, the current Southwestern ponderosa pine population. Potential low-elevation areas containing "old" trees could be identified for dendrochronological research, or, in longer time periods, the progression of ponderosa pine through the region could be modeled and cross-calibrated with packrat midden data. Conversely, output from predictive

models can be projected to new scenarios, whether they be other mountain islands in the Southwest or altered climate, to generate probabilities of suitable habitat for the modeled species. Using ecophysiological methods to confirm the importance of climatic and other variables (e.g, mycorrhizal associations) can only improve variable selection and directions for continued research on dynamic species distributions.

APPENDIX

Table A-1. Geographic coordinates and mean needle number for trees from the distribution study ("SCAT"). Universal Transverse Mercator (UTM) coordinates are for Zone 12S projected to World Geodetic System 1984. Elevation was interpolated from Topozone.com. Morphotype is based on Peloquin (1984): *Pinus ponderosa* var. *scopulorum* (PIN_PON), *P. arizonica* (PIN_ARI), and putative hybrid (Mixed).

WP	UTM-X	UTM-Y	Elevation (m)	Mean needle number	Morphotype
1	518198	3588043	2598.4	3.05	PIN_PON
1	518198	3588043	2598.4	3.63	Mixed
1	518198	3588043	2598.4	3.40	Mixed
1	518198	3588043	2598.4	3.61	Mixed
2	517666	3588386	2484.1	4.99	PIN_ARI
2	517666	3588386	2484.1	5.01	PIN_ARI
2	517666	3588386	2484.1	4.92	PIN_ARI
2	517666	3588386	2484.1	5.00	PIN_ARI
3	517260	3588735	2430.2	4.96	PIN_ARI
3	517260	3588735	2430.2	4.53	Mixed
3	517260	3588735	2430.2	4.88	PIN_ARI
3	517260	3588735	2430.2	5.05	PIN_ARI
4	516955	3589032	2346.0	4.86	PIN_ARI
4	516955	3589032	2346.0	5.00	PIN_ARI
4	516955	3589032	2346.0	4.89	PIN_ARI
4	516955	3589032	2346.0	4.91	PIN_ARI
5	516823	3589263	2368.8	5.00	PIN_ARI
5	516823	3589263	2368.8	4.98	PIN_ARI
5	516823	3589263	2368.8	4.65	PIN_ARI
5	516823	3589263	2368.8	5.00	PIN_ARI
6	517210	3590125	2193.1	4.97	PIN_ARI
6	517210	3590125	2193.1	4.78	PIN_ARI
6	517210	3590125	2193.1	4.93	PIN_ARI
6	517210	3590125	2193.1	4.75	PIN_ARI
7	517328	3590761	2266.3	4.80	PIN_ARI
7	517328	3590761	2266.3	4.82	PIN_ARI
7	517328	3590761	2266.3	4.78	PIN_ARI
7	517328	3590761	2266.3	4.88	PIN_ARI
7	517328	3590761	2266.3	4.86	PIN_ARI
8	517298	3590996	2252.1	4.95	PIN_ARI
8	517298	3590996	2252.1	4.08	Mixed
8	517298	3590996	2252.1	4.03	Mixed
8	517298	3590996	2252.1	4.97	PIN_ARI
9	517636	3592413	2221.3	4.90	PIN_ARI
9	517636	3592413	2221.3	3.93	Mixed
9	517636	3592413	2221.3	4.47	Mixed
9	517636	3592413	2221.3	4.59	Mixed
10	517417	3593325	2200.2	4.96	PIN_ARI
10	517417	3593325	2200.2	4.37	Mixed
10	517417	3593325	2200.2	4.74	PIN_ARI
10	517417	3593325	2200.2	4.54	Mixed
11	517429	3593667	2172.7	3.00	PIN_PON
11	517429	3593667	2172.7	3.00	PIN_PON

Table A-1. *Continued.*

WP	UTM-X	UTM-Y	Elevation (m)	Mean needle number	Morphotype
11	517429	3593667	2172.7	3.02	PIN_PON
11	517429	3593667	2172.7	3.14	PIN_PON
17	525172	3587947	2251.3	4.99	PIN_ARI
17	525172	3587947	2251.3	4.71	PIN_ARI
18	525234	3588017	2246.9	4.53	Mixed
18	525234	3588017	2246.9	4.90	PIN_ARI
18	525234	3588017	2246.9	5.01	PIN_ARI
18	525234	3588017	2246.9	4.85	PIN_ARI
19	525617	3588455	2110.2	4.51	Mixed
19	525617	3588455	2110.2	4.80	PIN_ARI
19	525617	3588455	2110.2	4.37	Mixed
19	525617	3588455	2110.2	4.24	Mixed
20	525467	3588808	2060.1	4.88	PIN_ARI
20	525467	3588808	2060.1	4.24	Mixed
20	525467	3588808	2060.1	4.98	PIN_ARI
20	525467	3588808	2060.1	4.60	Mixed
21	524432	3588773	2080.4	4.81	PIN_ARI
21	524432	3588773	2080.4	4.77	PIN_ARI
21	524432	3588773	2080.4	4.55	Mixed
21	524432	3588773	2080.4	4.78	PIN_ARI
22	524420	3590284	2083.4	4.72	PIN_ARI
22	524420	3590284	2083.4	4.66	PIN_ARI
22	524420	3590284	2083.4	5.00	PIN_ARI
22	524420	3590284	2083.4	4.91	PIN_ARI
23	524703	3590316	2083.6	4.80	PIN_ARI
23	524703	3590316	2083.6	4.70	PIN_ARI
23	524703	3590316	2083.6	4.98	PIN_ARI
23	524703	3590316	2083.6	4.94	PIN_ARI
24	524236	3590600	2134.2	4.72	PIN_ARI
24	524236	3590600	2134.2	4.65	PIN_ARI
24	524236	3590600	2134.2	4.69	PIN_ARI
24	524236	3590600	2134.2	4.99	PIN_ARI
25	523595	3590662	2256.7	4.60	Mixed
25	523595	3590662	2256.7	4.85	PIN_ARI
25	523595	3590662	2256.7	4.94	PIN_ARI
25	523595	3590662	2256.7	4.79	PIN_ARI
26	523343	3590272	2328.0	5.00	PIN_ARI
26	523343	3590272	2328.0	4.99	PIN_ARI
26	523343	3590272	2328.0	4.47	Mixed
26	523343	3590272	2328.0	4.86	PIN_ARI
28	528669	3582880	2133.7	4.91	PIN_ARI
28	528669	3582880	2133.7	4.70	PIN_ARI
28	528669	3582880	2133.7	4.54	Mixed
28	528669	3582880	2133.7	4.78	PIN_ARI
29	528529	3582872	2192.9	3.74	Mixed
29	528529	3582872	2192.9	4.97	PIN_ARI
29	528529	3582872	2192.9	4.84	PIN_ARI

Table A-1. *Continued.*

WP	UTM-X	UTM-Y	Elevation (m)	Mean needle number	Morphotype
29	528529	3582872	2192.9	4.77	PIN_ARI
30	528850	3582967	2135.3	4.93	PIN_ARI
30	528850	3582967	2135.3	4.77	PIN_ARI
30	528850	3582967	2135.3	4.32	Mixed
30	528850	3582967	2135.3	4.97	PIN_ARI
31	528339	3583418	2111.6	4.62	PIN_ARI
31	528339	3583418	2111.6	4.90	PIN_ARI
31	528339	3583418	2111.6	4.91	PIN_ARI
31	528339	3583418	2111.6	4.66	PIN_ARI
32	528636	3584094	2195.4	4.94	PIN_ARI
32	528636	3584094	2195.4	4.95	PIN_ARI
32	528636	3584094	2195.4	4.71	PIN_ARI
32	528636	3584094	2195.4	4.99	PIN_ARI
33	527366	3583739	2131.1	5.39	PIN_ARI
34	527280	3583339	2125.7	3.64	Mixed
34	527280	3583339	2125.7	5.04	PIN_ARI
34	527280	3583339	2125.7	4.72	PIN_ARI
34	527280	3583339	2125.7	4.95	PIN_ARI
35	525564	3586049	2504.2	3.56	Mixed
35	525564	3586049	2504.2	3.00	PIN_PON
35	525564	3586049	2504.2	3.02	PIN_PON
35	525564	3586049	2504.2	3.22	Mixed
36	525571	3585999	2492.3	3.07	PIN_PON
36	525571	3585999	2492.3	3.00	PIN_PON
37	526461	3585865	2400.7	5.15	PIN_ARI
37	526461	3585865	2400.7	5.04	PIN_ARI
37	526461	3585865	2400.7	4.61	PIN_ARI
37	526461	3585865	2400.7	4.99	PIN_ARI
37	526461	3585865	2400.7	5.01	PIN_ARI
38	527040	3585860	2428.2	4.97	PIN_ARI
38	527040	3585860	2428.2	4.79	PIN_ARI
38	527040	3585860	2428.2	4.96	PIN_ARI
38	527040	3585860	2428.2	4.99	PIN_ARI
39	526097	3586082	2487.4	3.46	Mixed
39	526097	3586082	2487.4	3.05	PIN_PON
39	526097	3586082	2487.4	4.91	PIN_ARI
39	526097	3586082	2487.4	3.06	PIN_PON
40	526177	3586133	2526.3	3.13	PIN_PON
40	526177	3586133	2526.3	3.38	Mixed
40	526177	3586133	2526.3	4.07	Mixed
40	526177	3586133	2526.3	3.01	PIN_PON
41	526231	3586172	2546.1	3.24	Mixed
41	526231	3586172	2546.1	3.02	PIN_PON
41	526231	3586172	2546.1	3.91	Mixed
41	526231	3586172	2546.1	3.37	Mixed
42	526206	3586225	2572.3	3.70	Mixed
42	526206	3586225	2572.3	3.52	Mixed

Table A-1. *Continued.*

WP	UTM-X	UTM-Y	Elevation (m)	Mean needle number	Morphotype
42	526206	3586225	2572.3	3.00	PIN_PON
42	526206	3586225	2572.3	3.00	PIN_PON
43	524405	3588019	2335.8	3.21	Mixed
43	524405	3588019	2335.8	3.05	PIN_PON
43	524405	3588019	2335.8	3.29	Mixed
43	524405	3588019	2335.8	2.99	PIN_PON
44	524395	3587937	2342.5	5.01	PIN_ARI
44	524395	3587937	2342.5	3.24	Mixed
44	524395	3587937	2342.5	4.99	PIN_ARI
44	524395	3587937	2342.5	3.00	PIN_PON
47	525002	3587025	2475.0	3.00	PIN_PON
47	525002	3587025	2475.0	3.36	Mixed
47	525002	3587025	2475.0	3.02	PIN_PON
47	525002	3587025	2475.0	3.01	PIN_PON
48	524884	3586716	2499.4	3.60	Mixed
48	524884	3586716	2499.4	3.23	Mixed
48	524884	3586716	2499.4	3.03	PIN_PON
48	524884	3586716	2499.4	3.08	PIN_PON
49	525728	3586553	2547.8	3.26	Mixed
49	525728	3586553	2547.8	3.00	PIN_PON
49	525728	3586553	2547.8	3.01	PIN_PON
49	525728	3586553	2547.8	3.02	PIN_PON
50	526064	3586493	2541.3	3.34	Mixed
50	526064	3586493	2541.3	3.03	PIN_PON
50	526064	3586493	2541.3	4.13	Mixed
50	526064	3586493	2541.3	4.08	Mixed
50	526064	3586493	2541.3	4.34	Mixed
51	526931	3586640	2581.4	3.03	PIN_PON
51	526931	3586640	2581.4	3.04	PIN_PON
51	526931	3586640	2581.4	3.01	PIN_PON
51	526931	3586640	2581.4	3.01	PIN_PON
52	529524	3584657	2198.4	4.95	PIN_ARI
52	529524	3584657	2198.4	4.98	PIN_ARI
52	529524	3584657	2198.4	4.95	PIN_ARI
52	529524	3584657	2198.4	5.00	PIN_ARI
53	529829	3584400	2193.1	5.03	PIN_ARI
53	529829	3584400	2193.1	4.99	PIN_ARI
53	529829	3584400	2193.1	4.92	PIN_ARI
53	529829	3584400	2193.1	4.79	PIN_ARI
54	530378	3584511	2010.5	4.64	PIN_ARI
54	530378	3584511	2010.5	4.95	PIN_ARI
54	530378	3584511	2010.5	4.64	PIN_ARI
54	530378	3584511	2010.5	4.94	PIN_ARI
55	530828	3584110	2110.0	5.08	PIN_ARI
55	530828	3584110	2110.0	4.82	PIN_ARI
55	530828	3584110	2110.0	4.97	PIN_ARI
55	530828	3584110	2110.0	4.81	PIN_ARI

Table A-1. *Continued.*

WP	UTM-X	UTM-Y	Elevation (m)	Mean needle number	Morphotype
57	531064	3583808	2162.7	4.96	PIN_ARI
57	531064	3583808	2162.7	4.92	PIN_ARI
57	531064	3583808	2162.7	4.42	Mixed
57	531064	3583808	2162.7	4.99	PIN_ARI
58	531692	3583274	2212.7	4.03	Mixed
58	531692	3583274	2212.7	4.11	Mixed
58	531692	3583274	2212.7	4.38	Mixed
58	531692	3583274	2212.7	3.81	Mixed
59	532261	3583539	2171.8	4.20	Mixed
59	532261	3583539	2171.8	4.98	PIN_ARI
59	532261	3583539	2171.8	5.00	PIN_ARI
59	532261	3583539	2171.8	4.46	Mixed
60	530739	3583800	2073.1	4.98	PIN_ARI
60	530739	3583800	2073.1	4.99	PIN_ARI
60	530739	3583800	2073.1	4.80	PIN_ARI
60	530739	3583800	2073.1	4.82	PIN_ARI
61	530500	3583244	2031.5	4.52	Mixed
61	530500	3583244	2031.5	4.96	PIN_ARI
61	530500	3583244	2031.5	4.96	PIN_ARI
61	530500	3583244	2031.5	4.87	PIN_ARI
62	530500	3583244	2031.5	4.82	PIN_ARI
62	530500	3583244	2031.5	4.96	PIN_ARI
62	530500	3583244	2031.5	4.95	PIN_ARI
62	530500	3583244	2031.5	5.00	PIN_ARI
65	523114	3590540	2378.6	4.86	PIN_ARI
65	523114	3590540	2378.6	4.99	PIN_ARI
65	523114	3590540	2378.6	4.84	PIN_ARI
65	523114	3590540	2378.6	3.44	Mixed
66	523015	3590116	2413.9	3.74	Mixed
66	523015	3590116	2413.9	3.40	Mixed
66	523015	3590116	2413.9	3.01	PIN_PON
67	522749	3589887	2406.1	3.23	Mixed
67	522749	3589887	2406.1	3.05	PIN_PON
67	522749	3589887	2406.1	3.00	PIN_PON
67	522749	3589887	2406.1	3.08	PIN_PON
68	523072	3589232	2438.0	4.91	PIN_ARI
68	523072	3589232	2438.0	3.00	PIN_PON
68	523072	3589232	2438.0	3.33	Mixed
68	523072	3589232	2438.0	3.00	PIN_PON
68	523072	3589232	2438.0	4.99	PIN_ARI
69	523212	3589207	2436.1	6.50	PIN_ARI
69	523212	3589207	2436.1	3.00	PIN_PON
69	523212	3589207	2436.1	3.33	Mixed
69	523212	3589207	2436.1	3.03	PIN_PON
70	521773	3590551	2398.3	5.00	PIN_ARI
70	521773	3590551	2398.3	4.99	PIN_ARI
70	521773	3590551	2398.3	5.23	PIN_ARI

Table A-1. *Continued.*

WP	UTM-X	UTM-Y	Elevation (m)	Mean needle number	Morphotype
70	521773	3590551	2398.3	5.02	PIN_ARI
71	521997	3592420	2069.5	4.87	PIN_ARI
71	521997	3592420	2069.5	4.65	PIN_ARI
71	521997	3592420	2069.5	4.88	PIN_ARI
71	521997	3592420	2069.5	4.88	PIN_ARI
72	522002	3593674	1745.0	3.00	PIN_PON
72	522002	3593674	1745.0	3.00	PIN_PON
72	522002	3593674	1745.0	3.00	PIN_PON
72	522002	3593674	1745.0	3.00	PIN_PON
73	523628	3593676	2127.0	3.11	PIN_PON
73	523628	3593676	2127.0	3.07	PIN_PON
73	523628	3593676	2127.0	2.98	PIN_PON
73	523628	3593676	2127.0	3.02	PIN_PON
74	524046	3592746	2295.7	3.23	Mixed
74	524046	3592746	2295.7	3.04	PIN_PON
74	524046	3592746	2295.7	3.01	PIN_PON
74	524046	3592746	2295.7	3.00	PIN_PON
75	523059	3587849	2268.4	3.05	PIN_PON
75	523059	3587849	2268.4	2.99	PIN_PON
75	523059	3587849	2268.4	3.00	PIN_PON
75	523059	3587849	2268.4	3.00	PIN_PON
76	522747	3588693	2321.7	3.49	Mixed
76	522747	3588693	2321.7	3.29	Mixed
76	522747	3588693	2321.7	3.24	Mixed
76	522747	3588693	2321.7	3.05	PIN_PON
77	522552	3589178	2344.7	3.01	PIN_PON
77	522552	3589178	2344.7	3.00	PIN_PON
77	522552	3589178	2344.7	3.02	PIN_PON
77	522552	3589178	2344.7	3.00	PIN_PON
78	521964	3590069	2422.0	3.03	PIN_PON
78	521964	3590069	2422.0	3.00	PIN_PON
78	521964	3590069	2422.0	3.06	PIN_PON
78	521964	3590069	2422.0	3.35	Mixed
79	521731	3590186	2465.4	3.22	Mixed
79	521731	3590186	2465.4	3.03	PIN_PON
79	521731	3590186	2465.4	3.01	PIN_PON
79	521731	3590186	2465.4	2.99	PIN_PON
80	520297	3590584	2572.5	3.00	PIN_PON
80	520297	3590584	2572.5	4.31	Mixed
80	520297	3590584	2572.5	3.25	Mixed
80	520297	3590584	2572.5	3.06	PIN_PON
81	520952	3589507	2680.4	3.13	PIN_PON
81	520952	3589507	2680.4	3.11	PIN_PON
81	520952	3589507	2680.4	4.99	PIN_ARI
81	520952	3589507	2680.4	3.99	Mixed
82	520361	3589357	2756.9	4.02	Mixed
82	520361	3589357	2756.9	3.64	Mixed

Table A-1. *Continued.*

WP	UTM-X	UTM-Y	Elevation (m)	Mean needle number	Morphotype
82	520361	3589357	2756.9	3.06	PIN_PON
82	520361	3589357	2756.9	3.68	Mixed
83	521521	3589530	2625.6	3.00	PIN_PON
85	523068	3587618	2314.2	4.85	PIN_ARI
85	523068	3587618	2314.2	4.97	PIN_ARI
85	523068	3587618	2314.2	4.98	PIN_ARI
85	523068	3587618	2314.2	4.98	PIN_ARI
86	522678	3587265	2410.5	5.00	PIN_ARI
86	522678	3587265	2410.5	5.07	PIN_ARI
86	522678	3587265	2410.5	5.10	PIN_ARI
86	522678	3587265	2410.5	5.00	PIN_ARI
87	521895	3587265	2472.8	4.64	PIN_ARI
87	521895	3587265	2472.8	5.00	PIN_ARI
87	521895	3587265	2472.8	4.86	PIN_ARI
87	521895	3587265	2472.8	4.89	PIN_ARI
88	521510	3587614	2478.7	4.99	PIN_ARI
88	521510	3587614	2478.7	5.00	PIN_ARI
88	521510	3587614	2478.7	4.98	PIN_ARI
88	521510	3587614	2478.7	5.00	PIN_ARI
89	521313	3588163	2434.8	4.90	PIN_ARI
89	521313	3588163	2434.8	4.52	Mixed
89	521313	3588163	2434.8	4.97	PIN_ARI
89	521313	3588163	2434.8	4.64	PIN_ARI
90	521837	3588153	2363.9	3.00	PIN_PON
90	521837	3588153	2363.9	3.04	PIN_PON
90	521837	3588153	2363.9	3.06	PIN_PON
90	521837	3588153	2363.9	3.00	PIN_PON
91	521198	3589037	2613.4	3.01	PIN_PON
91	521198	3589037	2613.4	3.02	PIN_PON
91	521198	3589037	2613.4	3.20	PIN_PON
91	521198	3589037	2613.4	3.70	Mixed
92	521161	3588666	2481.9	4.95	PIN_ARI
92	521161	3588666	2481.9	5.40	PIN_ARI
92	521161	3588666	2481.9	3.00	PIN_PON
92	521161	3588666	2481.9	4.60	PIN_ARI
93	520867	3588430	2372.2	4.98	PIN_ARI
93	520867	3588430	2372.2	4.95	PIN_ARI
93	520867	3588430	2372.2	3.51	Mixed
93	520867	3588430	2372.2	4.97	PIN_ARI
94	522536	3588172	2417.8	4.97	PIN_ARI
94	522536	3588172	2417.8	5.01	PIN_ARI
94	522536	3588172	2417.8	4.92	PIN_ARI
94	522536	3588172	2417.8	4.81	PIN_ARI
95	522408	3587860	2331.1	5.00	PIN_ARI
95	522408	3587860	2331.1	3.00	PIN_PON
95	522408	3587860	2331.1	3.05	PIN_PON
95	522408	3587860	2331.1	5.00	PIN_ARI

Table A-1. *Continued.*

WP	UTM-X	UTM-Y	Elevation (m)	Mean needle number	Morphotype
97	519443	3589532	2714.6	3.11	PIN_PON
97	519443	3589532	2714.6	3.00	PIN_PON
97	519443	3589532	2714.6	3.00	PIN_PON
97	519443	3589532	2714.6	3.14	PIN_PON
98	525491	3584718	2305.2	4.92	PIN_ARI
98	525491	3584718	2305.2	4.94	PIN_ARI
98	525491	3584718	2305.2	4.86	PIN_ARI
98	525491	3584718	2305.2	4.95	PIN_ARI
99	525777	3584681	2317.9	4.96	PIN_ARI
99	525777	3584681	2317.9	4.89	PIN_ARI
99	525777	3584681	2317.9	5.01	PIN_ARI
99	525777	3584681	2317.9	5.00	PIN_ARI
100	525551	3584070	2291.8	4.93	PIN_ARI
100	525551	3584070	2291.8	4.98	PIN_ARI
100	525551	3584070	2291.8	4.44	Mixed
100	525551	3584070	2291.8	4.94	PIN_ARI
101	526357	3585193	2365.6	4.98	PIN_ARI
101	526357	3585193	2365.6	4.41	Mixed
101	526357	3585193	2365.6	5.11	PIN_ARI
101	526357	3585193	2365.6	5.02	PIN_ARI
102	526350	3585532	2395.7	4.87	PIN_ARI
102	526350	3585532	2395.7	4.95	PIN_ARI
102	526350	3585532	2395.7	4.97	PIN_ARI
102	526350	3585532	2395.7	5.00	PIN_ARI
103	525110	3585720	2478.0	4.60	PIN_ARI
103	525110	3585720	2478.0	4.55	Mixed
103	525110	3585720	2478.0	4.84	PIN_ARI
103	525110	3585720	2478.0	4.97	PIN_ARI
104	525208	3586246	2489.2	3.10	PIN_PON
104	525208	3586246	2489.2	3.97	Mixed
104	525208	3586246	2489.2	3.40	Mixed
104	525208	3586246	2489.2	3.59	Mixed
105	528133	3585823	2482.1	4.40	Mixed
105	528133	3585823	2482.1	4.78	PIN_ARI
105	528133	3585823	2482.1	4.98	PIN_ARI
106	528204	3586238	2313.3	4.90	PIN_ARI
106	528204	3586238	2313.3	4.96	PIN_ARI
106	528204	3586238	2313.3	4.95	PIN_ARI
107	527998	3586344	2340.9	4.93	PIN_ARI
107	527998	3586344	2340.9	4.98	PIN_ARI
107	527998	3586344	2340.9	4.38	Mixed
107	527998	3586344	2340.9	4.85	PIN_ARI
108	527884	3586038	2467.4	5.11	PIN_ARI
108	527884	3586038	2467.4	5.45	PIN_ARI
108	527884	3586038	2467.4	4.57	Mixed
108	527884	3586038	2467.4	4.92	PIN_ARI
109	524358	3585856	2355.0	4.99	PIN_ARI

Table A-1. *Continued.*

WP	UTM-X	UTM-Y	Elevation (m)	Mean needle number	Morphotype
109	524358	3585856	2355.0	4.95	PIN_ARI
109	524358	3585856	2355.0	4.97	PIN_ARI
109	524358	3585856	2355.0	4.89	PIN_ARI
110	524331	3586423	2379.9	4.99	PIN_ARI
110	524331	3586423	2379.9	4.79	PIN_ARI
110	524331	3586423	2379.9	5.00	PIN_ARI
110	524331	3586423	2379.9	4.83	PIN_ARI
111	524607	3586710	2419.0	4.90	PIN_ARI
111	524607	3586710	2419.0	4.88	PIN_ARI
111	524607	3586710	2419.0	3.72	Mixed
111	524607	3586710	2419.0	4.78	PIN_ARI
112	524527	3586971	2451.1	4.94	PIN_ARI
112	524527	3586971	2451.1	3.00	PIN_PON
112	524527	3586971	2451.1	2.99	PIN_PON
112	524527	3586971	2451.1	4.49	Mixed
113	524083	3587031	2490.7	5.06	PIN_ARI
113	524083	3587031	2490.7	4.95	PIN_ARI
113	524083	3587031	2490.7	5.18	PIN_ARI
113	524083	3587031	2490.7	4.87	PIN_ARI
114	526916	3587500	2338.0	4.86	PIN_ARI
114	526916	3587500	2338.0	4.52	Mixed
114	526916	3587500	2338.0	4.98	PIN_ARI
115	527095	3587904	2309.0	4.65	PIN_ARI
115	527095	3587904	2309.0	4.58	Mixed
115	527095	3587904	2309.0	3.07	PIN_PON
115	527095	3587904	2309.0	4.85	PIN_ARI
116	527123	3588052	2232.9	4.90	PIN_ARI
116	527123	3588052	2232.9	4.95	PIN_ARI
116	527123	3588052	2232.9	4.74	PIN_ARI
117	526723	3588045	2172.7	4.97	PIN_ARI
117	526723	3588045	2172.7	4.76	PIN_ARI
117	526723	3588045	2172.7	5.13	PIN_ARI
118	526559	3587741	2108.5	5.00	PIN_ARI
118	526559	3587741	2108.5	4.66	PIN_ARI
118	526559	3587741	2108.5	4.88	PIN_ARI
119	525808	3587904	2142.4	4.99	PIN_ARI
119	525808	3587904	2142.4	5.02	PIN_ARI
119	525808	3587904	2142.4	4.80	PIN_ARI
120	527424	3586021	2419.8	4.81	PIN_ARI
120	527424	3586021	2419.8	4.99	PIN_ARI
120	527424	3586021	2419.8	4.97	PIN_ARI
120	527424	3586021	2419.8	4.98	PIN_ARI
121	527600	3586131	2451.6	4.96	PIN_ARI
121	527600	3586131	2451.6	4.95	PIN_ARI
121	527600	3586131	2451.6	5.00	PIN_ARI
121	527600	3586131	2451.6	4.75	PIN_ARI
122	527450	3586192	2470.8	4.94	PIN_ARI

Table A-1. *Continued.*

WP	UTM-X	UTM-Y	Elevation (m)	Mean needle number	Morphotype
122	527450	3586192	2470.8	4.94	PIN_ARI
122	527450	3586192	2470.8	4.97	PIN_ARI
122	527450	3586192	2470.8	4.70	PIN_ARI
123	527388	3586363	2554.3	3.16	PIN_PON
123	527388	3586363	2554.3	2.99	PIN_PON
124	527265	3586402	2551.7	3.02	PIN_PON
124	527265	3586402	2551.7	3.14	PIN_PON
124	527265	3586402	2551.7	3.42	Mixed
124	527265	3586402	2551.7	3.00	PIN_PON
125	527129	3586406	2521.1	3.26	Mixed
125	527129	3586406	2521.1	3.03	PIN_PON
125	527129	3586406	2521.1	3.04	PIN_PON
125	527129	3586406	2521.1	3.01	PIN_PON
126	527059	3586353	2508.2	3.01	PIN_PON
126	527059	3586353	2508.2	4.94	PIN_ARI
126	527059	3586353	2508.2	4.98	PIN_ARI
126	527059	3586353	2508.2	4.45	Mixed
127	519668	3589289	2768.9	3.06	PIN_PON
127	519668	3589289	2768.9	3.52	Mixed
127	519668	3589289	2768.9	3.08	PIN_PON
128	519615	3589131	2767.8	3.70	Mixed
128	519615	3589131	2767.8	3.68	Mixed
128	519615	3589131	2767.8	3.05	PIN_PON
128	519615	3589131	2767.8	3.08	PIN_PON
129	519183	3588867	2700.6	3.38	Mixed
129	519183	3588867	2700.6	3.00	PIN_PON
129	519183	3588867	2700.6	3.03	PIN_PON
129	519183	3588867	2700.6	3.63	Mixed
130	519136	3588734	2682.0	3.00	PIN_PON
130	519136	3588734	2682.0	3.00	PIN_PON
130	519136	3588734	2682.0	3.37	Mixed
130	519136	3588734	2682.0	3.02	PIN_PON
131	518926	3588551	2677.5	3.07	PIN_PON
131	518926	3588551	2677.5	3.38	Mixed
131	518926	3588551	2677.5	3.03	PIN_PON
131	518926	3588551	2677.5	2.93	PIN_PON
132	519369	3588742	2689.8	3.52	Mixed
132	519369	3588742	2689.8	3.97	Mixed
132	519369	3588742	2689.8	3.56	Mixed
132	519369	3588742	2689.8	2.99	PIN_PON
132	519369	3588742	2689.8	3.28	Mixed
133	519716	3588880	2712.0	3.01	PIN_PON
133	519716	3588880	2712.0	3.01	PIN_PON
133	519716	3588880	2712.0	3.14	PIN_PON
133	519716	3588880	2712.0	3.00	PIN_PON
134	519878	3588961	2730.1	3.00	PIN_PON
134	519878	3588961	2730.1	3.38	Mixed

Table A-1. *Continued.*

WP	UTM-X	UTM-Y	Elevation (m)	Mean needle number	Morphotype
134	519878	3588961	2730.1	3.09	PIN_PON
134	519878	3588961	2730.1	3.42	Mixed
135	529463	3584453	2334.9	4.84	PIN_ARI
135	529463	3584453	2334.9	4.75	PIN_ARI
135	529463	3584453	2334.9	4.42	Mixed
135	529463	3584453	2334.9	4.77	PIN_ARI
136	529496	3584309	2402.2	4.38	Mixed
136	529496	3584309	2402.2	5.22	PIN_ARI
136	529496	3584309	2402.2	4.68	PIN_ARI
136	529496	3584309	2402.2	4.32	Mixed
137	529406	3584161	2407.9	4.60	PIN_ARI
137	529406	3584161	2407.9	5.00	PIN_ARI
137	529406	3584161	2407.9	4.91	PIN_ARI
137	529406	3584161	2407.9	5.01	PIN_ARI
138	529469	3584041	2396.2	4.86	PIN_ARI
138	529469	3584041	2396.2	4.99	PIN_ARI
138	529469	3584041	2396.2	4.67	PIN_ARI
138	529469	3584041	2396.2	5.00	PIN_ARI
139	529396	3583820	2370.2	4.31	Mixed
139	529396	3583820	2370.2	4.99	PIN_ARI
139	529396	3583820	2370.2	5.00	PIN_ARI
139	529396	3583820	2370.2	5.00	PIN_ARI
140	529244	3583659	2319.5	5.02	PIN_ARI
140	529244	3583659	2319.5	4.95	PIN_ARI
140	529244	3583659	2319.5	5.00	PIN_ARI
140	529244	3583659	2319.5	5.25	PIN_ARI
141	528978	3583449	2228.5	5.00	PIN_ARI
141	528978	3583449	2228.5	5.10	PIN_ARI
141	528978	3583449	2228.5	4.80	PIN_ARI
141	528978	3583449	2228.5	4.95	PIN_ARI
142	528739	3583426	2173.4	4.94	PIN_ARI
142	528739	3583426	2173.4	4.89	PIN_ARI
142	528739	3583426	2173.4	4.89	PIN_ARI
142	528739	3583426	2173.4	4.88	PIN_ARI
143	528664	3584663	2190.9	4.96	PIN_ARI
143	528664	3584663	2190.9	4.51	Mixed
143	528664	3584663	2190.9	4.95	PIN_ARI
143	528664	3584663	2190.9	4.95	PIN_ARI
144	527887	3584178	2167.9	4.85	PIN_ARI
144	527887	3584178	2167.9	4.83	PIN_ARI
144	527887	3584178	2167.9	4.99	PIN_ARI
144	527887	3584178	2167.9	4.87	PIN_ARI
145	527156	3583655	2145.8	4.92	PIN_ARI
145	527156	3583655	2145.8	4.86	PIN_ARI
145	527156	3583655	2145.8	4.92	PIN_ARI
145	527156	3583655	2145.8	4.65	PIN_ARI
146	528445	3585778	2439.8	4.68	PIN_ARI

Table A-1. *Continued.*

WP	UTM-X	UTM-Y	Elevation (m)	Mean needle number	Morphotype
146	528445	3585778	2439.8	4.98	PIN_ARI
146	528445	3585778	2439.8	5.03	PIN_ARI
146	528445	3585778	2439.8	4.92	PIN_ARI
147	528272	3585635	2397.0	4.70	PIN_ARI
147	528272	3585635	2397.0	4.85	PIN_ARI
147	528272	3585635	2397.0	5.04	PIN_ARI
147	528272	3585635	2397.0	4.81	PIN_ARI
148	528482	3585409	2376.9	4.97	PIN_ARI
148	528482	3585409	2376.9	4.97	PIN_ARI
148	528482	3585409	2376.9	4.71	PIN_ARI
148	528482	3585409	2376.9	4.97	PIN_ARI
149	528480	3585146	2409.1	5.00	PIN_ARI
149	528480	3585146	2409.1	4.93	PIN_ARI
149	528480	3585146	2409.1	5.22	PIN_ARI
149	528480	3585146	2409.1	5.02	PIN_ARI
150	528592	3585010	2341.7	4.97	PIN_ARI
150	528592	3585010	2341.7	5.13	PIN_ARI
150	528592	3585010	2341.7	4.76	PIN_ARI
150	528592	3585010	2341.7	4.98	PIN_ARI
151	528877	3585124	2293.6	4.89	PIN_ARI
151	528877	3585124	2293.6	5.37	PIN_ARI
151	528877	3585124	2293.6	4.99	PIN_ARI
151	528877	3585124	2293.6	4.78	PIN_ARI
152	529181	3584828	2244.9	5.12	PIN_ARI
152	529181	3584828	2244.9	4.73	PIN_ARI
152	529181	3584828	2244.9	4.89	PIN_ARI
152	529181	3584828	2244.9	4.94	PIN_ARI
153	527783	3584801	2268.5	4.97	PIN_ARI
153	527783	3584801	2268.5	5.20	PIN_ARI
153	527783	3584801	2268.5	4.93	PIN_ARI
153	527783	3584801	2268.5	5.00	PIN_ARI
154	527563	3585623	2334.1	4.98	PIN_ARI
154	527563	3585623	2334.1	4.96	PIN_ARI
154	527563	3585623	2334.1	4.96	PIN_ARI
154	527563	3585623	2334.1	5.03	PIN_ARI
155	528120	3585438	2310.3	4.96	PIN_ARI
155	528120	3585438	2310.3	4.70	PIN_ARI
155	528120	3585438	2310.3	4.99	PIN_ARI
155	528120	3585438	2310.3	4.97	PIN_ARI
156	525955	3586763	2556.7	3.63	Mixed
156	525955	3586763	2556.7	3.07	PIN_PON
156	525955	3586763	2556.7	3.00	PIN_PON
156	525955	3586763	2556.7	3.20	Mixed
157	525565	3586272	2595.4	3.06	PIN_PON
157	525565	3586272	2595.4	3.13	PIN_PON
157	525565	3586272	2595.4	3.94	Mixed
157	525565	3586272	2595.4	3.07	PIN_PON

Table A-1. *Continued.*

WP	UTM-X	UTM-Y	Elevation (m)	Mean needle number	Morphotype
158	525782	3586502	2561.0	3.15	PIN_PON
158	525782	3586502	2561.0	3.44	Mixed
158	525782	3586502	2561.0	4.01	Mixed
158	525782	3586502	2561.0	3.17	PIN_PON
159	525333	3586998	2432.5	3.08	PIN_PON
159	525333	3586998	2432.5	3.03	PIN_PON
159	525333	3586998	2432.5	3.01	PIN_PON
159	525333	3586998	2432.5	3.00	PIN_PON
160	520065	3589172	2769.7	3.22	Mixed
160	520065	3589172	2769.7	3.01	PIN_PON
160	520065	3589172	2769.7	3.01	PIN_PON
160	520065	3589172	2769.7	3.40	Mixed
161	526520	3586370	2558.6	3.06	PIN_PON
161	526520	3586370	2558.6	3.01	PIN_PON
162	526504	3586244	2564.1	3.06	PIN_PON
162	526504	3586244	2564.1	3.35	Mixed
162	526504	3586244	2564.1	3.24	Mixed
162	526504	3586244	2564.1	4.51	Mixed
163	525218	3586605	2507.9	3.00	PIN_PON
163	525218	3586605	2507.9	3.00	PIN_PON
163	525218	3586605	2507.9	3.01	PIN_PON
163	525218	3586605	2507.9	3.02	PIN_PON
164	524790	3587570	2407.7	3.71	Mixed
164	524790	3587570	2407.7	4.86	PIN_ARI
164	524790	3587570	2407.7	3.00	PIN_PON
165	523505	3588328	2439.0	3.20	Mixed
165	523505	3588328	2439.0	5.10	PIN_ARI
165	523505	3588328	2439.0	4.98	PIN_ARI
165	523505	3588328	2439.0	4.02	Mixed
166	528831	3583112	2125.6	4.76	PIN_ARI
166	528831	3583112	2125.6	3.10	PIN_PON
166	528831	3583112	2125.6	4.99	PIN_ARI
166	528831	3583112	2125.6	3.39	Mixed
167	529014	3583212	2197.0	4.99	PIN_ARI
167	529014	3583212	2197.0	4.91	PIN_ARI
167	529014	3583212	2197.0	4.93	PIN_ARI
167	529014	3583212	2197.0	5.00	PIN_ARI
168	529195	3583607	2309.8	5.00	PIN_ARI
168	529195	3583607	2309.8	4.96	PIN_ARI
168	529195	3583607	2309.8	5.03	PIN_ARI
168	529195	3583607	2309.8	5.38	PIN_ARI
169	528976	3583398	2221.8	4.99	PIN_ARI
169	528976	3583398	2221.8	4.78	PIN_ARI
169	528976	3583398	2221.8	4.88	PIN_ARI
169	528976	3583398	2221.8	4.73	PIN_ARI
170	519676	3587162	2210.6	4.46	Mixed
170	519676	3587162	2210.6	4.89	PIN_ARI

Table A-1. *Continued.*

WP	UTM-X	UTM-Y	Elevation (m)	Mean needle number	Morphotype
170	519676	3587162	2210.6	4.47	Mixed
170	519676	3587162	2210.6	5.00	PIN_ARI
171	518348	3586331	2130.8	5.00	PIN_ARI
171	518348	3586331	2130.8	4.86	PIN_ARI
171	518348	3586331	2130.8	5.00	PIN_ARI
171	518348	3586331	2130.8	4.99	PIN_ARI
172	517083	3585705	2233.9	4.98	PIN_ARI
172	517083	3585705	2233.9	5.11	PIN_ARI
172	517083	3585705	2233.9	4.88	PIN_ARI
172	517083	3585705	2233.9	4.96	PIN_ARI
173	516251	3585092	2014.8	3.00	PIN_PON
174	516431	3585241	2066.6	3.58	Mixed
174	516431	3585241	2066.6	3.13	PIN_PON
174	516431	3585241	2066.6	3.01	PIN_PON
174	516431	3585241	2066.6	4.26	Mixed
175	516888	3585400	2215.3	4.97	PIN_ARI
175	516888	3585400	2215.3	4.10	Mixed
175	516888	3585400	2215.3	4.99	PIN_ARI
175	516888	3585400	2215.3	4.99	PIN_ARI
177	517261	3586397	2301.9	4.56	Mixed
177	517261	3586397	2301.9	4.99	PIN_ARI
177	517261	3586397	2301.9	4.84	PIN_ARI
177	517261	3586397	2301.9	4.98	PIN_ARI
178	517653	3587136	2330.9	4.95	PIN_ARI
178	517653	3587136	2330.9	4.99	PIN_ARI
178	517653	3587136	2330.9	4.96	PIN_ARI
178	517653	3587136	2330.9	4.96	PIN_ARI
179	517969	3587762	2493.1	3.01	PIN_PON
179	517969	3587762	2493.1	4.83	PIN_ARI
179	517969	3587762	2493.1	4.87	PIN_ARI
179	517969	3587762	2493.1	5.00	PIN_ARI
180	524999	3586496	2449.3	3.01	PIN_PON
180	524999	3586496	2449.3	4.98	PIN_ARI
180	524999	3586496	2449.3	4.90	PIN_ARI
180	524999	3586496	2449.3	3.13	PIN_PON
181	524595	3587330	2458.1	4.42	Mixed
181	524595	3587330	2458.1	3.41	Mixed
181	524595	3587330	2458.1	4.96	PIN_ARI
181	524595	3587330	2458.1	4.78	PIN_ARI
182	523842	3587780	2354.8	4.50	Mixed
182	523842	3587780	2354.8	4.97	PIN_ARI
182	523842	3587780	2354.8	4.99	PIN_ARI
182	523842	3587780	2354.8	4.99	PIN_ARI
183	522592	3584399	2155.0	4.93	PIN_ARI
183	522592	3584399	2155.0	4.36	Mixed
183	522592	3584399	2155.0	3.99	Mixed
183	522592	3584399	2155.0	4.71	PIN_ARI

Table A-1. *Continued.*

WP	UTM-X	UTM-Y	Elevation (m)	Mean needle number	Morphotype
184	522830	3585258	2248.2	4.87	PIN_ARI
184	522830	3585258	2248.2	4.88	PIN_ARI
184	522830	3585258	2248.2	4.18	Mixed
184	522830	3585258	2248.2	4.86	PIN_ARI
185	523842	3585874	2413.9	4.97	PIN_ARI
185	523842	3585874	2413.9	4.98	PIN_ARI
185	523842	3585874	2413.9	4.64	PIN_ARI
185	523842	3585874	2413.9	5.01	PIN_ARI
186	529520	3582208	1814.2	4.94	PIN_ARI
186	529520	3582208	1814.2	4.83	PIN_ARI
186	529520	3582208	1814.2	4.81	PIN_ARI
186	529520	3582208	1814.2	4.99	PIN_ARI
187	528657	3581733	1782.6	4.50	Mixed
187	528657	3581733	1782.6	4.55	Mixed
187	528657	3581733	1782.6	3.98	Mixed
187	528657	3581733	1782.6	4.72	PIN_ARI
188	528111	3581568	1758.0	5.01	PIN_ARI

Table A-2. Correlation matrix for mean (1971-2000; PRISM 2006) annual and monthly precipitation (Precip, *top*), minimum temperature (MinTemp, *bottom*), and maximum temperature (MaxTemp, *next page*) for the Santa Catalina Mountain study region.

Precip	Annual	Jan	Feb	Mar	Apr	May	June	July	Aug	Sept	Oct	Nov	Dec
Annual	1	0.94458	0.97221	0.9552	0.96357	0.91396	0.5068	0.90847	0.9434	0.92042	0.95803	0.97962	0.97257
Jan	0.94458	1	0.93047	0.95481	0.9735	0.91202	0.39207	0.79619	0.78819	0.81994	0.97392	0.93941	0.92777
Feb	0.97221	0.93047	1	0.95716	0.96423	0.92349	0.4359	0.81535	0.90707	0.82201	0.91813	0.96383	0.97343
Mar	0.9552	0.95481	0.95716	1	0.98747	0.92956	0.40568	0.76849	0.83745	0.82132	0.9299	0.92511	0.97348
Apr	0.96357	0.9735	0.96423	0.98747	1	0.93272	0.43765	0.79672	0.83877	0.82343	0.94979	0.93992	0.97023
May	0.91396	0.91202	0.92349	0.92956	0.93272	1	0.57535	0.7797	0.81126	0.78884	0.86764	0.87033	0.87385
June	0.5068	0.39207	0.4359	0.40568	0.43765	0.57535	1	0.6836	0.53906	0.6238	0.36576	0.37587	0.37253
July	0.90847	0.79619	0.81535	0.76849	0.79672	0.7797	0.6836	1	0.91805	0.95857	0.84493	0.86267	0.80757
Aug	0.9434	0.78819	0.90707	0.83745	0.83877	0.81126	0.53906	0.91805	1	0.90547	0.84122	0.92243	0.90214
Sept	0.92042	0.81994	0.82201	0.82132	0.82343	0.78884	0.6238	0.95857	0.84122	1	0.86047	0.87019	0.84256
Oct	0.95803	0.97392	0.91813	0.9299	0.94979	0.86764	0.36576	0.84493	0.84122	0.86047	1	0.96314	0.93423
Nov	0.97962	0.93941	0.96383	0.92511	0.93992	0.87033	0.37587	0.86267	0.92243	0.87019	0.96314	1	0.96074
Dec	0.97257	0.92777	0.97343	0.97348	0.97023	0.87385	0.37253	0.80757	0.90214	0.84256	0.93423	0.96074	1

MinTemp	Annual	Jan	Feb	Mar	Apr	May	June	July	Aug	Sept	Oct	Nov	Dec
Annual	1	0.98896	0.9929	0.99718	0.9951	0.99559	0.97479	0.97463	0.98919	0.99542	0.99565	0.99565	0.97722
Jan	0.98896	1	0.99476	0.99033	0.9811	0.98823	0.93989	0.93952	0.96666	0.97971	0.99001	0.99001	0.99169
Feb	0.9929	0.99476	1	0.99628	0.98924	0.99425	0.95065	0.9448	0.97044	0.98347	0.99665	0.99665	0.98851
Mar	0.99718	0.99033	0.99628	1	0.99409	0.99709	0.9639	0.95914	0.98023	0.99033	0.99764	0.99764	0.9828
Apr	0.9951	0.9811	0.98924	0.99409	1	0.99225	0.96635	0.96568	0.98648	0.99454	0.99553	0.99553	0.96389
May	0.99559	0.98823	0.99425	0.99709	0.99225	1	0.96397	0.95593	0.97665	0.98813	0.99709	0.99709	0.98063
June	0.97479	0.93989	0.95065	0.9639	0.96635	0.96397	1	0.98512	0.96845	0.96703	0.95947	0.95947	0.92829
July	0.97463	0.93952	0.9448	0.95914	0.96568	0.95593	0.98512	1	0.98492	0.97662	0.95434	0.95434	0.91825
Aug	0.98919	0.96666	0.97044	0.98023	0.98648	0.95593	0.98492	0.98492	1	0.99522	0.97751	0.97751	0.94509
Sept	0.99542	0.97971	0.98347	0.99033	0.99454	0.98813	0.96703	0.97662	0.99522	1	0.99011	0.99011	0.95908
Oct	0.99565	0.99001	0.99665	0.99764	0.99553	0.99709	0.95947	0.95434	0.97751	0.99011	1	1	0.97928
Nov	0.99565	0.99001	0.99665	0.99764	0.99553	0.99709	0.95947	0.95434	0.97751	0.99011	1	1	0.97928
Dec	0.97722	0.99169	0.98851	0.9828	0.96389	0.98063	0.92829	0.91825	0.94509	0.95908	0.97928	0.97928	1

Table A-2. Continued.

MaxTemp	Annual	Jan	Feb	Mar	Apr	May	June	July	Aug	Sept	Oct	Nov	Dec
Annual	1	0.99467	0.99846	0.99861	0.99892	0.99888	0.99787	0.99699	0.99863	0.99943	0.99909	0.99781	0.99198
Jan	0.99467	1	0.99541	0.99376	0.9921	0.99864	0.98795	0.98676	0.98951	0.99192	0.99144	0.99763	0.99711
Feb	0.99846	0.99541	1	0.99874	0.99753	0.99635	0.99375	0.99241	0.99486	0.99667	0.99624	0.99901	0.99433
Mar	0.99861	0.99376	0.99874	1	0.99691	0.997	0.99572	0.99504	0.99624	0.99712	0.99653	0.99765	0.99065
Apr	0.99892	0.9921	0.99753	0.99691	1	0.99918	0.99666	0.99476	0.99721	0.99857	0.99822	0.99592	0.9913
May	0.99888	0.98964	0.99635	0.997	0.99918	1	0.99881	0.99735	0.99871	0.99896	0.99856	0.99431	0.987
June	0.99787	0.98795	0.99375	0.99572	0.99666	0.99881	1	0.99932	0.99936	0.9983	0.99775	0.99198	0.98257
July	0.99699	0.98676	0.99241	0.99504	0.99476	0.99735	0.99932	1	0.99937	0.99761	0.99701	0.99102	0.98044
Aug	0.99863	0.98951	0.99486	0.99624	0.99721	0.99871	0.99936	0.99937	1	0.9992	0.99889	0.99357	0.98509
Sept	0.99943	0.99192	0.99667	0.99712	0.99857	0.99896	0.9983	0.99761	0.9992	1	0.99988	0.99584	0.98915
Oct	0.99909	0.99144	0.99624	0.99653	0.99822	0.99856	0.99775	0.99701	0.99889	0.99988	1	0.99555	0.98903
Nov	0.99781	0.99763	0.99901	0.99765	0.99592	0.99431	0.99198	0.99102	0.99357	0.99584	0.99555	1	0.99641
Dec	0.99198	0.99711	0.99433	0.99065	0.9913	0.987	0.98257	0.98044	0.98509	0.98915	0.98903	0.99641	1

REFERENCES

REFERENCES

- Adams, H.D., and T.E. Kolb. 2004. Drought responses of conifers in ecotone forests of northern Arizona: tree ring growth and leaf $\delta^{13}\text{C}$. *Oecologia* 140:217-225.
- Adams, H.D., and T.E. Kolb. 2005. Tree growth response to drought and temperature in a mountain landscape in northern Arizona, USA. *Journal of Biogeography* 32:1629-1640.
- Adams, J. 2007. *Vegetation-Climate Interaction: How Vegetation Makes the Global Environment*. Springer-Verlag, Berlin, Germany. 300p.
- Adams, W.W. III, C.R. Zarter, V. Ebbert, and B. Demmig-Adams. 2004. Photoprotective strategies of overwintering evergreens. *BioScience* 54(1):41-49.
- Alder N.N., W.T. Pockman, J.S. Sperry, and S. Nuismer. 1997. Use of centrifugal force in the study of xylem cavitation. *Journal of Experimental Botany* 48: 665-674.
- Alexander, K. 1991. *Paradise Found: The Settlement of the Santa Catalina Mountains*. Skunkwork Productions, Mount Lemmon, Arizona, USA. 115p.
- Anderson, E., and G.L. Stebbins, Jr. 1954. Hybridization as an evolutionary stimulus. *Evolution* 8:378-388.
- Anderson, R.P., A.T. Peterson, and M. Gómez-Laverde. 2002. Using niche-based GIS modeling to test geographic predictions of competitive exclusion and competitive release in South American pocket mice. *Oikos* 98:3-16.
- Anderson, R.P., D. Lew, and A.T. Peterson. 2003. Evaluating predictive models of species' distributions: criteria for selecting optimal models. *Ecological Modelling* 162:211-232.
- Andersson, L., and P. Milberg. 1998. Variation in seed dormancy among mother plants, populations and years of seed collection. *Seed Science Research* 8:29-38.
- Araújo, M.B., and R.G. Pearson. 2005. Equilibrium of species' distributions with climate. *Ecography* 28(5):693-695.

- Aronsson, A., and L. Eliasson. 1970. Frost hardiness in Scots pine (*Pinus sylvestris* L.). I. Conditions for test on hardy plant tissues and for evaluation of injuries by conductivity measurements. *Studia Forestalia Suecica* Nr77. 30p.
- Austin, M.P. 2002. Spatial prediction of species distribution: an interface between ecological theory and statistical modelling. *Ecological Modelling* 157:101-118.
- Axelrod, D.I. 1986. Cenozoic history of some western American pines. *Annals of the Missouri Botanical Garden* 73:565-641.
- Axelrod, D.I., and P.H. Raven. 1985. Origins of the Cordilleran flora. *Journal of Biogeography* 12:21-47.
- Bahn, V., and B.J. McGill. 2007. Can niche-based distribution models outperform spatial interpolation? *Global Ecology and Biogeography*, OnLine Early Articles, 15 May 2007:1-10.
- Baldrige, W.S. 2004. *Geology of the American Southwest*. Cambridge University Press, Cambridge, U.K. 280p.
- Barton, A.M. 1993. Factors controlling plant distributions: drought, competition, and fire in montane pines in Arizona. *Ecological Monographs* 63(4):367-397.
- Barton, A.M., and J.A. Teeri. 1993. The ecology of elevational positions in plants: drought resistance in five montane pine species in southeastern Arizona. *American Journal of Botany* 80(1):15-25.
- Bassman, J.H. 1987. Photosynthesis and water relations of ponderosa pine. Pages 45-58 in D.M. Baumgarnter and J.E. Lotan, editors. *Ponderosa pine: the species and its management*. Washington State University, Pullman, Washington, USA. 281p.
- Bazazz, F.A. 1979. The physiological ecology of plant succession. *Annual Review of Ecology and Systematics* 10:351-371.
- Betancourt, J.L., T.R. van Devender, and P.S. Martin, editors. 1990. *Packrat Middens: The Last 40,000 Years of Biotic Change*. The University of Arizona Press, Tucson, Arizona, USA. 467p.
- Bewley, J.D., and M. Black. 1985. *Seeds: Physiology of Development and Germination*. Plenum Press, New York, New York, USA. 367p.

- Beyer, H. L. 2006. Hawth's Analysis Tools for ArcGIS, Version 3.26. URL: <http://www.spataleecology.com/htools> (accessed 18 May 2007).
- Björkman, O., and B. Demmig. 1987. Photon yield of O₂-evolution and chlorophyll fluorescence characteristics at 77K among vascular plants of diverse origins. *Planta* 170:489-504.
- Björkman, O., and B. Demmig-Adams. 1994. Regulation of photosynthetic light energy capture, conversion, and dissipation in leaves. Pages 17-48 in E.-D. Schulze and M.M. Caldwell, Editors. *Ecophysiology of Photosynthesis*. Springer-Verlag, Berlin, Germany. 576p.
- Boorse, G.C., T.L. Bosma, A.-C. Meyer, F.W. Ewers, and S.D. Davis. 1998. Comparative methods of estimating freezing temperatures and freezing injury in leaves of chaparral shrubs. *International Journal of Plant Science* 159(3):513-521.
- Brown, G.N., T.M. Hinckley, and J.A. Bixby. 1972. Xylem sap pressure relationship to seedling survival after freezing. *Cryobiology* 9:314.
- Brown, J.H., and M.V. Lomolino. 1998. *Biogeography*, Second Edition. Sinauer Associates, Inc., Sunderland, Massachusetts, USA. 691p.
- Burr, K.E., R.W. Tinus, S.J. Wallner, and R.M. King. 1989. Relationships among cold hardiness, root growth potential and bud dormancy in three conifers. *Tree Physiology* 5:291-306.
- Burr, K.E., R.W. Tinus, S.J. Wallner, and R.M. King. 1990. Comparison of three cold hardiness tests for conifer seedlings. *Tree Physiology* 6:351-369.
- Burr, K.E., S.J. Wallner, and R.W. Tinus. 1991. Ethylene and ethane evolution during cold acclimation and deacclimation of ponderosa pine. *Canadian Journal of Forest Research* 21:601-605.
- Burr, K.E., C.D.B. Hawkins, S.J. L'Hirondelle, W.D. Binder, M.F. George, and T. Repo. 2001. Methods for measuring cold hardiness of conifers. Pages 369-401 in F.J. Bigras and S.J. Colombo, Editors. *Conifer Cold Hardiness*. Kluwer Academic Publishers, Boston, Massachusetts, USA. 596p.
- Barton, L.V. 1930. Hastening the germination of some coniferous seeds. *American Journal of Botany* 17:88-115.
- Cannell, M.G.R., and L.J. Sheppard. 1982. Seasonal changes in the frost hardiness of provenances of *Picea sitchensis* in Scotland. *Forestry* 55:137-153.

- Clausen, J., D.D. Keck, and W.M. Hiesey. 1940. Experimental studies on the nature of species. I. Effect of varied environments on western North American plants. Carnegie Institution of Washington, Publication 520. Washington, D.C., USA. 452p.
- Colorado Plateau Stable Isotope Laboratory (CPSIL). 2006. Sample submission – organics – $\delta^{13}\text{C}$ and $\delta^{15}\text{N}$ via EA-CFIRMS. URL: http://www4.nau.edu/cpsil/13c_15n_org.htm (accessed 19 May 2006).
- Conkle, M.T., and W.B. Critchfield. 1988. Genetic variation and hybridization of ponderosa pine. Pages 27-43 in D.M. Baumgarnter and J.E. Lotan, editors. Ponderosa pine: the species and its management. Washington State University, Pullman, Washington, USA. 281p.
- Coronado National Forest (CNF). 2002. Bullock Fire (Archival Site). URL: www.fs.fed.us/r3/coronado/bullock/ (accessed 14 May 2007).
- Coronado National Forest (CNF). 2003. Aspen Fire (Archival Site). URL: www.fs.fed.us/r3/coronado/aspen/ (accessed 14 May 2007).
- Cottam, G., and J.T. Curtis. 1956. The use of distance measures in phytosociological sampling. *Ecology* 37:451-460.
- Covington, W.W., R.L. Everett, R.W. Steele, L.I. Irwin, T.A. Daer, and A.N.D. Auclair. 1994. Historical and anticipated changes in forest ecosystems of the Inland West of the United States. *Journal of Sustainable Forestry* 2:13-63.
- Costa, J., A.T. Peterson, and C.B. Beard. 2002. Ecologic niche modeling and differentiation of populations of *Triatoma brasiliensis* Neiva, 1911, the most important chagas' disease vector in northeastern Brazil (Hemiptera, Reduviidae, Triatominae). *American Journal of Tropical Medicine and Hygiene* 67(5):516-520.
- Crawley, M.J. 2005. Statistics: An Introduction using R. John Wiley & Sons, Ltd., West Sussex, England. 327p.
- Cregg, B.M. 1994. Carbon allocation, gas exchange, and needle morphology of *Pinus ponderosa* genotypes known to differ in growth and survival under imposed drought. *Tree Physiology* 14:883-898.
- Critchfield, W.B., and E.L. Little, Jr. 1966. Geographic distribution of the pines of the world. USDA Misc. Publ. 991.

- Cui, M., and W.K. Smith. 1991. Photosynthesis, water relations and mortality in *Abies lasiocarpa* seedlings during natural establishment. *Tree Physiology* 8:37-46.
- Daubenmire, R.F. 1943. Soil temperature versus drought as a factor determining lower altitudinal limits of trees in the Rocky Mountains. *Botanical Gazette* 105(1):1-13.
- Davis, A.J., J.H. Lawton, B. Shorrocks, and L.S. Jenkinson. 1998. Individualistic species responses invalidate simple physiological models of community dynamics under global environmental change. *Journal of Animal Ecology* 67:600-612.
- Dawson, T.E., S. Mambelli, A.H. Plamboeck, P.H. Templer, and K.P. Tu. 2002. Stable isotopes in plant ecology. *Annual Review of Ecology and Systematics* 33:507-559.
- DeHayes, D.H. 1977. Genetic variation in cold hardiness and its effects on the performance of ponderosa pine (*Pinus ponderosa*) in Michigan. Unpublished dissertation, Michigan State University, East Lansing, Michigan, USA. 141p.
- Dodge, R.A. 1963. Investigations into the Ecological Relationships of Ponderosa Pine in Southeast Arizona. Unpublished dissertation, The University of Arizona, Tucson, Arizona, USA. 118p.
- Dreesen, D. 2003. Propagation protocol for production of container *Pinus ponderosa* plants (One-Gallon Tree Pot, 4"x4"x14"); Los Luna Plant Materials Center, Los Lunas, New Mexico. In Native Plant Network. URL: www.nativeplantnetwork.org (accessed 14 October 2005).
- Elton, C. 1927. *Animal Ecology*. Macmillan Company, New York, New York, USA. 207p.
- Elliott, K.J., and A.S. White. 1987. Competitive effects of various grasses and forbs on ponderosa pine seedlings. *Forest Science* 33(2):356-366.
- Engler, R., A. Guisan, and L. Rechsteiner. 2004. An improved approach for predicting the distribution of rare and endangered species from occurrence and pseudo-absence data. *Journal of Applied Ecology* 41:263-274.
- Epperson, B.K. F.W. Telewski, A.E. Plovanich-Jones, and J.E. Grimes. 2001. Clinal differentiation and putative hybridization in a contact zone of *Pinus ponderosa* and *P. arizonica* (Pinaceae). *American Journal of Botany* 88(6):1052-1057.

- Epperson, B.K., M.G. Chung, and F.W. Telewski. 2003. Spatial pattern of allozyme variation in a contact zone of *Pinus ponderosa* and *P. arizonica* (Pinaceae). *American Journal of Botany* 90(1):25-31.
- Environmental Systems Research Institute (ESRI), Inc. 2006. ArcGIS version 9.2. Redlands, California, USA.
- Evans, J., T. Luna, and D. Wick. 2001. Propagation protocol for production of container *Pinus ponderosa* Dougl. Plants (172 ml containers); Glacier National Park, West Glacier, Montana. *In* Native Plant Network. URL: <http://www.nativeplantnetwork.org> (accessed 14 October 2005).
- Faraway, J.J. 2002. Practical regression and Anova using R. URL: <http://cran.r-project.org/doc/contrib/Faraway-PRA.pdf> (accessed 15 June 2007). 213p.
- Farjon, A., and B.T. Styles. 1997. *Pinus* (Pinaceae), Flora Neotropica, Monograph 75. The New York Botanical Garden, Bronx, New York, USA. 293p.
- Farquhar, G.D., J.R. Ehleringer, and K.T. Hubick. 1989. Carbon isotope discrimination and photosynthesis. *Annual Review of Plant Physiology* 40:503-537.
- Farris, M.A., and J.B. Mitton. 1984. Population density, outcrossing rate, and heterozygote superiority in ponderosa pine. *Evolution* 38(5):1151-1154.
- Force, E.R. 1997. Geology and Mineral Resources of the Santa Catalina Mountains, Southeastern Arizona: A Cross-Sectional Approach. Monographs in Mineral Resource Science No. 1. The University of Arizona, Tucson, Arizona, USA. 135p.
- Fritts, H.C. 1963. Statistical evaluation of tree-ring series. Seventh Annual Meeting, Arizona Academy of Science, Biology Section, Tucson, Arizona, USA.
- Fritts, H.C. 1974. Relationships of ring widths in arid-site conifers to variations in monthly temperature and precipitation. *Ecological Monographs* 44:411-440.
- Fry, B. 2006. Stable Isotope Ecology. Springer Science+Business Media, LLC, New York, New York, USA. 308p.
- Fuller, G.D. 1916. Ecology of the Santa Catalina Mountains. *Botanical Gazette* 62(1):75-78.

- Germino, M.J., W.K. Smith, and A.C. Resor. 2002. Conifer seedling distribution and survival in an alpine-treeline ecotone. *Plant Ecology* 162:157-168.
- Gernandt, D.S., G.G. López, S.O. García, and A. Liston. 2005. Phylogeny and classification of *Pinus*. *Taxon* 54(1):29-42.
- Graybill, D.A. 1986. Green Mountain, Arizona, ponderosa pine. International Tree-Ring Data Bank. URL: <ftp://ftp.ncdc.noaa.gov/pub/data/paleo/treering/measurements/northamerica/usa/az520.rwl> (accessed 11 June 2007).
- Guisan, A., and W. Thuiller. 2005. Predicting species distribution: offering more than simple habitat models. *Ecology Letters* 8:993-1009.
- Guisan, A., C.H. Graham, J. Elith, F. Huettmann, and the NCEAS Species Distribution Modelling Group. 2007. Sensitivity of predictive species distribution models to change in grain size. *Diversity and Distributions* 13:332-340.
- Haase, E.F. 1970. Environmental fluctuations on south-facing slopes in the Santa Catalina Mountains of Arizona. *Ecology* 51(6):959-974.
- Haller, J.R. 1959. Factors affecting the distribution of ponderosa and Jeffrey pines in California. *Madroño* 15(3):65-96.
- Haller, J.R. 1965. The role of 2-needle fascicles in the adaptation and evolution of ponderosa pine. *Brittonia* 17:354-382.
- Hamrick, J.L., H.M. Blanton, and K.J. Hamrick. 1989. Genetic structure of geographically marginal populations of ponderosa pine. *American Journal of Botany* 76(11):1559-1568.
- Hanley, J.A., and B.J. McNeil. 1982. The meaning and use of the area under a receiver operating characteristic (ROC) curve. *Radiology* 143(1):29-36.
- Havranek, W.M., and W. Tranquillini. 1995. Physiological processes during winter dormancy and their ecological significance. Pages 95-124 in W.K. Smith and T.M. Hinckley, Editors. *Ecophysiology of Coniferous Forests*. Academic Press, Inc., San Diego, California, USA. 338p.
- Hawkins, B.J., H.J. Guest, and K. Kolotelo. 2003. Freezing tolerance of conifer seeds and germinants. *Tree Physiology* 23:1237-1246.
- Heidmann, L.J. 1987. Regeneration strategies for ponderosa pine. Pages 227-233 in D.M. Baumgarnter and J.E. Lotan, editors. *Ponderosa pine: the*

species and its management. Washington State University, Pullman, Washington, USA.

Helms, J.A. 1972. Environmental control of net photosynthesis in naturally growing *Pinus ponderosa* Laws. *Ecology* 53(1): 92-101.

Hernandez, P.A., C.H. Graham, L.L. Master, and D.L. Albert. 2006. The effect of sample size and species characteristics on performance of different species distribution modeling methods. *Ecography* 29:773-785.

Hijmans, R.J., and C.H. Graham. 2006. The ability of climate envelope models to predict the effect of climate change on species distributions. *Global Change Biology* 12:2272-2281.

Hirzel, A., and A. Guisan. 2002. Which is the optimal sampling strategy for habitat suitability modelling? *Ecological Modelling* 157:331-341.

Hobbie, E.A., S.A. Macko, and M. Williams. 2000. Correlations between foliar $\delta^{15}\text{N}$ and nitrogen concentrations may indicate plant-mycorrhizal interactions. *Oecologia* 122:273-283.

Hoch, G., and C. Körner. 2003. The carbon charging of pines at the climatic treeline: a global comparison. *Oecologia* 135:10-21.

Howard, Janet L. 2003a. *Pinus ponderosa* var. *arizonica*. In Fire Effects Information System. U.S. Department of Agriculture, Forest Service, Rocky Mountain Research Station, Fire Sciences Laboratory. URL: <http://www.fs.fed.us/database/feis> (accessed 21 March 2005).

Howard, Janet L. 2003b. *Pinus ponderosa* var. *scopulorum*. In Fire Effects Information System. U.S. Department of Agriculture, Forest Service, Rocky Mountain Research Station, Fire Sciences Laboratory. URL: <http://www.fs.fed.us/database/feis> (accessed 16 June 2007).

Hubbard, R.M., M.G. Ryan, V. Stiller, and J.S. Sperry. 2001. Stomatal conductance and photosynthesis vary linearly with plant hydraulic conductance in ponderosa pine. *Plant, Cell and Environment* 24:113-121.

Humphries, H.C., and P.S. Bourgeron. 2003. Environmental responses of *Pinus ponderosa* and associated species in the south-western USA. *Journal of Biogeography* 30:257-276.

Hutchinson, G.E. 1957. Concluding remarks. Cold Spring Harbor Symposium on Quantitative Biology 22:415-427.

- Jackson, G.E., I.J. Irvine, J. Grace, and A.A.M. Khalil. 1995. Absciscic acid concentrations and fluxes in droughted conifer saplings. *Plant, Cell and Environment* 18:13-22.
- Jacobsen A.L., R.B. Pratt, F.W. Ewers, and S.D. Davis. 2007. Cavitation resistance among twenty-six chaparral species of southern California. *Ecological Monographs* 77:99-115.
- Jarvis, P.G. 1976. The interpretation of the variations in leaf water potential and stomatal conductance found in canopies in the field. *Philosophical Transactions of the Royal Society of London. Series B, Biological Sciences* 273(927):593-610.
- Johnson, D.M., M.J. Germino, and W.K. Smith. 2004. Abiotic factors limiting photosynthesis in *Abies lasiocarpa* and *Picea engelmannii* seedlings below and above the alpine timberline. *Tree Physiology* 24:377-386.
- Jones, J.R. 1967. Regeneration of mixed conifer clearcuttings on the Apache National Forest, Arizona. Res. Note RM-79. Fort Collins, CO: U.S. Department of Agriculture, Forest Service, Rocky Mountain Forest and Range Experiment Station. 8 p.
- Kaufmann, M.R. 1968. Evaluation of the pressure chamber technique for estimating plant water potential of forest tree species. *Forest Science* 14(4):369-374.
- Kipfer, J.A., J. Balmat, and J.L. Smith. 2005. Shifts in the potential distribution of sky island plant communities in response to climate change. Pages 485-490 in G.J. Gottfried, B.S. Gebow, L.G. Eskew, and C.B. Edminster, Compilers. *Connecting Mountain Islands and Desert Seas: Biodiversity and Management of the Madrean Archipelago II*. Proceedings RMRS-P-36. U.S. Department of Agriculture, Forest Service, Rocky Mountain Research Station, Fort Collins, Colorado, USA. 631 p.
- Kolb, P.F., and R. Robberecht. *Pinus ponderosa* seedling establishment and the influence of competition with the bunchgrass *Agropyron spicatum*. *International Journal of Plant Science* 157(4):509-515.
- Kolb, T.E., K.C. Steiner, and H.F. Barbour. 1985. Seasonal and genetic variations in loblolly pine cold tolerance. *Forest Science* 31(4):926-932.
- Kozlowski, T.T., P.J. Kramer, and S.G. Pallardy. 1991. *The Physiological Ecology of Plants*. Academic Press, San Diego, California, USA. 657p.
- Kral, R. 1993. *Pinus*. Pages 373-398 in *Flora of North America* Editorial Committee, editors. *Flora of North America North of Mexico*. Volume 2.

- Pteridophytes and Gymnosperms. Oxford University Press, New York, New York, USA. 475pp.
- Krugman, S.L., and J.L. Jenkinson. 1974. *Pinus* L. Pine. Pages 598-638 in C.S. Schopmeyer, Technical Coordinator. Seeds of Woody Plants in the United States. U.S. Department of Agriculture, Forest Service, Agriculture Handbook No. 450, Washington, D.C., USA.
- Langsrud, Ø. 2003. ANOVA for unbalanced data: Use Type II instead of Type III sums of squares. *Statistics and Computing* 13:163-167.
- Larcher, W. 2005. *Physiological Plant Ecology: Ecophysiology and Stress Physiology of Functional Groups*, 4th Edition. Springer-Verlag, Berlin, Germany. 513p.
- Larson, M.M. 1961. Seed size, germination dates, and survival relationships of ponderosa pine in the Southwest. Research Note No. 66. Fort Collins, CO: U.S. Department of Agriculture, Forest Service, Rocky Mountain Forest and Range Experiment Station. 4 p.
- Larson, M.M., and G.H. Schubert. 1970. Cone crops of ponderosa pine in central Arizona, including the influence of Abert squirrels. Res. Pap. RM-58. Fort Collins, CO: U.S. Department of Agriculture, Forest Service, Rocky Mountain Forest and Range Experiment Station. 15 p.
- Latta, R.G., Y.B. Linhart, and J.B. Mitton. 2001. Cytonuclear disequilibrium and genetic drift in a natural population of ponderosa pine. *Genetics* 158:843-850.
- Leathwick, J.R. 1998. Are New Zealand's *Nothofagus* species in equilibrium with their environment? *Journal of Vegetation Science* 9:719-732.
- Lehdig, F.T. 1998. Genetic variation in pines. Pages 251-280 in D.M. Richardson, Editor. *Ecology and Biogeography of Pinus*. Cambridge University Press, Cambridge, U.K. 527p.
- Lemmon, P.E. 1957. A new instrument for measuring forest overstory density. *Journal of Forestry* 55(9):667-668.
- Li, X.J., P.J. Burton, and C.L. Leadem. 1994. Interactive effects of light and stratification on the germination of some British Columbia conifers. *Canadian Journal of Botany* 72:1635-1646.
- LI-COR. 2005a. Using the LI-6400 Portable Photosynthesis System, Version 5: Book 5. Leaf Chamber Fluorometer. LI-COR Biosciences, Inc., Lincoln, Nebraska, USA. 100p.

- Linhart, Y.B., and J.B. Mitton. 1985. Relationships among reproduction, growth rates, and protein heterozygosity in ponderosa pine. *American Journal of Botany* 72(2):181-184.
- Little, E.L., Jr., and W.B. Critchfield. 1960. Subdivisions of the genus *Pinus* (pines). United States Department of Agriculture Miscellaneous Publication 1144.
- Liu, C., P.M. Berry, T.P. Dawson, and R.G. Pearson. 2005. Selecting thresholds of occurrence in the prediction of species distributions. *Ecography* 28:385-393.
- Lu, P., S.J. Colombo, and R.W. Sinclair. 2007. Cold hardiness of interspecific hybrids between *Pinus strobus* and *P. wallichiana* measured by post-freezing needle electrolyte leakage. *Tree Physiology* 27:243-250.
- Maherali, H., and E.H. DeLucia. 2000. Xylem conductivity and vulnerability of ponderosa pine growing in contrasting climates. *Tree Physiology* 20:859-867.
- Maherali, H., B.L. Williams, K.N. Paige, and E.H. DeLucia. 2002. Hydraulic differentiation of Ponderosa pine populations along a climate gradient is not associated with ecotypic divergence. *Functional Ecology* 16:510-521.
- Marshall, J.D., and J. Zhang. 1994. Carbon isotope discrimination and water use efficiency of native plants of the north-central Rockies. *Ecology* 75:1887-1895.
- Martin, P.S., and P.J. Mehringer, Jr. 1965. Pleistocene pollen analysis and biogeography of the Southwest. Pages 433-451 in H.E. Wright, Jr. and D.G. Frey, editors. *The Quaternary of the United States: A Review Volume for the VII Congress of the International Association for Quaternary Research*. Princeton University Press, Princeton, New Jersey, USA. 922p.
- Martínez-Meyer, E., and A.T. Peterson. 2006. Conservatism of ecological niche characteristics in North American plant species over the Pleistocene-to-Recent transition. *Journal of Biogeography* 33:1779-1789.
- Maurer, B. 2002. Predicting distribution and abundance: thinking within and between scales. Pages 125-133 in J.M. Scott, P.J. Heglund, M.L. Morrison, J.B. Haufler, M.G. Raphael, W.A. Wall, and F.B. Samson, Editors. *Predicting Species Occurrences: Issues of Accuracy and Scale*. Island Press, Washington, D.C., USA. 868p.

- McPherson, J.M., W. Jetz, and D.J. Rogers. 2004. The effects of species' range sizes on the accuracy of distribution models: ecological phenomenon or statistical artefact? *Journal of Applied Ecology* 41:811-823.
- Melander, L., and W.H. Saunders. 1979. Reaction rates of isotopic molecules. Wiley, New York, New York, USA.
- Millar, C.I. 1993. Impact of the Eocene on the evolution of *Pinus* L. *Annals of the Missouri Botanical Garden* 80:471-498.
- Mitton, J.B., Y.B. Linhart, J.L. Hamrick, and J.S. Beckman. 1977. Observations on the genetic structure and mating system of ponderosa pine in the Colorado Front Range. *Theoretical and Applied Genetics* 51:5-13.
- Mitton, J.B., K.B. Sturgeon, and M.L. Davis. 1980. Genetic differentiation in ponderosa pine along a steep elevational gradient. *Silvae Genetica* 29(3-4):100-103.
- Moore, M.M., W.W. Covington, and P.Z. Fulé. 1999. Reference conditions and ecological restoration: a Southwestern ponderosa pine perspective. *Ecological Applications* 9(4):1266-1277.
- Muir, J. 1911. *My First Summer in the Sierra*. Houghton Mifflin Company, New York, New York, USA. 353p.
- National Climatic Data Center (NCDC). 2007. NNDP Climate Data Online. Station: East LANSING 4 S, MI, COOP-WBAN ID 202395-99999. National Climatic Data Center, Asheville, North Carolina, USA. URL: <http://www.ncdc.noaa.gov/oa/ncdc.html> (accessed 26 June 2007).
- Neilson, R.P., and L.H. Wullstein. 1983. Biogeography of two southwest American oaks in relation to atmospheric dynamics. *Journal of Biogeography* 10:275-297.
- Niebling, C.R., and M.T. Conkle 1990. Diversity of Washoe pine and comparisons with allozymes of ponderosa pine races. *Canadian Journal of Forest Research* 20:298-308.
- Nobel, P.S. 2005. *Physicochemical and Environmental Plant Physiology*, Third Edition. Elsevier Academic Press, Burlington, Massachusetts, USA. 567p.
- Norris, J.R., S.T. Jackson, and J.L. Betancourt. 2006. Classification tree and minimum-volume ellipsoid analyses of the distribution of ponderosa pine in the western USA. *Journal of Biogeography* 33:342-360.

- Oliver, W.W., and R.A. Ryker. 1990. Ponderosa Pine. *In* R.M. Burns and B.H. Honkala, technical coordinators. *Silvics of North America: Volume 1. Conifers. Agriculture Handbook 654.* U.S. Department of Agriculture, Forest Service, Washington, D.C. URL: www.na.fs.fed.us/spfo/pubs/silvics_manual (accessed 29 May 2007).
- Öquist, G., and N.P.A. Huner. 2003. Photosynthesis of overwintering evergreen plants. *Annual Review of Plant Biology* 54:329-355.
- Park, R., and S. Epstein. 1961. Metabolic fractionation of C13 and C12 in plants. *Plant Physiology* 36:133-138.
- Parker, J. 1955. Annual trends in cold hardiness of ponderosa pine and grand fir. *Ecology* 36(3):377-380.
- Pearson, R.G., C.J. Raxworthy, M. Nakamura, and A.T. Peterson. 2007. Predicting species distributions from small numbers of occurrence records: a test case using cryptic geckos in Madagascar. *Journal of Biogeography* 34:102-117.
- Peet, R.K. 1984. Forests of the Rocky Mountains. Pages 63-101 *in* M.G. Barbour and W.D. Billings, editors. *North American Terrestrial Vegetation.* Cambridge University Press, Cambridge, U.K. 434p.
- Peloquin, R.L. 1971. Variation and hybridization patterns in *Pinus ponderosa* and *Pinus engelmannii*. Ph.D. dissertation, University of California, Santa Barbara, California, USA. 196p.
- Peloquin, R.L. 1984. The identification of three-species hybrids in the ponderosa pine complex. *Southwestern Naturalist* 29(1):115-122.
- Perry, D.A., H. Margolis, C. Choquette, R. Molina, and J.M. Trappe. 1989. Ectomycorrhizal mediation of competition between coniferous tree species. *New Phytologist* 112:501-511.
- Perry, J.P., Jr. 1991. *The Pines of Mexico and Central America.* Timber Press, Inc., Portland, Oregon, USA. 231p.
- Peterson, A.T., J. Soberón, and V. Sánchez-Cordero. 1999. Conservation of ecological niches in evolutionary time. *Science* 285:1265-1267.
- Peterson, A.T., D.R.B. Stockwell, and D.A. Kluza. 2002. Distributional prediction based on ecological niche modeling of primary occurrence data. Pages 617-623 *in* J.M. Scott, P.J. Heglund, M.L. Morrison, J.B. Haufler, M.G. Raphael, W.A. Wall, and F.B. Samson, Editors. *Predicting Species*

- Occurrences: Issues of Accuracy and Scale. Island Press, Washington, D.C., USA. 868p.
- Phillips, S.J., M. Dudík, and R.E. Schapire. 2004. A maximum entropy approach to species distribution modeling. Pages 655-662 *in* Proceedings of the 21st International Conference on Machine Learning. ACM Press, New York, New York, USA.
- Phillips, S.J., R.P. Anderson, and R.E. Schapire. 2006a. Maximum entropy modeling of species geographic distributions. *Ecological Modelling* 190:231-259.
- Phillips, S.J., M. Dudik, and R.E. Schapire. 2006b. Maximum Entropy Species Distribution Modeling, Version 2.3. URL: www.cs.princeton.edu/~schapire/maxent/ (accessed 20 February 2007).
- Pima County Department of Transportation (PCDOT). 2007. Permanent Traffic Counter Stations for 2005-2006. URL: <http://www.dot.pima.gov/trafeng/trafcnt/> (accessed 29 June 2007).
- Piñol, J., and A. Sala. 2000. Ecological implications of xylem cavitation for several Pinaceae in the Pacific Northern USA. *Functional Ecology* 14:538-545.
- Pisek, A., and R. Schiessl. 1947. Die Temperaturbeeinflussbarkeit der Frosthärte von Nadelhölzern und Zwergsträuchern an der alpinen Waldgrenze. Berlin Naturwiss.-Med. Ver. Innsbruck 47:33-52.
- Potvin, C., and M.J. Lechowicz. 1990. The statistical analysis of ecophysiological response curves obtained from experiments involving repeated measures. *Ecology* 71(4):1389-1400.
- Price, R.A., A. Liston, and S.H. Strauss. 1998. Phylogeny and systematics of *Pinus*. Pages 49-68 *in* D.M. Richardson, editor. *Ecology and Biogeography of Pinus*. Cambridge University Press, Cambridge, U.K. 527p.
- PRISM. 2006. 30-arcsec (800m) Normals (1971-2000). PRISM Group, Oregon State University, Corvallis, Oregon, USA. URL: www.prismclimate.org (accessed 13 October 2006).
- Pulliam, H.R. 2000. On the relationship between niche and distribution. *Ecology Letters* 3:349-361.
- R Development Core Team. 2007. R: A Language and Environment for Statistical Computing. R Foundation for Statistical Computing, Vienna,

Austria. Version 2.5.0 (2007-4-23). URL: www.R-project.org (accessed 21 May 2007).

Radomes, Inc. 2005. Online Air Defense Radar Museum. URL: www.radomes.org/museum/ (accessed 8 June 2007).

Read, D.J. 1998. The mycorrhizal status of *Pinus*. Pages. 324-340 in D.M. Richardson, Editor. Ecology and Biogeography of *Pinus*. Cambridge University Press, Cambridge, United Kingdom. 527p.

Rehfeldt, G.E. 1986. Adaptive variation in *Pinus ponderosa* from Intermountain regions. I. Snake and Salmon River basins. Forest Science 32:79-92.

Rehfeldt, G.E. 1990. Genetic differentiation among populations of *Pinus ponderosa* from the upper Colorado River Basin. Botanical Gazette 151(1):125-137.

Rehfeldt, G.E. 1993. Genetic variation in the *Ponderosae* of the Southwest. American Journal of Botany 80(3):330-343.

Rehfeldt, G.E. 1999. Systematics and genetic structure of *Ponderosae* taxa (Pinaceae) inhabiting the mountain islands of the Southwest. American Journal of Botany 86(5):741-752.

Rehfeldt, G.E., B.C. Wilson, S.P. Wells, and R.M. Jeffers. 1996. Phytogeographic, taxonomic, and genetic implications of phenotypic variation in the *Ponderosae* of the Southwest. Southwestern Naturalist 41:409-418.

Reich, P.B., M.B. Walters, B.K. Kloeppel, and D.S. Ellsworth. 1995. Different photosynthesis-nitrogen relations in deciduous hardwood and evergreen coniferous tree species. Oecologia 104:24-30.

Riegel, G.M., R.F. Miller, and W.C. Krueger. 1992. Competition for resources between understory vegetation and overstory *Pinus ponderosa* in northeastern Oregon. Ecological Applications 2(1):71-85.

Ritchie, G.A. 1975. The pressure chamber as an instrument for ecological research. Advances in Ecological Research 9:165-254.

Ritchie, G.A. 1991. Measuring cold hardiness. Pages 557-582 in J.M. Lassoie and T.M. Hinckley, Editors. Techniques and Approaches in Forest Tree Ecophysiology. CRC Press, Inc., Boca Raton, Louisiana, USA. 599p.

- Rundel, P.W., and B.J. Yoder. 1998. Ecophysiology of *Pinus*. Pages 296-323 in D.M. Richardson, Editor. Ecology and Biogeography of *Pinus*. Cambridge University Press, Cambridge, United Kingdom. 527p.
- Schaberg, P.G., R.C. Wilkinson, J.B. Shane, J.R. Donnelly, and P.F. Cali. 1995. Winter photosynthesis of red spruce from three Vermont seed sources. *Tree Physiology* 15:345-350.
- Schmid, J.M., S.A. Mata, and J.C. Mitchell. 1986. Number and condition of seeds in ponderosa pine cones in central Arizona. *The Great Basin Naturalist*. 46: 449-451.
- Schreiber, U., W. Bilger, and C. Neubauer. 1994. Chlorophyll fluorescence as a nonintrusive indicator for rapid assessment of in vivo photosynthesis. Pages 49-70 in E.-D. Schulze and M.M. Caldwell, Editors. *Ecophysiology of Photosynthesis*. Springer-Verlag, Berlin, Germany. 576p.
- Schubert, G.H. 1974. Silviculture of southwestern ponderosa pine: the status of our knowledge. U.S. Department of Agriculture, Forest Service, Research Paper RM-123. Rocky Mountain Forest and Range Experiment Station, Fort Collins, Colorado, USA. 71p.
- Schütz, W., and G. Rave. 1999. The effect of cold stratification and light on the seed germination of temperate sedges (*Carex*) from various habitats and implications for regenerative strategies. *Plant Ecology* 144:215-230.
- Segurado, P., and M.B. Araújo. 2004. An evaluation of methods for modelling species distributions. *Journal of Biogeography* 31:1555-1568.
- Sheppard, P.R., A.C. Comrie, G.D. Packin, K. Angersbach, and M.K. Hughes. 2002. The climate of the US Southwest. *Climate Research* 21:219-238.
- Shreve, F. 1915. *The Vegetation of a Desert Mountain Range as Conditioned by Climatic Factors*. Carnegie Institution of Washington, Washington, D.C., USA. 112p.
- Shreve, F. 1922. Conditions indirectly affecting vertical distribution on desert mountains. *Ecology* 3(4):269-274.
- Shreve, F. 1924. Soil temperature as influenced by altitude and slope exposure. *Ecology* 5(2):128-136.
- Smith, R.H. 1977. Monoterpenes of ponderosa pine xylem resin in western United States. USDA Forest Service, Technical Bulletin 1532. 48p.

- Smith, T.M. 1986. Stratification reduced germination of ponderosa pine seed collected in New Mexico and southern Colorado. Pages 17-18 in T.D. Landis. Proceedings: Combined Western Forest Nursery Council and Intermountain Nursery Association Meeting. August 12-15, 1986. USDA Forest Service General Technical Report RM-137.
- Soberón, J., and A.T. Peterson. 2005. Interpretation of models of fundamental ecological niches and species' distributional areas. *Biodiversity Informatics* 2:1-10.
- Sperry J.S., J.R. Donnelly, and M.T. Tyree M.T. 1988. A method for measuring hydraulic conductivity and embolism in xylem. *Plant, Cell and Environment* 11:35-40.
- Stefferd, A., ed. 1961. The Yearbook of Agriculture 1961. U.S. Government Printing Office, Washington, D.C. 591p.
- Stockwell, D.R.B., and A.T. Peterson. 2002. Effects of sample size on accuracy of species distribution models. *Ecological Modelling* 148:1-13.
- Stout, D.L., and A. Sala. 2003. Xylem vulnerability to cavitation in *Pseudotsuga menziesii* and *Pinus ponderosa* from contrasting habitats. *Tree Physiology* 23:43-50.
- Sutinen, M.-L., J.P. Palta, and P.B. Reich. 1992. Seasonal differences in freezing stress resistance of needles of *Pinus nigra* and *Pinus resinosa*: evaluation of the electrolyte leakage method. *Tree Physiology* 11:241-254.
- Swetnam, T.W., and C.H. Baisan. 2003. Tree-ring reconstructions of fire and climate history in the Sierra Nevada and southwestern United States. Pages 154-191 in T.T. Veblen, W.L. Baker, G. Montenegro, and T.W. Swetnam, editors. *Fire and Climate Change in Temperate Ecosystems of the Western Americas*. Ecological Studies 160. Springer-Verlag, New York, New York, USA. 444p.
- Tanaka, Y. 1984. Assuring seed quality for seedling production: cone collection and seed processing, testing, storage, and stratification. Pages 27-39 in M.L. Duryea and T.D. Landis, editors. *Forest Nursery Manual: Production of Bareroot Seedlings*. Martinus Nijhoff/Dr W. Junk Publishers. The Hague/Boston/Lancaster, for Forest Research Laboratory, Oregon State University, Corvallis, Oregon, USA. 386p.
- Theophrastus. 1916. *Enquiry Into Plants*, Volume I, Books 1-5, with an English Translation by Sir Arthur Hort. Harvard University Press, Cambridge, Massachusetts, USA. 504p.

- Thompson, K., T. Keller-Wolf, and J. Franklin. 2002. A comparison of fine- and coarse-resolution environmental variables toward predicting vegetation distribution in the Mojave Desert. Pages 133-139 in J.M. Scott, P.J. Heglund, M.L. Morrison, J.B. Haufler, M.G. Raphael, W.A. Wall, and F.B. Samson, Editors. *Predicting Species Occurrences: Issues of Accuracy and Scale*. Island Press, Washington, D.C., USA. 868p.
- Thompson, R.S., K.H. Anderson, and P.J. Bartlein. 1999. Atlas of relations between climatic parameters and distributions of important trees and shrubs in North America. U.S. Geological Survey Professional Paper 1650 A&B, Denver, Colorado, USA. URL: pubs.usgs.gov/pp/p1650-a/ (accessed 27 May 2007).
- Thompson, R.S., and K.H. Anderson. 2000. Biomes of western North America at 18,000, 6000 and 0 ^{14}C yr BP reconstructed from pollen and packrat midden data. *Journal of Biogeography* 27:555-584.
- Tomback, D.F., A.J. Anderies, K.S. Carsey, M.L. Powell, and S. Mellmann-Brown. 2001. delayed seed germination in whitebark pine and regeneration patterns following the Yellowstone fires. 82(9):2587-2600.
- Tranquillini, W. 1979. *Physiological Ecology of the Alpine Timberline: Tree Existence at High Altitudes with Special Reference to the European Alps*. Springer-Verlag, Berlin, Germany. 137p.
- Tsoar, A., O. Allouche, O. Steinitz, D. Rotem, and R. Kadmon. 2007. A comparative evaluation of presence-only methods for modeling species distribution. *Diversity and Distributions*, OnLine Early Articles, 27 March 2007, 1-9.
- Tyree, M.T., and F.W. Ewers. 1991. The hydraulic architecture of trees and other woody plants. *New Phytologist* 119:345-360.
- U.S. Environmental Protection Agency (USEPA). 1998. *Climate Change and Arizona*. EPA 236-F-98-007c, Office of Policy, Washington, D.C., USA. 4p.
- U.S. Geological Survey (USGS). 2004. National Elevation Dataset (NED) 1/3 Arc Second. United States Geological Survey, Sioux Falls, SD. URL: <http://seamless.usgs.gov/index.asp> (accessed 18 May 2007).
- van Devender, T.R. 1990. Late Quaternary vegetation and climate of the Sonoran Desert, United States and Mexico. Pages 134-163 in J.L. Betancourt, T.R. van Devender, and P.S. Martin, editors. *Packrat Middens: The Last 40,000 Years of Biotic Change*. The University of Arizona Press, Tucson, Arizona, USA. 467p.

- van Devender, T.R., and W.G. Spaulding. 1979. Development of vegetation and climate in the southwestern United States. 204(4394):701-710.
- van Devender, T.R., J.L. Betancourt, and M. Wimberly. 1984. Biogeographic implications of a packrat midden sequence from the Sacramento Mountains, south-central New Mexico. *Quaternary Research* 22:344-360.
- Verhoeven, A.S., W.W. Adams III, and B. Demmig-Adams. 1999. The xanthophyll cycle and acclimation of *Pinus ponderosa* and *Malva neglecta* to winter stress. *Oecologia* 118:277-287.
- Vetaas, O.R. 2002. Realized and potential climate niches: a comparison of four *Rhododendron* tree species. *Journal of Biogeography* 29:545-554.
- Wagner, D.B. 1992. Nuclear, chloroplast, and mitochondrial DNA polymorphisms as biochemical markers in population genetic analyses of forest trees. *New Forests* 6(1-4):373-390
- Warrington, I.J., and A.K.H. Jackson. 1981. Injury to radiata pine as influenced by freezing and thawing rate, and low temperature duration. *New Zealand Journal of Forestry Science* 11(1):37-44.
- Watano, Y., M. Imazu, and T. Shimizu. 1996. Spatial distribution of cpDNA and mtDNA haplotypes in a hybrid zone between *Pinus pumila* and *P. parviflora* var. *pentaphylla* (Pinaceae). *Journal of Plant Research* 109:403-408.
- Wenny, D.L., and R.K. Dumroese. 2001. Propagation protocol for production of container *Pinus ponderosa* Laws. Var. *ponderosa* plants (90 ml (5 cu in) plugs); Forest Research Nursery, Moscow, Idaho. *In* Native Plant Network. URL: <http://www.nativeplantnetwork.org> (accessed 14 October 2005).
- Western Regional Climate Center. 2007. Western U.S. Historical Climate Summaries. URL: www.wrcc.dri.edu/Climsum.html (accessed 1 June 2007).
- White, A.S. 1985. Presettlement regeneration patterns in a Southwestern ponderosa pine stand. *Ecology* 66(2):589-594.
- Whittaker, R.H. and W.A. Niering. 1965. Vegetation of the Santa Catalina Mountains, Arizona: A gradient analysis of the south slope. *Ecology* 46(4):429-452.

- Whittaker, R.H. and W.A. Niering. 1968. Vegetation of the Santa Catalina Mountains, Arizona: IV. Limestone and acid soils. *Journal of Ecology* 56(2):523-544.
- Whittaker, R.H. and W.A. Niering. 1975. Vegetation of the Santa Catalina Mountains, Arizona: V. Biomass, production, and diversity along an environmental gradient. *Ecology* 56(4):771-790.
- Woodward, F.I. 1987. *Climate and Plant Distribution*. Cambridge University Press, Cambridge, UK. 174p.
- Yeaton, R.I., R.W. Yeaton, and J.E. Horenstein. 1980. The altitudinal replacement of digger pine by ponderosa pine on the western slopes of the Sierra Nevada. *Bulletin of the Torrey Botanical Club* 107(4):487-495.